DESIGN OPTIMISATION OF THE CHITRA TILTING DISC HEART VALVE PROSTHESIS

A thesis presented by

G. S. BHUVANESHWAR

in partial fulfilment of the requirements for
the degree of Doctor of Philosophy in
BIOMEDICAL ENGINEERING

Sree Chitra Tirunal Institute for
Medical Sciences and Technology
Trivandrum, India

May 1993

D E C L A R A T I O N

I, **G.S.BHUVANESHWAR** hereby declare that I personally carried out the work depicted in this thesis entitled **"DESIGN OPTIMISATION OF THE CHITRA TILTING DISC HEART VALVE PROSTHESIS"**, except where external help was sought and has been duly acknowledged.

Date: 26th May 1993.

G.S.BHUVANESHWAR
Div. of Artificial Internal Organs
Biomedical Technology Wing
SCTIMST, Trivandrum - 695 012

C E R T I F I C A T E

This is to certify that Sri **G.S.BHUVANESHWAR**, in the Biomedical Technology Wing of the Sree Chitra Tirunal Institute for Medical Sciences & Technology has fulfilled the requirements of regulations relating to the nature and prescribed period of research for the Ph.D degree of the Institute. The work relating to his thesis entitled **"DESIGN OPTIMISATION OF THE CHITRA TILTING DISC HEART VALVE PROSTHESIS"** was carried out under our joint supervision.

Dr. M.S.Valiathan
[Co-guide]
Prof. & Head
Dept. of Cardiovascular
& Thoracic Surgery
SCTIMST,
TRIVANDRUM - 695 011

Dr. T.S.Prahlad
[External Guide]
Project Director
Aeronautical
Development Agency
BANGALORE - 560 017

The thesis entitled

DESIGN OPTIMISATION OF THE CHITRA TILTING DISC HEART VALVE PROSTHESIS

Submitted

by

G.S.BHUVANESHWAR

for

Doctor of Philosophy

in

BIOMEDICAL ENGINEERING

of

Sree Chitra Tirunal Institute for
Medical Sciences and Technology
TRIVANDRUM, INDIA

Evaluated and approved by

Dr.T.S.Prahlad Guide	Dr.K.M.Patil I.I.T.,Madras	Dr.M.D.Deshpande NAL, Bangalore

This work is

dedicated to my family,

KAMINI, VIGNESH & KRITHIKA.

With love and thanks for your

patience, understanding and support.

ACKNOWLEDGEMENTS

The author wishes to express his gratitude and appreciation to the following persons and organisations, who have significantly contributed to the completion of this thesis :

Dr.T.S.Prahlad for his encouragement, advice and assistance throughout this research project as Guide and Chairman of the advisory committee.

Dr.M.S.Valiathan for the inspiration and confidence to persevere in this area despite the many set-backs; and for the concept and support to set up the Pulsed Ultrasound Doppler Velocimeter.

Mr.A.V.Ramani for the constant encouragement and invaluable discussions, and for combining such friendship with advice which made this work possible.

Mr.O.S.Neelakantan Nair and staff members of the Division of Toolroom and Engineering Services for their technical support and high level of workmanship in the fabrication of the test systems and components.

Liquid Propulsion Systems Centre, Department of Space, Bangalore for fabricating the force transducers and to Mr.M.Manjunath Naik in particular, whose personal interest made them available on time.

Dr.T.V.How of the University of Liverpool for the technical information and assistance in the setting up of the doppler velocimeter and its sample volume determination; to the British Council and the Institute for making his visit here possible.

Mr.C.V.Muraleedharan and colleagues of the Division of Artificial Internal Organs for their constant encouragement and unflinching support.

Dr.R.Sivakumar, Dr.G.A.V.Lal, Dr.S.N.Pal, friends and colleagues of the Institute, whose moral support and encouragement kept the work alive and the author going.

TABLE OF CONTENTS

LIST OF TABLES

LIST OF FIGURES

S Y N O P S I S

DESIGN OPTIMISATION OF THE CHITRA TILTING DISC HEART VALVE PROSTHESIS

Despite extensive development during the last three decades, problems continue to exist with all current artificial heart valves. Thrombus formation, thrombo-embolism and tissue overgrowth are the major complications of mechanical valves while tissue valves fail in 3 to 10 years due to calcification, leaflet thickening or material fatigue (Yoganathan *et al* 1978b; Reul *et al* 1986). Yoganathan *et al* contend that these problems of mechanical valves are directly related to the fluid dynamics of the valves. In tilting disc valves, the orifice is divided into two unequal parts by the eccentric pivoting of the disc. The smaller orifice is associated with the problem of tissue overgrowth due to the lower velocity of flow through it and the creation of a stagnation zone downstream (Yoganathan *et al* 1978a). In an attempt to mitigate this problem, the Bjork-Shiley valve was redesigned with a convexo-concave disc and an opening angle of 70^0 to widen the smaller orifice (Stevenson *et al* 1982). These changes resulted in an unacceptably high rate of failure of the valve due to strut fracture (Davis *et al* 1985; Joyce 1990). In hindsight, it is clear that the design changes caused a considerable increase in the impact forces during opening/closing of the valve.

The Chitra tilting disc valve was developed to meet the ever increasing demand for artificial valves in India. The design philosophy was principally drawn from the well established models with a quarter-chord pivot axis location, free floating disc and entrance-exit curvatures of the cage ring. A plano-convex disc permitted a wider minor orifice. The device currently in multi-centric trials, has a hydraulic performance that is better than the standard Bjork-Shiley valve.

The experimental works of Pierce *et al* (1968) and Knight (1973) in the use of aerofoil shaped discs and the computer assisted study of McQueen *et al* (1983) have demonstrated the possibility of improving the performance by suitable choice of disc shape, pivot axis location and opening angle.

This study was thus aimed at optimising the tilting disc design and the parameters studied were :

1. **Radial location of the pivot axis -**
   Eight test valves with the pivot axis moved centrally by 0.5 mm starting from the standard quarter chord point.

2. **Disc sliding**
   Sliding of the disc downstream during opening.

3. **Disc shape**
   Flat, mesa-shaped, plano-convex, concavo-convex disc shapes.

4. **Opening angle - varied from 45^0 to 85^0.**

5. **Cage entrance & exit curvatures.**

In addition, the clinically proven valve models - the St.Jude, Medtronic-Hall, Bjork-Shiley Monostrut, Bjork-

Shiley Standard and the Chitra valves were also studied to obtain base line data for comparison.

A force transducer was designed for the measurement of drag and impact forces. A new pulse duplicator system with computer based data acquisition and control was developed for testing under steady and pulsatile flow conditions. A Pulsed Ultrasound Doppler Velocity meter (PUDVEL) was also set up for velocity profile measurements under steady flow conditions.

The results indicate that the best orifice shape is that of a flow nozzle with only an entrance curvature and a straight outlet. The present practice of providing a radius both at the inlet and outlet edges of the cage results in larger pressure drops.

The steady flow test showed that the centre of pressure, which is at the disc centre at closure moves towards the leading edge as it tilts open. For the plano-convex disc shape, the valve opens fully (75^0 max) when the pivot axis is located at less than 0.32 disc diameter from the leading edge. The opening angle progressively reduces when the pivot axis is moved more centrally. If the disc is allowed to slide 1 mm downstream during opening, then full opening is obtained with a pivot axis location at 0.34 diameter and opens to 65^0 when the axis is at 0.364 diameter. The disc shape has considerable effect on the location of the centre of pressure. A convexo-concave disc exhibits less movement (i.e., its centre of pressure remains nearer the disc centre) in comparison to the plano-

convex disc, thus permitting the use of a more central pivot axis at 0.385 diameters. This design did not work practically as the disc could escape upwards through the inlet side of the cage.

The studies on closing regurgitation and impact forces bring out the effect of valve orientation and disc material density. The change in pivot axis location or disc sliding did not result in any increase in either of these two parameters. Among the standard valves, the Bjork-Shiley Monostrut with the convexo-concave disc showed maximum impact forces and it was considerably larger than the earlier standard model. This was confirmed by using concavo-convex and plano-convex discs in one of the test valves.

Thus the optimum design seems to be a pivot axis location between 0.34 and 0.364 disc diameters for the plano-convex disc with 1 mm of sliding. Under pulsatile tests, these two valves showed comparable pressure drop, regurgitation and impact forces to those of the standard valves. Steady flow measurements indicate considerably improved flow through the minor orifice, which was also confirmed by the PUDVEL measurements.

In conclusion, it is clear the shape of the disc and the pivot axis location determine the maximum opening angle. An optimum choice ensures that impact forces and closing volumes are not increased. The elimination of the outlet curvature of the cage ring results in reduced

pressure losses. In the optimised design, the 1 mm downstream sliding of the disc ensures clearance between the cage and the disc edge in the open position. With these improvements, it is hoped that this new model of the Chitra valve will result in reduced incidence of tissue overgrowth and thrombo-embolism under clinical use.

REFERENCES

Davis K.M. *et al* (1985) Ann. Thorac Surg 40:66

Joyce C (1990) New Scientist 125:1709, 22

Knight C.J. (1973) The development of an artificial heart valve. Ph.D. thesis, University of Edinburgh

McQueen D.M. *et al* (1983) Computer-assisted design of pivoting disc prosthetic mitral valves. J Thorac Cardiovasc Surg 86:126-135

Pierce W.S. *et al* (1968) A hinged prosthetic cardiac valve fabricated of rigid components. J Thorac Cardiovasc Surg 56:229-235

Reul H *et al* (1986) Comparative in vitro evaluation of porcine and pericardial bioprosthesis. Z. Kardiologie 75, Suppl.2,223-231

Stevenson D.M. *et al* (1982) The Bjork-Shiley heart valve prosthesis - flow characteristics of the new 70^0 model. Scand J Thor Cardiovasc Surg 16:1-7

Yoganathan A.P. *et al* (1978a) Wall shear stress measurements in the near vicinity of prosthetic aortic heart valves. J Bioengineering 2:369-379

Yoganathan A.P. *et al* (1978b) The Bjork-Shiley aortic prosthesis: flow characteristics, thrombus formation and tissue overgrowth. Circulation 58:70-76

~~~~~~
~~~~~~

CHAPTER 1

INTRODUCTION

1.1 BACKGROUND

The era of prosthetic heart valves began in 1953, when Charles Hufnagel implanted a plastic caged-ball valve in the descending thoracic aorta to correct severe aortic insufficiency. In 1953, Gibbon had introduced an effective heart-lung machine and by 1960, the techniques of heart-lung bypass for open-heart surgery were well established. Valve replacement became a standard surgical practice with the introduction of the caged ball valves in the subcoronary position by Dwight Harken and mitral valve replacement by Albert Starr in 1960.

By mid sixties, hundreds of valve replacements had been performed in centres all over the world, mostly with the Starr-Edwards ball valve. Long term results were good with a significant improvement in the quality of life of the patients. Surgical techniques improved, operative mortality fell and a good database of experience was accumulated. The medical complications were better understood and the correct use of anticoagulants to minimise thromboembolism was well defined. Sophisticated experimentation with valve design, valve materials and surgical techniques started taking place.

In this search for better valves, two major categories evolved :

i. mechanical valves

ii. tissue or bioprosthetic valves

The most commonly used mechanical valves today are :-

a. the Starr-Edwards caged ball valve
b. the Bjork-Shiley and Medtronic-Hall tilting disc valves
c. St. Jude Medical bileaflet valve

The merits of the mechanical valves are standardised construction and excellent durability. The main disadvantage is the need for constant anticoagulation measures to counter the risk of thromboembolism.

Two major types of tissue valves have emerged - (a) the porcine valve and (b) the pericardial valve. The advantages of tissue valves are good resistance to thrombosis with minimal need for anticoagulation, near natural flow patterns and little regurgitation. The main drawbacks are limited durability, variability of construction and in young patients below 40 years, calcification and leaflet thickening leading to valve dysfunction in 2-5 years. This last point is of considerable importance in the Indian context, where the average age of patients needing heart valve replacements is in the third decade.

1.2 MATERIAL & FUNCTIONAL REQUIREMENTS

During this period of development, a set of material and functional requirements gradually evolved, which can be summarised as :

Biological and Chemical Requirements :

a. Biocompatible - should be non-toxic and inert.
b. Blood compatible - should not induce blood clot formation on its surface.
c. Degradation and corrosion resistance in the body environment.

Physical and Mechanical Requirements :

a. Should be sterilisable.
b. Should not absorb water or other body fluids and change size or shape.
c. Should have adequate wear resistance and fatigue strength to withstand the constant cycling of 38 million cycles per year for the life of the patient.

Functional Requirements :

a. The valve must respond to pressure changes quickly, both while opening and closing
b. While open, the valve should offer minimal resistance to the forward flow of blood.
c. While closing and while closed, the valve should permit minimal or no regurgitation of the blood.
d. The presence of the valve in the flow stream should not generate areas of stagnation or low velocity flow.

There is no such thing as a perfect valve today. Cardiac surgeons have to be educated about the advantages and

1.2 MATERIAL & FUNCTIONAL REQUIREMENTS

During this period of development, a set of material and functional requirements gradually evolved, which can be summarised as :

Biological and Chemical Requirements :

a. Biocompatible - should be non-toxic and inert.
b. Blood compatible - should not induce blood clot formation on its surface.
c. Degradation and corrosion resistance in the body environment.

Physical and Mechanical Requirements :

a. Should be sterilisable.
b. Should not absorb water or other body fluids and change size or shape.
c. Should have adequate wear resistance and fatigue strength to withstand the constant cycling of 38 million cycles per year for the life of the patient.

Functional Requirements :

a. The valve must respond to pressure changes quickly, both while opening and closing
b. While open, the valve should offer minimal resistance to the forward flow of blood.
c. While closing and while closed, the valve should permit minimal or no regurgitation of the blood.
d. The presence of the valve in the flow stream should not generate areas of stagnation or low velocity flow.

There is no such thing as a perfect valve today. Cardiac surgeons have to be educated about the advantages and

disadvantages of each type of artificial valve and trained to select the most appropriate replacement for each individual patient. A rule of thumb generally used world wide, is to use tissue valves in patients over 40 years of age (calcification occurs in younger age groups), in patients unable or unwilling to take anticoagulants and in women who wish to bear children. Mechanical valves are used for the remaining patients.

1.3 PROBLEMS OF PRESENT DAY PROSTHESES

Despite the extensive developments during the last three decades, problems continue to exist in all the current valve models. The most serious are :

a. thrombus formation and thromboembolism.
b. tissue overgrowth
c. red-cell destruction
d. damage to the endothelial lining of the vessel wall
e. valve failure due to material fatigue or breakage
f. tearing of sutures
g. infection.

The extensive velocity profile and shear stress measurements carried out using Laser Doppler Anemometry (LDA) during the last two decades by various workers have shown that the first four problems are directly related to the fluid dynamics associated with the various prosthetic heart valves.

Clinical results, flow visualisation studies and velocity profiles by LDA have demonstrated the correlation between tissue overgrowth and thrombus formation to regions of low velocity flow or areas of flow stagnation. In tilting disc valves,

the orifice is divided into two unequal parts by the eccentric pivoting of the disc. The smaller orifice is associated with this problem due to lower velocity of flow through it and the creation of a stagnation zone downstream of the valve. Thus the need to widen the smaller orifice and increase the flow through it has been clearly established.

Failure of the valve due to fatigue fracture or breakage has generally been attributed to inadequate design or poor choice of materials and the tearing of the sutures to poor surgical technique or tissue annulus related problems like calcification. But what is not obvious is that, the design of the valve, especially the design of strut cross-sections governed by fatigue strength considerations is not direct, as no data exists on the magnitude of the forces acting on these valves during the different phases of the cardiac cycle. Further, no method has been devised so far to determine these forces, at least under in-vitro conditions in a pulse duplicator. Clearly, an understanding of the fluid dynamic forces acting on the valve during its cycling will help minimise these two problems.

A clear example of the failure to understand the nature of fluid forces is the modifications carried out on the Bjork-Shiley tilting disc valve. Following Yoganathan's findings of increased thrombus formation and tissue overgrowth in the smaller orifice, this valve was redesigned in 1979 with a convexo-concave disc to increase the flow through the smaller orifice. The standard Bjork-Shiley at that time had a plano-convex disc with the inlet side convex. In the further hope of improving the fluid dynamics of the convexo-concave (C-C) model, the opening angle was

Figure 1.1

BJORK-SHILEY STANDARD & CONVEXO-CONCAVE VALVES

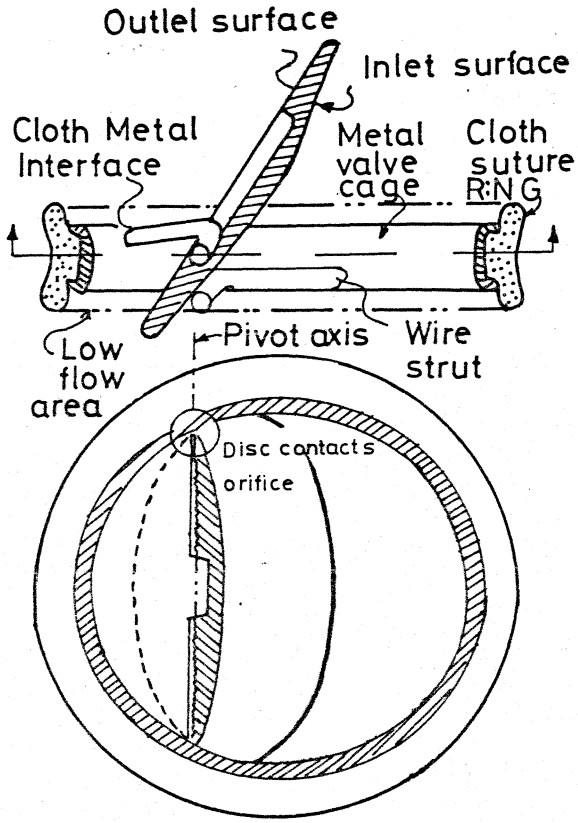

STANDARD DISC

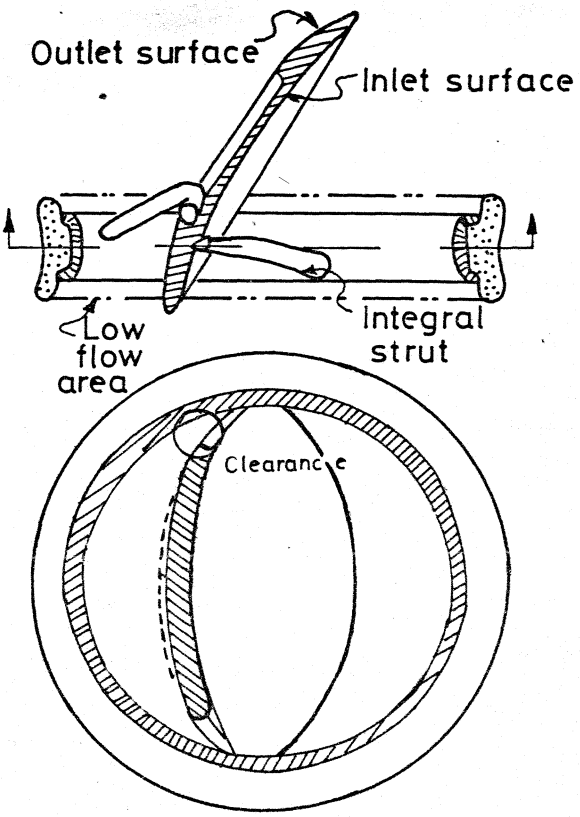

CONVEXO-CONCAVE DISC (60°)

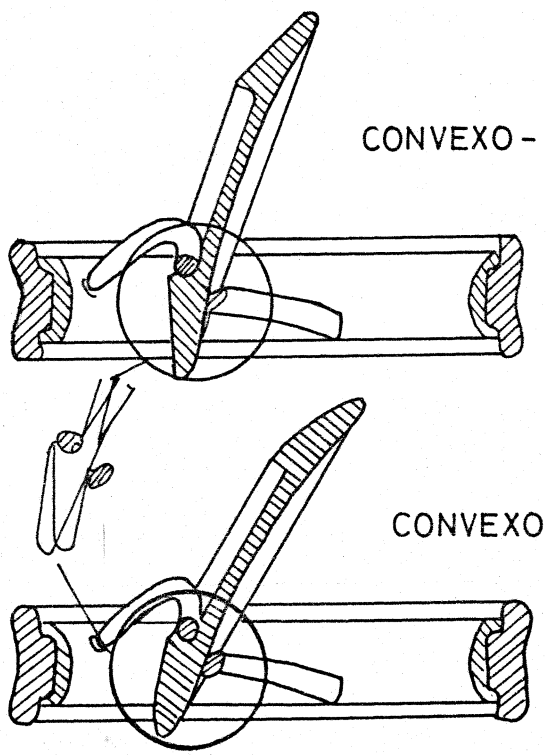

CONVEXO - CONCAVE - 70°

CONVEXO - CONCAVE - 60°

increased from 60^0 to 70^0. The changes are shown in **Figure 1.1.** These modifications did improve the fluid dynamics by reducing the size of the stagnation zone near the outflow face of the disc. During the following years of clinical use, over 300 fractures of the minor strut of this model occurred, especially in the larger 27 mm and 29 mm sizes.

At the outset, it is clear that the change in the disc shape increased the forces on the minor strut during the valve cycling and the stresses exceeded the fatigue limit of the welded joint. Though these design changes looked innocuous, the results were disastrous. This example clearly underscores the fact that there is a general trend to underestimate the importance of the complex fluid dynamic forces acting on prosthetic valves.

1.4 THE INDIAN PROBLEM

The population of India was 640 million and its 5-15 age group was over 200 million as per the census in 1981. The Indian Council of Medical Research (ICMR) had estimated that 6 out of every 1000 children in this age group were susceptible for rheumatic fever. Hence, the young population at risk for valvular heart disease was over 1.2 million then, and is increasing every year. According to the 1991 census, the population was 844 million and as a projection of the 1981 figures, the children at risk of valvular disease exceeds 1.5 million now. Clearly, prophylaxis at the community level is the ultimate answer to this enormous problem. Till such time, at

least for the next 3 to 4 decades, the demand for valve replacement will continue to be large and insistent. Due to the high cost of import, the development of an Indian valve thus became essential for the great majority of Indian patients. An inter-disciplinary effort to develop a prosthetic heart valve was thus started in 1976 at the Sree Chitra Tirunal Institute for Medical Sciences & Technology, Trivandrum.

1.5 DEVELOPMENT OF THE CHITRA TILTING DISC VALVE

The choice of the valve type was dictated by the demographic pattern of the patients and the need for a low profile model to suit mitral valve replacements in the small sized Indian hearts . The tilting disc design with its excellent hemodynamics suited the needs best.

The Chitra Valve in current clinical use is shown in **Figure 1.2.** The main features of this design are :-

a. Free floating disc of Ultra high molecular weight polyethylene (UHMW-PE).

b. Pivoted disc opening to 70^0 allowing almost central flow.

c. Non-seating disc helping to minimise blood damage and washing of the ring during the closed phase.

d. An integrally machined cage and struts of Haynes-25 alloy ensuring excellent fatigue strength and high surface finish.

e. Cage having entrance & exit curvature to help smooth entrance and exit of blood.

Figure 1.2

CHITRA HEART VALVE PROSTHESIS

In Chapter 3, a more detailed account of the development of the valve and the test systems are given. So far, the main efforts have been largely directed towards :

a. identifying suitable materials for the valve components.
b. developing fabrication techniques
c. developing test systems for the evaluation of the device performance - both in-vitro and in-vivo.

The clinical trial of the Chitra valve started in December 1990 and the performance has been good so far. The current expectation is that the performance will be similar to that of the Bjork-Shiley standard valve. Hence there is room for improvement.

1.6 AIM OF THE STUDY

Little work has been done till now towards experimentally optimising the design of the tilting disc valve. That such a study can lead to a better prosthesis is clear and therefore needed. However, any design changes introduced without understanding all the implications can at times be disastrous as shown by history. Hence the aim of this study was defined as :

1. Development of a technique for the measurement of forces acting on prosthetic heart valves in a pulse duplicator system as a prerequisite to understanding the effects of any design changes proposed.

2. Optimisation of the tilting disc valve from a fluid mechanical point of view based on :

   a. Minimisation of the steady flow pressure drop and drag forces.
   b. Maximisation of the minor orifice area to improve the flow through it.
   3. Minimisation of the pressure drop under pulsatile test in a pulse duplicator.
   4. Minimisation of the volume for valve closure.
   5. Minimisation of the impact forces during the valve closure.

The design parameters that could be varied to achieve this optimisation were :-

   i. Radial location of the pivot axis.
   ii. Shape of the disc.
   iii. Opening angle of the disc.
   iv. Bell-mouthing of the cage inlet and/or outlet edges.

1.7 OUTLINE OF THE PRESENT THESIS

This thesis is a record of an attempt to optimise the design of the Chitra tilting disc prosthesis. The investigation departed from the classical lines of academic research in that, it was directed towards a practical objective of achieving an improved model which could be commercialised. In pursuit of this aim, it was necessary to develop test methods to ensure a more rational and systematic design improvement, in order to avoid problems due to ad-hoc changes.

The account begins with a historical review of the development of valvular prosthesis in general and the tilting disc design in particular. From this emerges the fact that design

changes of clinical models have not resulted in improved clinical performance; but have resulted in serious failures. Hence, the need to understand the fluid dynamic forces at play during valve function became imperative. Further, the data on tilting disc valves clearly indicate the need to widen the minor orifice by moving the pivot axis or by choice of disc shape. This is followed by a short review of the fluid dynamic testing of prosthetic heart valves covering pulsatile testing and velocity profile measurements. One other problem that has recently come into focus is the possibility of cavitation, especially in mitral replacement. Another problem, which has not been investigated but could be a factor in valve thrombosis is the movement at the prosthesis-tissue interface. The last part of the review covers the major systematic attempt to improve the design of tilting disc valves. This section provided useful guidance for the design of this study.

The development work of the Chitra tilting disc valve, which forms the background to the present study is described in Chapter 3. The reasons for the choice of valve type and important design features are examined followed by a description of the search for suitable wear resistant materials, development of test systems and evaluation methods used.

Chapter 4 covers the aims of this study and the design of the experimental materials in detail. The design and development of a force transducer for the measurement of forces is described.

The fluid dynamic evaluation of the test valves and components under steady and pulsatile flow conditions are

covered in Chapters 5 and 6 respectively. From these test results, an optimum design emerges having improved function.

The improvements were evaluated by measuring the increase in flowrate through the smaller orifice and by determining velocity profiles, downstream of the valves. Chapter 7 covers this evaluation and the setting up of a pulsed ultrasound doppler velocimeter for this purpose.

The results of the study are summarised in Chapter 8. Its contributions and limitations are examined and further work that needs to be followed up are indicated.

The appendices cover the details of the design and calibration of various transducers developed and used in this study - force transducer, venturi flowmeter and pneumotachograph.

~~~~~~
~~~~~~

CHAPTER 2

REVIEW OF PROSTHETIC HEART VALVE DEVELOPMENT AND FLUID MECHANICAL STUDIES

2.1 HISTORY OF PROSTHETIC HEART VALVE DEVELOPMENT

Even as late as 1948, White stated that 'there is no cure for aortic valve disease itself' (White, 1948). Thus the development of prosthetic heart valves and surgical techniques for replacement covers a comparatively short period of time over the last four decades. During the early 1950s, Charles Hufnagel and Moore Campbell designed artificial valves made of Lucite tubes and spherical poppets (Campbell, 1950; Hufnagel, 1951). These devices used the caged ball valve principle commonly applied to soda-water bottle stoppers, which was well illustrated in 1858 by J.B.Williams in his patent application (Williams, 1858). Both implanted their valves in the descending thoracic aorta of dogs to improve the abnormalities due to aortic valve insufficiency. Campbell never implanted his valve in man. The era of prosthetic valves began on September 11, 1952 when Charles Hufnagel successfully implanted the first artificial valve into the descending thoracic aorta of a patient with severe aortic regurgitation (Hufnagel & Harvey, 1953).

In 1954, John Gibbon created a landmark in the field of medicine by his first successful use of total cardiopulmonary bypass for intra-cardiac surgery in man (Gibbon, 1954). In the following years, heart lung bypass was applied for the repair of congenital defects, open valvular commissurotomy and other valve repair procedures (Lefrak & Starr, 1979).

During the later half of 1950s, a number of leaflet type prostheses made of silastic, pericardium, teflon, dacron, polyurethane etc., mimicking the natural valves were tried. However, the leaflets tore, separated from the annulus or became rigid due to fibrous tissue ingrowth.

In 1960, Dwight Harken reported the survival in two of the seven patients in whom he had implanted a caged ball valve in the subcoronary position for severe aortic insufficiency (Harken *et al.*, 1960 & 1961). On September 21, 1960, Albert Starr performed the first long term successful mitral valve replacement with a caged ball valve (Lefrak & Starr, 1979). During the following 5 years, thousands of Starr-Edwards mitral and aortic valves were implanted throughout the world with good overall results. The ensuing decades witnessed the constant efforts toward improvement of this model and the development of several new synthetic and tissue prostheses.

Lefrak & Starr (1979) have traced the numerous developments of the caged ball, caged disc and other mechanical prostheses in detail. The following paragraphs briefly cover the major developments and modifications of these models as reviewed by these authors.

The first major modification of the ball valve was by Smellof and his associates to improve its hemodynamics. This valve consisted of an integral titanium cage and a silicone rubber ball. Unlike the Starr valve, the orifice was slightly larger than the ball diameter. This full orifice construction allowed a larger orifice diameter and also a smaller ball resulting in reduced pressure drops.

During the 1960s, valve replacement carried with it a high operative risk, due primarily to technical problems of implantation and myocardial ischemic injury associated with prolonged aortic cross-clamping. As a possible solution to this problem, Magovern and Cromie devised an ingenious automatic fixation mechanism to allow the rapid and secure implantation without the need for sutures. Interest waned in this design when myocardial protection techniques improved to a level of safety that outweighed the added risks associated with this valve; i.e., an increased incidence of perivalvular leak and postoperative thromboembolism.

Following the initial success, the caged ball design gained wide acceptance and use. However, little was known concerning the early and late risks that were to be faced and it was difficult to distinguish the valve related complications from the patient related ones. Many early deaths were attributed to outflow tract obstruction while some late deaths were ascribed to ventricular fibrillation induced by septal irritation by the cage apex rubbing against it. Some autopsy specimens demonstrated bulky and oversized ball valves projecting into a contracted left ventricular cavity, proving this point. This

resulted in a search for a low profile prosthesis in the mid 1960s.

Charles Hufnagel and Conrad described a polypropylene and silicone rubber caged disc valve. Similar disc valves were designed and used by many others. The notable ones are the Cross-Jones, Kay-Shiley, Harken-Cromie, Beall-Surgitool, Starr-Edwards and the Cooley-Cutter valves. Gott designed a hinged butterfly type of valve and Barnad and Goosen employed flat and cone-shaped poppets, while Juro Wada reported the implantation of the earliest tilting disc valve in man.

The early clinical trials established the vulnerability of these caged disc valves to catastrophic malfunction, high pressure drops and thrombus formation behind the disc. The discs had a high propensity for degradation, wear and to get stuck due to small thrombi on the struts.

Extensive in-vitro and in-vivo testing was carried out to find a compatible combination of cage and disc materials by the Starr-Edwards group for a caged-disc valve. The first model using a hollow Stellite 21 disc and cage eliminated the problem of edge wear. However, the incidence of thromboembolism was higher than with ball valves and the hydraulic function was poorer. As with all disc valves, there was a significant incidence of thrombotic entrapment of the disc. In-vitro wear testing of 14 different polymers to determine the best abrasion resistant material revealed Hifax (UHMWPE) and Delrin (acetal homopolymer) to be superior to the others in wear resistance. Because of the possibility of water absorption by Delrin, Hifax was chosen. However, due to poor hemodynamics and higher incidence of

thromboembolic complications, this model soon fell into disuse with the introduction of the tilting disc valves towards the end of the 1960s.

2.2 DEVELOPMENT OF TILTING DISC VALVES

The earliest attempt at the development of a tilting disc valve is reported by Frater & Ellis (1961). Their eccentrically hinged valve in animal studies became clogged with thrombi and was not tried in man. In 1967, Juro Wada introduced his so called 'hingeless' valve using a notched Teflon disc, which engaged in an another pair of notches in the cage (Wada, 1967). The effective tilt axis was placed at one-third of the diameter. He reported that there was no improvement in the pressure drops measured beyond 75° opening angle . The stepped occluder with notches was not free to rotate. This design permitted a large orifice diameter to be used when compared to equal sized ball and caged disc valves, thus reducing the forward pressure drops considerably. Clinical data during the next couple of years indicated catastrophic thrombus formation around the notches and wear of the teflon disc leading to severe valvular regurgitation or fatal disc embolization (Bjork, 1970).

Pierce *et al.*(1968) have reported the development and experimental evaluation of a hinged valve. The design was unique in many ways. The tilt axis located at 0.36 of the diameter from the leading edge of the disc (major and minor segments in the ratio of 1.75:1) was more centrally placed by present day standards. The initial model with a disc of uniform

thickness opened only to 45° under steady flow. The opening angle was improved by using an aerofoil cross-section for the disc, which provided lift forces. They have also reported that varying the location of the pivot axis altered the opening angle. This probably is the first report on the application of aerofoil shapes to heart valve design. Flow visualisation showed that the flow through the major orifice was laminar while that through the minor orifice was turbulent. In animal evaluation, tissue overgrowth was a major problem, which was reduced by anticoagulation, hinge modification and an improved sewing ring.

From these studies, it became clear that any type of hinge created an area of low flow and stasis, which led to thrombus formation around it. Hence, the need was to do away with the hinge and make the disc free floating.

The quest for a valve with optimal hemodynamics inspired Bjork to analyze the cardiac catheterisation data on early caged-ball and disc valves (Rodriguez, 1970; Bjork *et al.*, 1969). He switched over to the Wada-Cutter valve impressed by its low pressure drops. In patients, the mean pressure drops were much lower. However, catastrophic thrombosis and wear of the Teflon disc led to the abandonment of the device. He then collaborated with Donald Shiley to develop a new tilting disc valve.

The year 1969 saw the introduction of two truly hingeless free floating disc valves - the Bjork-Shiley (Bjork, 1969) and the Lillehei-Kaster (Kaster 1969). The Bjork-Shiley valve made use of a depression in the disc and two welded wire struts in the cage to retain the disc. This permitted the disc to tilt open and close, while it was free to rotate around its centre. The

Lillehei-Kaster valve used a pair of projecting arms on the outlet side and a pair of stubs on the inlet side to retain and allow the disc to tilt and rotate freely as well. The free rotation of the disc distributed the wear on the complete surface of the disc and allowed it to be washed well at the same time. This prevented thrombus build up on the disc.

The Bjork-Shiley valve used a Stellite-21 welded cage, a Delrin disc and a Teflon sewing ring. A couple of years later, the disc material was changed to Pyrolytic carbon as Delrin has a propensity to swell during autoclaving (due to water absorption) (Bjork, 1972a & 1972b). During the 1970s and early '80s, the Bjork-Shiley valve became the most widely used mechanical valve in the world.

The main features of these tilting disc valves compared to the caged ball and disc valves were :

a. a large orifice diameter for a given tissue annulus diameter resulting in very low pressure drops.

b. with an opening angle of 60° or more, the flow was more central.

c. the disc free to rotate around its centre thus preventing any build of thrombus.

In 1977, the Hall-Kaster valve (presently called the Medtronic-Hall valve) came into clinical use. This tilting disc valve had a disc of pyrolytic carbon with a central hole and corresponding struts to retain it in place. The disc pivot axis was more central than in the Bjork-Shiley valve. Also, in its pivoting action, the disc was allowed to slide downstream by

about a millimetre (Medtronic Blood Systems, 1980). The clinical results have been good and the valve has become more popular due to problems associated with the later models of the Bjork-Shiley valve.

A major complication with tilting disc valves has been the tendency for tissue overgrowth and thrombus formation near the smaller orifice leading to inadequate opening of the disc or lack of complete closure (Yoganathan *et al.*, 1978a). Many flow visualisation studies have demonstrated that flow through the major orifice is streamlined while that through the smaller orifice is of lower velocity and more disturbed (Pierce *et al.*, 1968; Bjork & Olin 1970; Valiathan *et al.*, 1978; Yoganathan & Letzing, 1983).

These disadvantages of the tilting disc valve saw the introduction of the bileaflet St. Jude valve in 1978 (Emery *et al.*, 1978a & 1978b; Emery & Nicoloff, 1979; Hehrlein *et al.*, 1980). With two nearly semi-circular tilting flaps, the valve orifice is divided into three regions with more central and symmetrical flow profiles. In the meantime, the disc of the Bjork-Shiley valve was redesigned following Yoganathan's report (Yoganathan *et al.*, 1978a; Bjork, 1978). The new disc had a Convexo-Concave (C-C) shape and was aimed at increasing the minor orifice area as shown in Fig.1.1. This did result in a reduction in the size of the stagnation zone behind the disc (Yoganathan *et al.*, 1980). In the further hope of improving the fluid dynamic characteristics, the opening angle of this C-C valve was increased from 60° to 70° and this did achieve the desired result (Stevenson *et al.*, 1982). However the changes

proved disastrous in other ways. The minor struts of the C-C valves fractured in over 300 patients (Davis *et al.*, 1985; Joyce, 1990; Fielder, 1991), especially in the larger sized valves of 27 mm and 29 mm leading to a Food & Drug Administration (FDA) Class I recall (Biomedical Safety & Standards, 1986). Bjork and colleagues have reported on one of the largest series of 3334 Bjork-Shiley valve replacements of different models over a 15 year period. In this series, they experienced 18 failures out of 1461 C-C valves implanted (Lindblom *et al.*, 1986).

It is now clear that the change in the disc shape was the culprit. The indications are that the changes resulted in a considerable increase in the impact forces on the minor strut, leading to the stresses exceeding the fatigue limit of the welded joint.

That this failure could happen, even though this design went through all the mandatory testing as specified by the Food & Drug Administration (FDA) of USA, indicates a serious gap in the testing of mechanical valves and understanding of the fluid dynamic forces involved. A system to measure the forces acting on the valve could probably have brought out the considerable increase in impact force caused by the change in the disc shape. FDA in its recent requirements for prosthetic valves has recommended Finite Element Modelling and individual fatigue testing of cage struts. However, the magnitude of the forces to be applied during the modelling/test has not been specified (Food & Drug Administration, 1990).

2.3 FLUID MECHANICAL TESTING

During the last three decades of heart valve development, a number of fluid mechanical systems have been developed and studies performed. Table 2.1 lists in chronological order the important studies in this area. The early studies were mainly on the measurement of pressure drops, regurgitation and flow visualisation. During the last decade there has been a considerable amount of test data generated on the prosthetic valve performance with the use of Laser Doppler anemometry (LDA) first by Yoganathan (Yoganathan *et al.*, 1978a) and followed by Reul, Chandran, and others (Hwang *et al.*, 1979; Affeld *et al.*, 1979; Philips *et al.*, 1980; Chandran *et al.*, 1983a & 1983d).

The introduction of the Wada-Cutter, Bjork-Shiley and Lillehei-Kaster tilting disc valves in the late 1960s saw a considerable reduction in the forward pressure drops. Studies by Knight (1973), Gentle (1977), Yoganathan *et al.*, (1979a) and others have shown that :

> ***The pressure drop across a circular orifice is inversely proportional to the fourth power of its diameter.***

Hence, the valve should be designed with as large a flow area as is possible subject to the design of the sewing ring and cage. This point immediately explained the considerable improvement in the performance of the tilting disc valves in comparison to the ball and caged disc valves. These tilting disc valves had relatively thin sewing rings and cage cross-sections and therefore comparatively larger orifice areas.

Table 2.1
Major Fluid Mechanical Studies

Sl.No	Investigator	Year	Type of Study
1.	Smeloff et al	1966	Pressure drop, retrograde flow & flow visualisation.
2.	Weiting	1969	Velocity measurements using photographic technique. Also pressure drop & flow visualisation.
3.	Duff	1969	Pressure drop, retrograde flow.
4.	Kaster et al	1970	Pressure drop, retrograde flow & flow visualisation
5.	Bjork & Olin	1970	Pressure drop, retrograde flow & flow visualisation
6.	Swanson	1972	Flow visualisation & pressure drop
7.	Wright et al	1971	Pressure drop and flow visualisation
8.	Black et al	1976	Pressure drop & regurgitation
9.	Gentle	1977	Pressure drop
10.	Yoganathan et al	1978	Velocity profiles & shear stress by LDA. Pressure drop, regurgitation & flow visualisation
11.	Reul et al	1979	Pressure drop, regurgitation, velocity profiles & shear stress by LDA
12.	Chandran et al	1983	Flow visualisation, velocity profiles & shear stress by LDA

Knight (1973) in addition points out that the performance of the valve orifice could be further improved by having :

a. Sufficient length in the flow direction to permit good 'fairing' of the orifice section, subject to the condition that it does not foul with the myocardium.

b. Freedom from abutments or strut projections into the flow stream.

Pulse duplicator testing during the late 1970s and 1980s have brought out the additional facts on tilting disc valves :

(a) Forward pressure drops can be reduced by increasing the opening angle of the disc.

(b) Increased opening angles lead to increased closing volumes due to the larger sweep of the disc.

(Knott *et al.*, 1988; Willshaw *et al.*, 1986)

In clinical situations of high heart rate and low cardiac outputs, the second point above can be dangerous as the reflux volume can form a significant part of the cardiac output (Yoganathan & Letzing, 1983).

i. Flow Visualisation Studies on Tilting Disc Valves :

In-vitro visualisation of the velocity profiles and their measurement in the near vicinity of prosthetic valves have been studied by many workers in order to understand their effect on the performance of the valves. One of the earliest was by Leyse *et al.* (1961), who used a birefringent 1% bentonite suspension in a glycerine-water mixture and illuminated the particles using polarised light. Weiting *et al.*, (1969) have reported that dye, india ink, aluminium particles & hydrogen bubble have been tried before. Even kitchen pepper has been used to visualise the flow patterns and photograph them using both still and high speed cine cameras (Wada, 1969). The first report of flow visualisation on a tilting disc valve was by Pierce *et al.* (1968) who also used the birefringent 1% bentonite

suspension in a glycerine-water mixture technique. They have reported that the flow through the major orifice of their hinged valve was laminar while that through the minor orifice was turbulent. Although these investigations made it possible to observe qualitatively areas of stagnation or stasis and turbulence in a random flow situation, they did not provide quantitative measurements of velocity magnitude and direction at points of interest within the flow field. Therefore, it was not possible to calculate the shear stress or to predict blood-wall interaction, parameters of interest in hemolysis and thrombosis.

The next major study was by Weiting (1969) who measured velocities using suspended polystyrene particles and a narrow beam of light to illuminate them. This resulted in a two-dimensional flow pattern being seen in the tracer particles suspended in the fluid. He used test chamber geometries to provide cross-sectional areas 30 mm proximal and distal to the valve, analogous to such areas in the human heart by obtaining RTV silicone rubber casts of natural human hearts. The velocities were calculated from the streak lengths of the particles in photographs of the flow profiles (Weiting et al., 1969). This technique of lighting and flow visualisation has subsequently been used by many workers (Wright & Temple, 1977; Valiathan *et al.*, 1978; Yoganathan & Letzing, 1983; Chandran *et al.*, 1983c). The photographic technique has many drawbacks. Weiting (1969) was unable to measure velocities immediately distal to the valve. His nearest measurement was 51 mm downstream

from the valve. Nearer the valve, the flow was too turbulent for good measurement.

ii. Velocity Profile & Turbulent Stress Measurements :

Velocity profile and turbulent stress measurements have been carried out using hot-wire and hot-film anemometers (Swope & Falsetti, 1976; Figliola & Mueller, 1977; Chandran *et al.*, 1983b). The hot-wire or film was mounted on a probe and inserted into the flow stream. The velocity profile could be determined by moving the probe across a diameter of the flow channel and taking measurements at various points. However, the probe itself disturbed the velocity field in its vicinity leading to errors (Affeld *et al.*, 1976). These techniques also have the disadvantage of low signal/noise ratio, low frequency response, need for frequent calibration & more importantly, lack a directional signal for identifying forward or reverse flow. (Yoganathan *et al.*, 1979).

Laser Doppler Anemometry (LDA) has been used by several workers during the last 15 years to determine the velocity profiles in the near vicinity of prosthetic heart valves, both in steady flow and pulsatile flow (Yoganathan *et al.*, 1979; Hwang *et al.*, 1979; Chandran *et al.*, 1983d; Bruss *et al.*, 1983). The main advantages of LDA are :

(a) requires no probe to be inserted into the flow field.
(b) requires no calibration
(c) has a high signal/noise ratio
(d) can be used very close to the walls of the flow channel
(e) has a high frequency response ($>10^5$ Hz)
(f) can distinguish between forward and backward flow.

Early velocity profile measurements using LDA were performed under steady flow conditions (Yoganathan *et al.*, 1978a,

1979) and later extended to pulsatile conditions (Hwang *et al.*, 1979; Yoganathan *et al.*, 1979a). In the 1980s, the introduction of three beam LDA enabled the measurement of both the axial and radial velocity components (Woo & Yoganathan, 1986, 1986a) and the calculation of turbulent shear stresses.

These measurements clearly highlighted the stagnation zones and areas of high turbulent stresses. Improved designs of tilting disc valves like the Medtronic-Hall, Bjork-Shiley monostrut, Omni-carbon etc., have clearly superior hemodynamic performance compared to the earlier generation of tilting disc valves (Yoganathan *et al.*, 1988). However, all these valves still continue to create regions of flow separation or stagnation and elevated turbulent shear stresses around 1000 dynes/cm^2, which can cause lethal or sublethal damage to blood elements. According to Yoganathan *et al.* (1988), these newer designs are unlikely to eliminate the problems of thrombosis, complications of thromboembolism and hemolysis. Whether these problems of thrombosis, thromboembolism and tissue-overgrowth are only due to these fluid dynamic factors or are related to other factors also, is still not understood.

The work of Yoganathan *et al.*, (1978a) on the Bjork-Shiley aortic valve, correlating clinical findings of thrombus formation and tissue-overgrowth to areas of low flow brought new insights. In the Bjork-Shiley type of tilting disc valves, the disc in the open position divides the orifice into two unequal regions. LDA studies have shown that the velocities in the smaller or minor flow region of these valves are much lower. Clinical data clearly show that these minor flow regions are maximally prone for

tissue overgrowth and thrombus formation. These overgrowth encroaching into the smaller flow area reduce the flow further leading to a vicious cycle which ends in valve failure. This data indicated the need to widen the minor orifice of tilting disc valves and increase the flow through it.

LDA studies of mechanical valves in general indicate that the high turbulent shear stresses observed with the prosthetic valves in use today could lead to sublethal or lethal damage to red blood cells and platelets. Current clinical data from the use of these valves do not indicate blood damage of clinical significance. However, valve thrombosis, thromboembolism and tissue overgrowth continue to be the major complications in the use of mechanical valves despite permanent anticoagulation therapy. It is possible that these problems are triggered by the sublethal damage to the blood cells.

2.4 CAVITATION

Graf *et al.* (1991) have reported from in-vitro studies that cavitation could also be a problem associated with prosthetic valves just like engineering check valves. Cavitation may primarily occur in the mitral position due to the water-hammer effect leading to high mechanical stresses in the valve itself and of blood cells. They studied ten different models of mechanical heart valves in the mitral position of a pulse duplicator by cinematographic techniques. All these valve prostheses showed cavitation up to a ventricular pressure gradient of 5000 mmHg/s; the threshold depended on the valve

type and in some, were within the physiological range below 2000 mmHg/s. They have suggested that vapour cavitation may be an important factor for material and blood damage. The results also indicate that valve models with the lowest leakage rates commonly have the lowest cavitation thresholds, indicating that tight sealing at valve closure promotes the generation of high negative pressures downstream of the sealing area.

In tilting disc valves, by slowing down the disc towards the end of closure can reduce this effect of cavitation as well as reducing the impact forces. This study also indicates that reducing the leak during the closed phase of the valve to very low levels may not be advisable from this point. An engineering compromise may be necessary between this factor and the physiological need to have zero leak.

2.5 MOVEMENT OF PROSTHESIS - TISSUE INTERFACE

Whalen (1983) has demonstrated using a series of experiments involving an intracorporeal compliance chambers that relative movement between a smooth surface implant and the encapsulating tissue around induced mechanical trauma to the healing tissue. This trauma resulted in an inflammatory reaction leading to increased tissue growth and vigorous encapsulation.

In the case of prosthetic heart valves, there is a junction between the fabric sewing ring and the highly polished metal or carbon cage which is exposed to blood. Normal healing on the sewing ring fabric usually extends up to this junction. However, in areas of low velocity flow, there is a tendency for the

tissue to overgrow and push into the orifice (Yoganathan *et al.*, 1978a).

In pulse duplicator studies and accelerated testing, one can clearly observe that during valve closure, the closing impact force pushes the valve cage back resulting in a small relative movement at the sewing ring-metal interface. It seems possible that the periodic relative movement between the edge of the polished cage and the edge of the healing tissue on the fabric could be one of the causes for tissue overgrowth. Reduction of impact forces, especially during valve closure could thus help reduce this relative movement and probably lead to a reduced tissue overgrowth.

2.6 DESIGN OF TILTING DISC VALVES

i. Requirements :

The basic fluid mechanical requirements of a prosthetic heart valve can be summarised as :

(i) minimum total pressure drops across the valve during its opening and open phase.

(ii) minimum total regurgitation during its closing and closed phases.

(iv) minimum areas of low or static flow during the forward flow to minimise thrombus formation and tissue overgrowth.

(v) minimisation of forces acting on the valve to reduce the incidence of mechanical failure, wear, tearing of sutures and blood damage.

The review of literature in the previous sections on fluid mechanical testing of tilting disc valves shows that these design requirements can be simplified as :

(a) maximum orifice area for a given tissue diameter with minium allowance for sewing ring and the cage wall.

(b) good 'fairing' of the cage orifice to minimise pressure drops and flow separation.

(c) optimisation of the disc shape, pivot location and opening angle to minimise flow separation, regions of stagnation and wall shear stresses.

(d) minimisation of impact forces during the opening and closing of the valve to minimise the probability of fatigue fracture and reduce wear, tearing of sutures, tissue overgrowth, thrombo-embolic complications, blood damage and effects of cavitation.

(e) Cage and disc shapes which can be practically realised using the very few blood compatible and wear resistant materials available for prosthetic valve fabrication today.

Pierce *et al.*(1968) have reported the earliest attempt to optimise the design of a tilting disc valve. In their design, the pivot axis was located at 0.36 disc diameters from the leading edge and the initial model with a flat disc opened only to 45° in steady flow test. By using aerofoil shapes for the disc, they could get the valve to open up to 75°. They have also reported that the opening angle was dependent on the location of the pivot axis and the opening angle could be increased for the same disc by moving the pivot axis away from the centre of the valve. However, the optimum location of the pivot axis was not studied in detail. The use of a hinge resulted in thrombi around it in animal implants and the valve development does not seem to have been pursued further.

There is hardly any data on how the design of the first models of tilting disc valves, viz., the Wada-Cutter, Bjork-Shiley and Lillehei-Kaster were arrived at. The opening angles of both

the Wada-Cutter and Bjork-Shiley valves were optimised from steady flow experimental data (Wada *et al.*, 1969: Bjork, 1969). Wada *et al.*, (1969) state that an eccentric axis of one third the disc diameter gave the best flow characteristics. The basis for the pivot axis location of the other models are not available in literature. The pivot location and shape of the disc were apparently chosen from the use of general engineering principles. However, they have incorporated a few of the design principles like maximising orifice area and minimising disc thickness.

So far, there has been little experimental study to optimise the design of the tilting disc valve in terms of all the requirements cited earlier. There have been two notable efforts in this direction to use fluid mechanical principles to optimise valve design as indicated in the following sections.

2.7 THE EDINBURGH AEROFOIL VALVE

The first effort in this direction is the work of Macleod and associates at Edinburgh during the 1970s (Macleod *et al.*, 1976 & 1977; Knight *et al.*, 1977; Turina & Macleod, 1975; Knight, 1973). The main design criterion initially adopted for this model was that the disturbance to forward flow should be minimal (the requirement for valve closure was not identified). The best design to achieve this was felt to be a pivoted disc arrangement with no obstruction to the flow field other than the disc and its housing. The design was based on the premise that a pivoted disc will not open fully unless the pivot axis was located very asymmetrically and such asymmetry would cause a

considerable disturbance to the flow field. This premise was validated later by the LDA studies of Yoganathan & others. This problem was overcome by using an aerofoil shaped disc occluder which enabled the valve to open very nearly to 90° with the pivot axis only slightly eccentric from the centre.

Despite the improved disc shape, more central pivot location and absence of projecting struts in the flow stream, the valve showed high pressure drops. Modifications to the cage profile from conical to a hyperboloidal shape resulted in a very much thinner cage cross-section leading to similar performance with the standard Bjork-Shiley valve (Macleod *et al.*, 1976).

Though there are no projecting struts in the flow field in this design, the very thick 'faired' leading edge of the aerofoil disc seems to cause sufficient flow obstruction to nullify the gain of the large opening angle and improved flow profiles. Further the regurgitation of this valve is comparable to the Bjork-Shiley despite the fact that there is no leak on closure. This indicates a large closing volume probably due to the large opening angle and more central pivot axis. Hence this parameter has not been considered for optimisation in the design.

The complexities involved in the fabrication of the complex shaped disc and the hyperboloidal bore of the cage to the required tight tolerances has probably been one deterrent in its commercialisation. Further the need for a hinge and the absence of disc rotation was probably the second deterrent in view of the history of thrombus formation and disc immobilisation in such configurations.

2.8 COMPUTER ASSISTED DESIGN

The second notable effort has been by McQueen & Peskin (1983, 1985), who have carried out computer assisted mathematical simulation of the performance of flat and curved pivoting disc and bileaflet mitral valves. Simulated prosthetic heart valves were evaluated in a computer test chamber with contractile walls that model the left side of the heart. The model was two dimensional and the Reynolds number was artificially reduced by a factor of 25 (Peskin, 1977; Peskin *et al.*, 1980). The design parameters considered were the radius of curvature of the occluder and the position of the pivot axis. The performance criteria were the net stroke volume, the mean forward pressure drop and the peak velocity in the minor orifice region.

Their study on tilting disc valve has indicated that the best overall valve has a disc with a radius of curvature equal to 1.5 times the diameter of the occluder and a pivot point located at 0.39 mitral ring diameter from the anterior border of the mitral annulus with a maximum opening angle of about 70°. The detailed analysis obtained by computer simulation is very interesting. However, as noted by the authors themselves, it is important to keep in mind the principal limitations of the study, namely :-

(a) mathematical model was two dimensional.
(b) the Reynolds number was artificially low.
(c) the model did not take into the account the physical dimensions of any clinical valve in use.
(d) the valves were tested under a fixed set of conditions - resting conditions of a canine heart.

(e) the sliding of the disc during opening and closing was not considered.

This simulation can therefore mainly be a useful guide for an experimental study aimed at improving the design of tilting disc valves.

An important fact to be noted is the absence of any report on the measurement of impact forces acting on heart valves and the study of the closing mechanics of valves, till very recently (after the present study was completed). Chang *et al.*, (1992) have presented data on the effect of sewing ring compliance on impact force and closing mechanics of the Duromedics valve.

2.9 SUMMARY

Despite extensive development during the last three decades, problems continue to exist with all current artificial heart valves. Thrombus formation, thrombo-embolism and tissue overgrowth are the major complications of mechanical valves. Some authors contend that these problems of mechanical valves are directly related to the fluid dynamics of the valves. In tilting disc valves, the orifice is divided into two unequal parts by the eccentric pivoting of the disc. It is clear that the smaller orifice is associated with the problem of tissue overgrowth due to the lower velocity of flow through it and the creation of a stagnation zone downstream of the disc. In an attempt to mitigate this problem, the Bjork-Shiley valve was redesigned with a convexo-concave disc and an opening angle of

70° to widen the smaller orifice. These changes resulted in an unacceptably high rate of failure of the valve due to strut fracture. In hindsight, it is clear that the design changes caused a considerable increase in the impact forces during closing of the valve. This clearly shows the tendency to underestimate the importance of the complex fluid dynamic forces acting on prosthetic valves and the need to develop a technique for measuring these forces, at least under in-vitro conditions.

The occurrence of cavitation under in-vitro test conditions in the mitral position has been demonstrated recently. Whether cavitation can occur under in-vivo conditions inside elastic chambers is still debatable. Another problem, which has not been investigated but could be a factor in valve thrombosis is the movement at the prosthesis-tissue interface. Both these are linked to the closing impact force as they occur at the instance of valve closure.

The experimental works of Pierce *et al.* (1968) and Knight (1973) in the use of aerofoil shaped discs and the computer assisted study of McQueen & Peskin (1983) have demonstrated the possibility of improving the performance by suitable choice of disc shape, pivot axis location and opening angle. These studies provide the basic information for a more detailed study aimed at improving the design of a tilting disc valve.

~~~~~~
~~~~~~

CHAPTER 3

DEVELOPMENT OF THE CHITRA VALVE PROSTHESIS

A design optimisation study aimed at improving an existing heart valve model has real significance, only when the improved version can be further developed and evaluated to realise a clinically usable model. A heart valve prosthesis must satisfy various material and functional requirements as listed in §1.2. Once the design is optimised, a considerable amount of work in terms of durability testing, animal evaluation and clinical trials needs to be carried out before regular clinical use can commence.

In this chapter, the reasons for the initial choice of Chitra valve type and some of the important design features are examined. This is followed by a description of the search for a suitable wear resistant material combination and the test methods developed. The author has been a principal contributor to the design and development of the Chitra valve and it is mainly this contribution that is brought out in this chapter. Further, incorporation of possible improvements in the basic design of the Chitra valve has been the main motivation for the fluid mechanical studies described in subsequent chapters.

3.1 CHOICE OF DESIGN AND MATERIALS

i. Choice valve type :

The choice of valve type was a major consideration. With the majority of our patients below 30 years and the poorly organised beef and pork industries in India, the choice was limited to a mechanical valve. Among the mechanical designs, the choice was again narrowed down to the time tested ones, viz., the CAGED BALL, CAGED DISC and the TILTING DISC [1]. With mitral valve replacements being more in number, the caged-ball design with its high profile had to be dropped. Between the other two, the tilting disc with its superior hemodynamics (lower pressure drops, more central flow and lower incidence of thrombo-embolism) was considered a better choice.

ii. Design Features :

The Chitra Valve in current clinical use is shown in Figure 3.1. At the beginning, the basic design features of the Chitra Tilting disc valve were drawn from the established designs like the Bjork-Shiley and the Lillehei-Kaster valves. They were :

a. Free floating disc :

The disc was designed to be free floating and able to rotate on its centre to avoid the problems of thrombosis around a hinge and to distribute the wear over the surface of the disc.

---

[1] **Note:** The bileaflet valve model was not considered at that time as it was not in clinical use then.

Figure 3.1

CROSS-SECTION OF CHITRA HEART VALVE PROSTHESIS

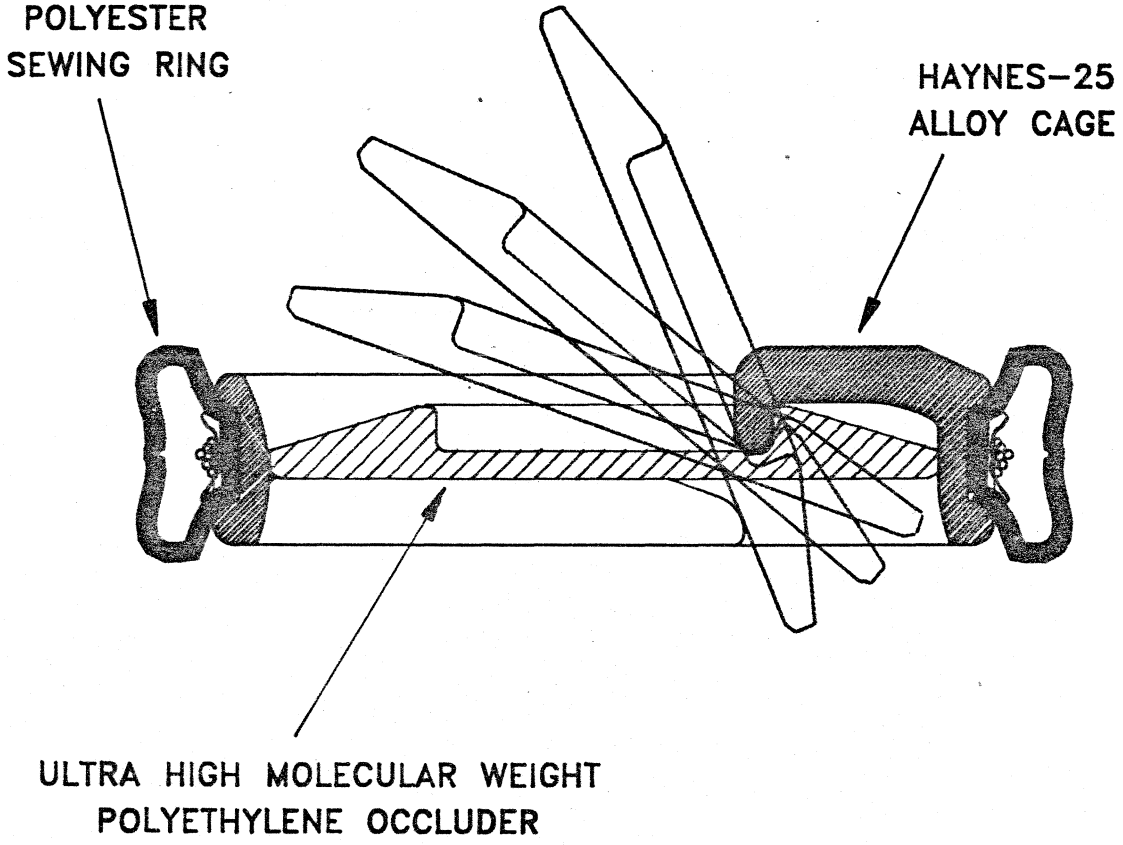

b. Pivot Location :

The tilt axis of the disc was retained close to the quarter chord point, i.e., at one-fourth the diameter of the disc.

c. Cage Entrance & Exit curvature :

Both the inlet and outlet edges of the valve cage were bell mouthed to permit smooth entrance and exit of blood, thereby minimising the resistance to flow.

d. Disc Shape :

A plano-convex shape with the inlet side flat was chosen for the disc to :

(1) increase the inflow area into the minor-orifice thereby increasing the flow through it.

(2) make the fabrication of the cage and disc easier.

e. Opening Angle :

A 70° opening angle was chosen to achieve reduced pressure drops and more central flow.

f. Cage Structure :

An integral cage design was arrived at, with the struts being machined integral with the ring from a solid block. This particular design enabled the integral machining of the cage with the indigenous capability at that time without the need for expensive CNC machines.

iii. Materials :

During the last one and half decades of mechanical valve development, three combinations of materials have been tried for the cage and disc as listed in Table 3.1

Table 3.1
Materials used in the different models of the Chitra valve

Valve Model	CAGE		DISC		SEWING RING
	Material	Fabrication	Material	Fabrication	
1.	Titanium	Integral major strut; Electron beam welded minor strut.	Polyacetal (Delrin)	Injection moulded	Polyester knitted fabric
2.	Haynes-25 alloy with TiN coating	Integrally machined struts	Single crystal synthetic Sapphire	Machined and polished	-do-
3.	Haynes-25 alloy	-do-	UHMW-PE	Solid state polishing & cryo-machining	-do-

The first model using a titanium cage and a polyacetal disc was given up because of the propensity of this plastic to swell during steam sterilisation. This was a potential hazard in the absence of adequate drying, which was none too uncommon a problem in most sterilisers used in the country. The second model used a Titanium nitride (TiN) coated Haynes-25 alloy cage and a synthetic sapphire disc. This model successfully completed the accelerated durability test. In animal evaluation, the sapphire disc fractured in 5 animals in a total of 14 implants

and hence the combination had to be discarded. However, in all these implants sapphire proved to be a an excellent blood compatible material (Bhuvaneshwar *et al.*, 1991b).

The search for a better combination began immediately and resulted in the third model having an all integral cage of Haynes-25 alloy and a UHMW-PE disc. In this search for a suitable combination, a set of screening tests for wear resistance was developed and used. Once it became clear that UHMW-PE was the best choice, prototype valves were fabricated and evaluated as per international standards.

3.2 MATERIALS & DEVICE EVALUATION

The heart of a normal human beats about 38 million times a year. For an artificial heart valve to perform in the adverse environment inside the heart for periods of 50 years or more, the materials used should be tough with an extremely high wear resistance and fatigue strength. Thus the study of the wear properties is an inseparable part of any valve development programme.

Based on the need for low wear, high fatigue resistance, high toughness and known biocompatibility, the choice of materials was headed by UHMW-PE and followed by Delrin ST (super-tough), PTFE-Delrin, EKONOL (composite of PTFE & a high temperature polyester). These tough engineering plastics were evaluated to determine the most suitable one. These tests and results have been published earlier (Bhuvaneshwar *et al.*, 1991a).

i. Water absorption :

Water absorption of Delrin-ST, Delrin-AF and UHMW-PE were measured by soaking five circular coin like specimens of 25 mm diameter and 2 mm thick in distilled water for periods up to 15 days. The samples were then carefully dried and weighed at intervals of 24 hours, 96 hours and 360 hours. The weighings were carried out in an analytical balance (Sartorius) with an accuracy of ± 0.1 mg and the weight gain noted.

ii. Screening Tests for Wear :

The two main types of wear occurring in this situation are ADHESIVE and ABRASIVE wear. Adhesive wear is predominant when highly polished surfaces in contact articulate against each other (Rabinowicz 1965).

a. Adhesive wear by Pin-on-wheel test :

The test set up shown in **Figure 3.2** is a modified version of the ASTM recommended test for hip joint materials (ASTM, 1986). It consists of a platform rotating at a constant speed of 55 RPM and a pin loading arm. The polymer specimen is a flat ended circular disc of 25 mm diameter and 10 mm length. The metal pin, polished to the prosthetic implant quality of the valve cage and having a 3 mm diameter circular contact area slides against the surface of the disc. The loading arm is free to move vertically so as to follow the specimen as the wear occurs. The entire set up is covered to eliminate any foreign particle coming between the wearing surfaces.

Figure 3.2

PIN-ON-WHEEL TEST SETUP

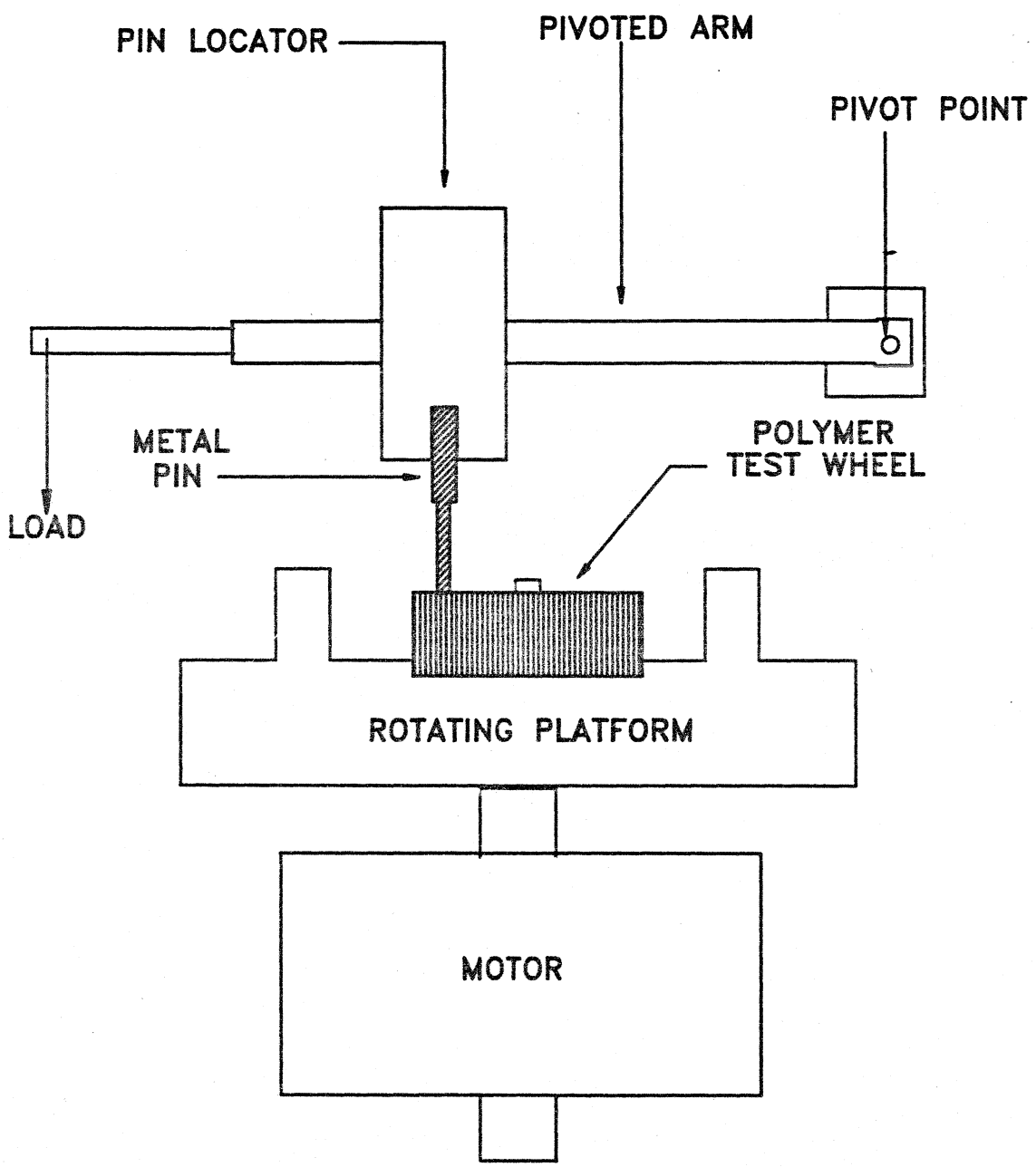

A load of 9.8 Newtons (1 Kgf) is applied along the longitudinal axis of the pin, so that the average contact stress is 1.373 MPa (14 Kgf/sq.cm). The pin is loaded at a radial distance of 9 mm from the centre of the disc to produce a sliding speed of 50 mm/second. There are no lubricants between the sliding surfaces. A time totaliser records the duration of the test, which is 100 hours so that sufficient wear occurs for accurate measurement of weight loss even in low wear materials. A minimum of three samples are tested for each material. The weight loss measured are converted to volume losses from the known densities of the test materials. With polymer samples, the weight loss of the metal pin was not not measurable at a resolution of ±0.1 mg.

The material pairs tested were **TITANIUM PIN** on the different polymers and **HAYNES-25 ALLOY PIN** on UHMW-PE disc.

b. Abrasive wear by Sand Slurry test :

The schematic of the setup is shown in **Figure 3.3** and has been modified from that of a polymer manufacturer (Himount, 1986). The test specimen is mounted on a 1/2 HP motor shaft. Alumina powder of 350 to 1000 micron particle size (20 to 40 BS-mesh) in an equal volume of water forms the abrasive slurry. The specimen is rotated at 3000 RPM for six hours inside the slurry. The height of the specimen from the bottom of the polystyrene container and the volume of the slurry are kept constant and the slurry changed after every test. A control sample of the same material is kept immersed in water for the same duration as the test and the weight gain of this is used

Figure 3.3

SAND SLURRY TEST SETUP

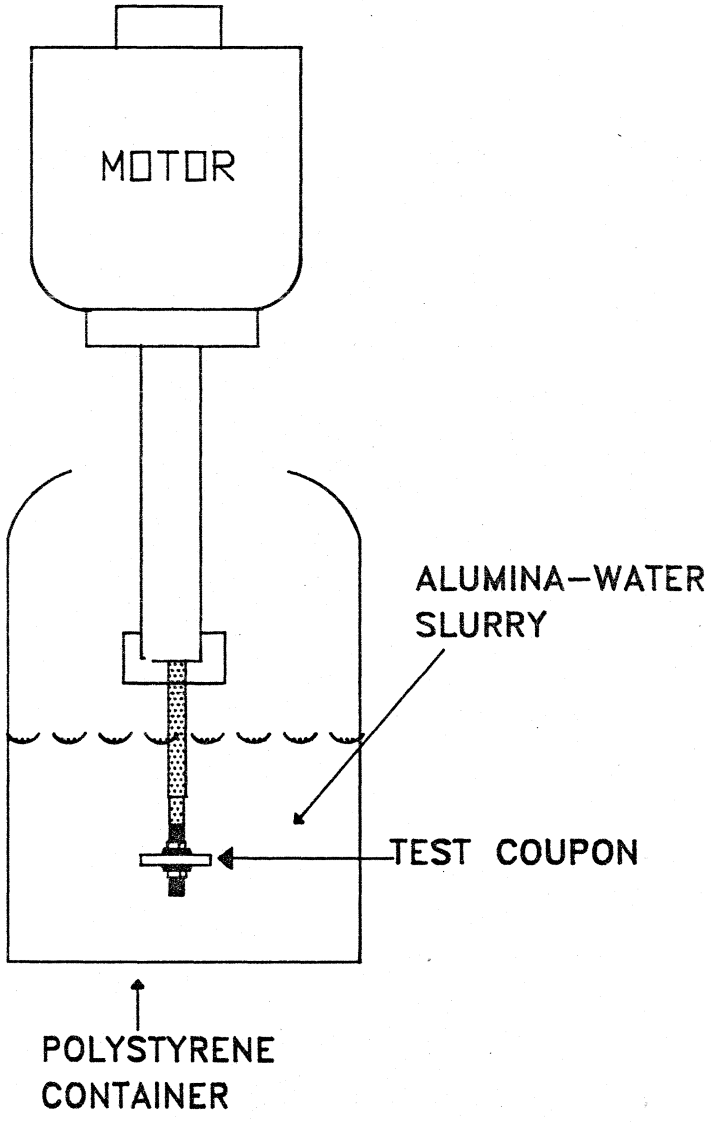

to correct for water absorption of the material. This weight-loss is then converted to volume-loss as before. A minimum of five samples are tested for each material.

c. Effect of thermal cycling on UHMW-PE

UHMW-PE was later chosen as the potential candidate material for valve discs. The process of fabricating the disc involves many thermal cycling stages like compression moulding, die polishing, annealing, autoclaving of the valve for sterilization etc. The effect of thermal cycling on UHMW-PE was also studied by the above two methods.

iii. Accelerated durability test :

The durability of artificial heart valves is determined by Accelerated life cycle testing to determine their mechanical wear resistance and fatigue properties. To test new designs at normal heart rates, whether in mechanical systems or in animal models for periods over 10 years is totally unrealistic. Several methods of accelerated testing of prosthetic valves have been used, including pneumatic cycling, several variations of mechanical cycling, hydraulic cycling and a combination of these (Fettel *et al.*, 1980).

Figure 3.4 is a schematic of the accelerated test system in use for the past 10 years. The hardware of this basic system presently in use is third generation and many problems with the equipment have been minimised so that the test results can be interpreted with reasonable accuracy. Different pairs of cage and occluder materials have been tested in this system to

Figure 3.4

SCHEMATIC – ACCELERATED DURABILITY TEST SYSTEM

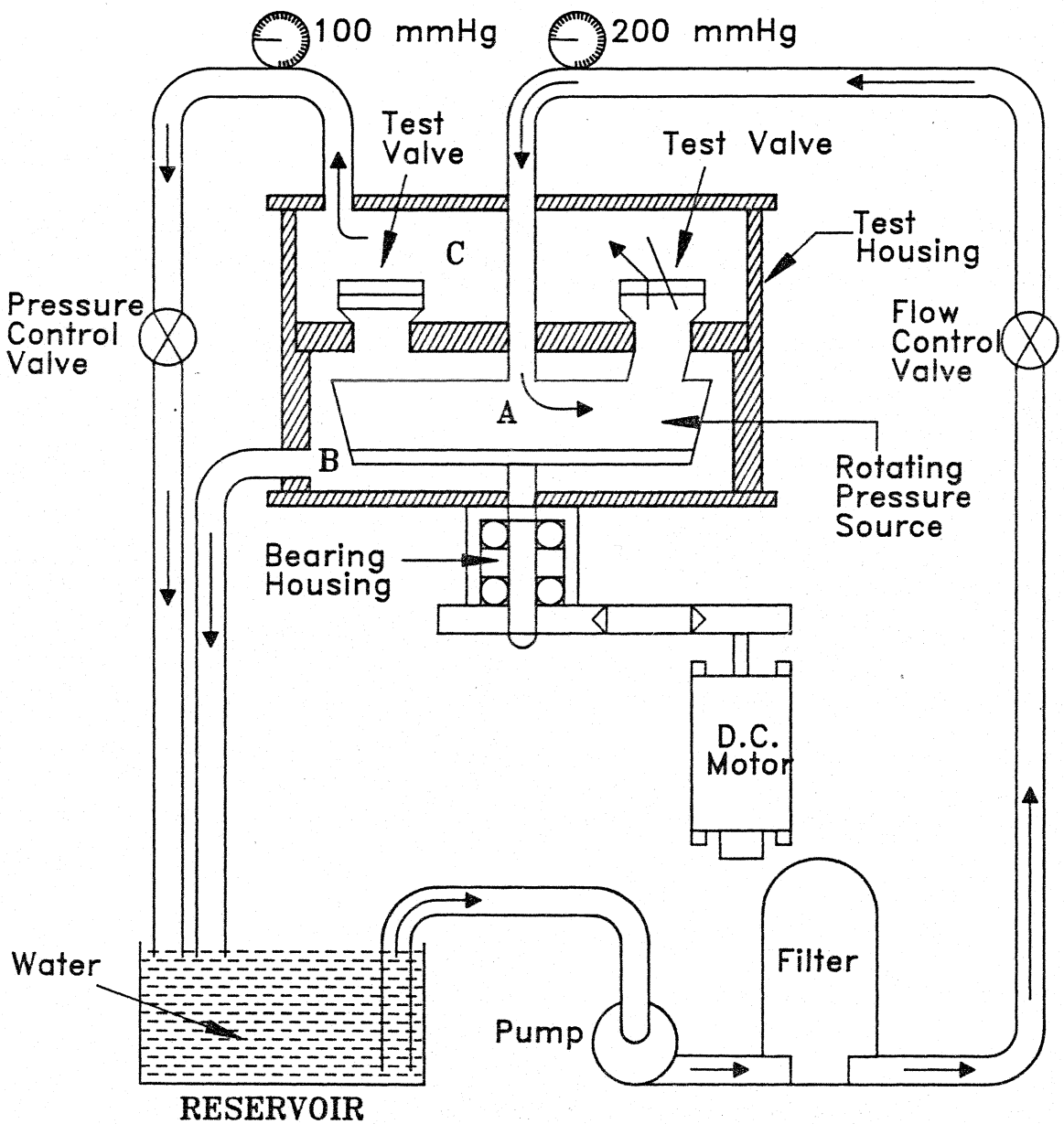

arrive at a suitable wear resistant combination. Five equally spaced valves are mounted on a stationary housing and covered with an acrylic chamber. The test fluid (plain water treated with trace amounts of copper sulphate to control fungal growth) is supplied through the centre inlet of the test housing. A D.C. motor with a variable speed control drives the rotor inside the housing. The fluid at a pressure of 26.7 kPa (200 mmHg, chamber A) is distributed by the rotor to sequentially actuate each of the five test valves. Two diametrically opposite fluid passages are incorporated in the rotor of the actual mechanism, so that a single revolution actuates each valve twice. This balances the rotor and reduces the number of revolutions. (*Note : for the sake of clarity, only one supply passage in the rotor is shown in figure 3.4).* When a fluid supply passage is directly under the inlet of a valve, the higher pressure of the chamber 'A' forces that valve to open and the fluid passes through the valve into the outer chamber 'C'. From here, the fluid returns to the reservoir through a pressure control valve. The pressure of chamber 'C' is kept at 13.35 kPa (100 mmHg) using the pressure control valve.

The portion of the rotating member not containing the fluid passage is relieved. When this portion of the rotor is directly under the inlet of a valve, that valve's inlet is connected to the inner chamber 'B'. The pressure of this chamber is less than atmospheric, as it is connected to the reservoir through a large bore tube and the reservoir is kept at a level lower than the test housing. At this point of time, the higher pressure of 'C' on the outlet side of the valve, forces it to

close quickly. Thus, as the pressure source 'A' rotates, the test valves are sequentially opened and closed, their rate being determined by the rotor speed.

The fluid is pumped through a 10 micron filter to remove foreign particles. Pressure control valves and monitoring gauges are placed as shown in the figure. The test valves are mounted with their sewing rings stitched to silicone rubber supports to isolate and damp their vibrations during cycling.

Table 3.2
Different Models of Chitra Valves Tested for Durability

Sl. No.	Valve Model	Cage Material	Disc Material
1.	Titanium cage with outlet strut electron-beam welded	Titanium	Polyacetal
2.	All integral machined cage	Titanium	Sapphire
3.	All integral machined cage	Haynes-25	Sapphire
4.	All integral machined cage	Haynes-25 TiN coated	Sapphire
5.	All integral machined cage	Titanium	UHMW-PE
6.	All integral machined cage	Haynes-25	UHMW-PE
7.	Bjork-Shiley standard valve	Stellite	Pyrolytic carbon

Table 3.2 shows the valve models that have been tested in this system for various periods and their durability assessed. The wear of the valve components has been measured by weighing the components and cage/disc assembly to an accuracy of ± 0.1 mg in a single pan electronic balance (Sartorius). The cage and disc are weighed separately before assembly. The assembly is weighed again after inspection. Control weights of titanium are

used to monitor the reliability & consistency of the weighing balance over the prolonged period of the test.

The test valves are cycled at 800-840 times a minute. The calibration of the d.c. motor speed controller is periodically checked with a stroboscope. The valves are removed after 1, 2, 5, 10, 20, 40 million cycles and there after at intervals of 40 million cycles. At these instances, the assemblies are removed from their sewing ring holder, cleaned, degreased and dried before weighing.

The end of the cycling of any valve is determined when :-

(i) there is a failure of any its components

(ii) excessive wear is noticed and the valve is expected to fail very soon or

(iii) the valve reaches 400 million cycles without failure.

At the end of the test, the valves are dismantled and the components weighed again. They are also inspected for signs of wear and other degradation. The volume of wear is calculated from the weight loss and the density of the material. During cycling, since the cage and disc cannot be weighed separately, the weight loss is attributed to the component which wears most. The error due to this has been found to be small as borne out by the final weighings.

The extrapolation of the wear data obtained from accelerated wear testing to predict actual implant durability depends on the relation of the wear occurring in-vivo to that measured in the test system. To assess this factor, valves implanted in sheep for various intervals of time have been

accurately monitored for weight loss. The number of cycles that the valve has gone through is estimated by assuming that on an average, the heart of the animal beats at 70 per minute.

3.3 RESULTS & DISCUSSION

i. Water absorption :

Figure 3.5 gives the data obtained from water absorption tests. The results show the higher water absorption of Delrin based polymers compared to the UHMW-PE. The low water absorption of UHMW-PE ensures that the disc will not unduly swell and change shape like the Delrin disc occluder of the first Bjork-Shiley model (Teuvo & Karkola, 1974).

ii. Wear tests :

Figure 3.6 shows the results obtained from the adhesive wear test. The reported volume losses are the combined losses from the pin and the wheel.

The results from the sand slurry test are given in **Figure 3.7**, where mild steel was used as the control.

The results from tests for studying the wear behaviour of UHMW-PE undergoing thermal cycling are shown in **Figure 3.8.**

These results establish that any thermal cycling of the material above 135°C can cause deterioration in its wear properties (The reported glass transition temperature of UHMW-PE is 136-138°C). These tests showed that steam sterilisation does not considerably change the wear properties of UHMW-PE.

Figure 3.5
WATER ABSORPTION CHARACTERISTICS

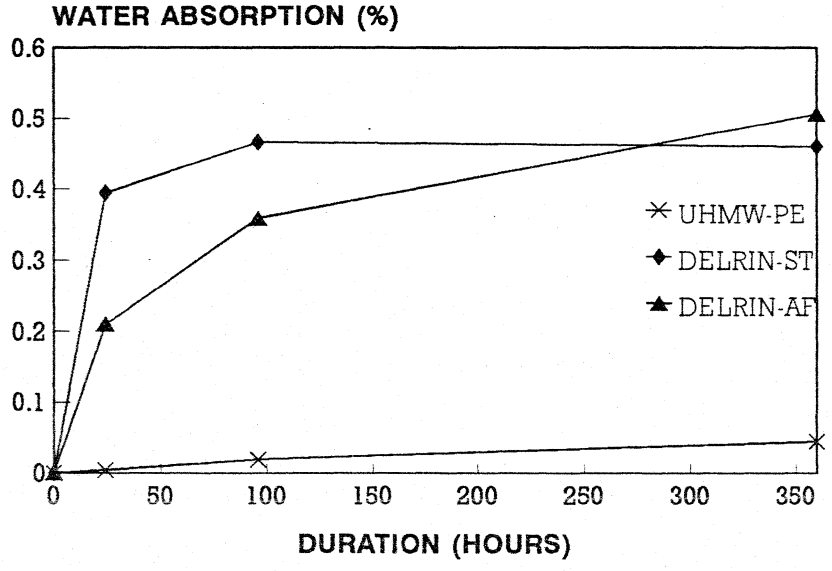

Figure 3.6
PIN ON WHEEL TEST RESULTS
Test Duration : 100 Hours

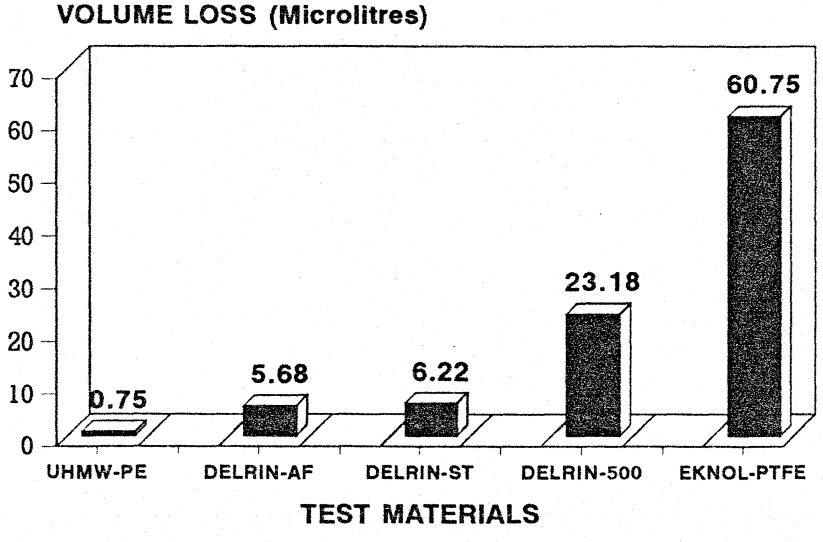

Figure 3.7
SAND SLURRY TEST RESULTS
Test Duration : 6 Hours

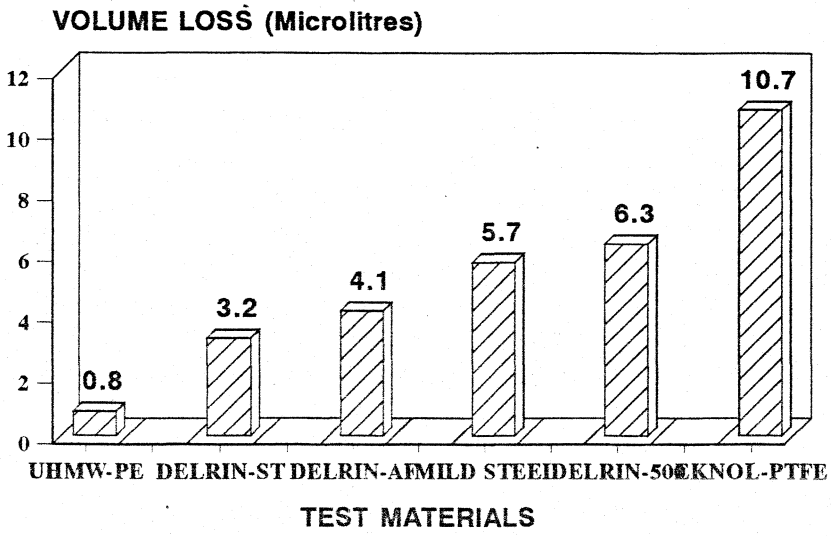

Figure 3.8
EFFECT OF THERMAL CYCLING OF UHMW-PE

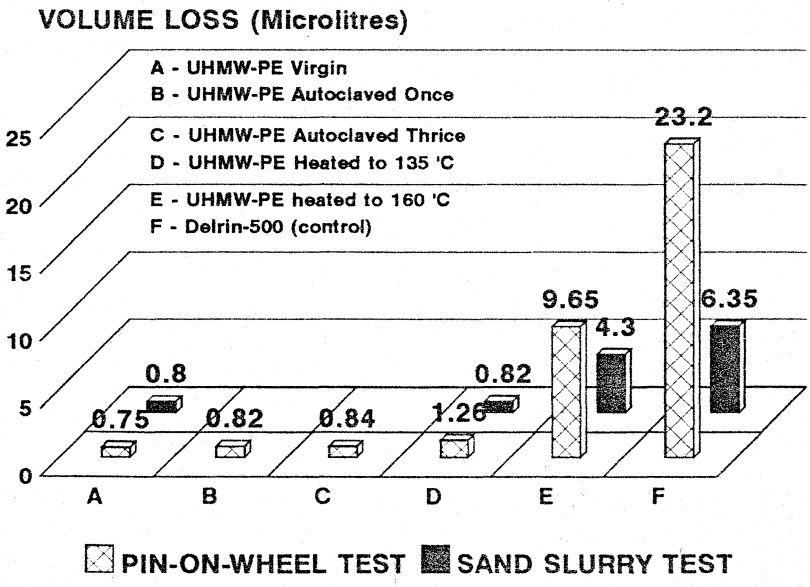

The pin-on-wheel and sand-slurry wear tests indicated that UHMW-PE is an extremely good material for heart valve occluders. These results are also confirmed by the accelerated durability testing of valves with UHMW-PE discs. These tests further helped to establish the correct processing cycles for its fabrication. Though steam sterilisation does not create noticeable changes in its wear properties, it is advisable to minimise the thermal cycling of the assembled valve as a measure of precaution. Fabrication of prototype valves followed by accelerated durability testing and animal trials takes a minimum of six to twelve months before any meaningful data become available. These tests can quickly screen more material combinations and help reduce the development time.

iii. Accelerated durability testing :

Figure 3.9 shows the relative wear rates of the various combinations tested during the last 8 years. The lowest wear rate is for the Bjork-Shiley valve with the Stellite/Pyrolytic carbon combination. The titanium sapphire combination shows an extremely high wear rate. In fact, this combination failed in animals between 1 to 3 months due to wear of the titanium cage.

The TiN coated Haynes-25 cage gives the best durability when sapphire disc is used. UHMW-PE with Haynes-25 combination has turned out be the best. The wear rate is marginally higher than the proven Bjork-Shiley valve and extrapolation gives an estimate of durability in excess of 50 years.

Figure 3.9

ACCELERATED WEAR TEST RESULTS

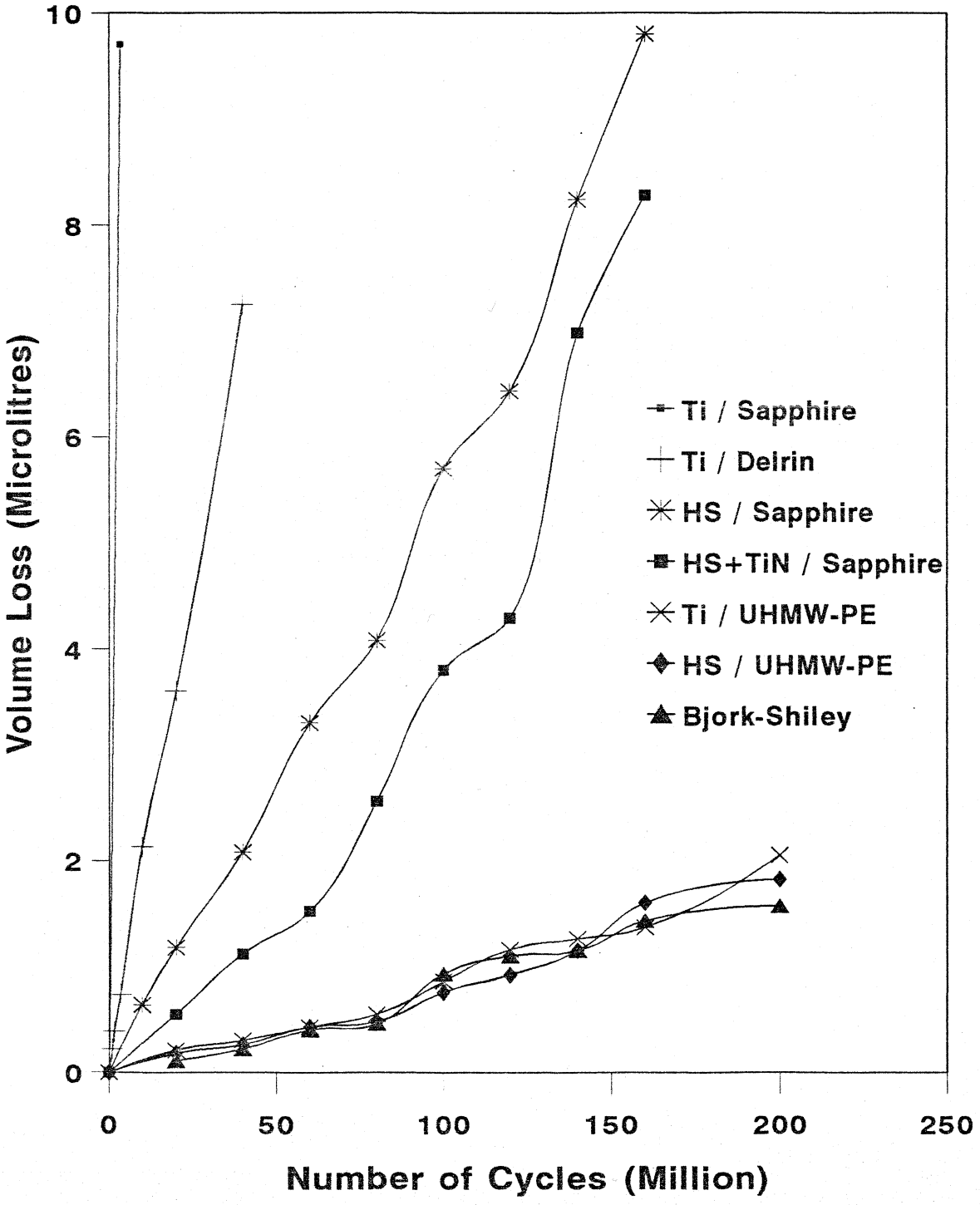

Table 3.3 shows the weight loss of valves recovered from animal implantations and the corresponding weight loss interpolated from accelerated wear testing data.

Table 3.3
Weight loss from Animal Implants & Accelerated Testing

Valve Model	Animal Implantation		Accelerated Testing	
	Cycles millions	Wt.Loss mg	Cycles millions	Wt.loss mg
TiN coated Ti cage with Sapphire disc	5.9	16.9	0.6	16.8
Haynes-25 cage with Sapphire disc	11.55	5.9	11.55	5.2
TiN coated Haynes-25 cage with Sapphire disc	50.5	20.4	50.5	19.1

Many problems and difficulties are encountered with accelerated testing, most of which are related to interpreting results and relating them to the clinical application. Wear rates are generally greater at the beginning of the testing and tend to level off after a short "WEAR IN" period, once the mating parts have seated. Because structural fatigue failures are particularly difficult to predict, projections of valve life based on wear rate projections would not be appropriate if structural fatigue were the limiting factor.

Accelerated testing inherently imposes unrealistically severe conditions because of (a) the inability to achieve adequate system damping (b) increased pressures that are required to achieve full valve excursion (c) inferior lubricating properties of the test fluid and (d) high frequencies imposing

stresses that are not found at lower rates (Fettel, BE et al. 1980).

The durability of the test apparatus itself is a significant problem when one considers that it must outlive a relatively simplistic device that is designed to withstand an equivalent of 38 million cycles per year of use for over 50 years or more. All of these factors must be considered during both the design of the test system and subsequent evaluation of results.

Accurate prediction of device durability is of paramount importance in the development of life saving implants like artificial heart valves. The present test system developed here has proved to be reliable in terms of long term performance. The wear rates observed in this system give a good 1 : 1 correspondence to the wear rates obtained from implanted devices.

Thus the study of the mechanical and physical properties of the materials intended for use in artificial valves becomes an inseparable part of the valve development process itself. In the Indian context, the durability of the valve is all the more important because the average age of an Indian patient undergoing valve replacement is between 20 and 30 years, whereas this is in the sixties in developed countries. Having gone through 3 models during the last 10 years with the failure of the first two, this set of test methods has been developed to ensure that the material requirements of the device are met.

The Bjork-Shiley standard valves have been in clinical use since 1971 and have a good track record of durability. Their durability based on wear rates was estimated to be 400 years

(Fettel *et al.*, 1980). The wear rate of Haynes-25/UHMW-PE combination is marginally higher than that of the Bjork-Shiley. Since, it is the disc that wears in these two models unlike those with Sapphire, the wear gets distributed over the surface of the disc as it rotates during working. Hence, for a given volume loss of wear, the thickness of the component worn out is very much smaller than it would be, if the cage struts were to wear. Clinical use of UHMW-PE in artificial hip joints over the last 25 years has shown this material to be extremely stable in the body environment. Considering all this, it is clear that the Haynes-25/UHMW-PE combination should last for over 50 years of implant life.

However, it should be emphasised that all this simulated testing does not preclude or eliminate the need for animal trials of the device. Early on in our development effort, the titanium/sapphire combination showed acceptable wear rates in the accelerated life cycle test. However, in animal implants, this model repeatedly failed due to strut wear of the metallic cage between 1 and 3 months. Though the problem was traced to the lubricating effect of glycerine in the test fluid of the accelerated system, it is clear that one cannot exactly simulate the in-vivo conditions. Another example is the high failure rate of the Bjork-Shiley convexo-concave model in patients due to strut fracture (Davis *et al.*, 1985; Joyce, 1990), though their earlier standard model had an excellent record of safety and the manufacturers would have tested the new model adequately in their accelerated tester. This problem was consequent to the change in shape of the disc. Design changes, however minor can

lead to deleterious effects and hence necessitates a full cycle of retesting in critical implantable devices.

3.4 FUNCTIONAL EVALUATION

The fluid dynamic performance of the Chitra Valve was compared with the popular and extensively used Bjork-Shiley standard valve in a pulse duplicator. The details of the test system and the results have been published earlier (Bhuvaneshwar *et al.*, 1983).

The results showed comparable performance of the Chitra valve exhibiting reduced pressure drops and marginally increased closing volumes due to a larger opening angle of 70^0 against 60^0 for the Bjork-Shiley standard. The data are summarised in Tables 3.4 & 3.5.

Table 3.4
Regurgitant Volumes per Cycle

	CHITRA	BJORK-SHILEY
AORTIC POSITION #23	***ml***	***ml***
Closing volume	1.9	1.4
Diastolic leak	3.4	4.7
TOTAL	**5.3**	**6.1**
MITRAL POSITION #27	***ml***	***ml***
Closing volume	4.0	3.1
Systolic leak	8.8	8.8
TOTAL	**12.8**	**11.9**

Table 3.5
Effective Orifice Areas of
Bjork-Shiley Standard & Chitra valves

Effective Orifice Areas in cm^2

Valve Model	AORTIC Size 23mm	MITRAL Size 27mm
Bjork-Shiley Standard	1.95	2.67
Chitra Valve	2.33	2.94

3.5 ANIMAL EVALUATION

Chitra valves of 23 mm sewing diameter were implanted in the mitral position of sheep under heart lung bypass. After initial difficulties, postoperative survival became routine and five animals were available for long term study. The animals received no anti-coagulants. Three animals were electively terminated at 6 months and a complete autopsy performed in addition to haematologic investigations for blood damage. The pathologic studies showed excellent healing of the valve and no organ or blood damage. Two animals continue to live at present, nearly 3 years after implantation.

3.6 CLINICAL TRIALS

On the basis of the engineering and in-vivo data, the Institute Ethics committee approved the trial of the Chitra valve in patients. This trial, which commenced in December 1990 is in progress. About 70 valves have been implanted in the Institute with good clinical results so far. The patients are on

anti-coagulant therapy just like in the case of any other current mechanical valve in use.

3.7 CURRENT STATUS

As noted earlier, the efforts so far have been largely directed towards :

a. identifying suitable materials for the valve components.

b. developing fabrication techniques

c. developing test systems for the evaluation of the device performance - both in-vitro and in-vivo.

A decade and a half ago, when this development was started, the technology of biomaterials and bioimplants scarcely existed in India. Little data existed in the literature then, linking the fluid dynamics of the valve with its clinical performance. A decade later the Chitra valve was almost a reality and extensive data on the fluid dynamics of prosthetic heart valves became available. At that point of time, the natural question that came up was : "Can the performance of this tilting disc valve be improved by design ? "

The following chapters are an account of the attempt to answer this question.

CHAPTER 4

AIM, METHODS AND EXPERIMENTAL MATERIALS

4.1 AIM OF THE STUDY

As stated in §1.6, the aim of this study was to experimentally optimise the design of the tilting disc valve so that :

a) hydraulic performance of the valve was optimised in terms of its effective orifice area and closing volume by suitable choice of disc shape, opening angle and entrance/exit curvature of the cage ring.

b) flow through the minor orifice area was maximised so that tissue overgrowth problems could be reduced by increasing the shear stresses at the ring margins. This could be achieved by locating the pivot axis as centrally as possible and having the maximum opening angle.

c) ensuring that the closing impact forces were not increased, if not minimised due to the design changes introduced. Large closing impact forces could be a source of suture dehiscence leading to paravalvular leaks and fatigue failures of the valve components.

4.2 SCOPE OF THE STUDY

The hydraulic performance of the various valve models and components were tested in a **1 : 1** model test chamber simulating the proximal and distal parts of the heart adjacent to the mitral valve. The chamber dimensions were those as obtained by Weiting from casts of the natural heart (Weiting, 1969). These are described in more detail in § 4.4. The tests were conducted using a blood analogue of glycerine/water mixture (approximately 35% v/v; specific gravity 1.08) under various conditions as given below.

i. Steady Flow :

Under steady flow conditions of 0 to 35 lpm, pressure drops, opening angle of the valve disc and drag forces were measured for the various test valves and components to study the effect of the various design parameters. Details of this study are given in the next chapter. Based on these data, a smaller set of viable test valves were taken up for further study under pulsatile conditions.

ii. Pulsatile Tests :

Static pulsatile tests were conducted for the measurement of closing volumes and closing impact forces. Pressure drops, closing volumes and impact forces were also determined under dynamic conditions for the selected test valves and the standard valves. The static tests with better control on the test conditions yielded more precise data.

Chapter 6 contains the complete details of the test systems, methods, results and discussions. From this study an optimum valve model emerged.

iii. Relative Flows and Velocity Profiles :

The improvement in the minor orifice flow for this optimum model was measured under steady flow conditions of 15 to 25 lpm and compared with those for the other standard valves in current clinical use. The velocity profiles downstream of this valve and the standard valves were determined using a Pulsed Ultrasound Doppler velocimeter (PUDVEL), set up for this purpose. The velocity profiles clearly show the improvement in the velocity of flow through the minor orifice. The details of the test methods and the results are discussed in Chapter 7.

4.3 LIMITATIONS OF THE STUDY

The incidence of valve thrombosis and thrombo-embolism is higher in mitral valve replacements and in India, the majority of valve replacements are in the mitral position. Hence, it was decided to restrict this study to mitral valves. Further, 27 mm mitral valve is one of the most widely used sizes in clinical practice. Also, many of the current investigators have used this size for comparative evaluation in their pulse duplicator studies and hence extensive data exist for this size. Because of this, all prototype and test valves used in this study have been of size 27 mm sewing diameter. This will enable a limited comparison

of the data from this study with those of others for existing valve models.

In view of the expertise available in the fabrication of the Chitra Valve and the need to fabricate different prototypes quickly, the basic design of the valve in terms of the strut shapes and the concept of a free floating disc were retained. The length of the struts were modified depending on the requirements for pivot location and/or disc shape.

4.4 DESIGN OF EXPERIMENTAL VALVES AND COMPONENTS

i. Pivot axis location :

One way to increase the minor orifice area is to have as central a pivot axis as possible. To determine the optimum location of this axis, 8 valves as shown in **Figure 4.1** were fabricated, by moving the pivot point 0.5 mm radially towards the centre for each cage, from No.1 to No.8. The well in the disc was suitably reduced in diameter by 1 mm and the taper marginally adjusted to suit the well diameter. The cages were machined from brass and electroplated to make their fabrication easier and quicker. The discs were machined from UHMW-PE rods.

ii. Opening angle of the disc :

The unique design of the Chitra valve with independent major struts made this study possible. Any opening angle from 45^0 to 85^0 could be obtained by radially repositioning the major struts. This study was carried out with the present model of the Chitra valve.

Figure 4.1

TEST VALVES WITH DIFFERENT PIVOT AXIS LOCATIONS

TV-11

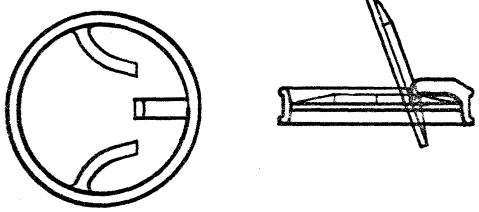

TV-55

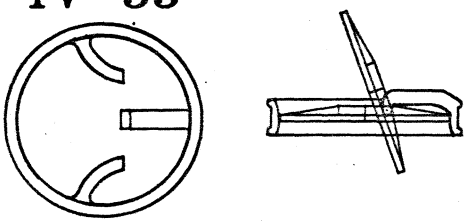

TV-22

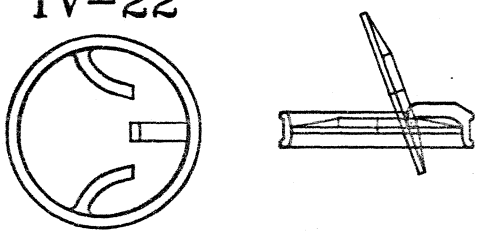

TV-66

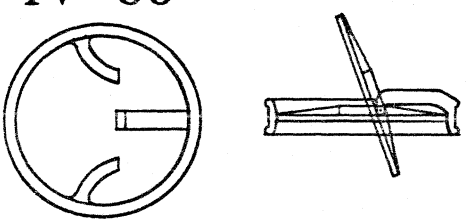

TV-33

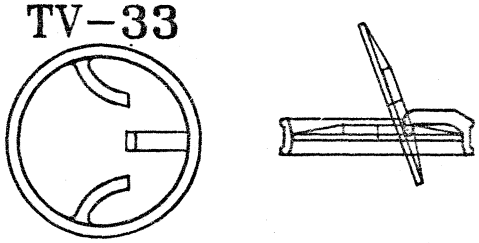

TV-77

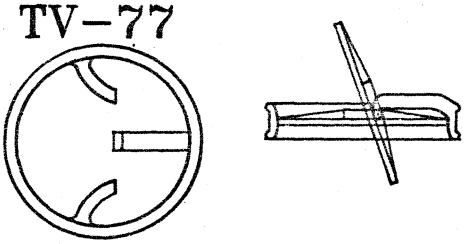

TV-44

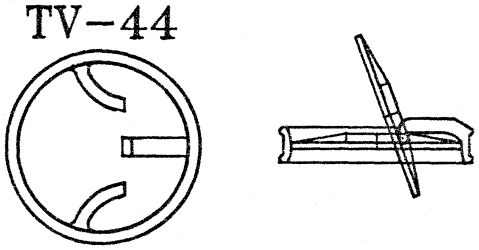

TV-88

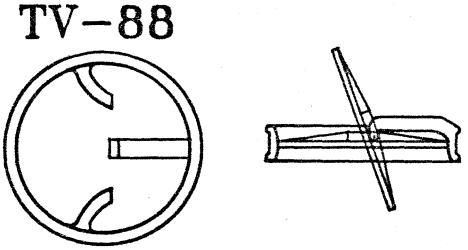

iii. Entrance and/or exit curvatures of the cage ring :

Bellmouthing or providing a radius at the entrance and exit edges of the cage ring started in the mid sixties with the ball valves and has been shown to improve the flow through the valve (Viggers *et al.*, 1968). This practice has been extended to the design of the tilting disc valves like the Bjork-Shiley (standard and more recently the Monostrut models), Medtronic-Hall, Bicer, etc. and was also adopted in the current model of the Chitra valve. The basic premise in this has been that the entrance and exit curvatures reduce the resistance to flow. In the late seventies, the St.Jude bileaflet valve was introduced with a straight bore ring without any entrance/exit curvatures, most probably to make the fabrication and assembly easier. Hence, it is clear that the shape of the bore has so far not been designed with any fluid mechanical considerations.

To study this, rings without struts but having a similar cross-section as the valve cages were fabricated. These had radius on one edge, radius on both edges **(radii = 5 mm)** and a straight bore as shown in **Figure 4.2.** The first ring with one edge having radius was used to study independently, the effect of inlet and outlet curvatures by reversing the ring in the test system.

iv. Disc shape :

Various disc shapes have been employed in different models. The Bjork-shiley started with a mesa shaped disc, which was subsequently changed to a convex shape in their standard model. In 1979, they introduced the convexo-concave disc (Fig.1.1). Other

Figure 4.2

RINGS WITH ENTRANCE AND EXIT CURVATURES

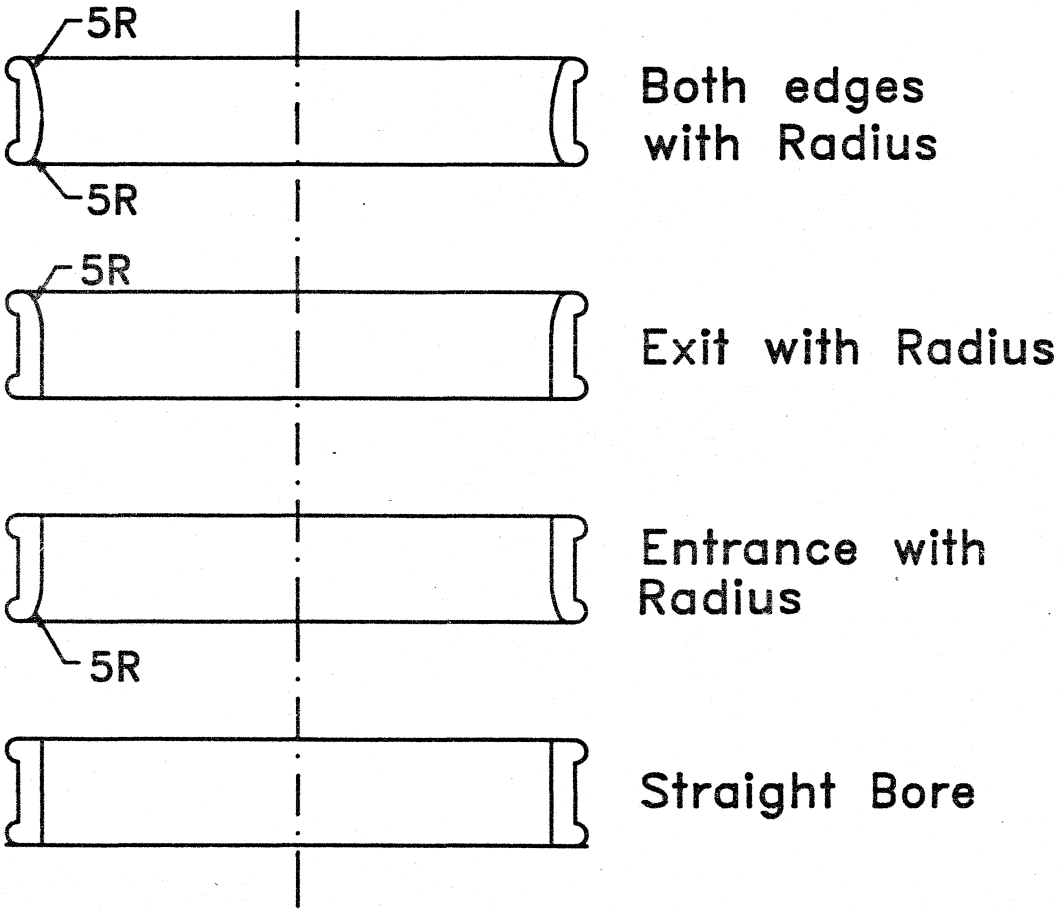

models like the Lillehei-Kaster and Medtronic-Hall have used flat discs. A plano-convex disc with inlet side flat was chosen for the present model of the Chitra valve to improve the flow through the minor orifice (Fig.1.2).

The experimental work of Pierce *et al.*, (1968), Knight (1973) and the modelling work of McQueen & Peskin (1983) have shown that the shape of the disc can considerably influence the opening and closing mechanics of the valve. The failure of the Bjork-Shiley valve due to strut fractures consequent to the change in the shape of the disc strengthens this observation.

Flat, mesa-shaped, plano-convex and concavo-convex shaped discs were machined from UHMW-PE as shown in **Figure 4.3** with different well diameters. These could be fitted to the brass test cages by manually repositioning the struts. To be in line with the maxim of keeping to simple shapes that could be easily fabricated, other complex aerofoil shapes were not tried in this study.

The nomenclature **PLANO-CONVEX** and **CONCAVO-CONVEX** is preferred as the first part indicates the shape of the inlet side and the second part, the shape of the outlet side of the disc. The Bjork-Shiley model, which has been discontinued was called the **CONVEXO-CONCAVE.** The disc of their current model MONOSTRUT VALVE is also referred to as convexo-concave. However, for consistency here, all these discs will be termed as **CONCAVO-CONVEX or C-C.**

Figure 4.3

DISC SHAPES EVALUATED

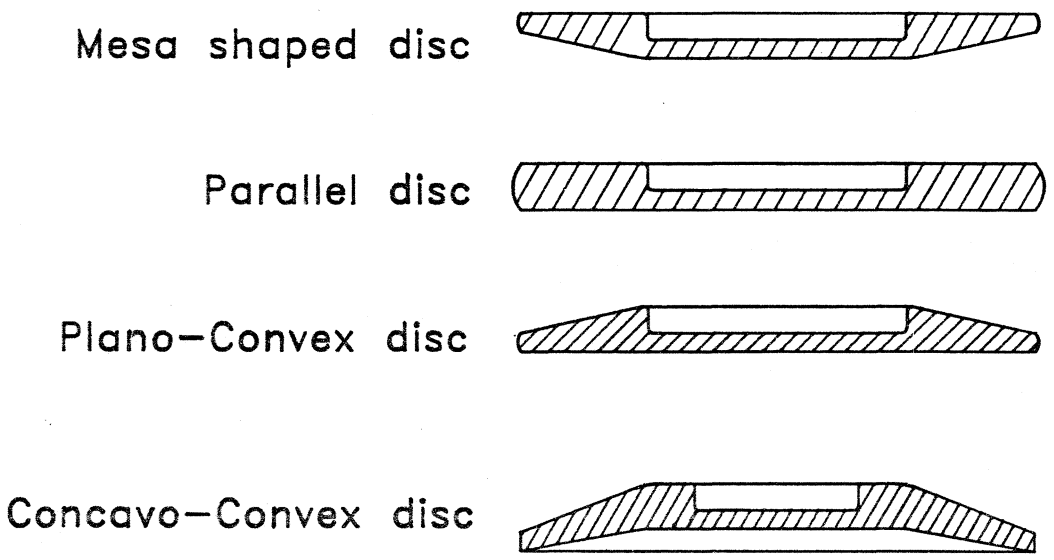

v. Effect of Disc Sliding :

Flow through the valve can be marginally improved by allowing the disc to slide axially down in the direction of opening. This permits a better clearance between the edge of the disc and cage in the open position and reduces the projected area of the disc within the cage orifice. However, this could lead to increased edge wear of the disc, especially when large sliding distances are used. Also, with large sliding distances the possibility of the disc getting stuck seemed possible. A sliding distance of 1 mm for the 27 mm size valve was considered optimum.

The effect of disc sliding was studied by using discs with a larger well diameter. A sliding distance of 1.0 mm was obtained by using a disc with a well radius that is 1 mm larger than the radial length of the minor strut as shown in **Figure 4.4.**

vi. Standard Valves :

In-vitro evaluation of the hydraulic performance of artificial heart valves under steady and pulsatile conditions have given invaluable data on their performance. However, since all the test systems used rigid chambers and only approximate the real in-vivo conditions, direct correlation of these data to clinical situations has been very difficult, if not impossible. Generally, the comparative performance of the valves, evaluated in in-vitro test systems have a good correlation with their comparative performance in-vivo. Because of this, almost all in-vitro studies so far, rely on comparative evaluation of any new designs or models with popularly used clinical valves to predict

Figure 4.4

VALVE ASSEMBLIES WITH SLIDING

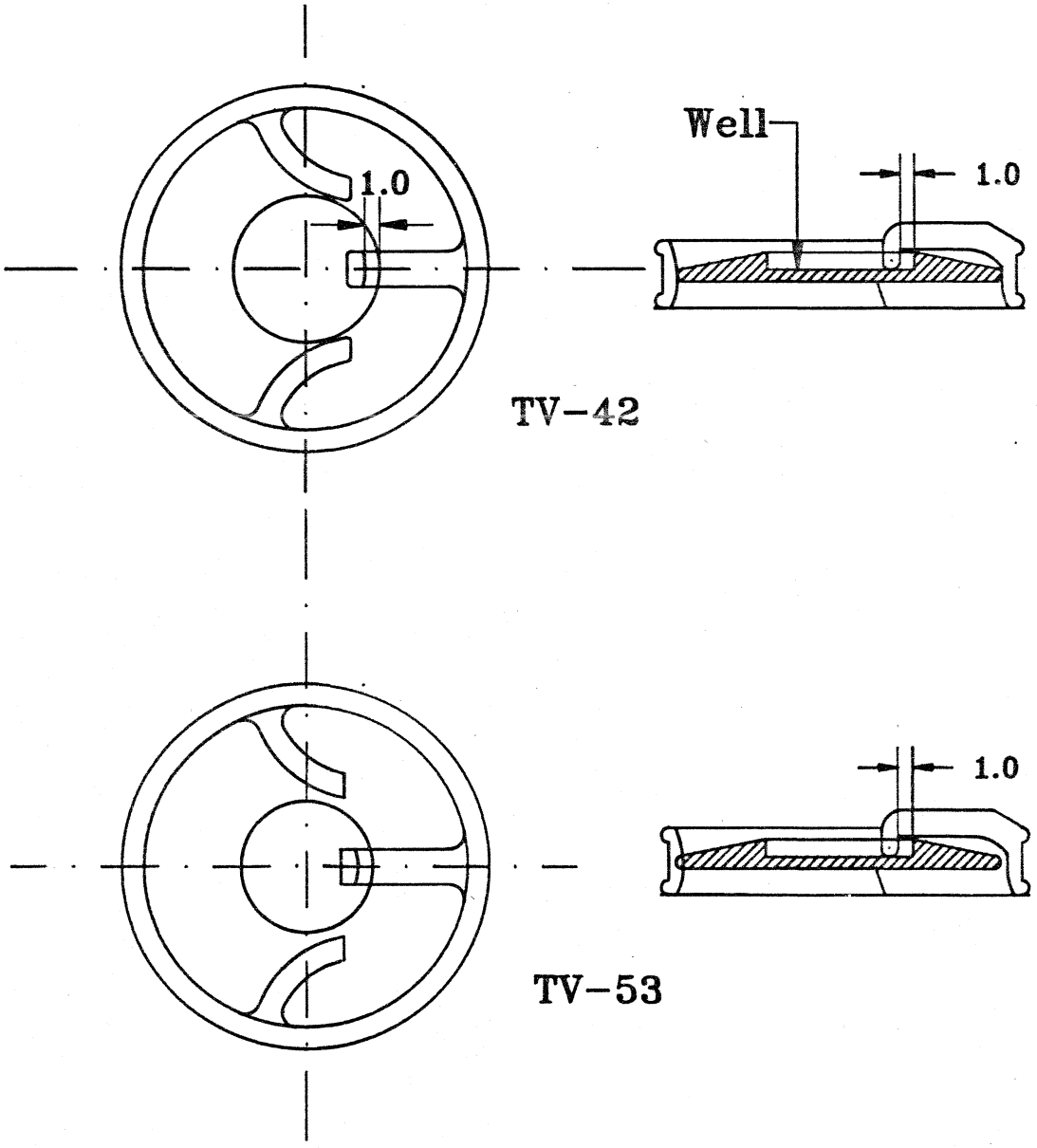

their clinical performance (Bjork, 1970; Kaster *et al.*, 1970; Macleod *et al.*, 1976; Willshaw *et al.*, 1986; Emery *et al.*, 1978a).

The standard mitral valves shown in **Figure 4.5** were evaluated in the present study for obtaining the base data for comparison and are also listed in Table 4.1.

Table 4.1
Standard Valves Tested

	Valve Model	Abbreviation
1	Starr-Edwards 28 mm silastic ball valve Model 6100.	**SE**
2	St. Jude Medical bileaflet valve 27 mm mitral.	**SJM**
3	Medtronic-Hall Prosthetic Heart Valve 27 mm mitral.	**MHV**
4	Bjork-Shiley Monostrut tilting disc valve 27 mm mitral.	**BSM**
5	Bjork-Shiley Standard tilting disc valve 27 mm mitral.	**BSS**
6	Chitra Tilting disc valve -- 27 mm mitral with UHMWPE disc.	**CHU**
7	Chitra Tilting disc valve -- 27 mm mitral with Sapphire disc.	**CHS**

4.5 VALVE NOMENCLATURE & ABBREVIATIONS

The eight test cages and discs with the different pivot axis locations were numbered 1 to 8. Starting with 1 for the present design, each subsequent cage had the pivot axis moved towards the centre by 0.5 mm. The discs with corresponding well diameters to the cages, were also numbered 1 to 8.

Figure 4.5

STANDARD VALVES

View from Inlet side

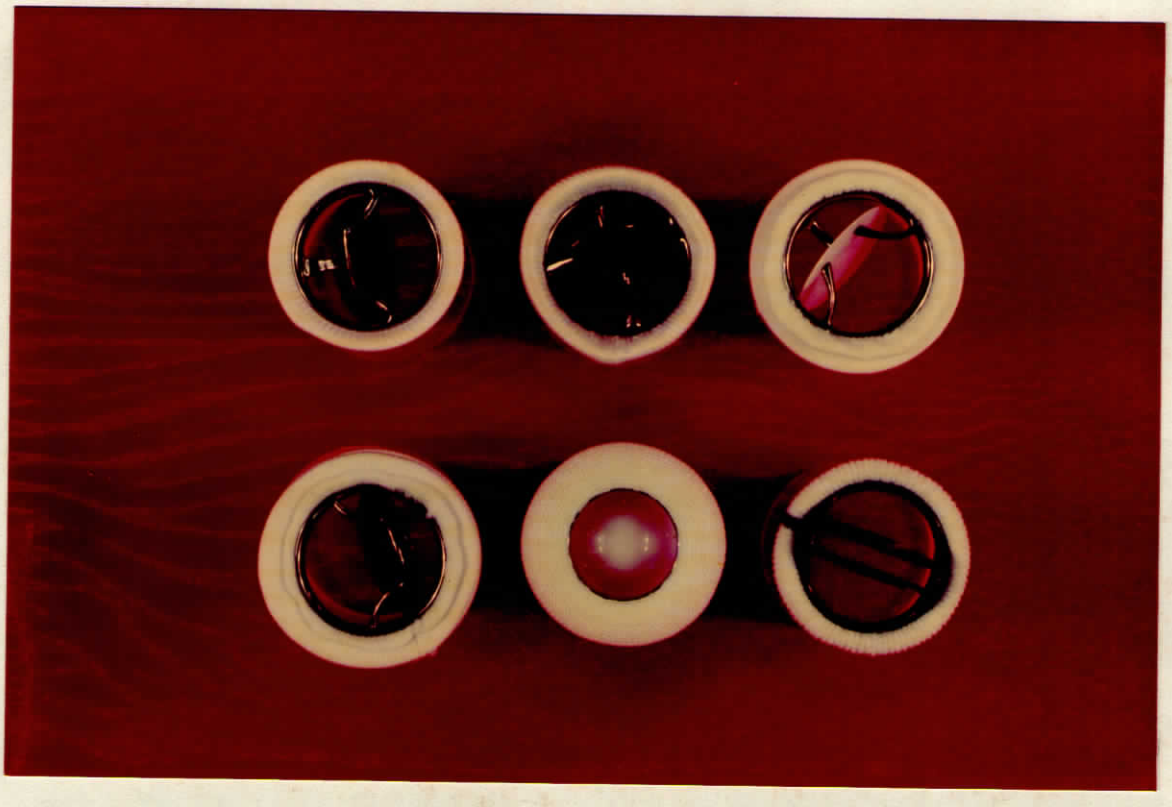

1	2	3
4	5	6

1. Bjork–Shiley Monostrut
2. Medtronic–Hall
3. Chitra
4. Bjork–Shiley Standard
5. Starr–Edwards
6. St. Jude Medical

A two digit number following the abbreviation 'TV-' was used to designate a particular assembly of cage and disc. The first digit referred to the cage number and the second to the disc number. For example, TV-11 refers to the valve assembly with cage no.1 and corresponding disc no.1, TV-66 to cage no.6 and disc no.6 etc. In the case of assemblies where disc sliding of 1 mm was desired, discs with 2 mm larger well diameters were used. Thus TV-42 would refer to the assembly with cage no.4 and disc no.2 and TV-53 to cage no.5 and disc no.3.

'C' was used to designate a concavo-convex disc. Thus TV-2C refers to the assembly with cage no.2 and corresponding C-C disc no.2, etc.

Among the Chitra valve models tested, 'CHU' refers to a Chitra valve with UHMW-PE disc and 'CHS' refers to the valve with Sapphire disc.

The abbreviations used to refer to the standard valves are given against each in Table 4.1.

4.6 VALVE FLOW CHANNELS

The flow channels proximal and distal to the aortic and mitral valves were patterned on the published work of D.W.Weiting & Yoganathan and provide cross-sectional areas analogous to the flow tracts in the human heart (Weiting et al., 1969; Yoganathan & Letzing, 1983). The cross-sections of the channels with pressure taps are shown in **Figure 4.6**. The pressure tap P1 was located one valve diameter upstream and the tap P2, 4 diameters downstream of the test valve. This ensured that full pressure

Figure 4.6

VALVE TEST FLOW CHANNELS

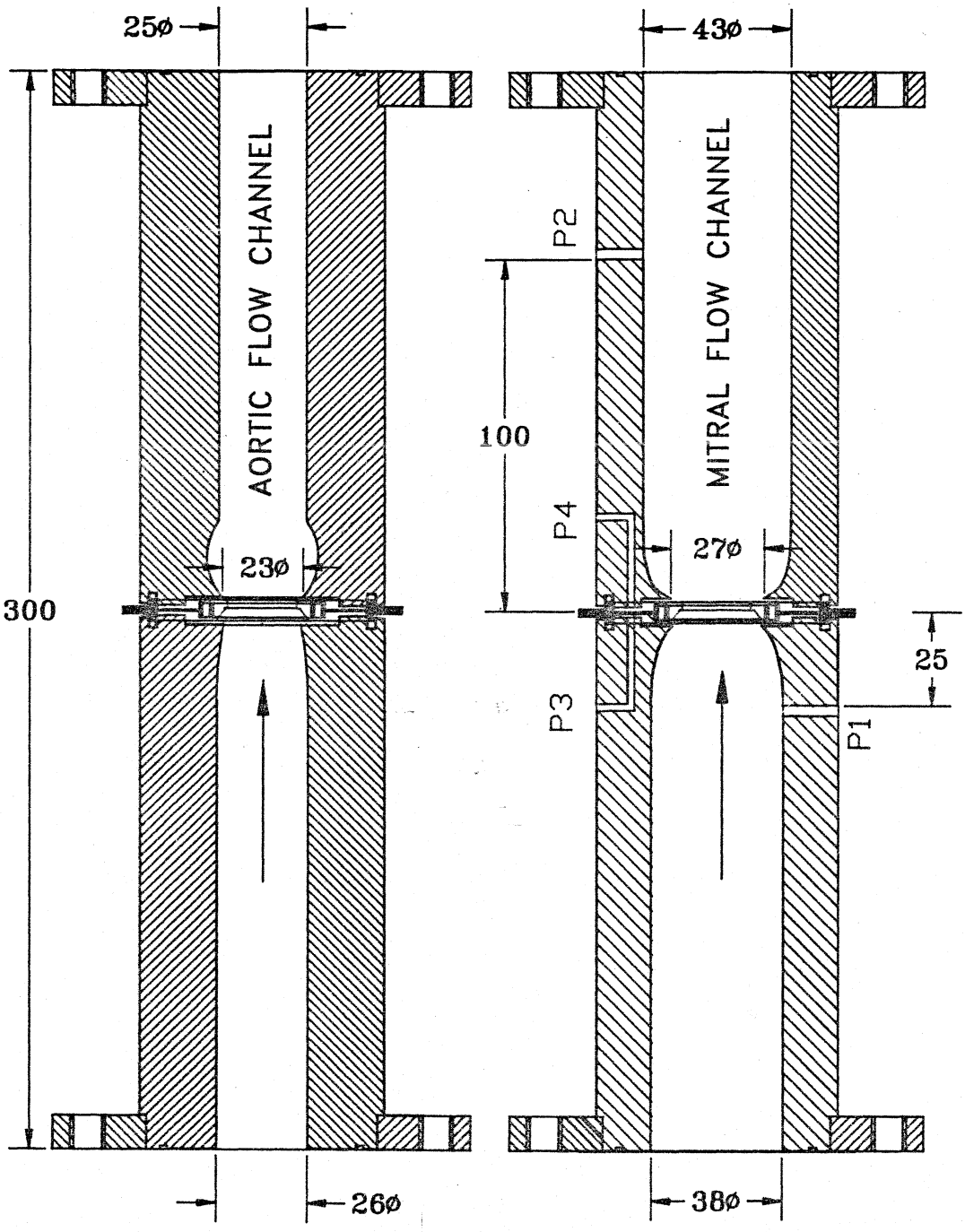

recovery had taken place at the point of measurement (Bruss *et al.*, 1983).

Additional taps were also placed to facilitate velocity measurements using a PUDVEL. The flow channels were machined from 70 mm square, 150 mm long polymethyl methacrylate rods and consist of two sections each - an inlet and outlet for the aortic and mitral channels. The test valves, sutured to a machined stainless-steel holder are held between the two sections. The aortic sinuses were modelled as a circular axisymmetric groove rather than as individual sinuses to simplify fabrication. This was considered adequate as all the testing in this study has been limited to the mitral position as explained before (§ 1.7).

Previous investigators have designed the flow channels to accommodate a range of test valve sizes, usually from 21 to 27 for aortic and 25 to 33 mm (Yoganathan & Letzing, 1983; Weiting et al., 1969). This feature naturally leads to a discontinuity in diameter between the valve and the adjacent internal diameters of the channel. To avoid this problem, the mitral flow channel was specifically designed for a 27 mm sized valve and the aortic for a 23 mm valve. Many investigators have preferred the 27 mm size for evaluation (Knott *et al.*, 1988; Bruss *et al.*, 1983; Reul *et al.*, 1986; Yoganathan & Letzing, 1983) and considerable amount of data is available on this size for comparison. The aortic valve size of 23 mm was chosen to correspond to the mitral size of 27 mm.

4.7 FORCE TRANSDUCER DEVELOPMENT

i. Design considerations

The test valve in a mechanical pulse duplicator test system needed to be affixed to a holder using the valve's sewing ring to ensure that :

a) the valve was evaluated in its final configuration
b) there was no leakage path around the perimeter of the valve.
c) placement and removal of the test valve was easy.
d) the holder was thin and preferably no thicker than the valve cage itself to minimise obstruction for flow visualisation and velocity profile measurement.

In view of these considerations, many investigators have used valve holders which are 5 to 6 mm thick annular plates (Weiting et al., 1969; Yoganathan & Letzing, 1983).

ii. Transducer selection :

Force measurements can be carried out using a variety of transducers. With the limitations on size described above, the bonded strain-gauge technique seemed most practical. It would be ideal if strain-gauges could be directly bonded to the cage struts for direct measurements. However, the small size of the struts and the much larger strain-gauges presently available do not make this possible at present. Also, preparing a large number of different valve models would be very time consuming. Hence, an approach that seemed practical was to convert the valve holder into a transducer. Conversion of the annular plate

generally used to hold valves into a diaphragm type transducer with bonded strain-gauges mounted seemed the simplest approach.

iii. Dimensions & material of the annular diaphragm :

An annular diaphragm rigidly held at the outer edges and subjected to an axial load will have maximum radial strain at the outer edges like a beam. Also, a thinner diaphragm would naturally deflect more leading to higher strain. Hence, to obtain maximum sensitivity it was necessary to design for the largest and thinnest diaphragm possible. But the limitations were :-

i) The holder sealing diameter was limited to 60 mm in view of the test chamber dimensions (§ 4.4). The internal diameter had to be fixed at 28 mm to accommodate 27 mm mitral valves. With these limits, the practical dimensions of a valve holder/transducer was realised as shown in **Figure 4.7.**

ii) The need to immerse the transducer in the glycerine-water test fluid and local availability, limited the choice of the diaphragm material to stainless-steel.

With the radial dimensions of the diaphragm fixed, the next step needed was to estimate its thickness so that adequate sensitivity could be realised. To do this, it was first necessary to determine the minimum acceptable sensitivity based on the magnitude of the forces to be measured and the resolution required, keeping in mind the minimum acceptable signal level at the input of the strain bridge amplifier.

iv. Forces on prosthetic heart valves :

The pulsatile nature of flow and the valving action imposes a cyclic time dependent force on the valve. This can be

Figure 4.7

FORCE TRANSDUCER DIMENSIONS

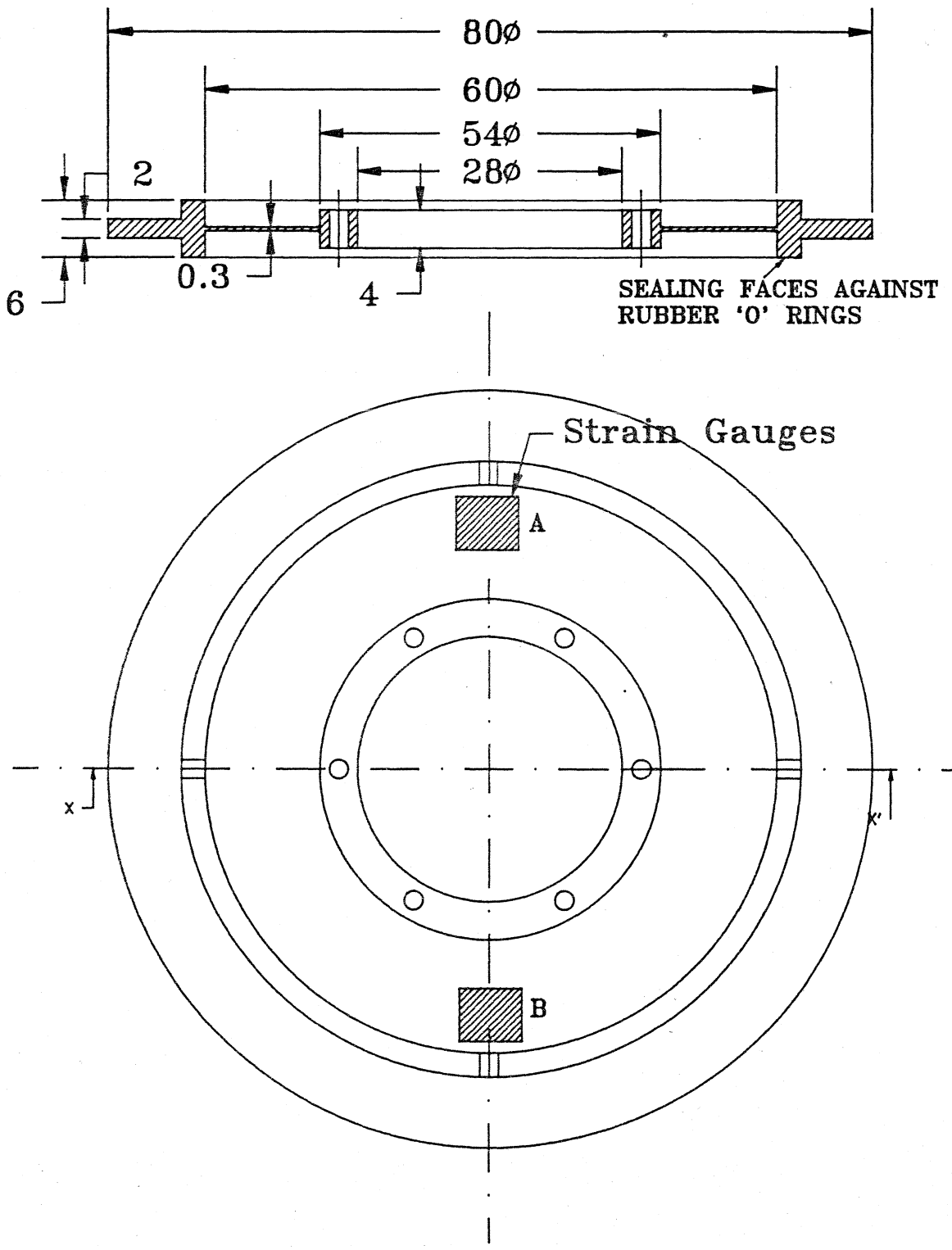

described as :-

a) A very small impact in the direction of the forward flow, when the valve opens.

b) A small drag force proportional to the forward pressure drop during the open phase of the valve.

c) A large impact in the direction of reversed flow during the valve closure.

d) A large drag force proportional to the pressure drop across the valve during its closed phase.

The smallest forces are during the forward flow phase. Peak pressure drops across 27 mm tilting disc valves are in the range of 5 to 10 mmHg for 5 to 7 lpm cardiac output. For a complete comparative study of the forces on different valves, it was felt desirable that these drag forces should be measurable. Hence, a transducer sensitivity that would enable the measurement of forces due to a pressure drop of 1 mmHg across the diaphragm was considered desirable.

v. Strain & signal considerations :

Bonded metal strain-gauges presently available for transducer applications have a gauge factor of 2 and a maximum linear range of 1000 micro-strains. A five volt excitation of the strain-gauge bridge is considered best from a point of thermal dissipation and temperature stability. A 5 volt excited full bridge then gives an output of 10 μV per micro-strain.

The low noise instrumentation amplifiers that were easily available had an input noise level of 0.8μV (INA101 of Burr-Brown). The 50 Hz mains frequency interference picked up by a

shielded cable of 3 metres length was found to be approximately 10 μV under laboratory conditions here.

Pulse duplicator measurements are generally carried out by computerised data acquisition with signal averaging over 32 to 64 cycles (Knott *et al.*, 1988; Yoganathan *et al.*, 1984). Hence, a signal to noise ratio of 2 was considered just acceptable.

This then placed the minimum acceptable signal at 20μV or 2 micro-strains for the 5 volt excited bridge. Thus, to be able to measure the force due to a 1 mmHg pressure difference, the average surface strain under the strain-gauges should be 2 micro-strains.

vi. Practical considerations :

The fabrication of good quality strain-gauge transducers requires considerable experience, especially in the mounting of the strain-gauges and their wiring. Hence, the help of the engineers at the transducer section of the Liquid Propulsion Systems Centre of Indian Space Research Organisation, Bangalore was sought. They advised that the minimum thickness of diaphragms of this size that could be fabricated was 0.2 mm and the stainless-steel used by them for transducers had the following physical properties :

Young's modulus : $E = 2 \times 10^5$ MPa

Poisson's ratio : $\nu = 0.28$

Further, the strain-gauges available were 3 mm wide and 3 mm long and if mounted close to the outer edge would result in a mean radial distance of 27 mm from the centre of the annular holder plate.

vii. Theoretical estimation of diaphragm thickness:

The strain at a point 'r' from the centre of an annular plate subject to a pressure difference and axial load can be calculated using the theory of bending of thin plates. The derivation of the equations for the strain in terms of the load applied, properties of the material and dimensions of the diaphragm are given in detail in Appendix A.

These equations were set up on a PC-AT compatible computer using a spread-sheet software. The strain could then be calculated for a given diaphragm thickness. By trial and error, a diaphragm thickness of 0.3 mm yielded a calculated strain of 2.07 microstrains, which is close to the required value.

viii. Fabrication & calibration :

Based on the above, two transducers, one with 0.2 mm and the second of 0.3 mm thick diaphragms were designed and fabricated. Each transducer has 8 strain gauges fixed on it to form two full bridges A and B (Fig.4.7). Each bridge consisted of two pairs of matched strain gauges; a pair being mounted on each surface of the diaphragm and opposite to each other.

The thinner one developed a stress concentration crack at the inner edge during its calibration and had to be discarded. The second one, which actually had a thickness of 0.32 mm yielded a measured output sensitivity of 13 μV/mmHg. This is within 35% of the theoretical estimated output of 20 μV/mmHg.

One of the reasons for the lower sensitivity was the fairly thick multi-layer protective coating over the strain-

gauges, which was necessary to protect them from corrosion. This involved 4 layers of a thin epoxy coating, a layer of teflon and then a thick layer of silicone rubber adhesive as recommended by the gauge manufacturer. The data on the force transducer calibration is given Appendix B.

Figure 4.8 shows the force transducer in its final form. Individual 4 core shielded cable connections were provided from each of the two bridges, A and B as seen in the figure.

~~~~~~
~~~~~~

Figure 4.8

THE FORCE TRANSDUCER

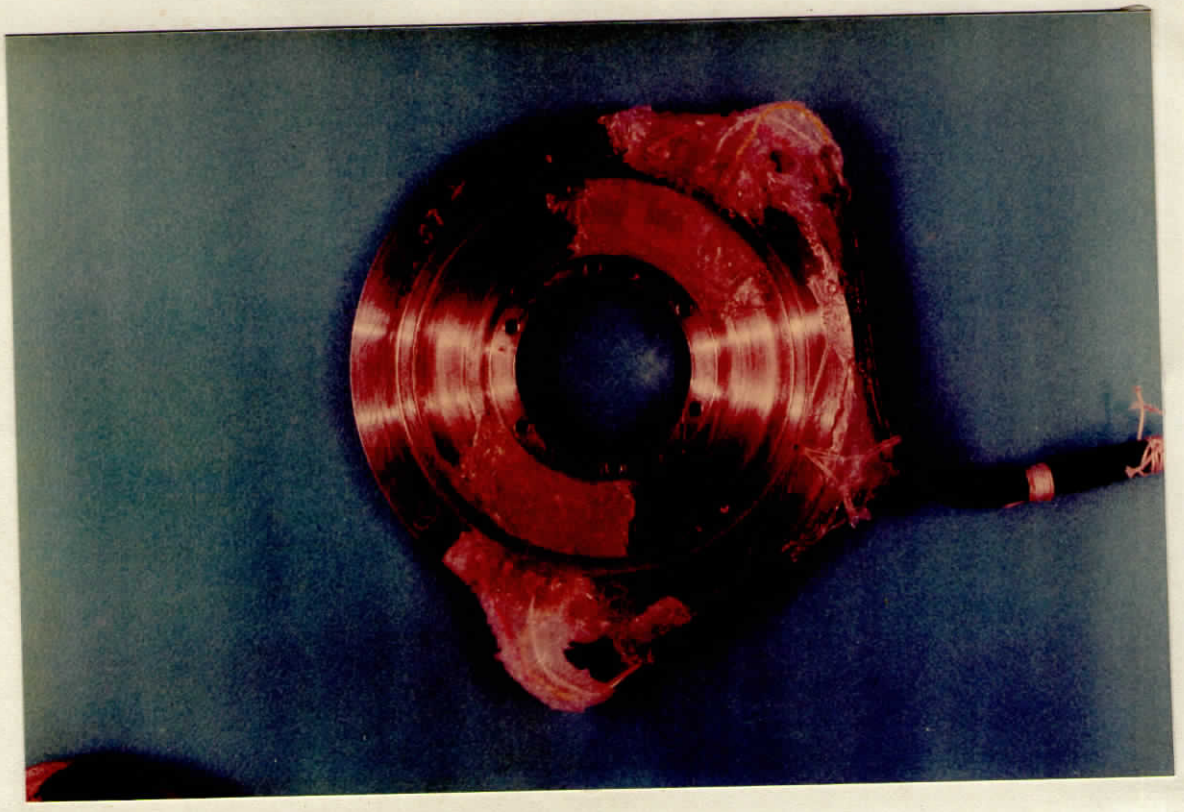

CHAPTER 5

STEADY FLOW EVALUATION

5.1 EXPERIMENTAL SETUP

Figure 5.1 is a schematic of the steady flow system used for pressure drop and drag force measurements. It consists of the Mitral flow channel connected on its inlet side to a constant level tank via a venturi flow probe and a 1.5 metre long straight entrance section. The outlet of the test channel was connected to a flow control valve, which discharged into the main reservoir. The entrance section had the same internal diameter as the inlet side of the mitral test channel. This ensured that the flow entering the channel had reached a steady state with a stable velocity profile.

Accurate metering of the flowrate was obtained using a venturi flow probe. The design of the probe and its calibration data are given in Appendix C. Semiconductor differential pressure transducers were used for obtaining the pressure drop signals across the valve, venturi probe and the force transducer. The pressure drop and force signals were acquired by a PC-AT compatible computer. The signals were digitised using an analog to digital converter board plugged in the computer. This instrumentation is described in detail in following sections.

Figure 5.1

SCHEMATIC OF STEADY FLOW SYSTEM

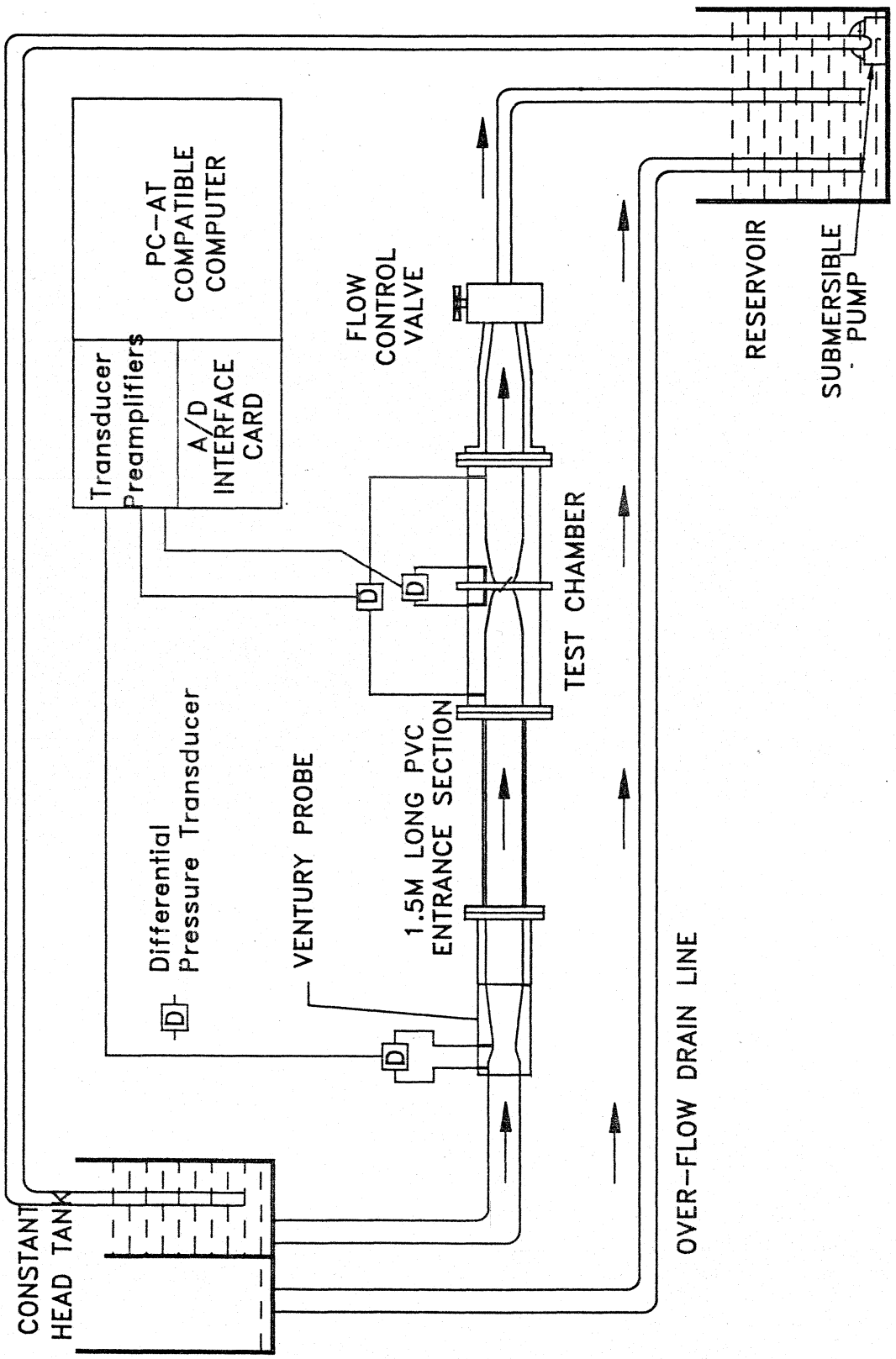

THE STEADY FLOW SETUP

5.2 INSTRUMENTATION

i. Venturi Tube flow meter :

EM flowmeters are generally the measurement system of choice for most investigators of artificial heart valves because of its good frequency response for pulsatile measurements and ability to distinguish between forward and reverse flow. However, these flow meters suffer from one main drawback - the impedance of the probe is extremely high like a pH-electrode. Because of this, the measurement system is susceptible to noise, especially mains frequency 50 Hz and zero drift. Generally, the overall accuracy is about ±5 %. A few investigators have used rotameters, which can give an accuracy of 2% of the full scale.

To improve the accuracy of the steady flow measurement over that of the available EM flowmeter, a Venturi tube was designed as recommended by the American Society for Mechanical Engineers (ASME, 1971). The probe was machined in perspex. The pressure drop of the probe was measured using a semiconductor differential pressure transducer and amplifiers, which are described in more detail in the following section. The probe was calibrated in-situ in the steady flow system by carefully timed collection. The design and calibration details are given **Appendix-C.** A parabolic least square curve, fitted to the data points was used for the actual flow settings and measurements during the testing. As can be seen the fit was excellent. Because of the square law relationship between the flow and pressure drop, the accuracy of the setting/measurement at high flowrates, especially above 10 lpm was very good.

ii. Pressure drop measurements :

The pressure drops across test valves, the venturi tube, the air flow meter (used in pulsatile tests) and across the force transducer were all measured using Semiconductor Differential Pressure Transducers. The pressure drops across the test valves and the force transducer in both steady flow and pulsatile flow tests were measured using the Sensym LX1601D signal conditioned transducer, while the other two were measured using LX06005D temperature compensated transducers. The LX1601D transducers have a built-in amplifier to minimise ambient noise pickup and provide an amplified output at 1 volt/psi. The LX06005D are temperature compensated sensors, providing a signal output of 10mV/psi, thus requiring signal amplification.

These transducers were mounted in a machined perspex holder as shown in **Figure 5.2.** Using vacuum, the transducers were back filled with silicone oil to protect them from water ingress. Standard luer fittings fixed to the perspex holders enabled fluid coupling to the test points using equal lengths of rigid polyethylene tubings. The very high frequency response and the high sensitivity of these transducers enable accurate differential pressure measurements better than ± 0.1 mmHg.

iii. Preamplifiers for force transducer :

Low noise instrumentation amplifiers (Burr-Brown INA101) were used at a gain of 1000 to amplify the low level signals from the force transducer. The output signals of the instrumentation amplifiers were buffered with unity gain followers before being fed to the A/D card of the computer.

Figure 5.2

DIFFERENTIAL PRESSURE TRANSDUCER ASSEMBLY

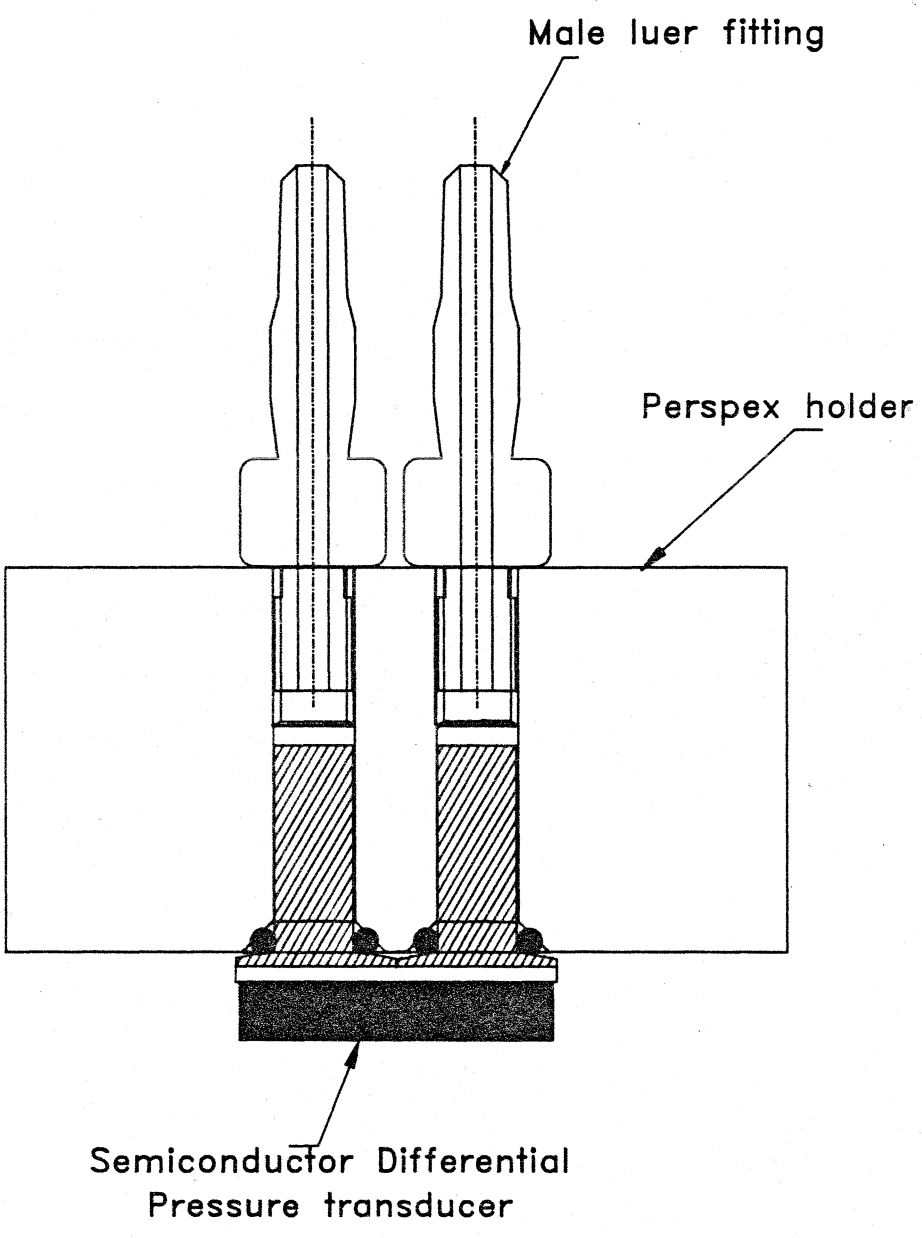

iv. Computerised Data Acquisition hardware & software

Fig.5.1 also shows the data acquisition hardware employed for the steady flow and pulsatile tests. The pressure, force and flow-meter signals were amplified & fed to the PC-AT compatible computer (Aurelec 2AT6-XL) through a 12 bit analog to digital converter card (Metrabyte DASH16). Steady flow data were acquired at 200 samples/sec per channel for 10 seconds and averaged.

Data acquisition was carried out using menu driver programmes written under the ASYST Ver.3.0 data analysis and acquisition software package. ASYST is a very versatile software base providing simple routines for data acquisition, control and analysis. The averaged data were then converted to Lotus123 compatible worksheet files. The final analysis and plotting were done using spreadsheet software.

5.3 PRESSURE DROP AND FORCE MEASUREMENTS

Pressure drop and drag force measurements were made under steady flow rates of 0 to 35 lpm in the mitral channel. The pressure drops across the test valve was measured at wall taps P_1 & P_2 as shown in Fig.4.6 using a differential pressure transducer. The connections were made using equal lengths of rigid polyethylene tubing filled with the test fluid. The two force signals, one from each bridge on the force transducer and the pressure drop across the force transducer diaphragm (from pressure taps P_3 & P_4) were acquired. The flow settings were

made using this calibration curve for the venturi tube (appendix C).

Measurements were taken at 5 lpm steps starting at 35 lpm and coming down to zero. At each measurement point, data were acquired at 200 samples/s for 10 seconds (total 2000 samples). The mean and standard deviation of these 2000 samples for each signal was calculated and stored in hard disk memory. The signal zero's were recorded at the start and end of each run to ensure that there was no significant zero shift.

i. Drag force calculations :

During steady flow through the test valve, the force transducer deflects due to two forces acting on it as shown in **Figure 5.3(a)** :

a) due to the drag force on the valve - F_d
b) due to the pressure difference across the transducer diaphragm - $F_{\Delta p}$

The actual measured signal is a sum of the two forces and hence to determine the drag force on the valve, the force $F_{\Delta p}$ due to the pressure drop has to be subtracted.

To achieve this, a static differential pressure calibration of the force transducer was carried out by blocking the central orifice of the transducer as shown in **Figure 5.3(b)**. The transducer was mounted in the mitral chamber held vertically and filled with water. The pressure drop across the force transducers (from taps P_3 & P_4) and the force signals due to this differential pressure (V_{PR}) were measured for different heads of the water column. This signal corresponds to the total

Figure 5.3(a)

DRAG FORCE MODEL

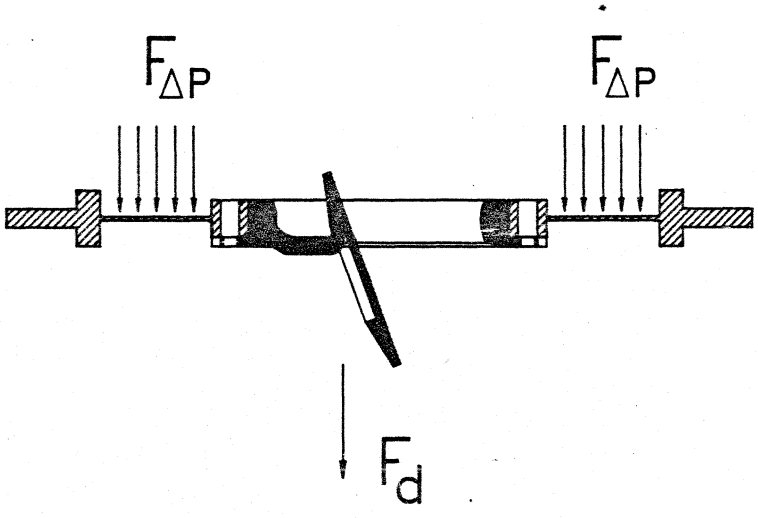

$$F_T = F_{\Delta P} + F_d$$

F_T = Total force on transducer due to pressure difference & drag on disc

$F_{\Delta P}$ = Force on transducer diaphragm due to pressure drop (ΔP)

F_d = Drag force on the valve due to fluid flow through it

Figure 5.3(b)

STATIC DIFFERENTIAL PRESSURE CALIBRATION

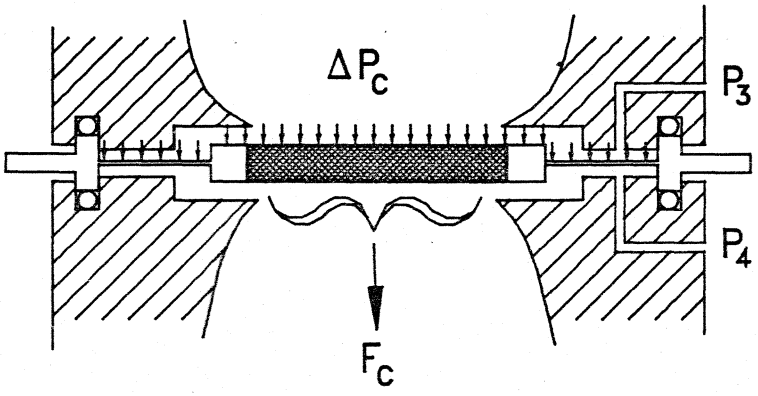

ΔP_C = Pressure of fluid column

F_C = Force on valve mounting area

= $\Delta P_C \times A_C$, A_c is the area of central orifice

C_F = Static calibration factor for transducer

V_c = F_C / C_F , voltage signal corresponding to F_C

$V_{\Delta P} = V_{PR} - V_C$

V_{PR} = Total signal due to liquid column

$V_{\Delta P}$ = Signal due to pressure on diaphragm alone

force on the diaphragm including the valve mounting central area of 28 mm diameter. The force on this central area (F_c) was calculated from the measured pressure drop and its equivalent force signal V_c obtained from the static force calibration curve (Appendix B). Subtracting the latter (V_c) from the total signal due to the differential pressure (V_{PR}) gave the Force offset $V_{\Delta P}$ due to the pressure drop across the diaphragm.

This correction was employed to determine the drag force from the measured total signal in steady flow measurements.

ii. Components & Valve Models tested under Steady Flow :

The components and valves that were tested under steady flow conditions are :-

i. Brass rings with entrance/exit radii and straight bore as shown in Fig. 4.2. This was followed by a cage (i.e., with struts added) and a valve (i.e., a cage with disc added) to determine the increase in pressure drop due to these additions.

ii. Chitra valve with opening angles set between 45° and 85° (in steps of 5°). The different opening angles were obtained by manually adjusting the major struts in the plane of the cage. The opening angles were measured with templates and were within ± 2°.

iii. Test valves Nos. 1 to 8. In these valves, the cage struts were positioned to limit the disc opening angle to a maximum of 75°. The effect of disc sliding was obtained by using discs with 2 mm larger well diameters in cages No.4 and No.5 (Fig.4.4).

iv. Effect of disc shape on opening angle. Discs of different shapes as shown in Fig. 4.3 were inserted in test valve cage No.1. In the second series, the discs (with suitably reduced well diameters) were inserted in test valve cage No.5. In both these series, the opening angle was limited to a maximum of 75°, mechanically by the major struts.

v. Standard valves (Fig. 4.5).

5.4 RESULTS & DISCUSSION

i. Entrance & exit curvature of the cage ring :

Pressure drop across the rings with entrance, exit curvature and straight bore are shown in **Figure 5.4.** The results show that the present practice of providing a radius at both the inlet and outlet edges of the cage as in the Bjork-Shiley, Medtronic-Hall and Chitra valves results in higher pressure drops than that with only the entrance curvature. The straight bore ring as used in the St. Jude valve results in still higher pressure drops while that with exit curvature shows the highest losses.

From the fluid dynamic point of view, these results are not surprising, when one considers the cage ring to be a Flow Nozzle. The recommended form of a flow nozzle is a radius or elliptical inlet and a cylindrical throat extending up to its exit. There must no bell mouth or diameter increase near the outlet end (ASME, 1971). The radius at the exit of the ring causes an

Figure 5.4

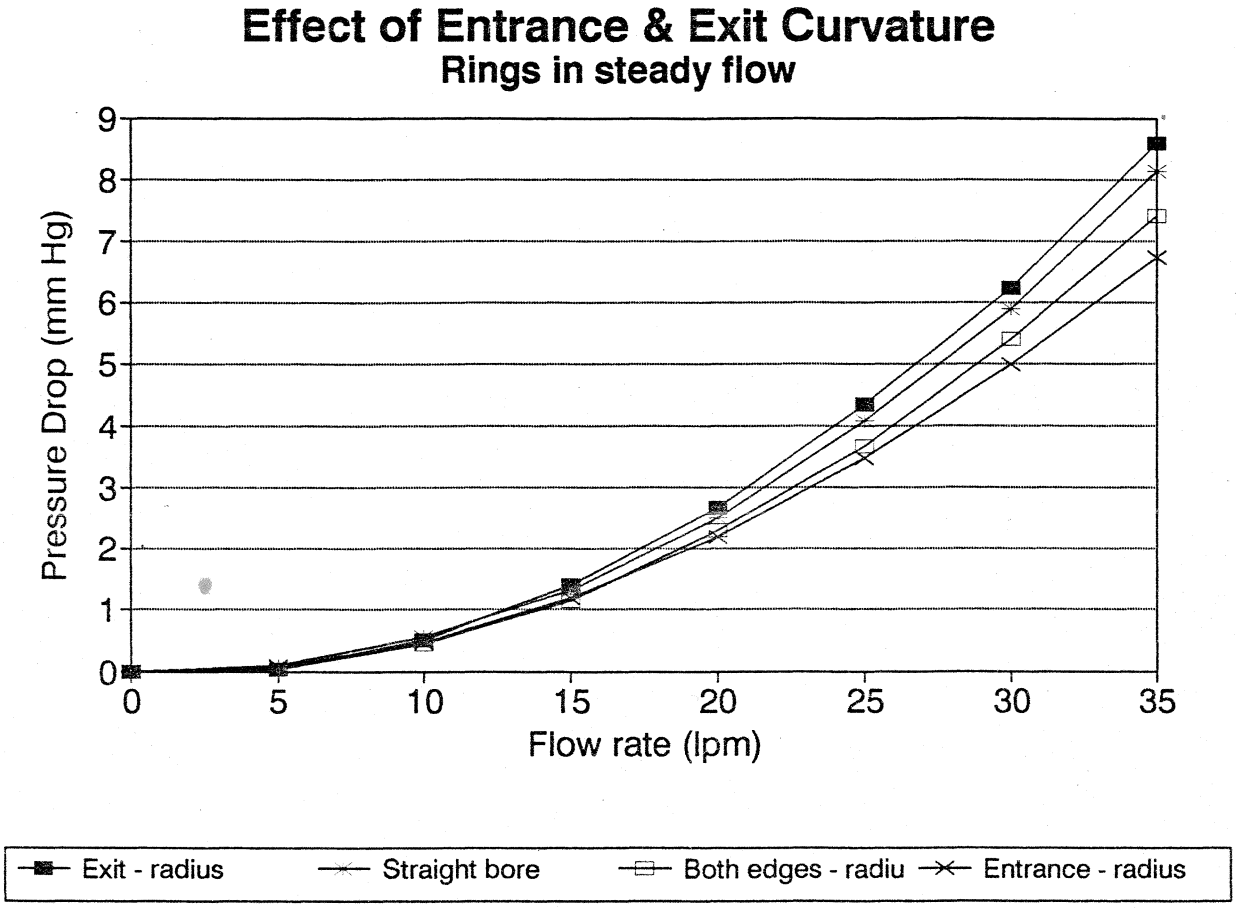
Effect of Entrance & Exit Curvature
Rings in steady flow
Pressure Drop (mm Hg)
0
1
2
3
4
5
6
7
8
9
0
5
10
15
20
25
30
35
Flow rate (lpm)
Exit - radius
Straight bore
Both edges - radiu
Entrance - radius

adverse pressure gradient and can lead to flow separation at the ring exit edge, causing higher pressure loss if the curvature is not carefully controlled.

ii. Effect of introducing Struts and Disc :

The pressure drop across a ring, plain cage (Cage = ring + struts) and a valve (Valve = cage + disc) are shown in **Figure 5.5.** It is clear that the major percentage of the pressure drop increase is due to the disc, while the struts contribute less. The reduction in diameter of the flow area due to the sewing ring and the cage itself causes about 50 % of the overall pressure drop. This is clearly due to the fact that the pressure drop across an orifice is inversely proportional to the fourth power of its diameter (Gentle, 1977). Profiling the struts in the direction of flow to give an aerofoil, teardrop or elliptical shape to minimise their contribution will definitely be helpful. However, a major improvement could be obtained by reducing the pressure drag of the disc by suitable design.

iii. Effect of Disc Opening Angle :

Figure 5.6 shows the effect of increasing the opening angle of the disc on pressure drop at flow rates from 10 to 35 lpm; the pressure drop reducing with increasing opening angle at a given flow rate as expected from fluid dynamic theory. At flow rates of 15 to 25 lpm, there is 'knee' around 60°, beyond which the reduction in pressure drop is only marginal. However, at

Figure 5.5

EFFECT OF STRUTS & DISC

Steady flow testing

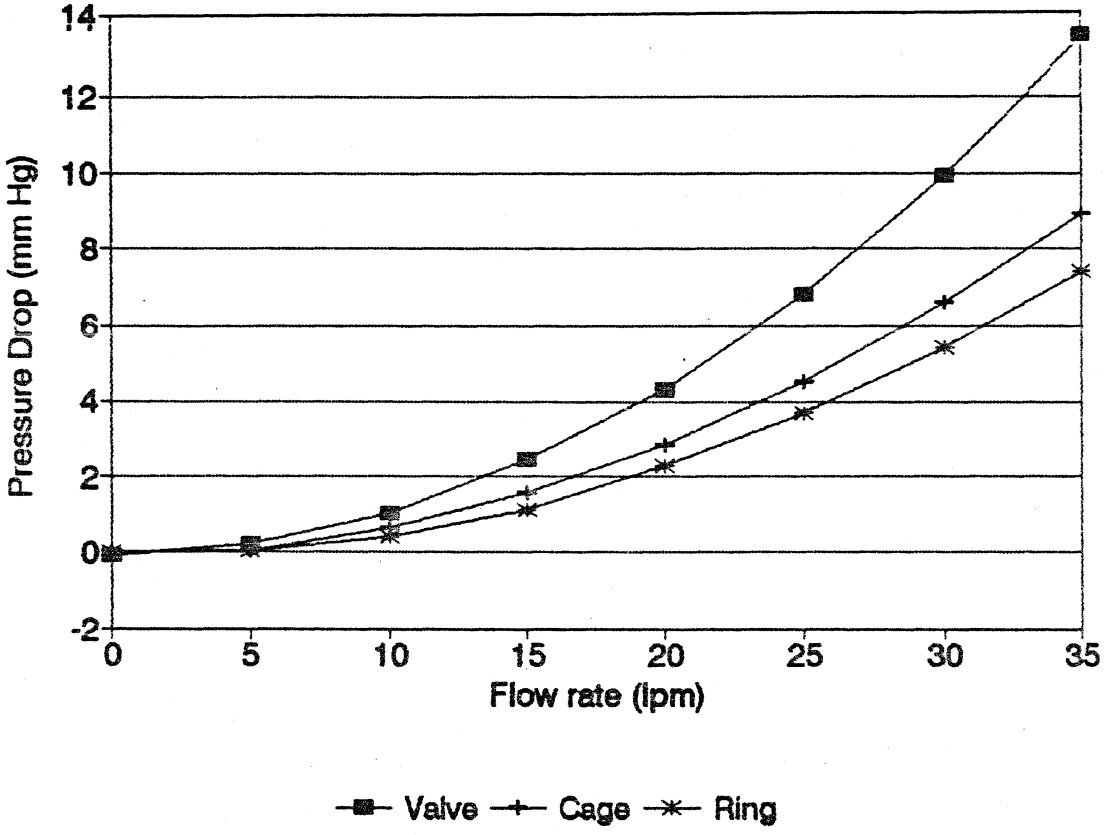

Figure 5.6
PRESSURE DROP and OPENING ANGLE
Chitra Valve in Steady Flow

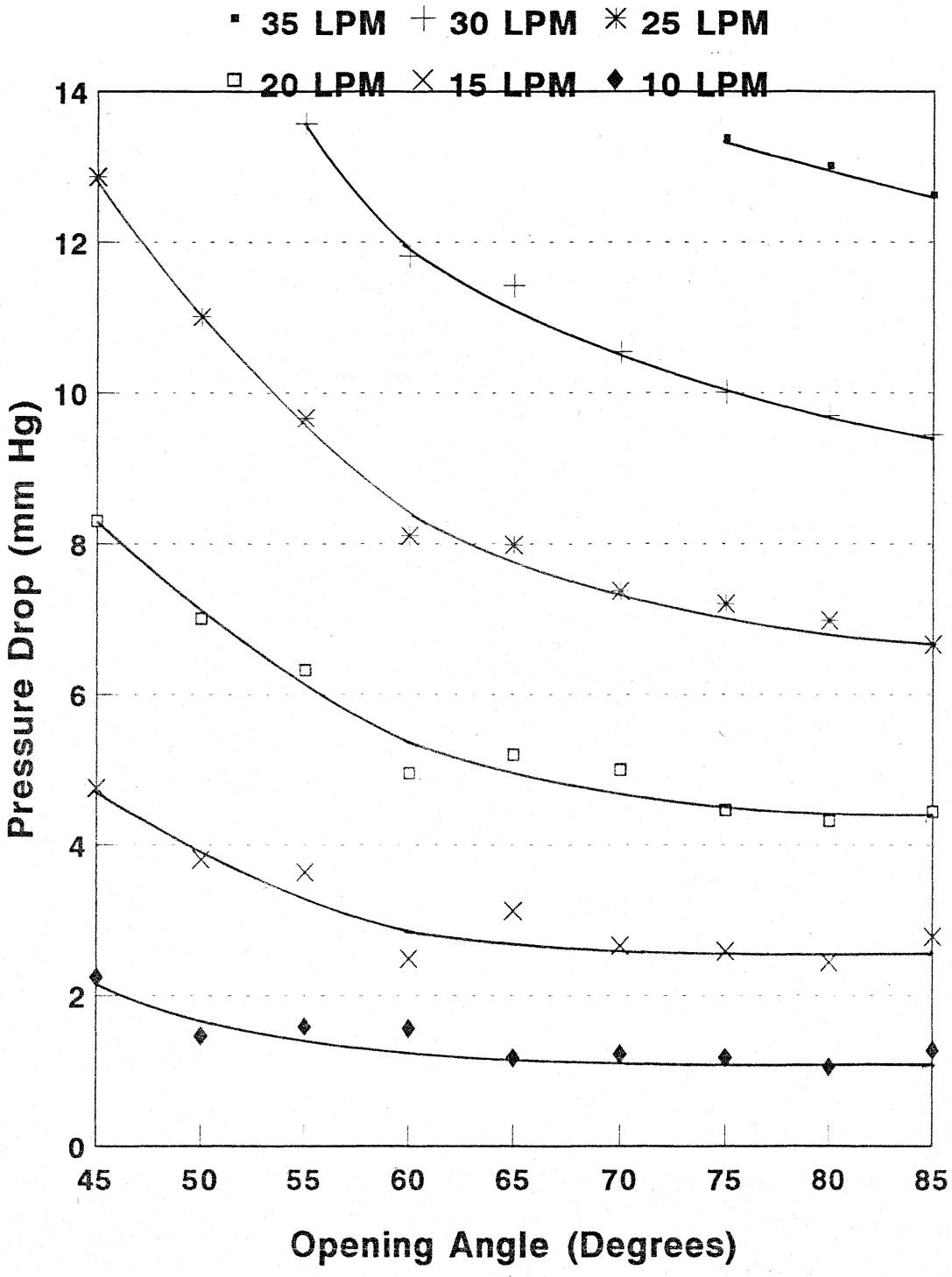

Curve fit by eye judgement

higher flow rates over 25 lpm, the reduction in pressure drop is not negligible. The currently used values of 70 to 75° seems a reasonable compromise between minimum pressure drop and closing regurgitation. Bjork (1969) has reported a minimum pressure drop at 68° opening angle and at larger opening angles, the pressure drop increased substantially. This is inconsistent with the general expectations from fluid dynamic theory. In Fig.5.6, a small variation at 60° is seen; however this is within the experimental error. Wada *et al.*, (1969) have reported that there was no significant improvement to flow resistance beyond 75° to 80°, which is in agreement with the present results.

iv. Effect of Pivot Location :

Under steady flow conditions of 0 to 35 lpm, test valves TV-11 to TV-88, TV-42, TV-53 and valves with concavo-convex discs TV-5C to TV-8C were found to open to different angles as shown in **Figure 5.7.** It was noticed that the disc reached a stable opening angle at a very low flowrate of 1 lpm and there was no further change in the opening angle at higher flow rates. Where the opening angle was determined by fluid forces, the disc fluttered over an angle of 5° to 10° due to the onset of turbulent flow conditions around 10 lpm[1]. However, where the opening angle was limited by the struts of the valve, there was no flutter even at the high flow rate of 35 lpm. The opening angle was estimated by using triangular templates. The error was estimated to be ±3°.

---

[1]Reynolds no. is 3300 at 10 lpm & disc dia of 22 mm

higher flow rates over 25 lpm, the reduction in pressure drop is not negligible. The currently used values of 70 to 75° seems a reasonable compromise between minimum pressure drop and closing regurgitation. Bjork (1969) has reported a minimum pressure drop at 68° opening angle and at larger opening angles, the pressure drop increased substantially. This is inconsistent with the general expectations from fluid dynamic theory. In Fig.5.6, a small variation at 60° is seen; however this is within the experimental error. Wada *et al.*, (1969) have reported that there was no significant improvement to flow resistance beyond 75° to 80°, which is in agreement with the present results.

iv. Effect of Pivot Location :

Under steady flow conditions of 0 to 35 lpm, test valves TV-11 to TV-88, TV-42, TV-53 and valves with concavo-convex discs TV-5C to TV-8C were found to open to different angles as shown in **Figure 5.7.** It was noticed that the disc reached a stable opening angle at a very low flowrate of 1 lpm and there was no further change in the opening angle at higher flow rates. Where the opening angle was determined by fluid forces, the disc fluttered over an angle of 5° to 10° due to the onset of turbulent flow conditions around 10 lpm[1]. However, where the opening angle was limited by the struts of the valve, there was no flutter even at the high flow rate of 35 lpm. The opening angle was estimated by using triangular templates. The error was estimated to be ±3°.

---

[1]Reynolds no. is 3300 at 10 lpm & disc dia of 22 mm

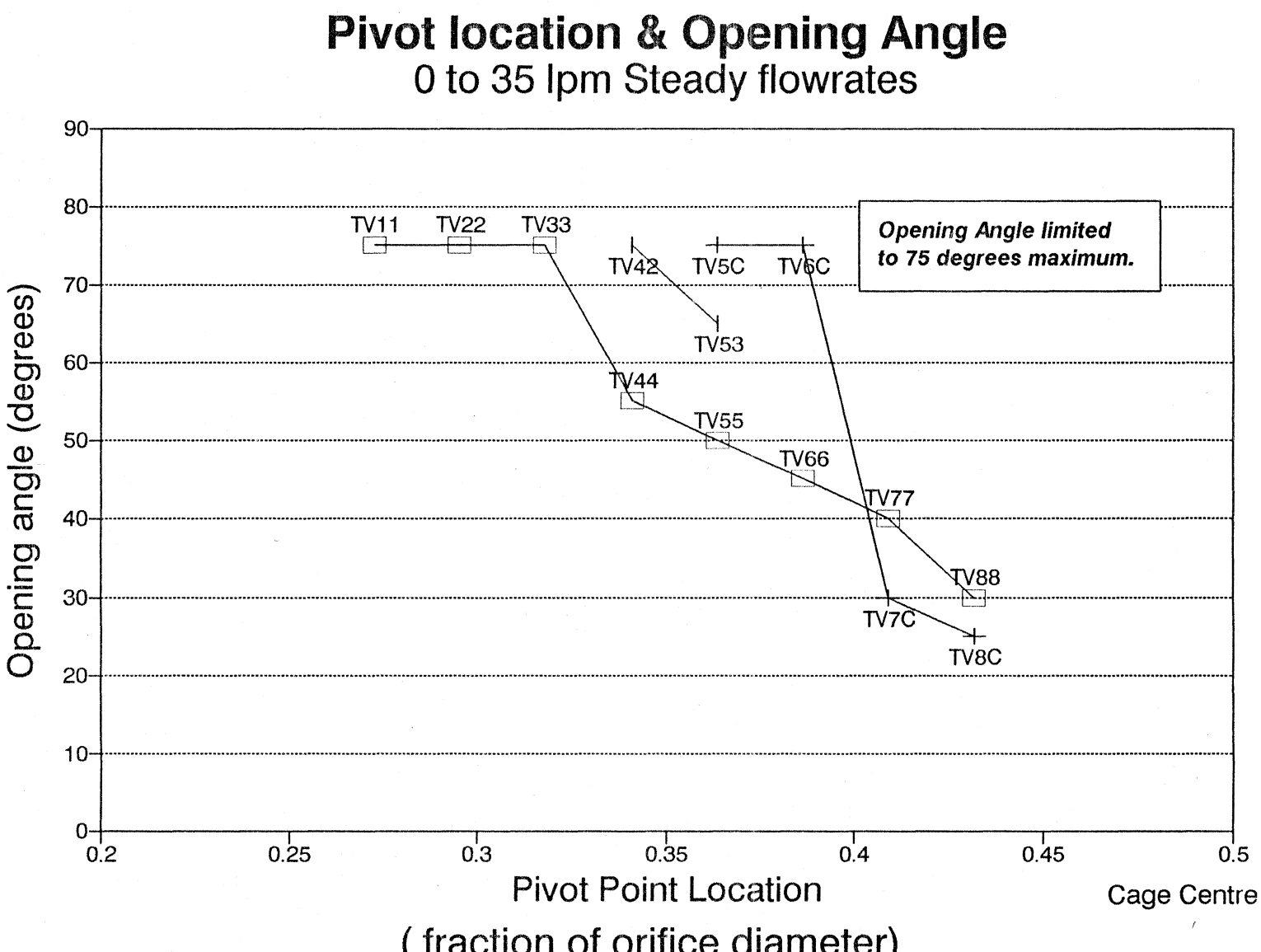
Pivot location & Opening Angle
0 to 35 lpm Steady flowrates
Opening angle (degrees)
90
80
70
60
50
40
30
20
10
0
0.2
0.25
0.3
0.35
0.4
0.45
0.5
Pivot Point Location
(fraction of orifice diameter)
Cage Centre
TV11
TV22
TV33
TV42
TV5C
TV6C
TV53
TV44
TV55
TV66
TV77
TV88
TV7C
TV8C
Opening Angle limited
to 75 degrees maximum.

Figure 5.7

As the pivot axis was moved towards the centre of the cage, test valves TV-11, TV-22 & TV-33 (with plano-convex disc) opened fully to 75° while the others (TV-44 to TV-88) opened less; the angle in these latter valves being determined by the fluid forces rather than the mechanical stoppage of the cage struts. It is clear from this data that the centre of pressure, which lies at the centre of the disc in the closed position, moves towards the leading edge (or inlet edge) as it tilts open. The disc reaches a stable opening angle, when the centre of pressure reaches the pivot point (provided the disc is not mechanically stopped). The line joining the points of the valves TV-11 to TV-88 is thus the locus of the centre of pressure at various opening angles for the plano-convex shaped disc. This data is in agreement with the predictions for flat discs by McQueen & Peskin (1983) from computer simulation and with the experimental data of Pierce *et al.*, (1968). The latter have reported that at a pivot axis location of 0.36 diameter from the leading edge, the flat disc opened only to 45° and larger opening angles were obtained with aerofoil shaped discs. In the present study, valve TV-55 with a plano-convex disc and a pivot axis location of 0.365 diameter opened to 50°.

Allowing the disc to slide 1 mm downstream leads to an increased opening angle for the same pivot location; for in this case, the centre of pressure has to move another 1 mm towards the leading edge before it reaches the pivot, as seen for valves TV-42 and TV-53.

The concavo-convex shaped discs behaved differently. While valves TV-5C and TV-6C opened fully to 75°, TV-7C and TV-8C

opened considerably less. The transition from full opening to reduced opening is also sharper than the plano-convex case. This effect of the centre of pressure remaining near the centre of the disc due to aerofoil shapes has been indicated in the work of Pierce *et al.*, (1968) and clearly explained by Knight (1973) using thin aerofoil theory. The computer simulation study by McQueen & Peskin (1983) clearly predicts this behaviour of the curved disc.

Figure 5.8 shows the pressure drop against flowrate for some of the practical valve designs. TV-44, which opened to about 55° shows a significantly higher pressure drop. Amongst the valves which opened fully, the difference is very small. TV-53, which opened to about 65° also shows a comparable pressure drop.

v. Effect of Disc Shape :

The disc shape has considerable effect on the opening angle as shown in **Figure 5.9.** These data underscore the fact that, in concavo-convex shaped discs, the centre of pressure remains much closer to the centre of the disc than in the original standard or mesa shaped discs of the Bjork-Shiley valve. This results in a significant increase in the opening moment on the disc.

vi. Standard Valves :

Figure 5.10 gives the data on the standard valves. Among the standard valves, the Starr-Edwards ball valve showed the

Figure 5.8

PRESSURE DROP OF TEST VALVES

Steady flow testing

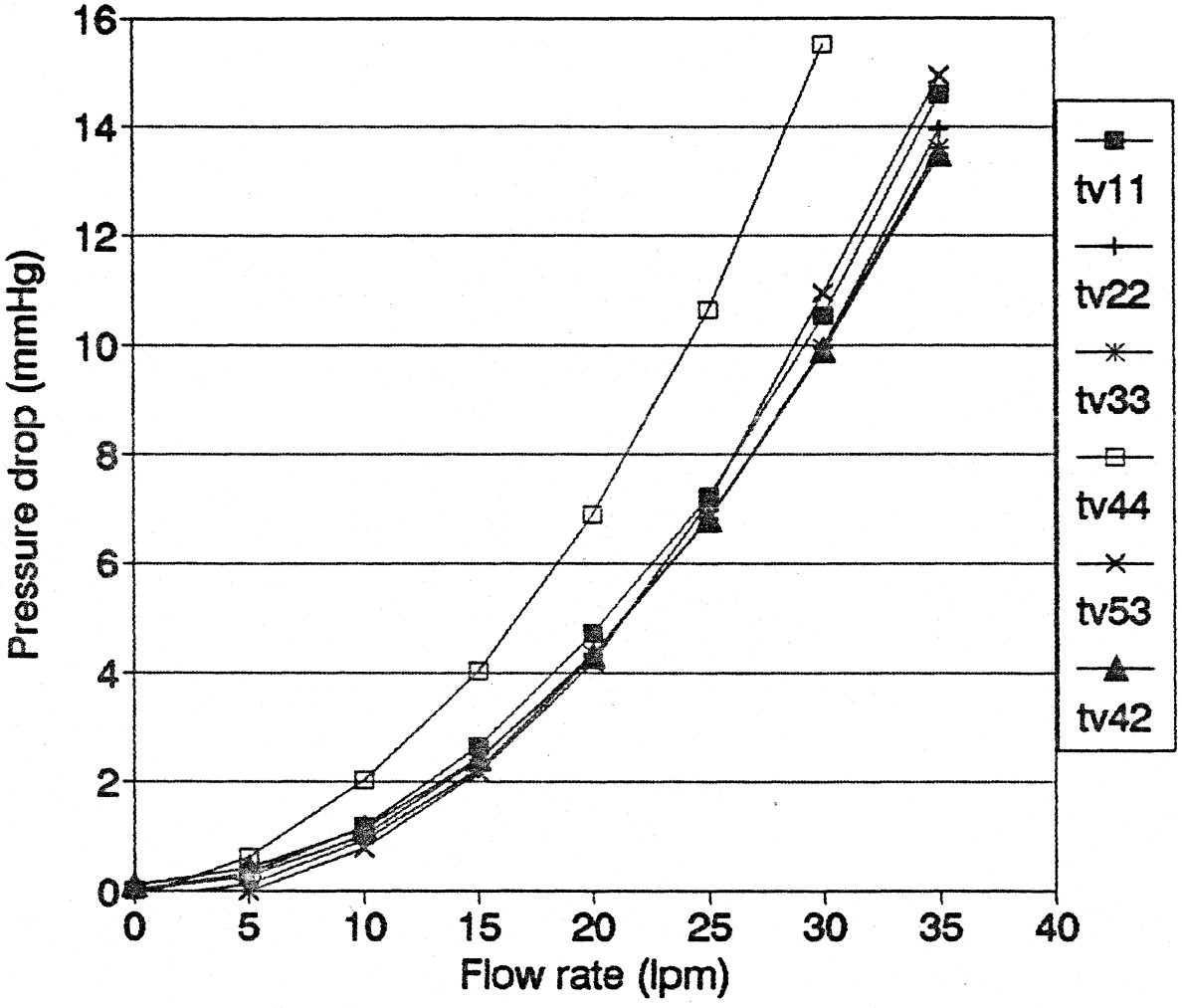

Figure 5.9

EFFECT OF DISC SHAPE

Pivot location = 0.273 diameters from leading edge.
Standard Valves
35 lpm Steady flow

		Opening Angle
B–S Standard disc	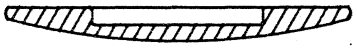	57°
Mesa shaped disc	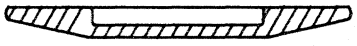	60°
Parallel disc	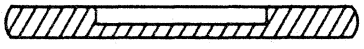	73°
Plano–Convex disc	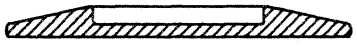	75° **

Pivot location = 0.364 diameters from leading edge.
Test Valves
30 lpm Steady flow

Mesa shaped disc	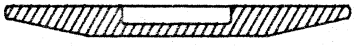	45°
Plano–Convex disc	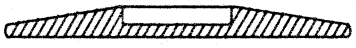	50°
Concavo–Convex disc	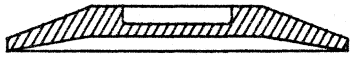	75° **

** Opening angle limited to a maximum of 75° by valve cage.

Figure 5.10

PRESSURE DROP OF STANDARD VALVES

Steady flow testing

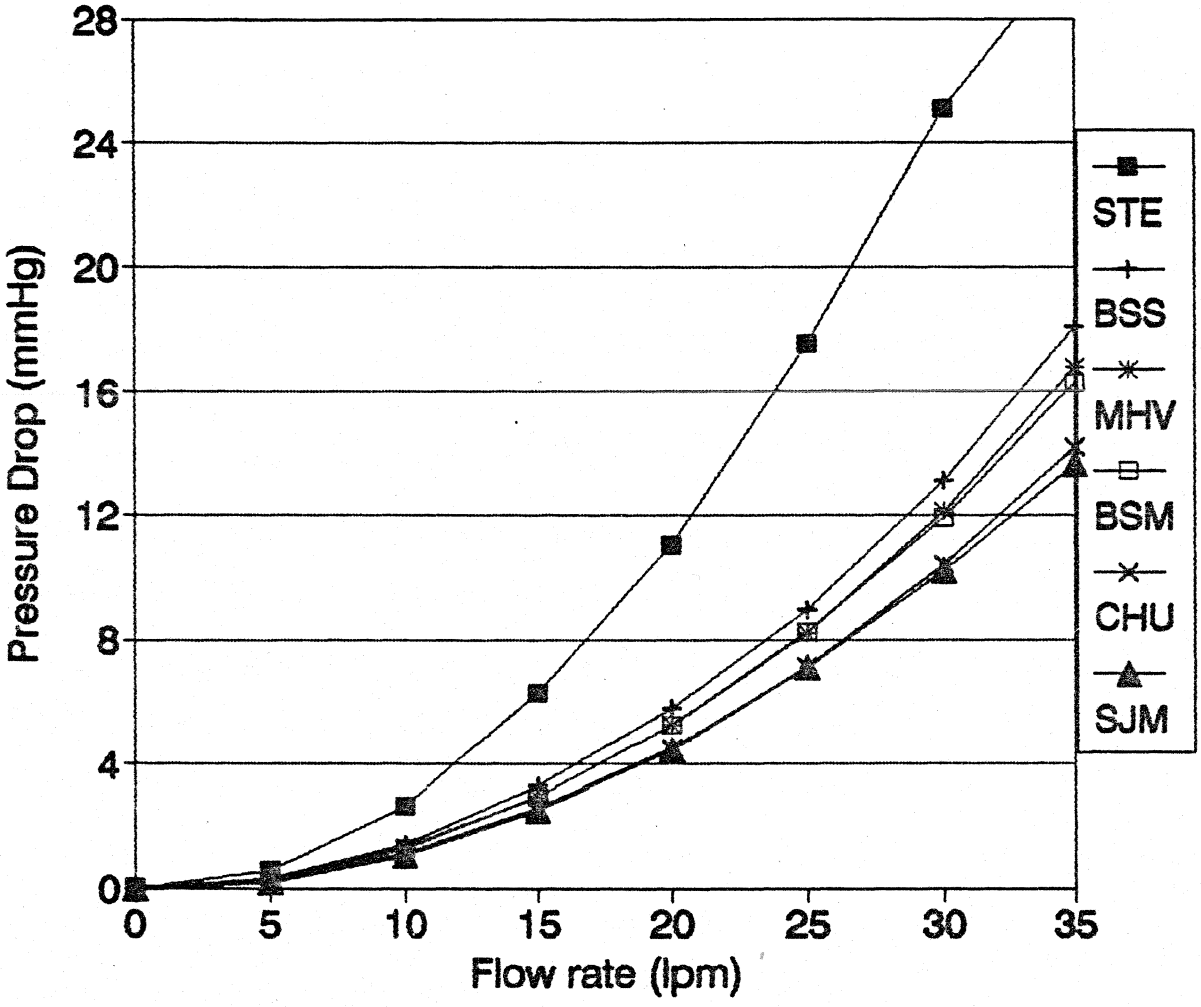

highest pressure drop due to its lower orifice diameter. Next was the Bjork-Shiley standard valve, which has a higher pressure drop than the other tilting disc valves due to its lower opening angle of 60°. A mild flutter was noticed at higher flow rates showing that for this disc shape, the centre of pressure is just at the pivot point at full opening. The Medtronic-Hall valve also showed a similar flutter at its opening angle of 70° while the Bjork-Shiley monostrut with its concavo-convex disc did not show any. Woo & Yoganathan (1986) have reported a similar observation that the occluder of the MHV was oscillating during diastole under pulsatile testing in the mitral position of a pulse duplicator and indicate that the flow could become non-stationary. The M-H valve is able to open to 70° inspite of its more central pivot location and a flat disc shape due to the presence of disc sliding. As shown by many workers, the St.Jude valve exhibited the lowest pressure drop, while the Chitra valve showed marginally higher. The higher pressure drop of the BSM valve than the Chitra valve is probably due to use of thicker struts. However, it should be noted that these differences between the tilting disc valves are marginal from a clinical point of view.

vii. Drag Forces :

In general, the drag forces are proportional to the pressure drop across the valves as seen in **Figures 5.11 & 5.12** for test and standard valves respectively. This is as expected from fluid mechanical considerations. The only inconsistent point is the reversal of trend for the SJM in comparison to CHU. The

Figure 5.11

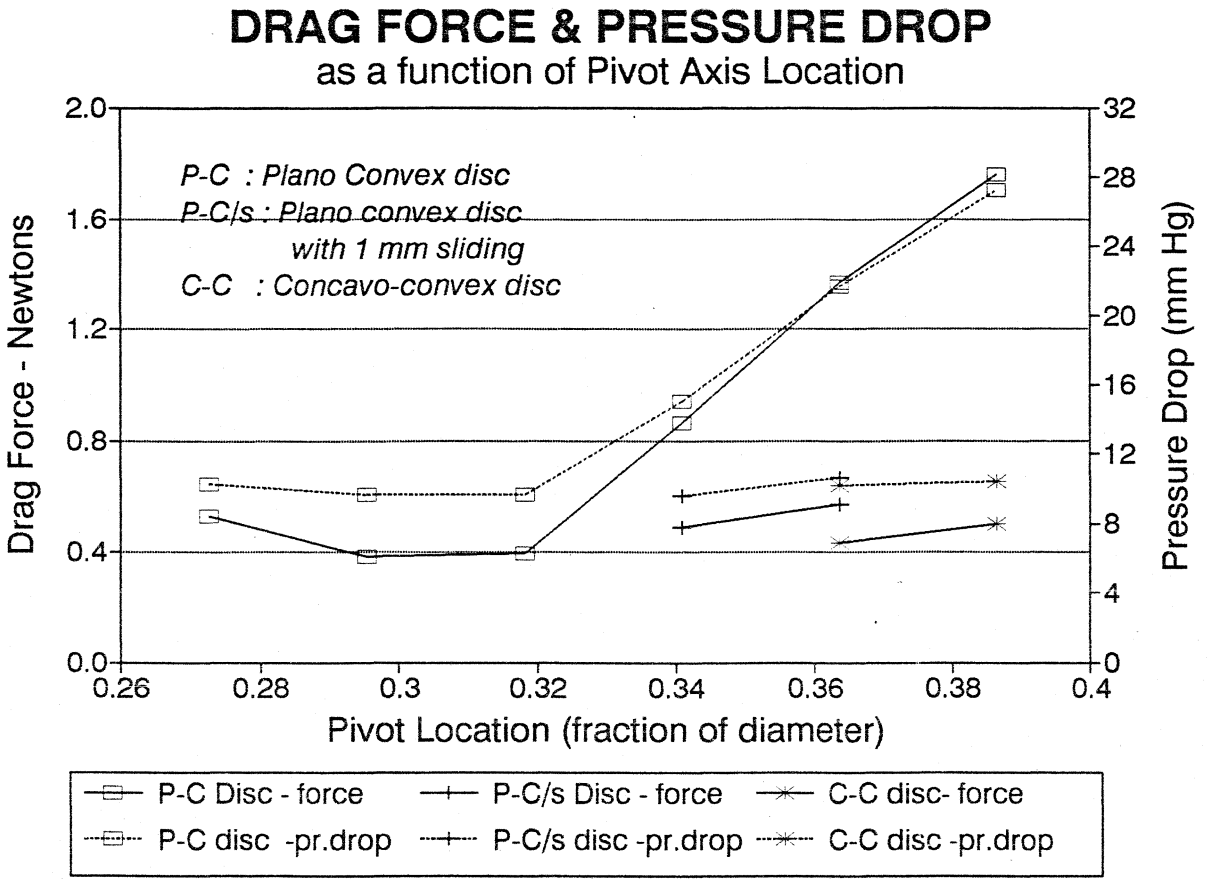
DRAG FORCE & PRESSURE DROP
as a function of Pivot Axis Location
P-C : Plano Convex disc
P-C/s : Plano convex disc with 1 mm sliding
C-C : Concavo-convex disc
Drag Force - Newtons
Pressure Drop (mm Hg)
Pivot Location (fraction of diameter)
2.0
1.6
1.2
0.8
0.4
0.0
32
28
24
20
16
12
8
4
0
0.26
0.28
0.3
0.32
0.34
0.36
0.38
0.4
P-C Disc - force
P-C/s Disc - force
C-C disc- force
P-C disc -pr.drop
P-C/s disc -pr.drop
C-C disc -pr.drop

Figure 5.12

DRAG FORCE ON STANDARD VALVES

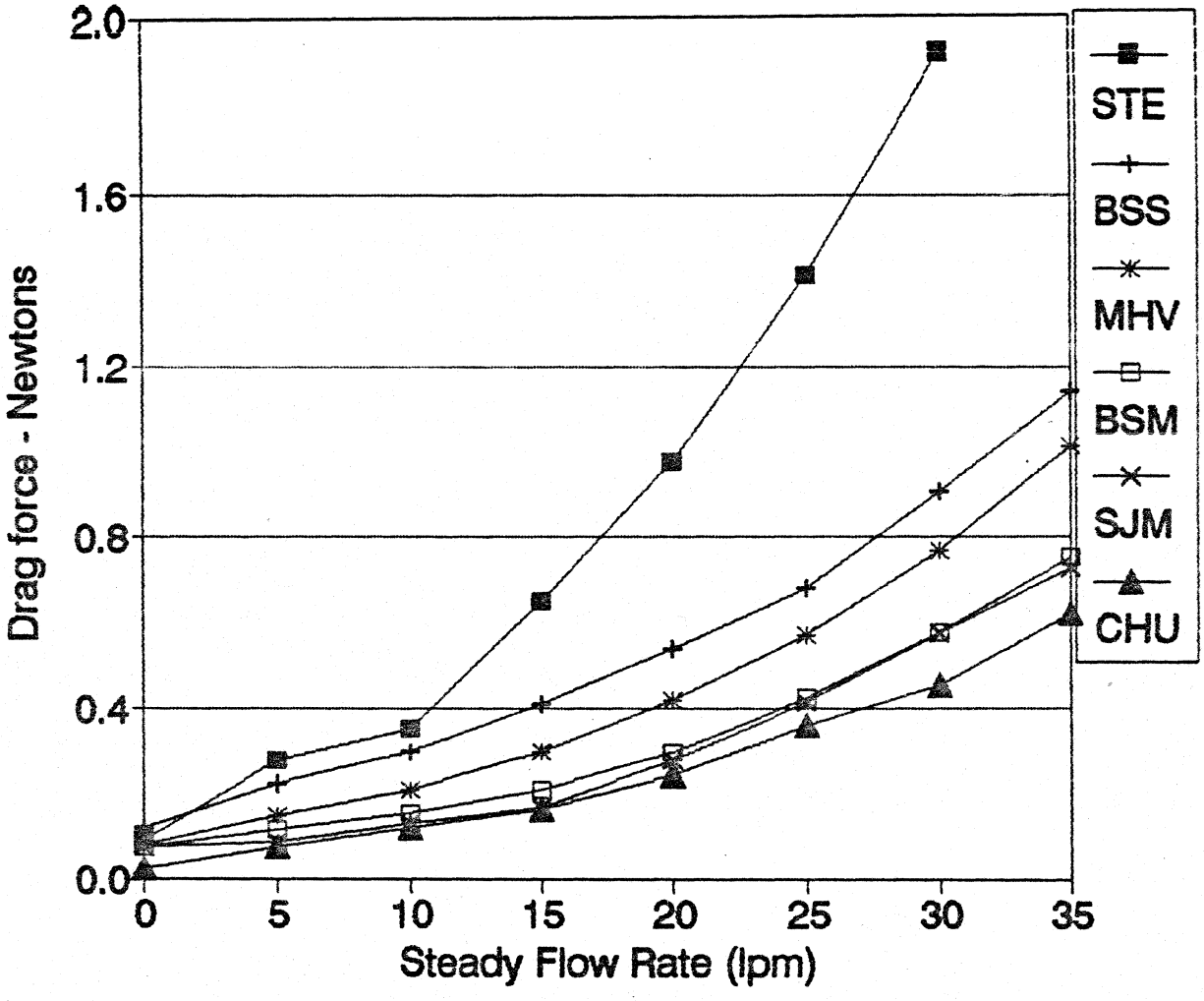

difference between these two valves are very small and within the measurement error.

Figure 5.13(a) shows the measured drag force on the whole valve and the drag on the disc as function of the disc opening angle at a steady flowrate of 35 lpm. The drag on the cage [determined in § 5.4(ii)] was subtracted from the total drag on the valve to obtain the drag force on the disc. It was assumed that the total drag on the valve can be considered as the sum of the drag on the disc plus the cage.

Reif *et al.*, (1986) have modelled drag and lift forces by potential flow theory (flow over a semi-circular shaped aerofoil for opening angles $\geq 60°$). They have determined the drag and lift coefficients experimentally for a Lillehei Kaster valve with a disc diameter of 20 mm. The drag forces on the disc were calculated on the assumption that this model could be applied here approximately. **Figure 5.13(b)** shows that the calculated and measured forces on the disc are of the same magnitude and have the same trend with increasing opening angle. At reducing opening angles of less than 60°, the measured drag on the valve shows a larger increase than the pressure drop across the valve.

These results clearly validate the basic technique of drag force measurements developed here and show the magnitude of the forces on the valve during its open phase. However, improvements to the technique are needed to differentiate the effects of disc shape and presence/absence of struts, etc.

Figure 5.13

DRAG FORCES

At a steady flowrate of 35 lpm

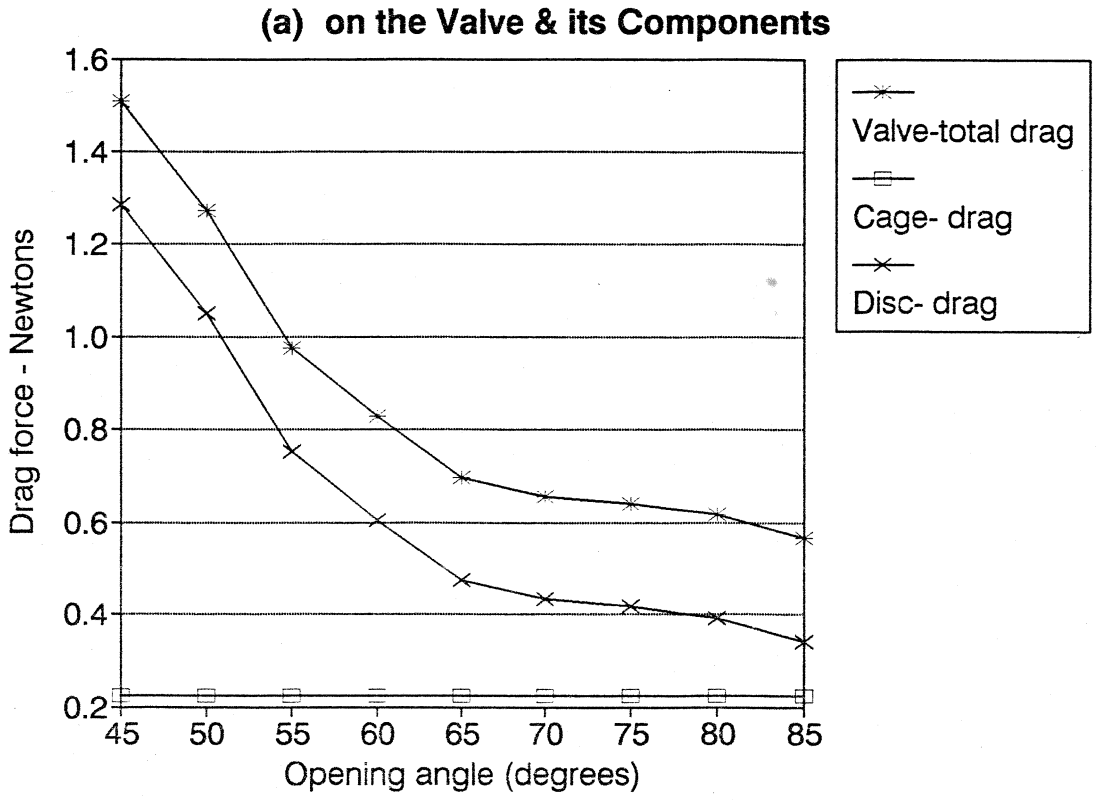

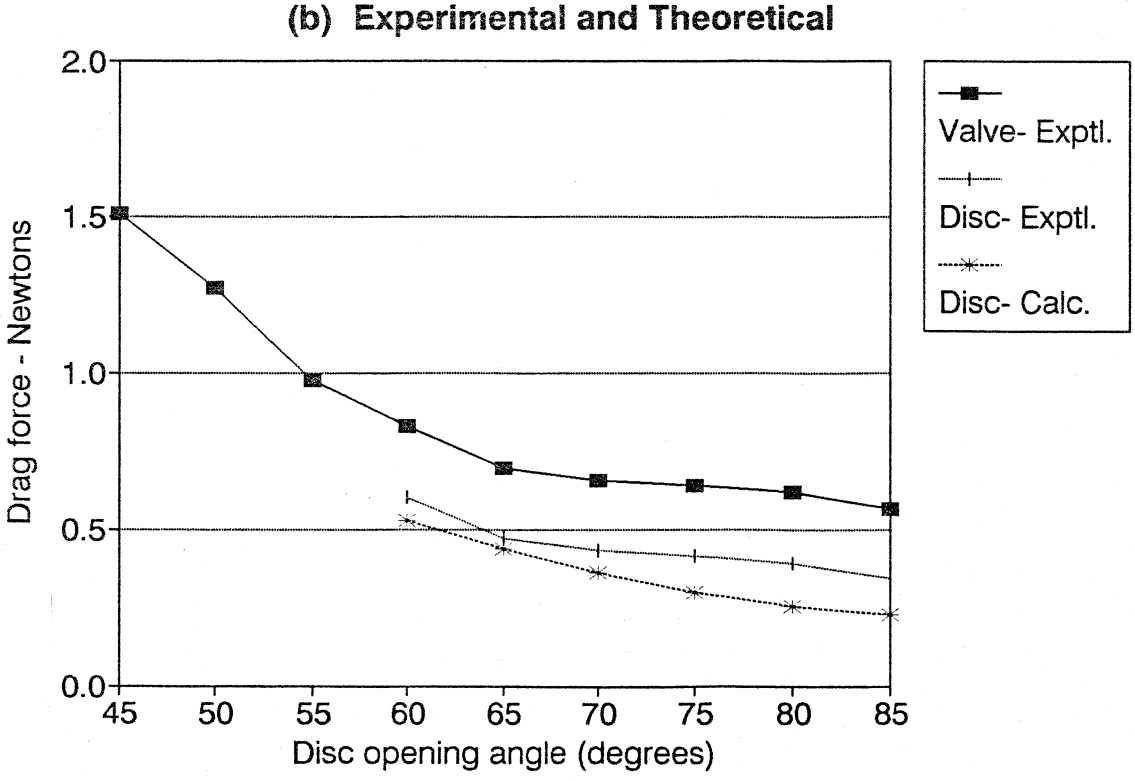

5.5 SUMMARY

The results indicate that the best orifice shape is that of a flow nozzle with only an entrance curvature and a straight outlet. The present practice of providing or not providing a radius at both the inlet and outlet edges of the cage results in larger pressure drops.

The centre of pressure, which is at the disc centre at closure, moves towards the leading edge as it tilts open. For the plano-convex disc shape, the valve opens fully (75° max) when the pivot axis is located at less than 0.32 disc diameters from the leading edge. The opening angle progressively reduces when the pivot axis is moved more centrally. If the disc is allowed to slide 1 mm downstream during opening, then full opening is obtained with a pivot axis location at 0.34 disc diameters and opens to 65° when the axis is at 0.364 disc diameters. The disc shape has considerable effect on the location of the centre of pressure. A convexo-concave disc exhibits less movement (i.e., its centre of pressure remains nearer the disc centre) in comparison to the plano-convex disc, thus permitting the use of a more central pivot axis at 0.385 diameters. This design did not work practically, as the disc, in its open position is very close to the diameter of the cage and so can escape upwards through the cage.

The data on the effect of opening angle clearly indicate that the range 70 to 75° is optimum. At higher angles, the reduction in pressure drop is only marginal.

A technique for the measurement of drag force on the valve has been demonstrated successfully. However, it is not sensitive enough to determine accurately the effect of the disc shape, effect of struts or other design changes. A more detailed study to improve the technique is necessary.

Amongst the standard valves, the St.Jude valve showed the least pressure drop followed by the Chitra. However, it should be noted that these differences between the tilting disc valves is very small and probably not significant from a clinical point of view. Amongst the test valves, all those that opened fully showed comparable pressure drops; the minor differences are probably due to the small dimensional differences amongst the different test pieces and the error in measurement.

The use of a venturi tube greatly increased the repeatability of the flow settings in this study. The square law relationship between flowrate and the pressure drop of the probe greatly enhances the precision at the higher flowrates. The use of sensitive semiconductor differential pressure transducer ensures precise measurement of these pressure drops.

Models TV-77, TV-88, TV-5C and TV-6C which were not practically usable under pulsatile conditions as the discs could escape upwards and models TV-55 & TV-66, which opened very poorly were not taken up for further evaluation under pulsatile conditions.

~~~~~~
~~~~~~

CHAPTER 6

PULSATILE TESTING

6.1 PULSE DUPLICATOR DESIGN

The requirements and concepts for the design of a left heart pulse duplicator have been described by many workers (Weiting, 1969; Wright & Temple, 1971;Swanson & Clark, 1976a; Martin & Black, 1976; Reul, 1983). The variety of systems that have been used reflects the problems and constraints involved in modelling the left ventricular dynamics and systemic circulation (Weiting et al., 1969; Klain *et al.*, 1969; Wright & Temple, 1971; Swanson & Clark, 1976b; Martin & Black; 1976; Yoganathan & Letzing, 1983; Knott *et al.*, 1988). Hence, the results from these different investigators are not strictly comparable (Tindale *et al.*, 1982; Swanson, 1984). The Food & Drug Administration (FDA) of U.S.A. have recommended an interlaboratory comparison protocol so that use of identical and reproducible test conditions will enable representative comparison of data from different authors (FDA, 1985).

Considering all these, no attempt was made here to either simulate the systemic circulation accurately or to match the performance of any other well known investigator in this field. The design of the present duplicator was an improvement of the

earlier system developed here (Bhuvaneshwar et al., 1983). The improvements were mainly in the simulation of the systemic impedance, ventricular compliance control and instrumentation.

The schematic of the pulse duplicator is shown in **Figure 6.1.** The mitral and aortic flow channels were the same as those used in the steady flow test. To obtain similarity in the pulsatile flow, the output impedance (or Systemic Impedance) of the left side of the human circulatory system was simulated by means of hydraulic elements consisting of two capacitances and resistances as shown in the figure. The pulsatile flow is obtained by using a balloon inflated and deflated in a ventricular chamber using compressed air.

Table 6.1
Values of Systemic Impedance Components

Inertance gram cm^{-4}		Resistance dynes sec cm^{-2}		Compliance cm^{3} $dyne^{-1}$	
L_1	L_2	R_1	R_2	C_1	C_2
3.0	0.9	108	1912	5.6×10^{-4}	3.0×10^{-4}

i. Systemic Impedance :

The design of the systemic impedance using resistances and compliance chambers was based on earlier work (Martin & Black, 1976; Reul *et al.*,1975). The electrical analogue used to simulate the impedance and the physical realisation of this model are shown in **Figure 6.2.** The values are given in Table 6.1. The resistances were made by using 16 gauge thin walled stainless steel capillary tubings. The resistance values were calculated

THE PULSE DUPLICATOR SETUP

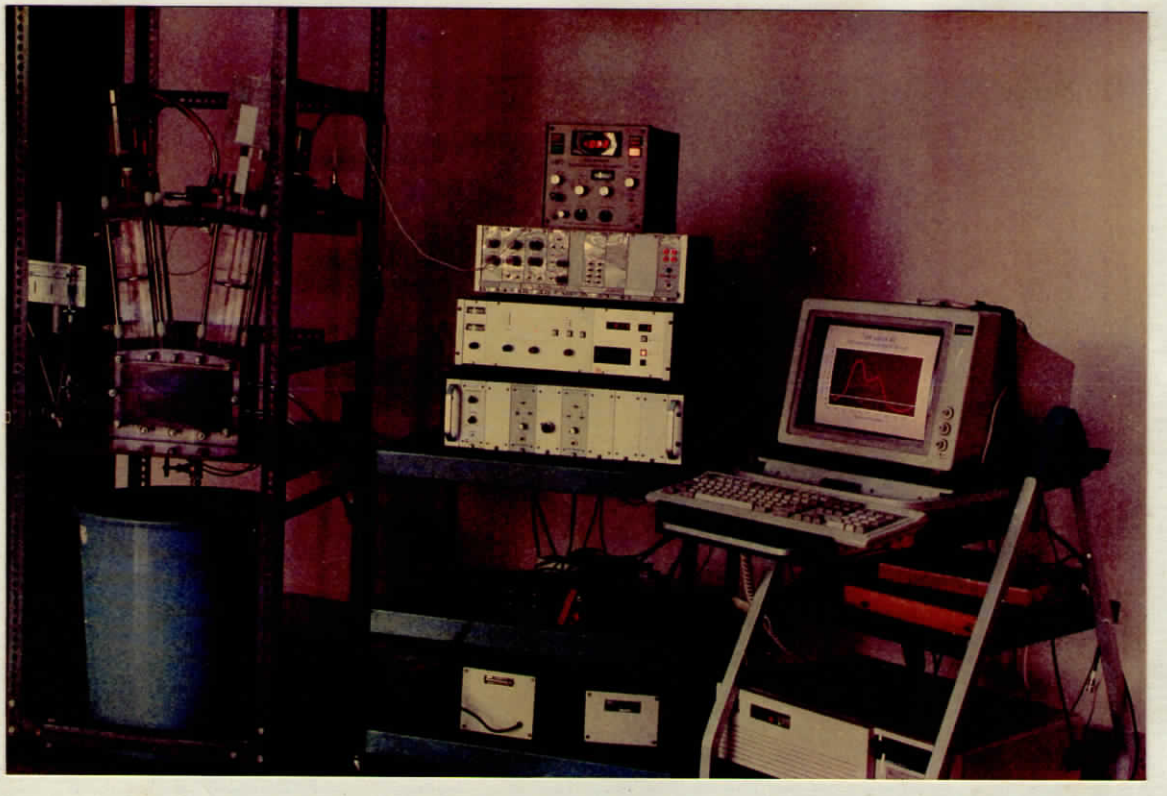

Figure 6.1

PULSE DUPLICATOR SCHEMATIC

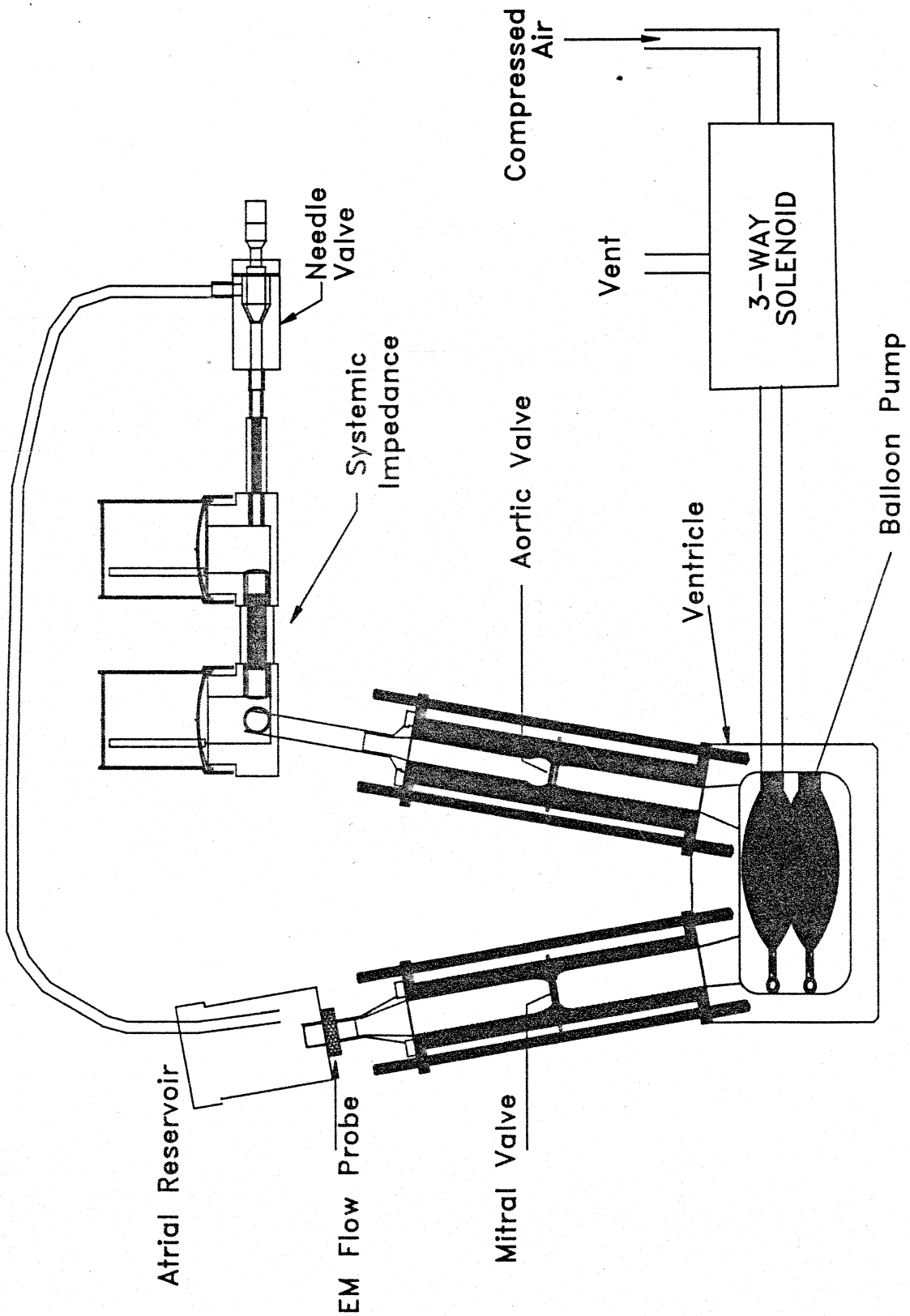

Figure 6.2

SYSTEMIC-IMPEDANCE REALISATION

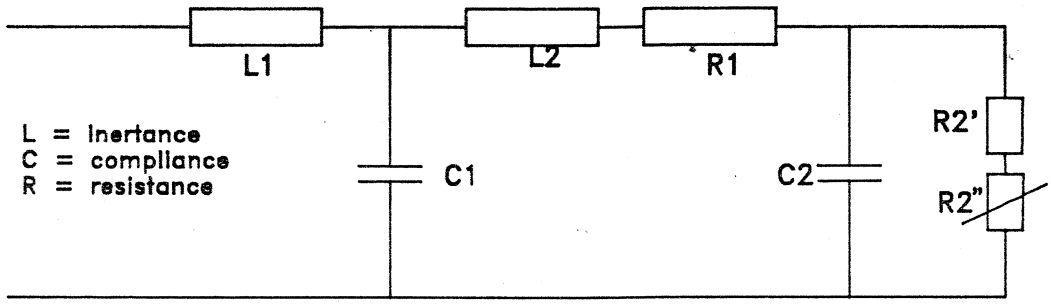

Electrical Analogue of the Systemic Impedance

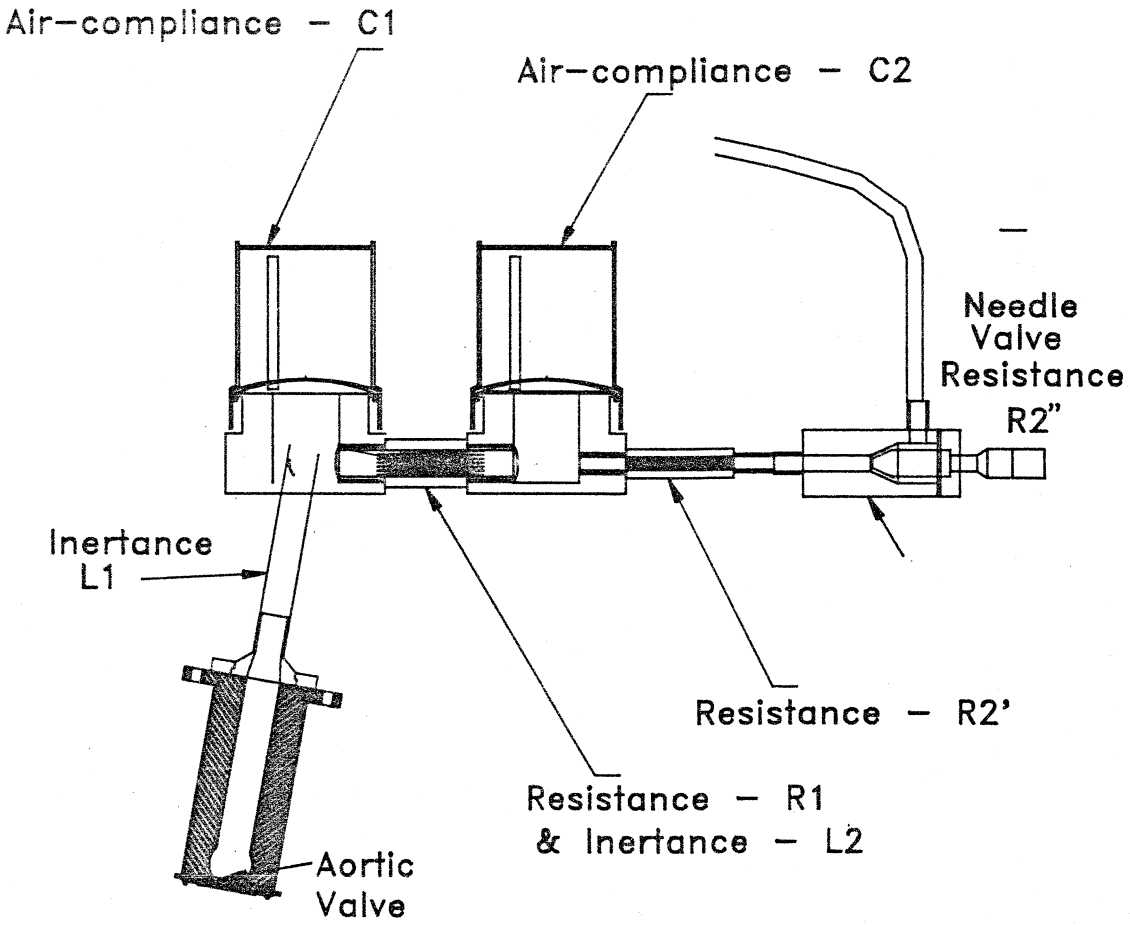

Physical Realisation of the Systemic Impedance

using Poisseuille's law as :

$$R=\frac{8\mu l}{\pi r^4 n} \qquad (1)$$

where :

R = resistance
μ = fluid viscosity
l = length of the capillary
r = radius of the capillary
n = number of capillaries used.

The minimum lengths of these capillaries to ensure good quality factor and frequency response were met by suitable design. The detailed calculations and the design of the resistances are given Appendix D. The resistance R_2 consisted of a fixed part and a variable part consisting of a needle valve as shown in Fig.6.2. The needle valve was used to make fine adjustments to the systemic resistance so as to obtain the required mean aortic pressure.

The capacitances consisted of a plastic container fixed to a machined block of polypropylene with suitable water-tight sealing. The value of the capacitance were set by controlling the volume of the air column over the fluid level inside. This could be adjusted by using a squeeze bulb to pump in air or to let out till the set mark on the transparent chamber.

ii. Ventricular Chamber :

The ventricular chamber was machined from a block of perspex, to which the valve test chamber could be mounted as shown in the Fig.6.1. Two rubber balloons were fitted inside with

external connections for inflation. the upper balloon was inflated and deflated using compressed air to achieve the ventricular pumping action. The lower balloon was used to control the compliance of the chamber in order to adjust the rise time of the ventricular pressure wave and keep it within physiological limits.

iii. Atrial Reservoir :

The atrial reservoir consisted of a plastic tank so as to obtain mitral inlet pressures in the range of 10 to 20 mmHg.

iv. Inter-connections :

A 22 mm diameter Carolina Instruments Electro-magnetic cannulating probe connected between the atrial reservoir and the mitral inlet provided the instantaneous flow signal. The different units were connected with 22 mm internal diameter thick-walled silicone rubber hose. The final outlet from the systemic reservoir consisted of a 12.5 mm i.d. PVC tubing. The needle valve served to make fine adjustments of the systemic resistance to obtain a mean aortic pressure of 100 mmHg.

v. Pressure drop measurements :

The pressure drops across the test valves during pulsatile flow was measured using a LX1601D semiconductor pressure transducer as previously described in § 5.2.

vi. Atrial and Ventricular Pressures :

Atrial and ventricular pressures were measured using clinical quality disposable pressure transducers (Spectramed) with a sensitivity of 5μV/V/mmHg. These were interfaced through instrumentation amplifiers to the data acquisition system.

vii. Cycle control, Data acquisition and analysis :

At present, pulsatile testing is generally carried out using computer based data acquisition and control to enable ensemble averaging of cycles, calculation of the various quantities (rms of flowrate, mean pressure drops, EOAs, etc.) (Yoganathan *et al.*, 1984; Knott *et al.*, 1988).

The digital output of the A/D interface card was used to generate the trigger signal for the pulse duplicator solenoid and also acted as the starting reference for the pulse cycle. Data was acquired at 500 or 1000 samples/s for 64 or 32 consecutive cycles respectively and stored. The data were then ensemble averaged off line, over the 64/32 cycles to obtain an averaged cycle waveform for each signal. Mean and standard deviation was calculated for the ensemble at each sampling point in the cycle.

Solenoid triggering, data acquisition and ensemble averaging were all carried out using menu driven programmes developed under the ASYST Ver.3.0 (Asyst Software Technologies, Inc., Rochester, N.Y., USA) data acquisition and analysis software package.

6.2 STATIC CLOSING VOLUME MEASUREMENT SYSTEM

All prosthetic heart valves require a certain volume of backflow for it to close. In some designs, there may be a gap between the occluder and the cage ring in the closed position thus permitting a leak during the closed phase. Regurgitant volumes are generally measured under pulsatile flow conditions in a pulse duplicator using an Electro-magnetic (EM) flowmeter. However, the accuracy of the instrument restricts the determination of small changes in the closing volumes due to design changes such as those proposed in this study. Hence, a better measurement technique was considered essential.

Willshaw *et al.*, (1986) have used an artificial heart and a pneumotachograph to obtain more accurate measurements of the closing volumes and leaks of tilting disc valves. In this system, there is no dynamic pulsatile flow of the fluid at a given mean flow rate. The system essentially works with only the test valve thus ensuring more controlled conditions of measurement. **Figure 6.3** shows the schematic of the system used here. The ventricular pumping chamber of the pulse duplicator and the mitral flow channel were used. The aortic side of the pumping chamber was sealed and the valve under test was placed in the mitral position in the conventional manner.

The system was filled with the test fluid to a level of 10 cm above the valve, leaving a column of air-space above. The pumping action is generated by inflating and deflating the rubber bag using compressed air. The flow of compressed air is controlled by the computer through the solenoid valve. A

Figure 6.3

STATIC CLOSING VOLUME & IMPACT FORCE TEST SETUP

Valve Opening Downwards

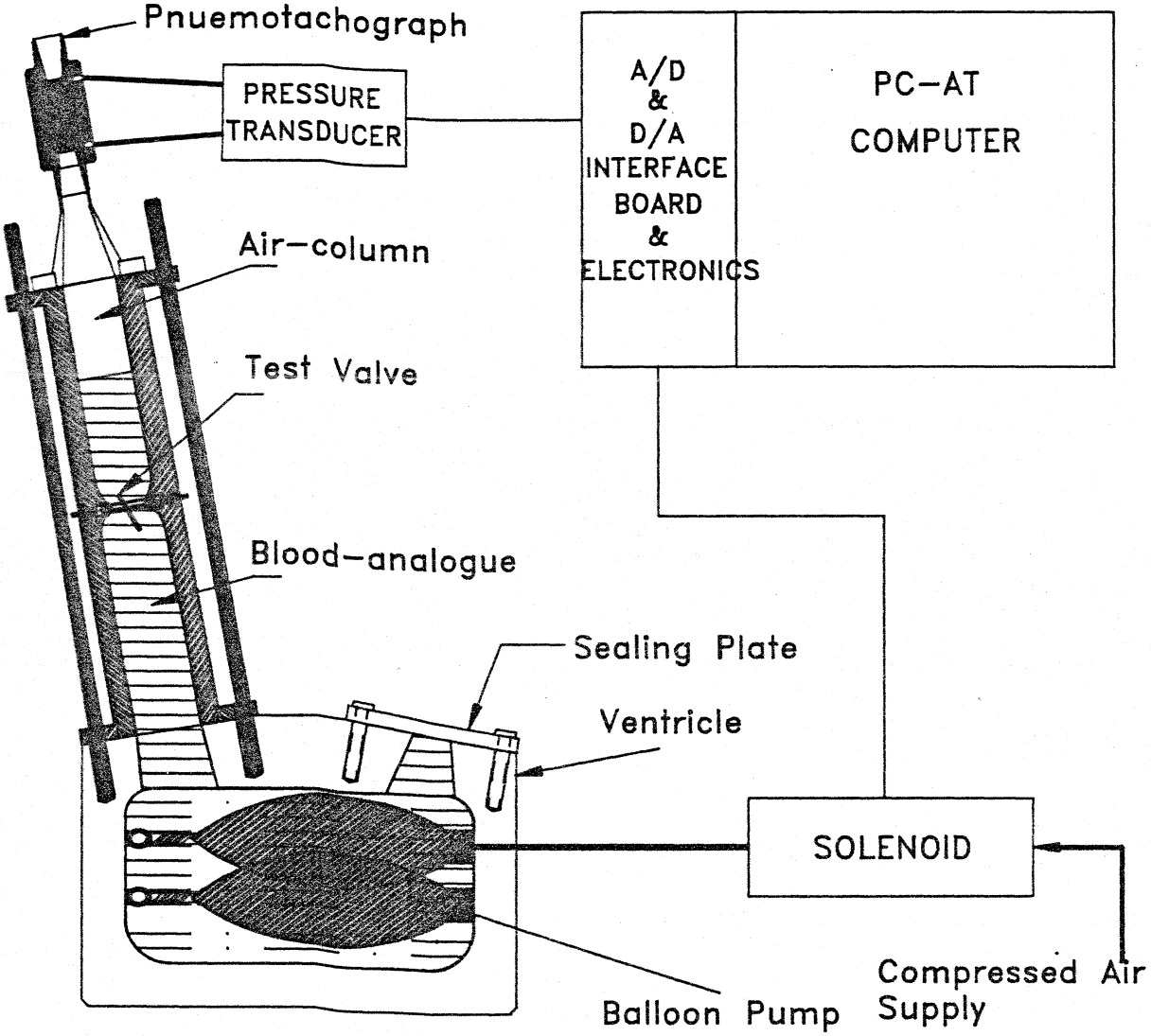

pneumotachograph was designed, fabricated and calibrated. This is described in Appendix E. The device acts like a resistance and produces a differential pressure proportional to the rate of air-flow through it.

The principle of measurement in this system is based on the fact that any volume of water which passes through the valve under test must displace an equal volume of air through the pneumotachograph probe. As the differential pressure across the probe is kept small by design, the volume change due to the compressibility of air is negligible in comparison to the total flow. The flowrate signal appearing as a differential pressure is transduced using a sensitive semi-conductor differential pressure transducer (Sensym LX06001D, 0-1 psi range), amplified and fed to the data acquisition system.

This setup functions well with valves, whose occluders are denser than the test fluid, like all the imported valves. In the case of the Chitra and test valves with UHMW-PE discs (specific gravity of UHMW-PE = 0.94), the disc opens down fully at the start of forward flow. However, since the forward flow is small (equal to the total regurgitant volume), the flowrate falls to zero towards the end of the filling phase. At this point, these discs float up and are in a semi-closed position. At the start of the systole (bag inflation here), the valves close rapidly exhibiting a small closing volume.

In order to test UHMW-PE disc valves more fully, the system was modified as shown in **Figure 6.4** with the disc opening upwards. UHMW-PE discs float up to a fully open position, while the denser discs tend to move down to a small opening angle. In

Figure 6.4

STATIC CLOSING VOLUME & IMPACT FORCE TEST SETUP

Valve Opening Upwards

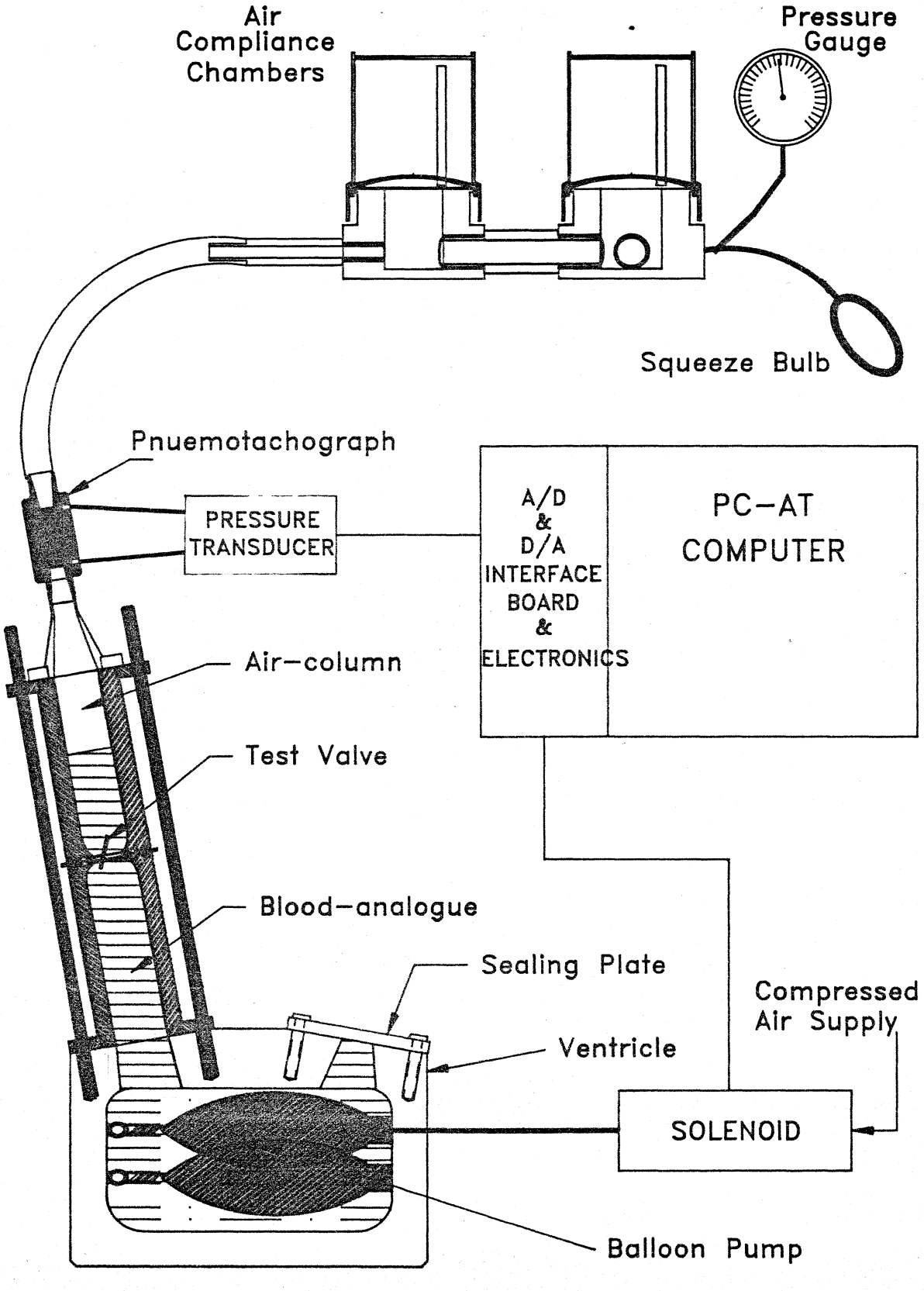

this mode, the pneumotachograph probe was connected to a compliance chamber as shown in the figure. This compliance could be pressurised by pumping air into it. The valve mounting direction was reversed to open upwards in a manner similar to the aortic valve of the pulse duplicator. The mitral test chamber was used for all the tests. During systole (inflation), the fluid flows up, displacing air into the compliance chamber. During diastole (deflation of the bag), the air-pressure in the compliance chamber forces the valve to close; the movement of air being equal to the closing volume as before.

All the tests were conducted at a cycling rate of 70 per minute, systolic duration of 300-330 ms and a peak ventricular pressure of 125 mmHg. Signals were digitised and acquired at 1000 samples/s for two sets of 32 consecutive cycles. Each set of 32 cycles were then ensemble averaged separately and the closing volume determined from the averaged waveforms.

Figure 6.5(a) shows typical ventricular pressure and air-flow rate ensemble averaged waveforms for the valve opening downwards. In this figure, four phases may be seen. Phase 1 consists of a delay between the starting pulse from the computer (time zero) and the moment at which fluid begins to flow through the valve (point a). The delay, approximately 20 ms, was caused by the time required for the solenoid valve actuation and the build up of air pressure in the ventricular bag. Phase 2 was the closing phase, during which water accelerated rapidly through the valve reaching a peak flowrate, which was abruptly terminated by valve closure. This abrupt termination produces resonance in the air-space above the water column, which was

Figure 6.5

ENSEMBLE AVERAGED AIR-FLOWRATE WAVEFORM

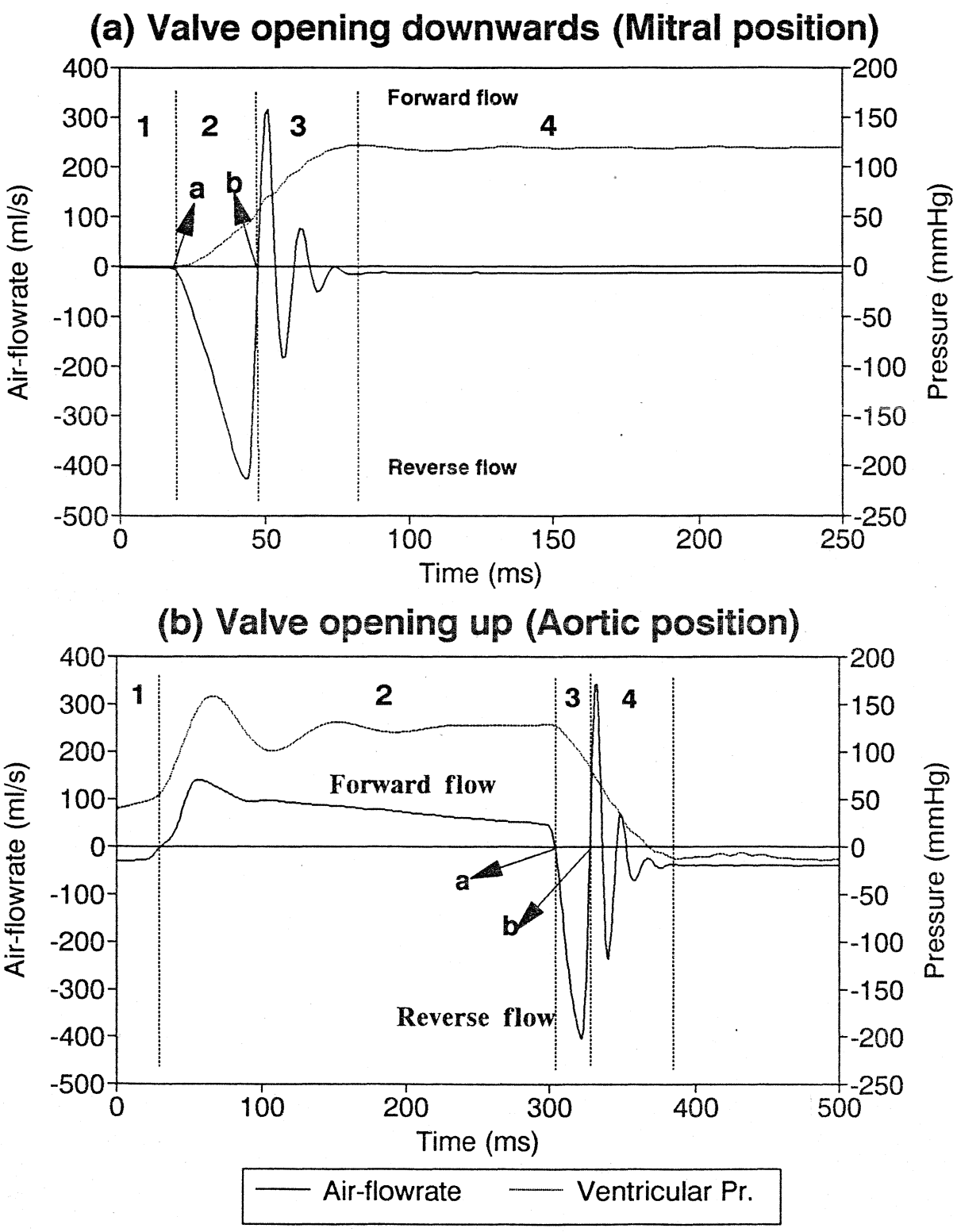

phase 3. The start and finish of the closing phase was detected by the change in sign of the values. The valve closure was defined as the first zero crossing of the resonant phase (point 'b' in the figure).

Figure 6.5(b) shows typical ensemble averaged waveforms in the case of the valves opening upwards. As before, phase 1 was the delay for the inflation of the bag to start. Here phase 2 was the forward flow through the valve, when the air above the valve was displaced into the compliance chamber with consequent build up of pressure there. At the start of deflation (diastole), the forward flow was terminated by the fall in ventricular pressure, resulting in valve closure due to the higher pressure in the compliance chamber - this was phase 3, the closing phase of the valve. The end of valve closure (point b) was followed by phase 4, when the air column resonates.

The closing volume was therefore the area under the curve during the closing phase; i.e., between points 'a' and 'b'. The closing volume, (CV in ml) was determined by integrating the flow signal from the start to the finish points and the closure time (CT in ms) as the time interval between these two points.

6.3 STATIC CLOSING IMPACT FORCE MEASUREMENTS

For the efficient working of any one-way flow control valve, it is necessary that the valve closes quickly at the start of reverse flow. This is more so in prosthetic heart valves, where valve efficiency is critical for the efficient functioning of the heart. To achieve this quick closure, the

occluder has to accelerate from its fully open position to the closed position and impact with the cage mechanism before coming to a rest. This impact at closure results in an impact force of short duration being transmitted through the cage, sewing ring & sutures to the heart muscle. Large impact forces are naturally a source of problems - suture dehiscence, fatigue fracture, wear of components and probably tissue overgrowth due to chronic inflammatory response of the host tissue.

The static closing impact forces were measured in the same set-up as for the static closing volume measurements (§6.2). The test valve was sutured to the force transducer instead of the holder plate. The air-flow probe was removed. Tests were conducted with the valves opening down for the denser discs and opening up for UHMW-PE discs for the same reasons as before. The test and data acquisition conditions were also similar. However, the peak impact force for each cycle was detected and then the values averaged over the 64 cycles of data to eliminate errors arising from cycle to cycle timing variations. **Figures 6.6 (a) & (b)** show typical ventricular pressure and force waveforms for the two cases.

In the case of valves opening downwards, the initial force is zero with the valve open. At the onset of systole (inflation), the valve closes rapidly with an impact followed by a short ringing. The force signal then settles at a high value due to the ventricular pressure during systole. In the case of valve opening upwards, the closure occurs at the start of diastole (deflation). During systole, the force is almost zero as the valve is open.

Figure 6.6

CLOSING IMPACT FORCE WAVEFORM

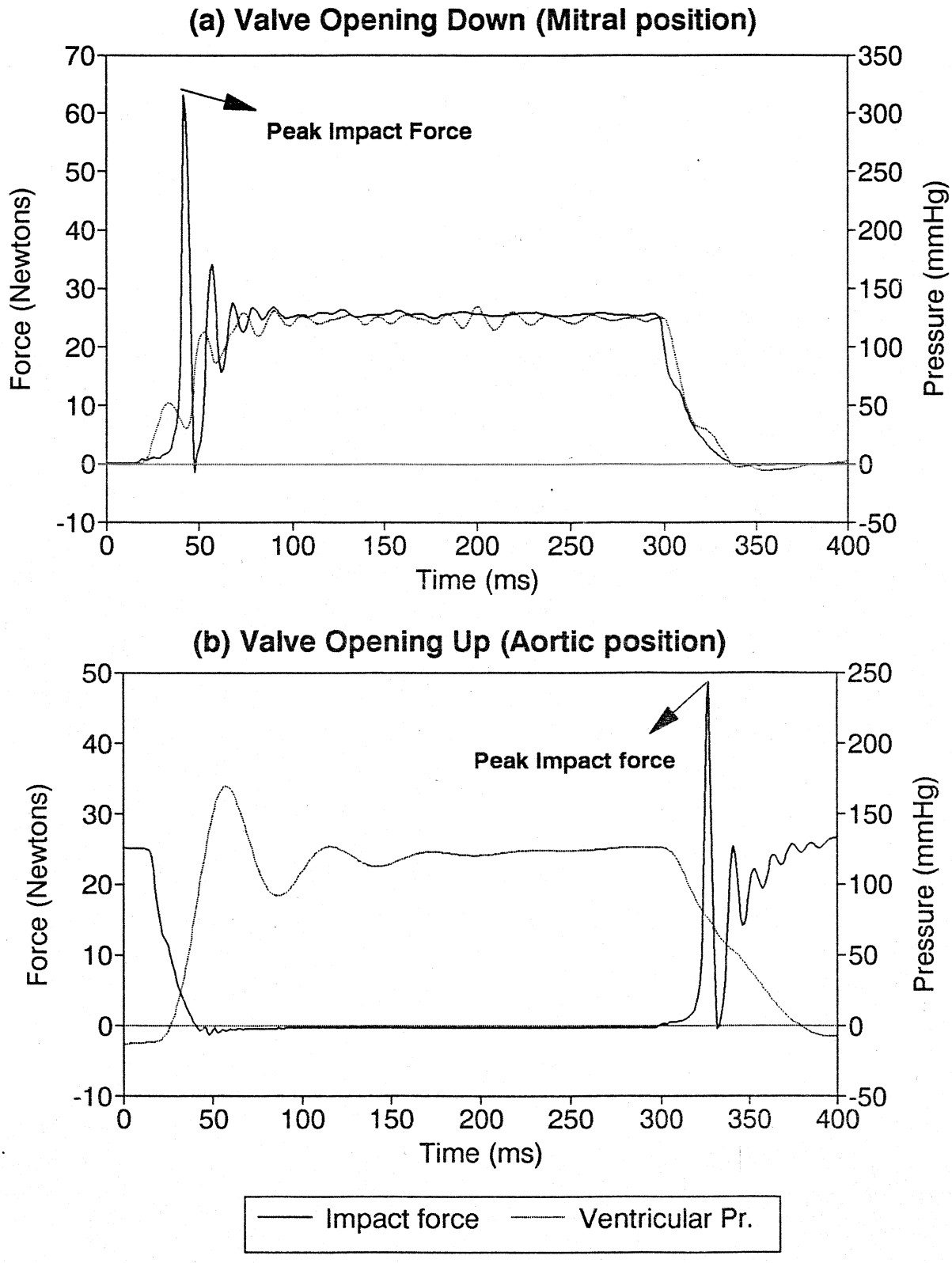

The closing impact force was taken as the peak value of the force waveform. The two outputs A and B from the force transducers (§ 4.7 viii) were converted to their force units using the static calibration data (Appendix B) and the resultant total force determined by the sum of the two.

6.4 DYNAMIC PULSATILE TESTS

Following the static measurements of closing volume and closing impact forces for the various valve models, dynamic testing under pulsatile flow conditions was carried out in the pulse duplicator system (Fig.6.1). The blood analogue fluid was a 35% solution (v/v) of glycerol in water having a specific gravity of 1.08 and a viscosity of 3.1 centipoise at the room temperature of 28 to 30 °C.

The atrial, ventricular and aortic pressures were measured using the disposable Spectramed transducer; the pressure drop across the valve with a LX1601D semiconductor pressure transducer and the pulsatile flowrate with the EM flowmeter (Square wave electromagnetic flowmeter, Carolina Medical Electronics Inc., USA). The valve under study was sutured to the force transducer. All the signals were interfaced to the PC-AT computer.

The cycling was controlled by the computer and the system adjusted to obtain :

Cycling rate : 70 per minute
Cycle time : 856 ms
Systolic duration : 300 ms (approx)
Mean aortic pressure = 100 ± 2 mmHg

The mean atrial pressure varied between 12 to 18 mmHg depending on the mean flow. The mean aortic pressure of 100 mmHg was obtained by adjusting the variable systemic resistance and controlling the pressure of the driving air supply. Tests were conducted at mean flow rated of 2.5, 3, 4, 5.25 lpm. Signals were acquired at 1000 samples/s for 32 consecutive cycles. Two such ensembles of data were acquired at each flowrate and each ensemble averaged separately. The closing volume, peak impact force, mean diastolic pressure and the rms diastolic flowrate were all calculated from the ensemble averaged data.

i. Effective Orifice Area:

From the pressure drop measurements (steady and pulsatile flow), the effective orifice area (EOA) of each valve was calculated using the following equation (Yoganathan & Letzing, 1983) :-

$$EOA = \frac{Q_{rms}}{51.6\sqrt{\Delta p}} \qquad (2)$$

where Q_{RMS} = rms diastolic flowrate or steady flowrate in cm^3/s.

ΔP = mean diastolic measure drop or the mean pressure drop mmHg.

The equation for EOA is derived using the relation

$$\frac{v^2}{2g} = \Delta P$$

where v = velocity of fluid

g = acceleration due to gravity

The EOA is an index of how well the valve utilizes its primary orifice area. The EOA for both steady flow and pulsatile flow were calculated for comparison.

ii. Closing volumes

Closing volumes were obtained by integrating the area under the EM-flowmeter signal for the duration of the closure period.

iii. Closing impact forces

The peak force during the closing phase as described in the previous section was taken as the closing impact force.

6.5 VALVE MODELS TESTED

The list of test valves was pruned, with TV-44, TV-55 & TV-66 being left out as they did not open fully under steady flow conditions and hence were not acceptable. A test cage no.2 was assembled with a corresponding concavo-convex (C-C) disc to determine if it produced increased impact forces in comparison to the plano-convex disc. A Chitra valve with a Sapphire disc was also included at this stage to see the effect of density difference (density of Sapphire=3.98 compared to 0.93 of UHMWPE).

6.6 RESULTS & DISCUSSION

i. Effective Orifice areas (EOA) :

Table 6.2
Effective Orifice Areas of Test Valves

Valve	Steady Flow cm^2	Pulsatile Flow cm^2
TV 11	2.98 ± 0.01	2.76 ± 0.01
TV 22	3.15 ± 0.12	2.53 ± 0.14
TV 33	3.11 ± 0.06	2.39 ± 0.01
TV 44*	2.41 ± 0.09	2.18 ± 0.08
TV 55*	2.05 ± 0.01	-
TV 66*	1.83 ± 0.01	-
TV 42	3.08 ±0.04	2.66 ± 0.01
TV 53*	3.16 ± 0.28	2.06 ± 0.03
TV 2C	-	2.89 ± 0.01
TV 5C	3.12 ± 0.18	-
TV 6C	3.11 ± 0.18	-

± one standard deviation
* Valves NOT opening fully

The EOA for the test and standard valves under both steady and pulsatile flow are given in Tables 6.2 and 6.3. Movement of the pivot axis centrally seems to result in a marginal increase in the EOA. In general, all the test valves which open fully have comparable EOA as expected.

The test valves with the most central pivot axis and opening fully under steady flow were TV-5C and TV-6C. However, they are not practically usable as the discs tend to escape through the cage ring due to the close proximity of the disc

edge to the cage diameter in the open position. Hence, among the practically realisable models, TV-42 had the most central pivot axis and still opening fully to 75°.

Table 6.3
Effective Orifice Area of Standard Valves

Valve	Steady Flow cm^2	Pulsatile Flow cm^2
St. Jude Medical	3.07 ± 0.05	2.51 ± 0.10
Medtronic-Hall	2.80 ± 0.02	2.41 ± 0.09
Bjork-shiley Monostrut	2.82 ± 0.02	2.57 ± 0.13
Bjork-shiley standard	2.68 ± 0.01	2.51 ± 0.10
Chitra - UHMW-PE	3.03 ± 0.02	2.47 ± 0.14
Chitra Sapphire	-	2.56 ± 0.04

± one standard deviation.

Among the standard valves, under steady flow, St. Jude had the maximum EOA. The Chitra valve came a close second. Under pulsatile flow, all the standard valves showed comparable EOA's. This difference in EOA relationships between valves in steady flow and pulsatile flow is probably due to the larger error in flowrate measurement using the EM flowmeter as discussed earlier. Yoganathan *et al.*, (1979a) have clearly brought out the close correlation between steady flow EOA and that measured under pulsatile flow using rms flowrate. Hence, in this study, comparison based on steady flow data is probably more realistic.

ii. Closing volumes :

The closing volumes of the standard and test valves measured under static and dynamic flow conditions are given in

Figure 6.7

CLOSING VOLUMES OF STANDARD VALVES

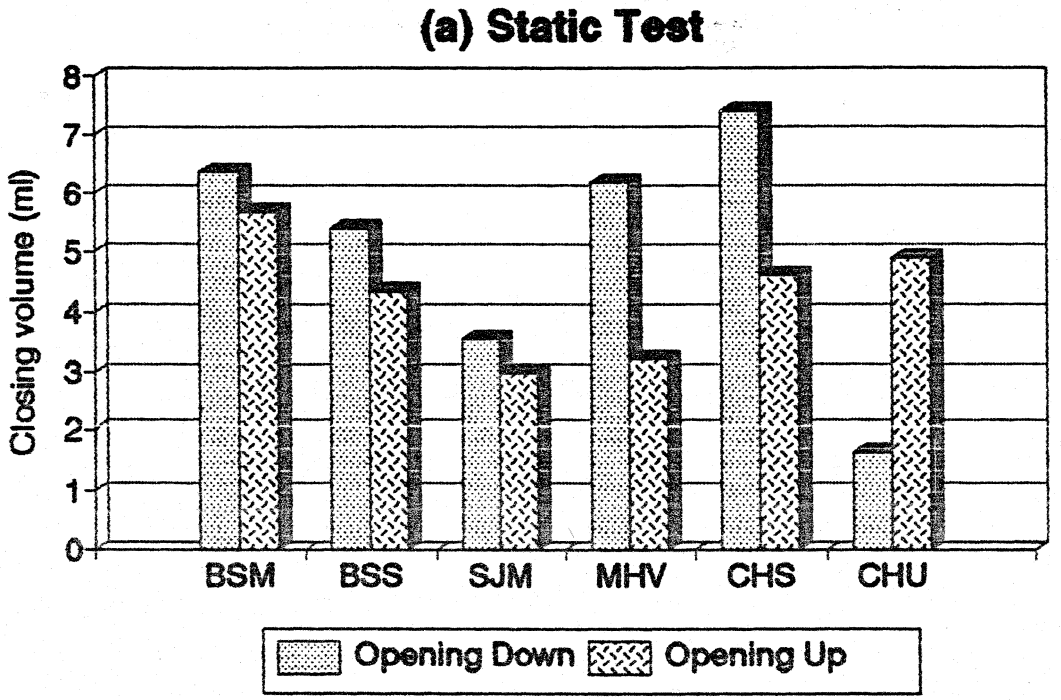

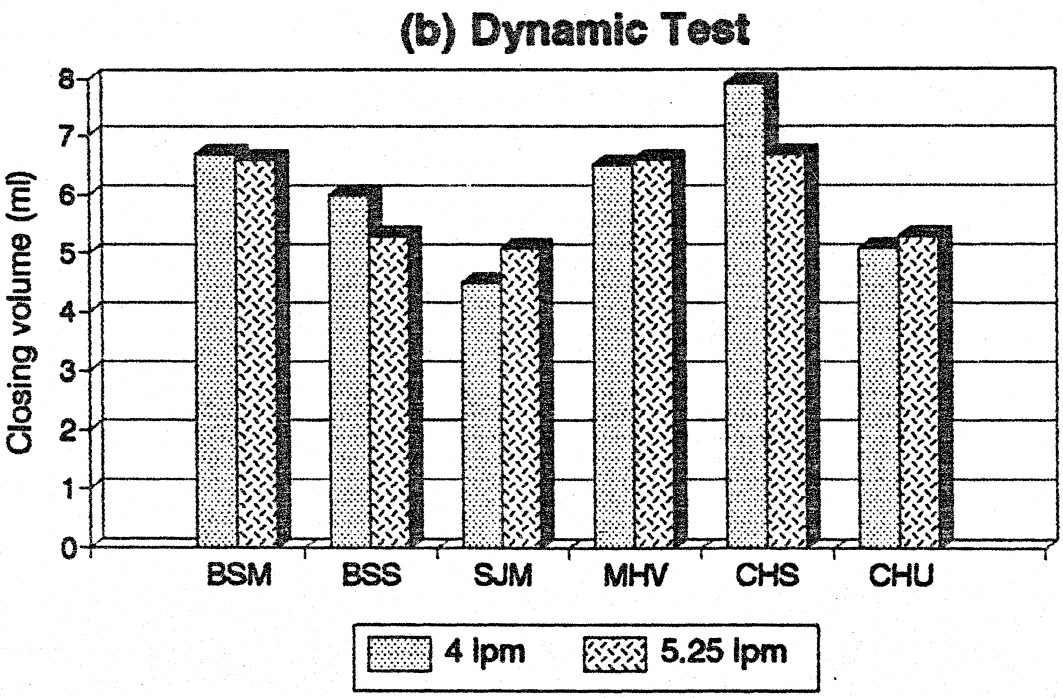

Figure 6.8

CLOSING VOLUMES OF TEST VALVES

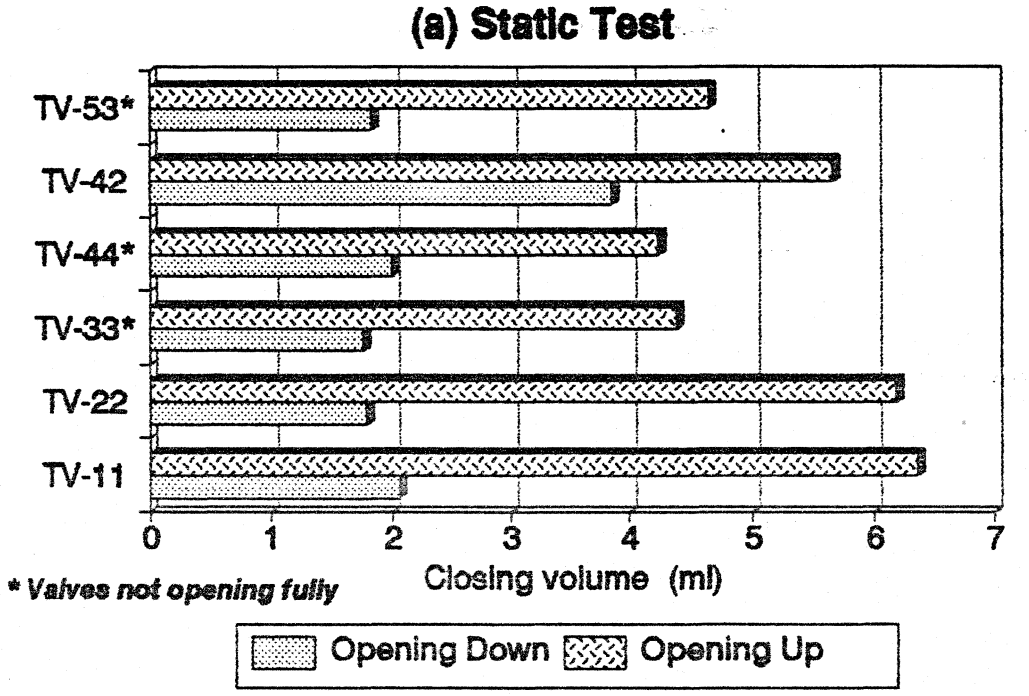

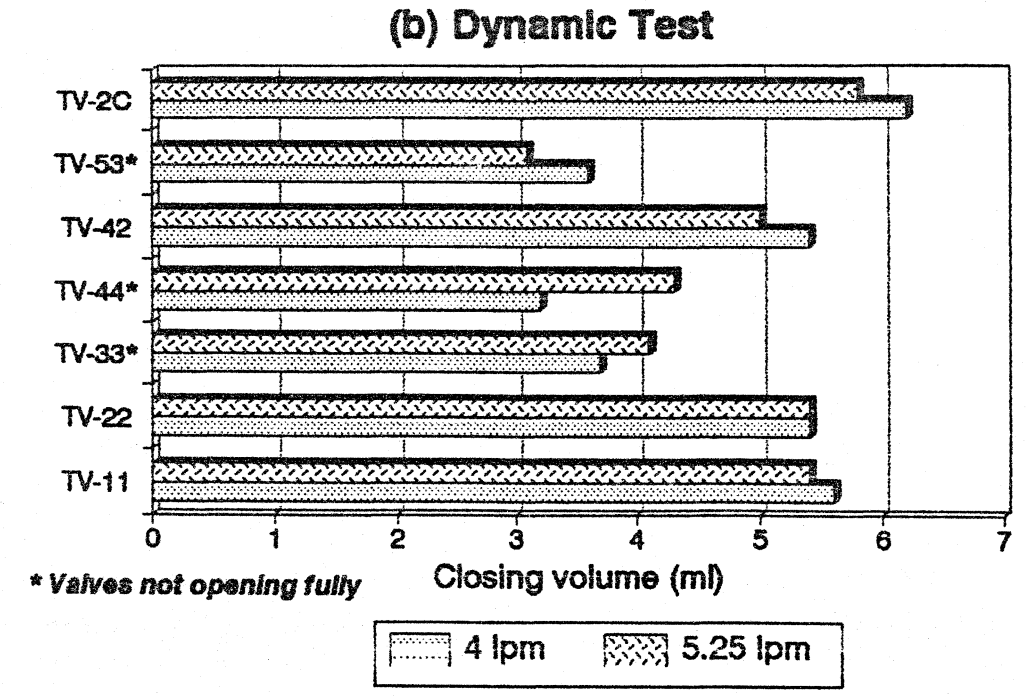

Figures 6.7 & 6.8 respectively. Movement of the pivot axis centrally results in a marginal decrease in closing volume. When the valves do not open fully, there is a significant reduction due to a decrease in the swept volume of the disc. Among the test valves which opened fully, the C-C disc valve TV-2C showed the largest closing volume, more than its associate TV-22 with the same cage and a plano-convex disc. TV-42 with the most central pivot axis showed the minimum closing volume amongst the valves that opened fully, though the difference is not significant from the present valve TV-11.

Amongst the standard valves, the Chitra model with sapphire disc exhibited the maximum closing volume, while the St.Jude had the minimum followed by the Chitra-UHMWPE. The large difference between Sapphire and UHMWPE valves of same design clearly brings out the effect of the specific gravity of the disc material. Sapphire (sp.gr=3.98) also exhibits the maximum difference (under static tests) between the two orientations. UHMW-PE under static tests shows the opposite effect due to its low specific gravity (0.94).

The St.Jude valve with its minimal leaflet travel shows the lowest closing volume. Other investigators (Dellsperger *et al.*, 1983; Yoganathan & Letzing, 1983; Knott *et al.*, 1988) have shown that the closing volumes for the SJM is comparable to others like MHV and BSM. However Knott *et al.*, indicate that closure volumes are mainly dependent on the opening angles.

The BSM with a C-C disc shows a significantly larger closing volume than the B-S standard; the comparison being similar to the test valves TV-22 and TV-2C. Regurgitation

measurements of Scotten *et al.*, (1983) in the mitral position under pulsatile tests show a similar difference between the BSS 60° and BS C-C 60° valves. They contend that the 9% heavier C-C disc closes more slowly. This may be so, as the still heavier Sapphire discs exhibit the largest closing volume. However, the difference between the TV-22 (disc mass 0.44 gm) and TV-2C (disc mass 0.42 gm) are not explained. Dellsperger *et al.*, (1983) have obtained similar results in the aortic position for these two valve models. They contend that the C-C disc presents less drag to the reverse flow and therefore closes slower. In the present study, no significant difference in their closing times could be observed and as seen in the next section, the closing impact forces for the C-C disc was significantly higher, suggesting the opposite. Hence, it seems that the increased closing volume of the C-C disc valve may be due to the simple spooning effect of the curved inflow surface as against the convex shape of the other.

On an overall assessment, the design changes in TV-42 results in a marginal decrease in closing volume inspite of the 75° opening angle. The closing volume is still comparable to the present day standard valve like MHV, though larger than the St.Jude medical.

iii. Effect of Opening Angle :

The effect of opening angle on the closing volume under static conditions is shown in **Figure 6.9(a)**. The closing volume increases with increasing opening angle clearly showing its dependence on the disc swept volume.

Figure 6.9

EFFECT OF VALVE OPENING ANGLE ON

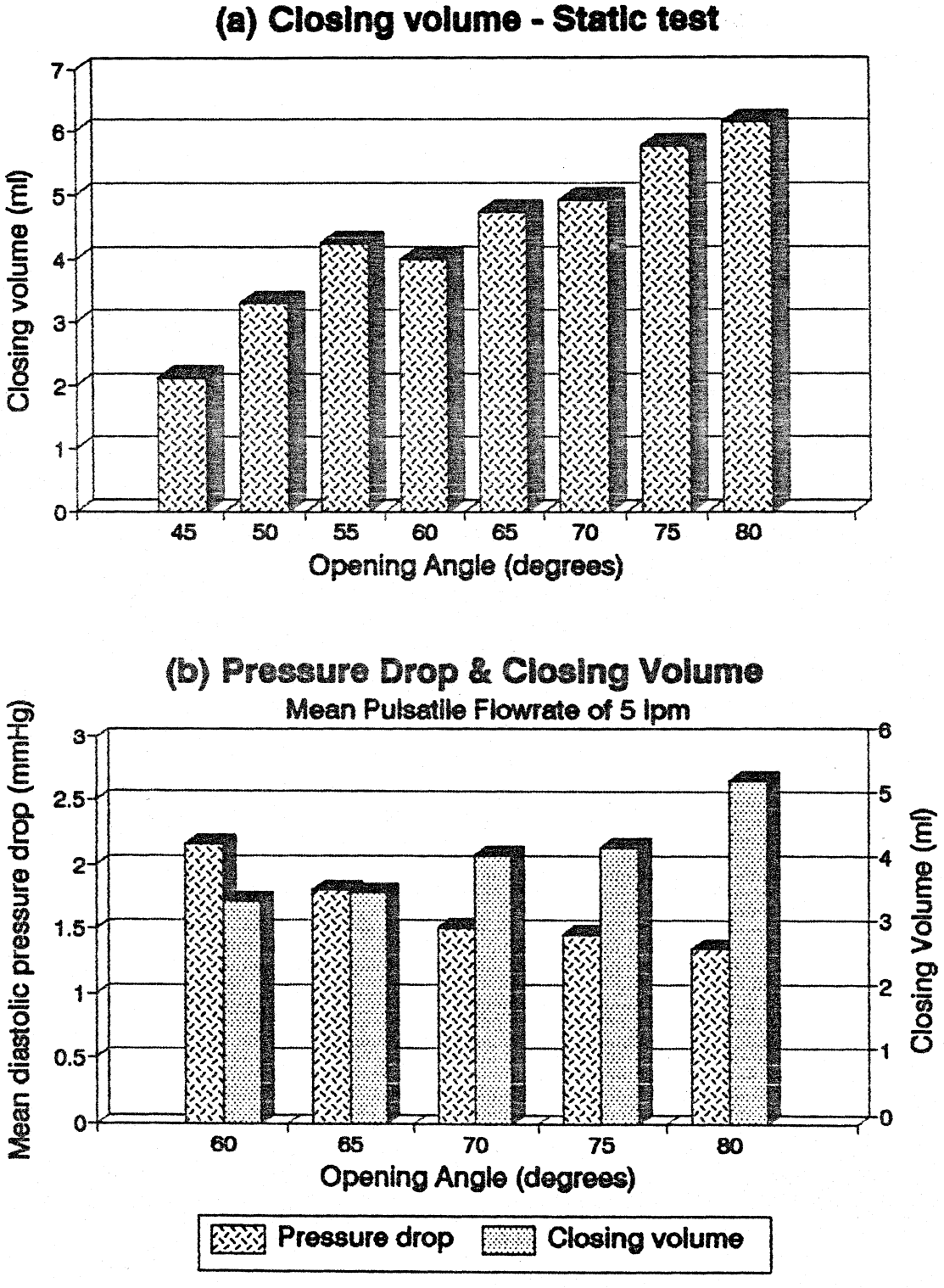

Under pulsatile conditions at a mean flowrate of 5 lpm, the mean diastolic pressure drop across the valve and the closing volume are given in **Figure 6.9(b).** The figure clearly brings out the conflicting change between pressure drop and closing volume due to increasing opening angle. From the figure, it is clear that in the range of 70-75° opening angle, the change in these two parameters is small indicating an optimum region.

iv. Closing Impact forces :

a. Effect of sewing ring & ventricular dP/dt

Figure 6.10(a) shows the effect of a direct rigid mounting of the valve on the force transducer as against that by stitching the sewing ring. The sewing ring acts as a shock absorber reducing the impact force by 20-25%. This has also been demonstrated very recently by Chang *et al.,* (1992).

Figure 6.10(b) shows the effect of increased ventricular peak pressure and its rate of rise. The rate of ventricular pressure rise dP/dt - IMPACT was taken as the slope of the pressure curve between the points 5 ms before and 5 ms after the peak impact force point. The dP/dt - OVERALL was taken as the slope between the 10% and 90% points of the maximum ventricular pressure.

Though there is an increase in the impact force, the change is far less marked than that due to the absence of a sewing ring as seen in previous test. Olsen and colleagues (Olsen *et al.,* 1976; Dew *et al.,* 1984; Olsen, 1988) contend that the failure of mechanical valves (Bjork-Shiley & Hall-Kaster) used in

Figure 6.10

CLOSING IMPACT FORCE

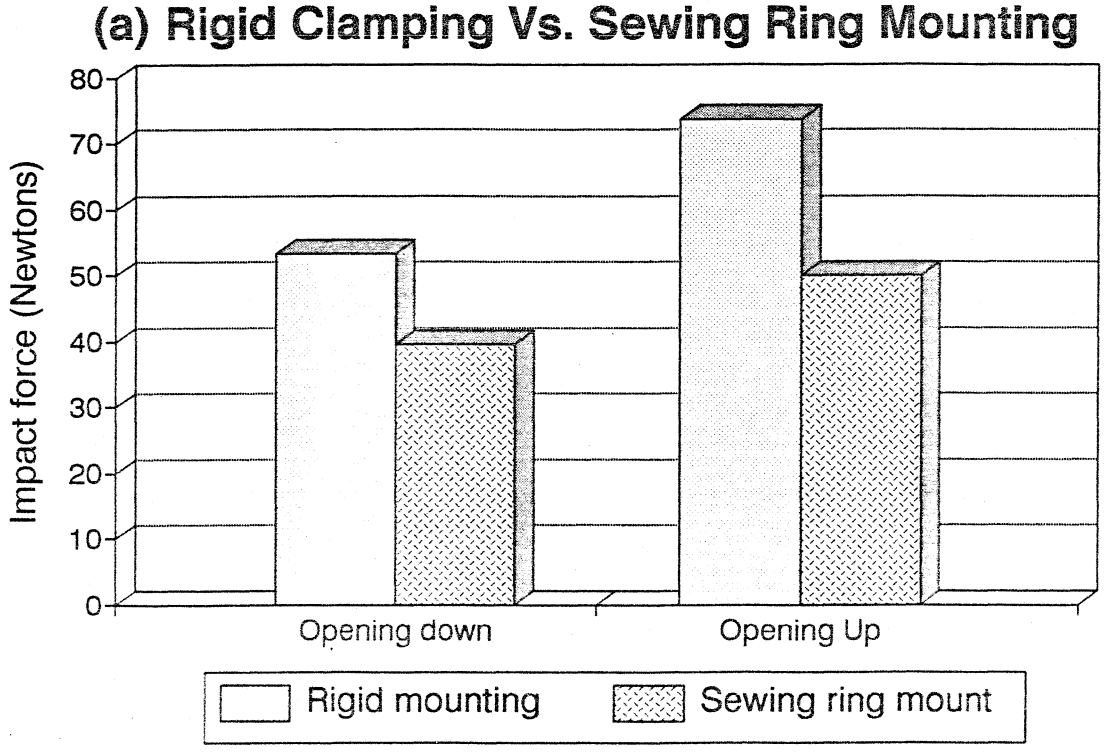

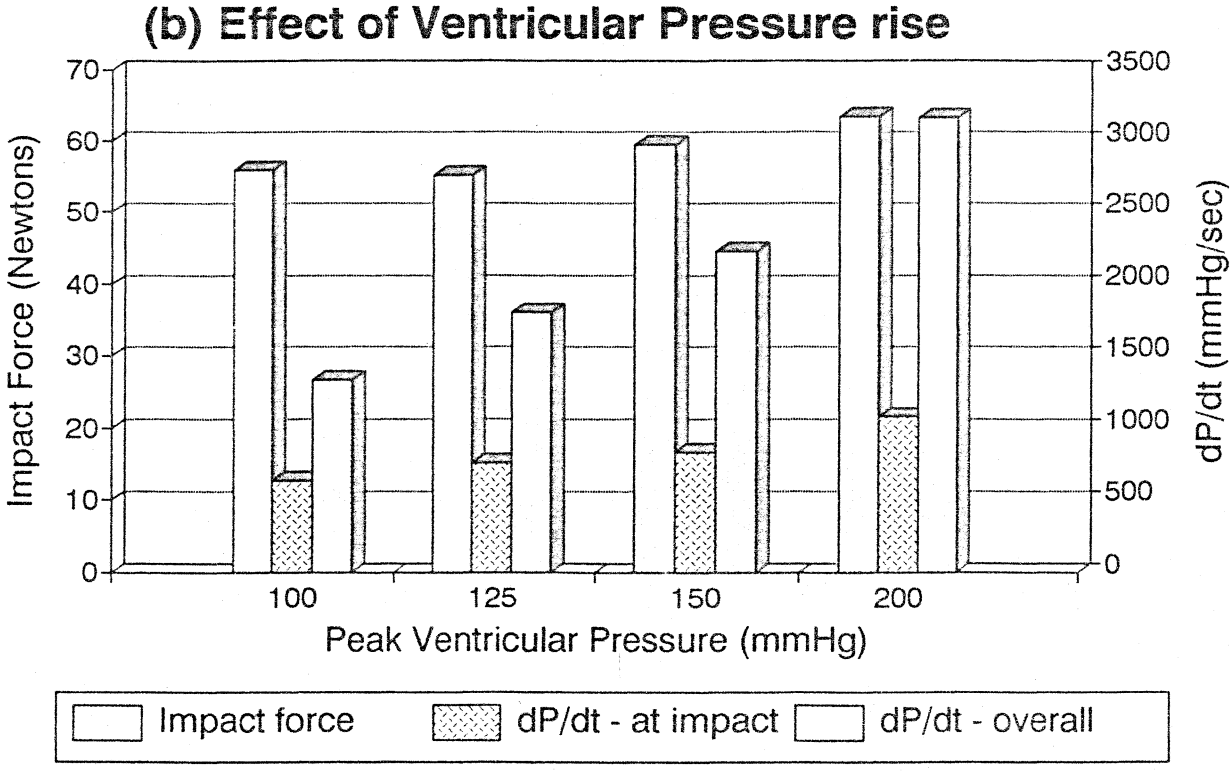

artificial hearts was due to the much higher rate of rise (dP/dt) of the ventricular pressure and the more rigid mounting of the valve in the artificial heart. Olsen in his later work (1988) contends that valve failures after reduction of the ventricular pressure dP/dt has been completely eliminated. But during this period, the valve mounting clamp also used to fail and was redesigned to be more durable. However, its effect in reduction of valve failures has not been considered. From the present data, it is clear that the rigid mounting of the valves contributes far more to increased impact forces on the valve than the ventricular dP/dt.

The importance of the sewing ring as a shock absorber during valve closure has not been studied in detail so far, especially in relation to its material and construction. Improving its shock absorbing ability may result in improved performance of mechanical valves. Another information that is not available is the nature of the impact forces in the case of tissue valves. The leaflets of the tissue valves may absorb bulk of the impact, leading to considerable reduction at the prosthetic-tissue interface. This could very well be an important factor in the incidence of thrombo-embolism and tissue overgrowth, which are seen more in mechanical valves. Reduced impact forces may naturally lead to reduced incidence of suture dehiscence and paravalvular leak, especially in cases with calcified roots.

b. Disc shape

Figure 6.11 shows the effect of disc shape on closing impact force. Though flat and mesa shaped disc exhibit similar

Figure 6.11

EFFECT OF DISC SHAPE ON
Closing Impact Force - Static Test

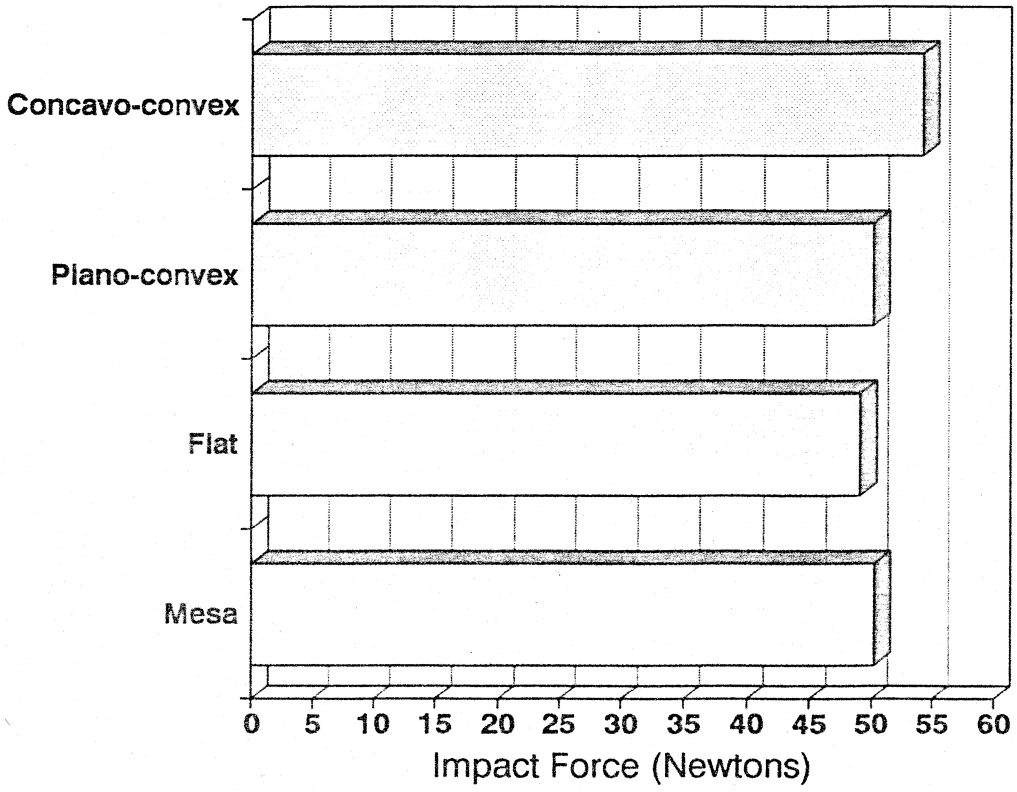

values, there is a marginal increase in the case of the plano-convex disc. The C-C disc shows a definite increase. Hence, the plano-convex disc shape as presently used seems to be a reasonable compromise; considering the improved minor orifice flow and ease of fabrication.

c. Standard valves

Under static testing, the impact forces of the standard valves [**Figure 6.12(a)**] show a similar effect of valve orientation and disc material density like the closing volumes. The BSM showed the maximum impact force followed by the MHV and the SJM. The CHS though using a more rigid disc, shows a smaller impact force, probably due the softer sewing rings of the Chitra valves. Under dynamic testing [**Figure 6.12(b)**], the same differences persist, though these differences are reduced in magnitude. The increase in the closing impact force was probably one of the factors in the minor strut fracture of the Bjork-Shiley C-C models during the mid 1980's.

d. Test valves

Figure 6.13 shows the closing impact force of the test valves, which under static conditions decreases with a more central pivot axis. Among the valves which open fully, TV-42 again shows the minimum impact force. This is also seen under dynamic testing, though with reduced difference at high flowrates.

Figure 6.12

CLOSING IMPACT FORCE OF STANDARD VALVES

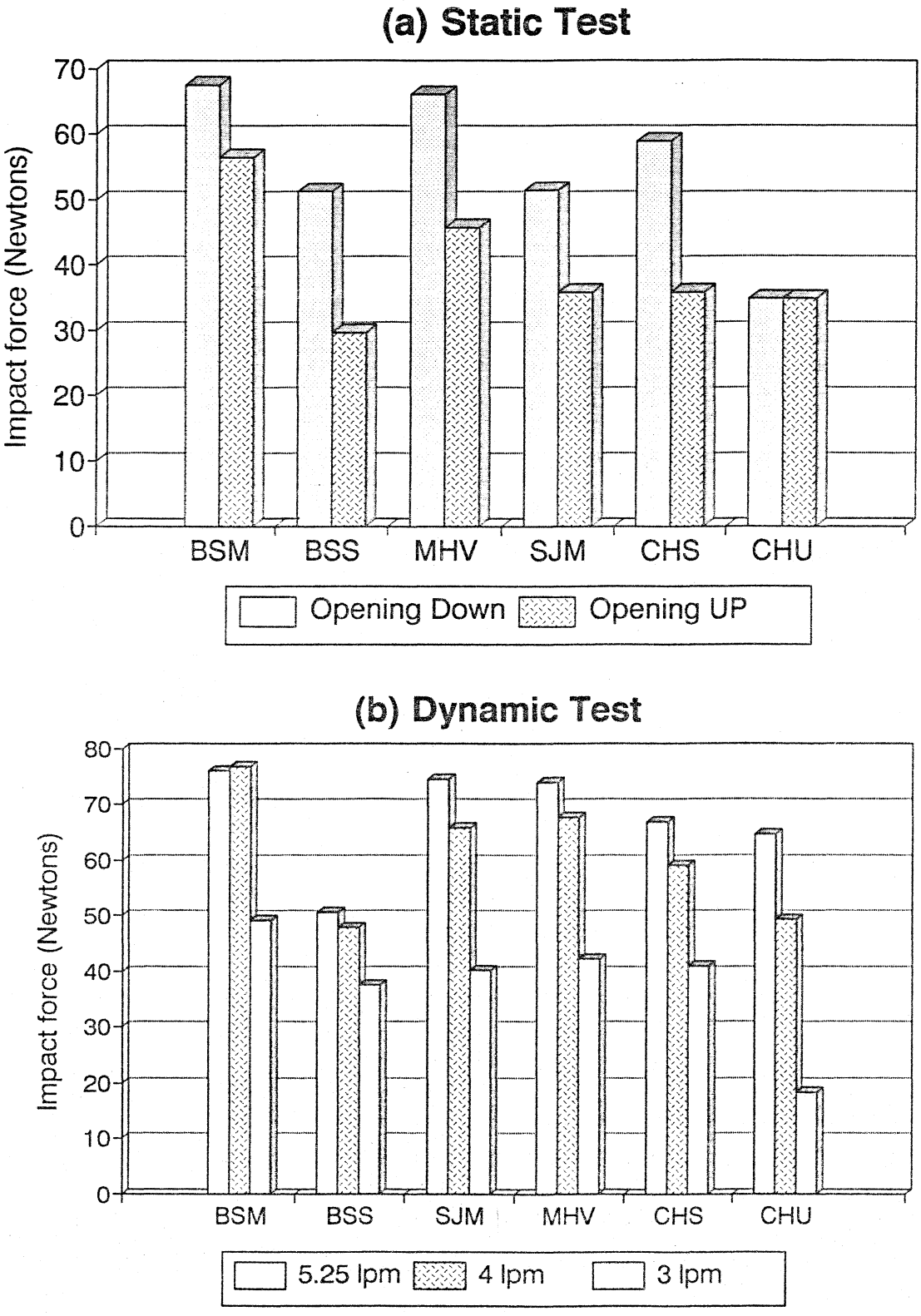

Figure 6.13

CLOSING IMPACT FORCE OF TEST VALVES

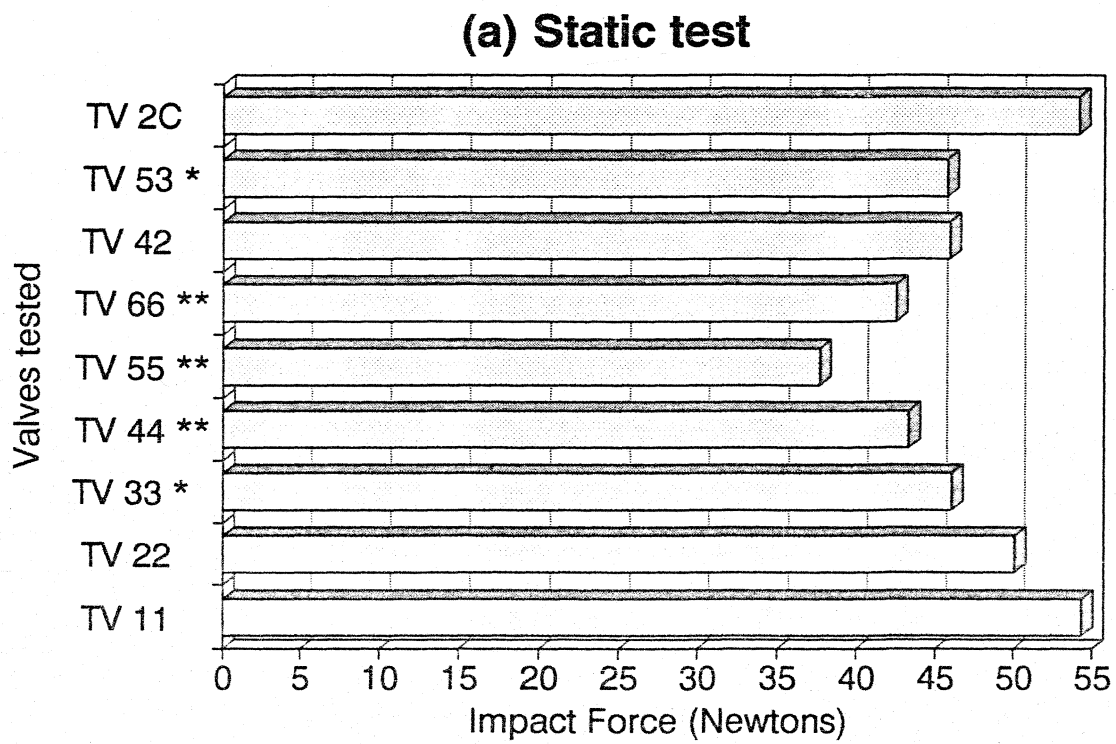

*Note: * Valve opens 60 to 70 degrees only*
*** Valve opens less than 60 degrees*

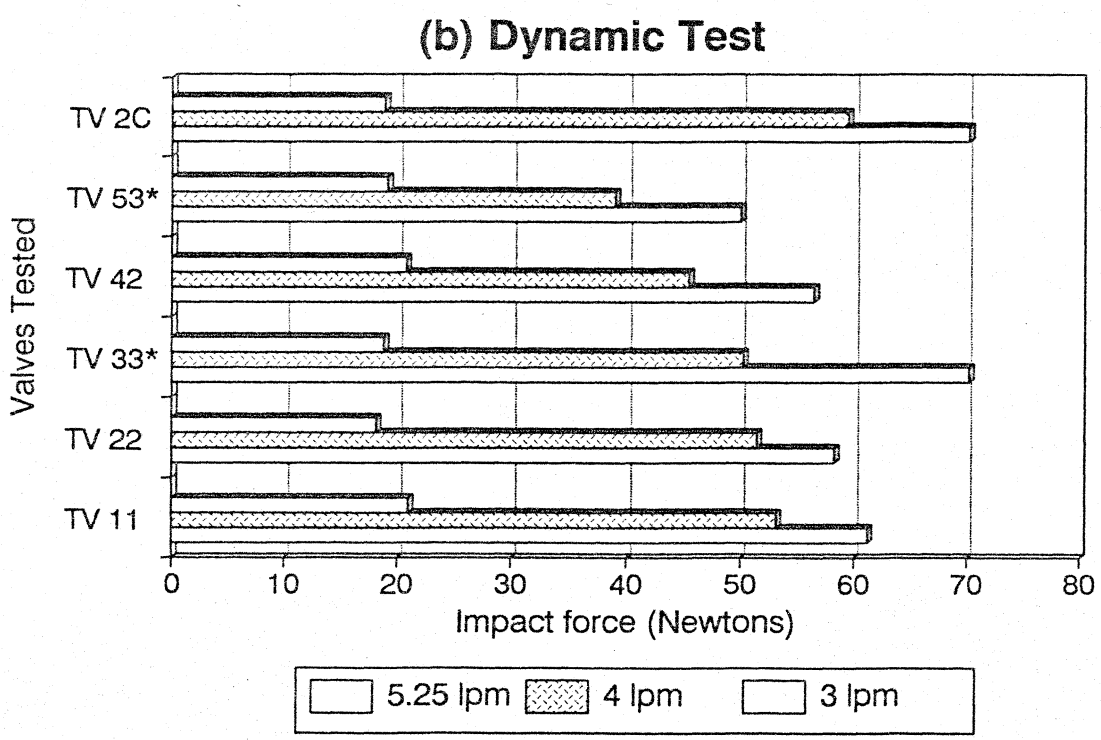

6.7 SUMMARY

Overall, the above data indicate that TV-42 is the optimum valve in terms of EOA, closing volume and closing impact forces, having the most central pivot axis and the condition that the valve must open fully to 75°. The most important observations are that the impact forces and closing volumes are definitely NOT INCREASED (if not marginally reduced) over the current model, ensuring that the design changes have produced no deleterious changes on valve function. EOA of the TV-42 seems to be similar to the current design. The effect of introducing the disc sliding on wear of the disc has not been studied and needs to be carried out. From experience, the expectations are that the disc wear will not be significantly increased. However, prototype valves of clinical quality have to be fabricated and tested in the accelerated durability system and animal trials for sufficient durations to rule out this possibility and confirm the expectations.

A technique for the measurement of closing impact forces has been developed and the effect of sewing ring, ventricular pressure rate of rise, disc shape, etc. have been studied. It is clear that the sewing ring plays a major role as a shock absorber. The concavo-convex discs consistently show higher impact forces and closing volumes.

The sewing ring of the present Chitra valve being softer than that of the standard valves like the Bjork-Shiley and Medtronic-Hall, absorbs more of the impact force. The UHMW-PE disc, being a plastic also helps reduce the impact. This may

already have some beneficial effect, which may come to light during the next couple years from the clinical trials. Further work on improving the shock absorbing capacity of sewing rings is indicated.

~~~~~~~~~~~~~~~~~~~~~~~~~~~~~~
~~~~~~~~~~~~~~~~~~~~~~~~~~~~~~

CHAPTER 7

RELATIVE ORIFICE FLOWS AND VELOCITY PROFILES

After having determined that the valve model TV42 is the optimum one from steady flow and pulsatile tests, it was considered necessary to quantify the improvement in the flowrate through the minor orifice. In the first part, the relative flowrate through the major and minor orifices were directly measured. In the second part, velocity profiles 18 mm downstream of the valve (measured from the edge of the valve ring) were determined using a Pulsed Ultrasound Doppler velocimeter (PUDVEL) system. Apart from the model TV42, the standard valves were also evaluated for comparison.

7.1 RELATIVE FLOW BETWEEN MAJOR & MINOR ORIFICE AREAS

The relative flowrates through the major and minor orifice areas of tilting disc valves were measured under steady flowrates of 15 to 25 lpm[1] using the steady flow set-up described in §5.1.

Pressure drop across the fully-open test valves were carefully measured at three flowrates of 15, 20 and 25 lpm; the flowrate being set using the venturi flow-meter. Then with the

[1]Reynold's nos. are 5000 to 8400 at the valve i.d. of 2.2 cm

disc in the fully open position, the minor-orifice was blocked by sewing a piece of teflon sheet over it and then filling the well thus formed in the valve with RTV silicone adhesive. In this state, the flowrate through the major orifice was measured using the venturi meter at the same pressure drops as measured first with the fully open valve. This procedure was then repeated with the major orifice similarly blocked. The percentage flowrate through each orifice was then calculated and averaged over the three flowrates. The results are shown in **Figure 7.1.**

The basic assumption in this technique is that the potential field across the valve is not significantly disturbed due to the blocking of the major or the minor orifice and remains nearly the same as when the valve is fully open. This of course is not strictly true and hence results in some error. Over this flowrate range (which corresponds to pulsatile mean flowrate of 4 to 8 lpm in the mitral position), it can be seen that the technique yields fairly good estimates of the relative flowrate through the two orifices and the effect of the design changes introduced can be observed.

The present model of the Chitra valve exhibits a 4% improvement over the BSS due to the use of the plano-convex disc. The good improvement of flow through the minor orifices of the newer generation tilting disc valves, viz., Medtronic-Hall and Bjork-Shiley Monostrut over the Bjork-Shiley standard design can also be seen. The test valve TV42 shows the maximum minor orifice flow through it with an 8% increase over the present Chitra model and a good 12% increase over the Bjork-shiley standard. This increase should contribute significantly to

Figure 7.1

RELATIVE FLOW IN MAJOR & MINOR ORIFICES

15 to 25 lpm Steady flowrate

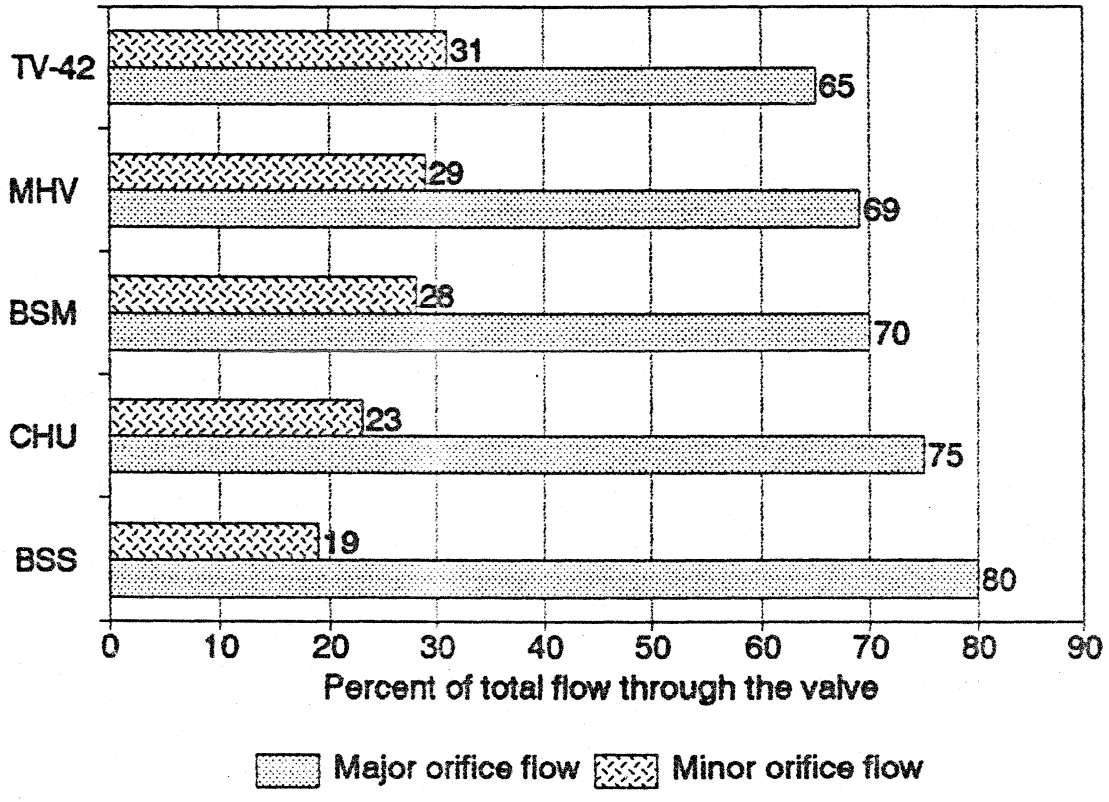

reducing the problem of tissue overgrowth in the minor orifice region.

This improvement in the minor orifice flow for the BSM & MHV has been documented by LDA velocity profile measurements by a number of investigators (Yoganathan & Letzing, 1983; Yoganathan *et al.*, 1988; Reul *et al.*, 1986; Bruss *et al.*, 1983; Chandran *et al.*, 1983a). However, there are no reports of such quantification of volumetric flowrates, which are probably more meaningful to the cardiac surgeon.

7.2 PULSED ULTRASOUND DOPPLER VELOCITY METER SYSTEM (PUDVEL)

The PUDVEL system developed by Black & How (1989) for the hydrodynamic testing of tapered prosthetic arteries was suitably modified for this application and is described below.

The doppler signals were obtained from a commercially available variable range, single gated 10 MHz PUDVEL (Crystal Biotech, USA). Briefly, a miniature piezoelectric crystal of size 1 mm X 1 mm, which alternately acts as the transmitter and receiver was excited at 10 MHz with a pulse repetition frequency of 62.5 kHz. Each transmitted pulse had a duration of 0.4μs. The receiver gate can be varied between 1 and 13 μs in order to detect the signals originating from 1 to 10 mm from the face of the crystal. The transmitted pulses were reflected by the structures in the beam path of the ultrasound and the resulting echoes were converted to a voltage signal by the crystal transducer. The signal was processed through a phase quadrature detection circuit, whose outputs were in the form of two

quadrature audio signals. The quadrature signals were frequency tracking demodulated.

Figure 7.2 is a schematic of the system used. A frequency tracking demodulator (type 55N20 Dantec Electronics, UK) designed for use with laser anemometer systems was used to obtain real time estimates of the doppler frequency. The tracker can process doppler signals of frequencies from 1 kHz to 10 MHz by means of seven overlapping ranges. The quadrature signals from the doppler velocimeter were frequency shifted to the 3 to 33 kHz range of the tracker using custom built instrumentation. The tracker processed the signal to give a voltage output proportional to the doppler frequency. The analogue output from the frequency tracker was sampled at 400 Hz by the microcomputer and stored for subsequent analysis. A 200 Hz low pass filter prevented aliasing of the signal.

7.3 PROBE DESIGN AND MOUNTING

The 10 MHz PUDVEL range gate has a maximum range of 10 mm at a pulse repetition frequency (PRF) of 62.5 kHz and a 20 mm at a PRF of 31.25 kHz. Hence, to measure velocity profiles in the mitral channel of 43 mm diameter, it was necessary to introduce the crystal into the flow channel. To minimise the disturbance to the flow field in the region of measurement, the crystal was mounted on the side of a 1.5 mm diameter stainless steel tubing for support and bringing out the signal wires. This assembly is henceforth termed a velocity **PROBE**. The probe was placed diametrically across the flow channel, downstream of the valve

Figure 7.2

SCHEMATIC OF PUDVEL

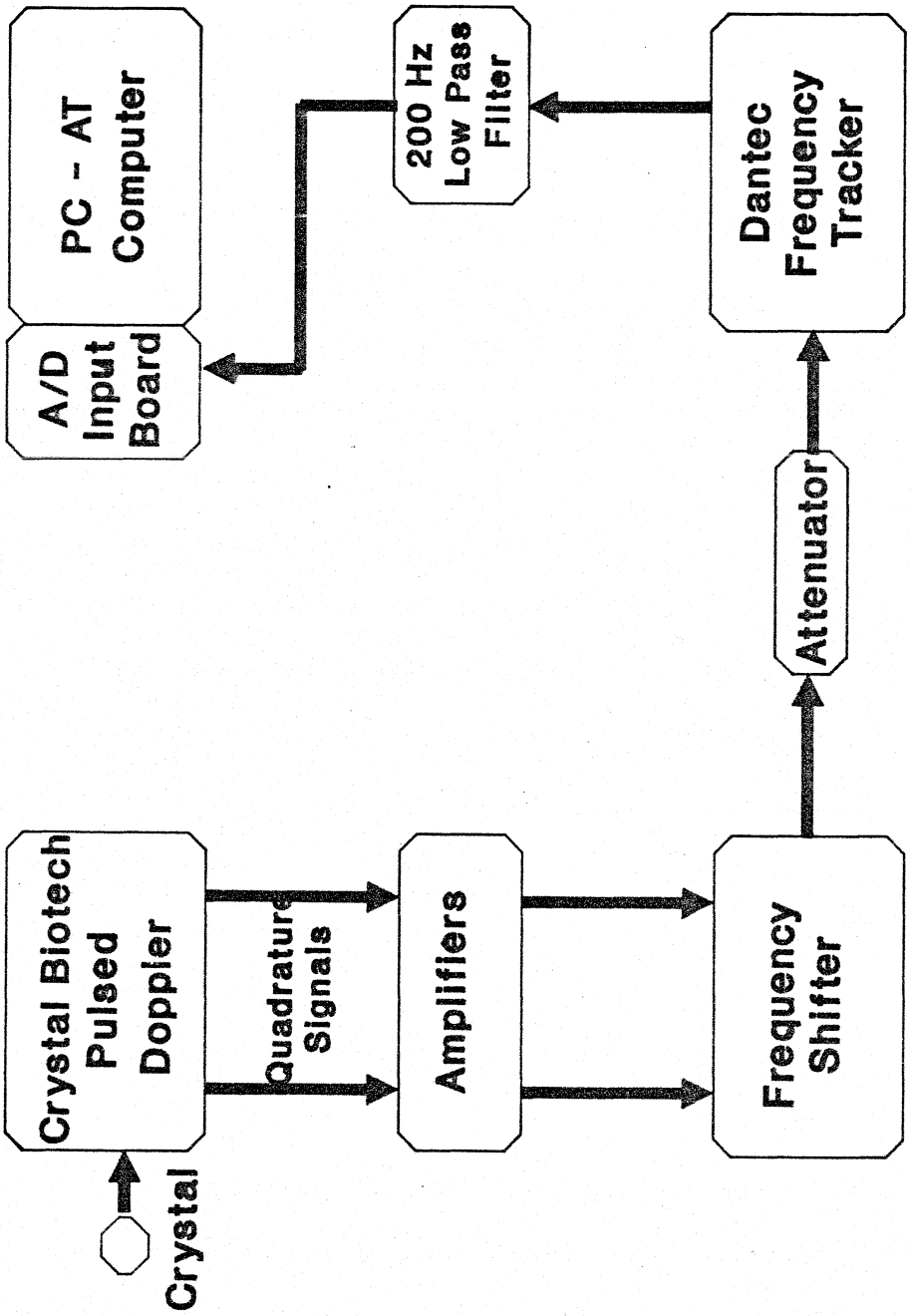

as shown in **Figure 7.3.** Further, the crystal was pointed axially upstream towards the valve and the velocity profiles measured 8 mm (i.e., >5 probe diameters) upstream from the face of the crystal. Under these conditions, it was assumed that the probe did not cause any disturbance to the flow field at the measurement point.

7.4 STEPPER MOTOR DRIVEN PROBE MOVEMENT

The probe was mounted on a stepper motor driven screw positioning system, which was fabricated in-house, as shown in **Figure 7.4.** The stepper motor was controlled using an interface card in the PC-AT computer. With a 1 mm pitch screw and 200 steps/revolution motor, the system was theoretically capable of a positioning accuracy of ±5 microns. However, the accuracy of the machined screw pitch, backlash and other parameters gave a location accuracy better than ±0.1 mm, non-cumulative. The probe position was visually monitored using a vernier scale fitted to the positioning unit as shown in the figure.

7.5 MEASUREMENT OF VELOCITY PROFILES

The doppler probe was positioned diametrically 26 mm downstream from the edge of the valve with the crystal pointing upstream. The doppler range was set at 8 mm resulting in a measurement traverse 18 mm downstream of the valve. This resulted in the traverse being just 1 to 2 mm beyond the edge of the fully open disc of the tilting disc valves.

Figure 7.3

VELOCITY PROFILE MEASUREMENT : Probe Insertion & Traverse Axes

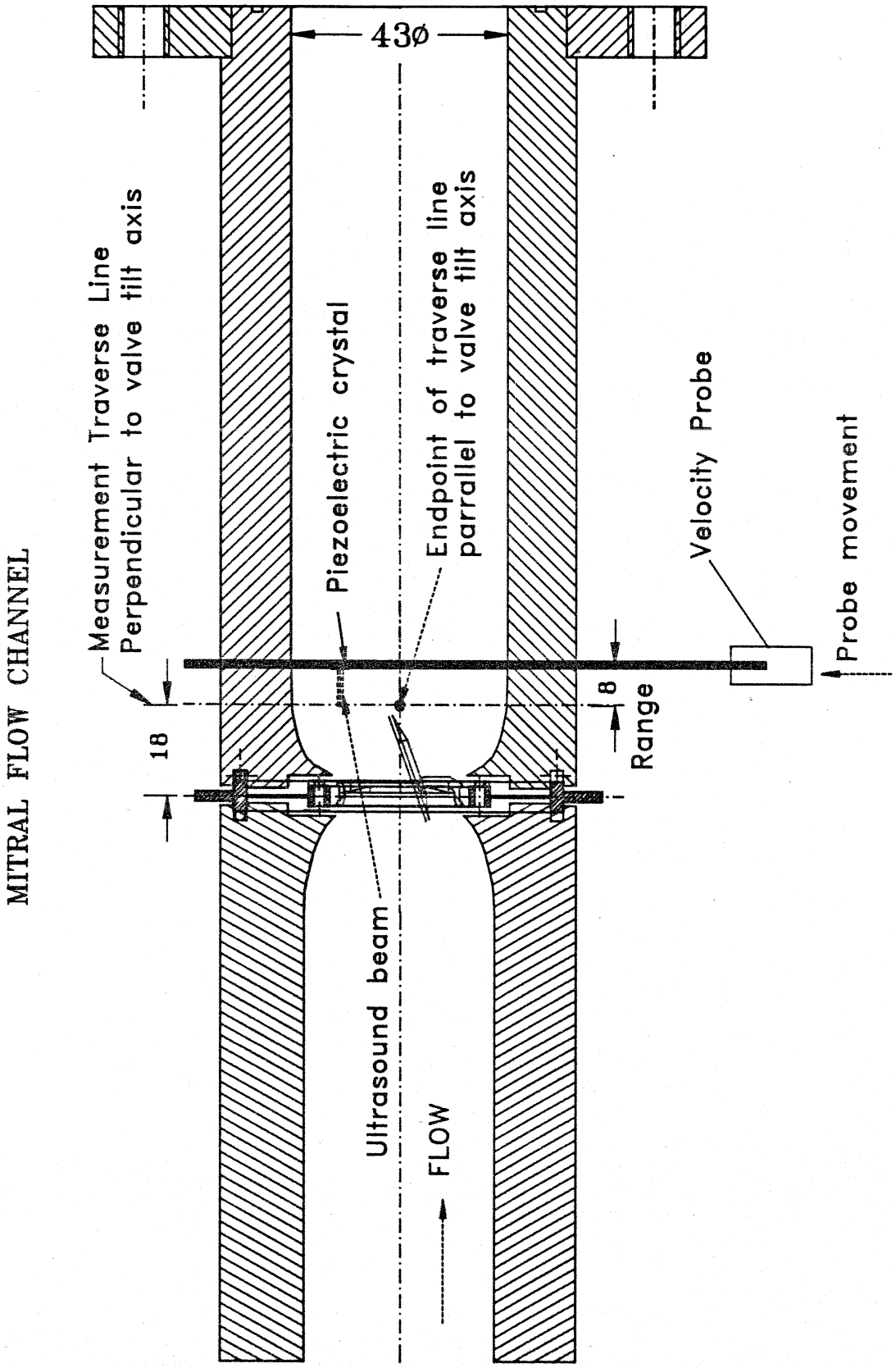

ULTRASOUND PROBE POSITIONING UNIT

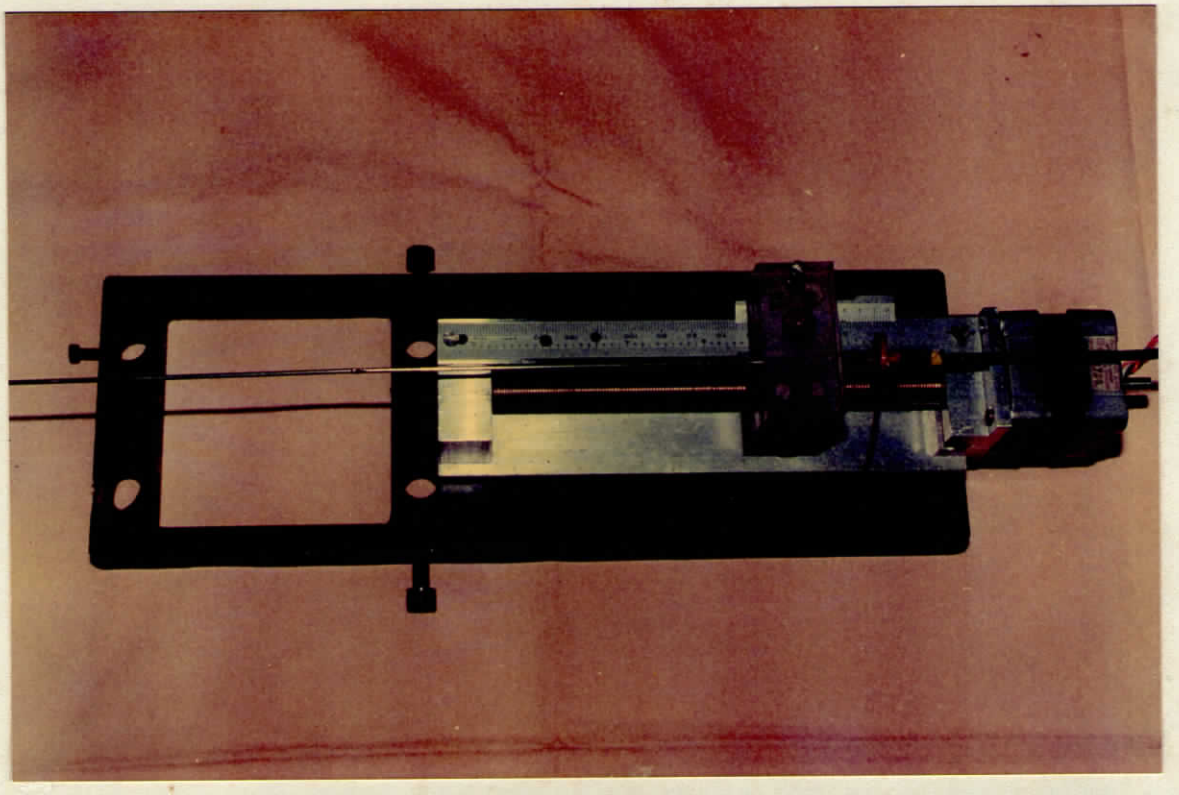

THE PULSE DUPLICATOR SETUP

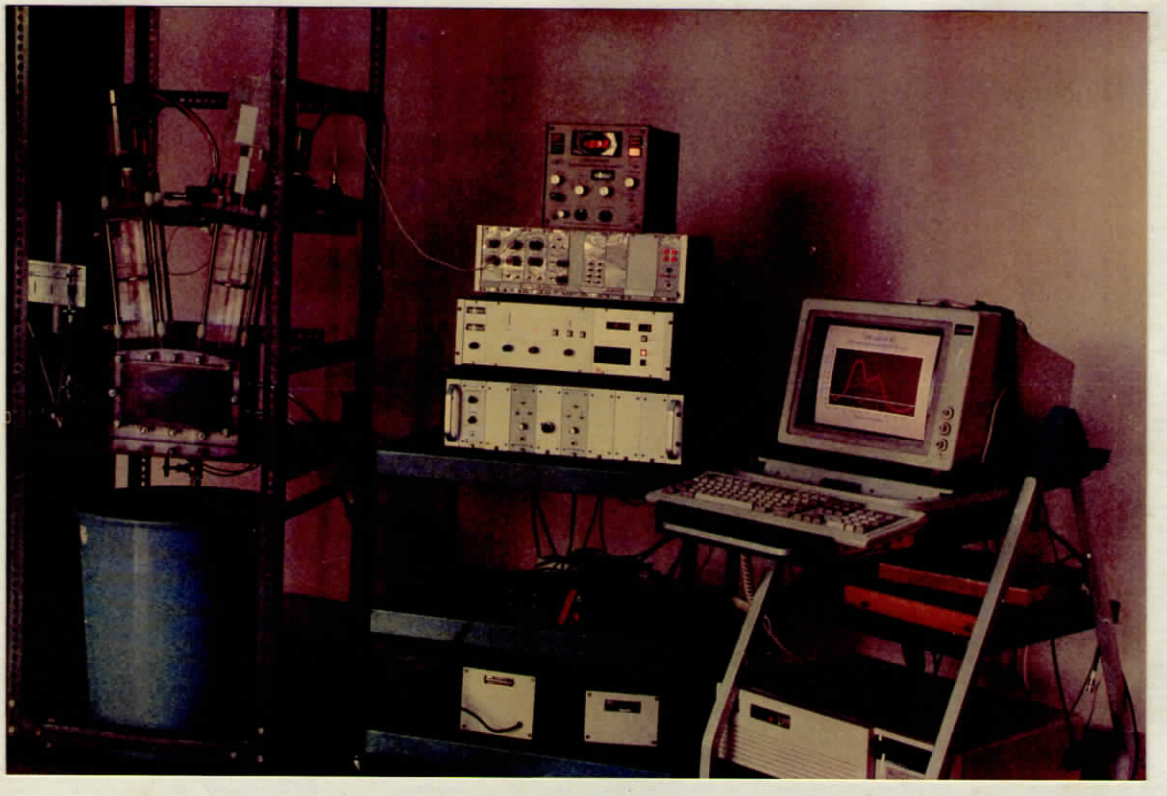

CLOSE-UP OF THE PULSE DUPLICATOR

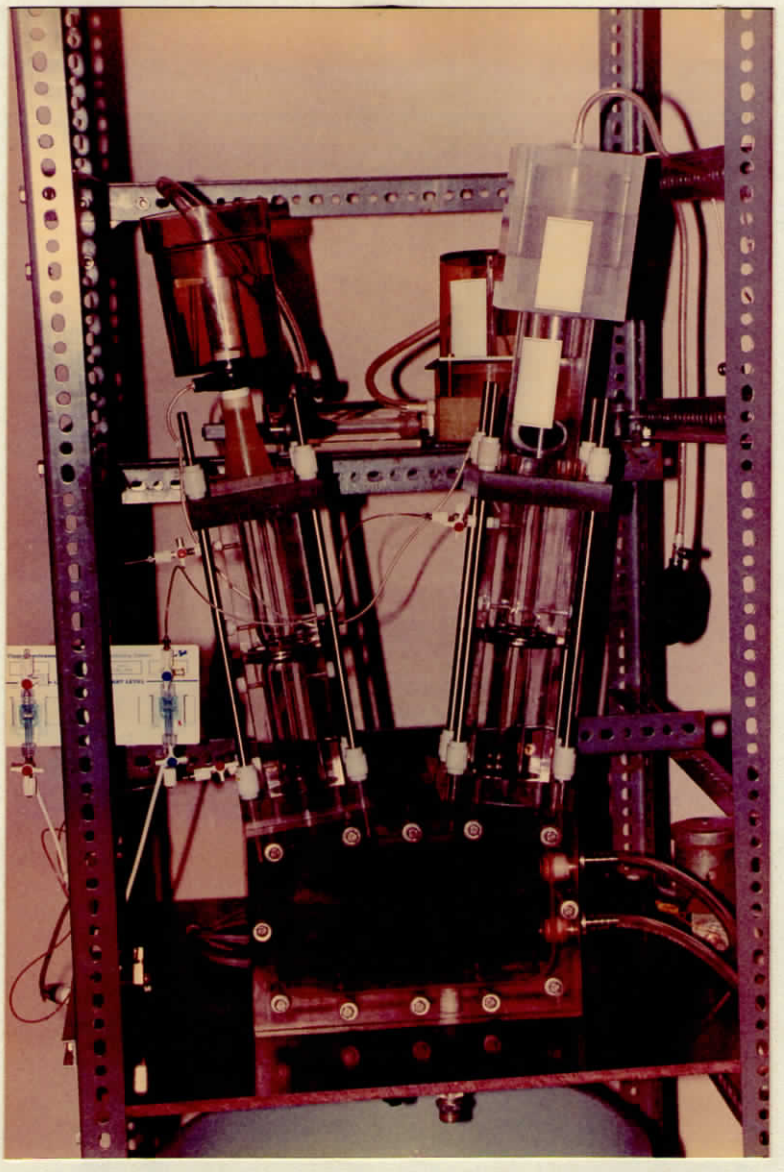

Figure 7.4

ULTRASOUND PROBE POSITIONING UNIT

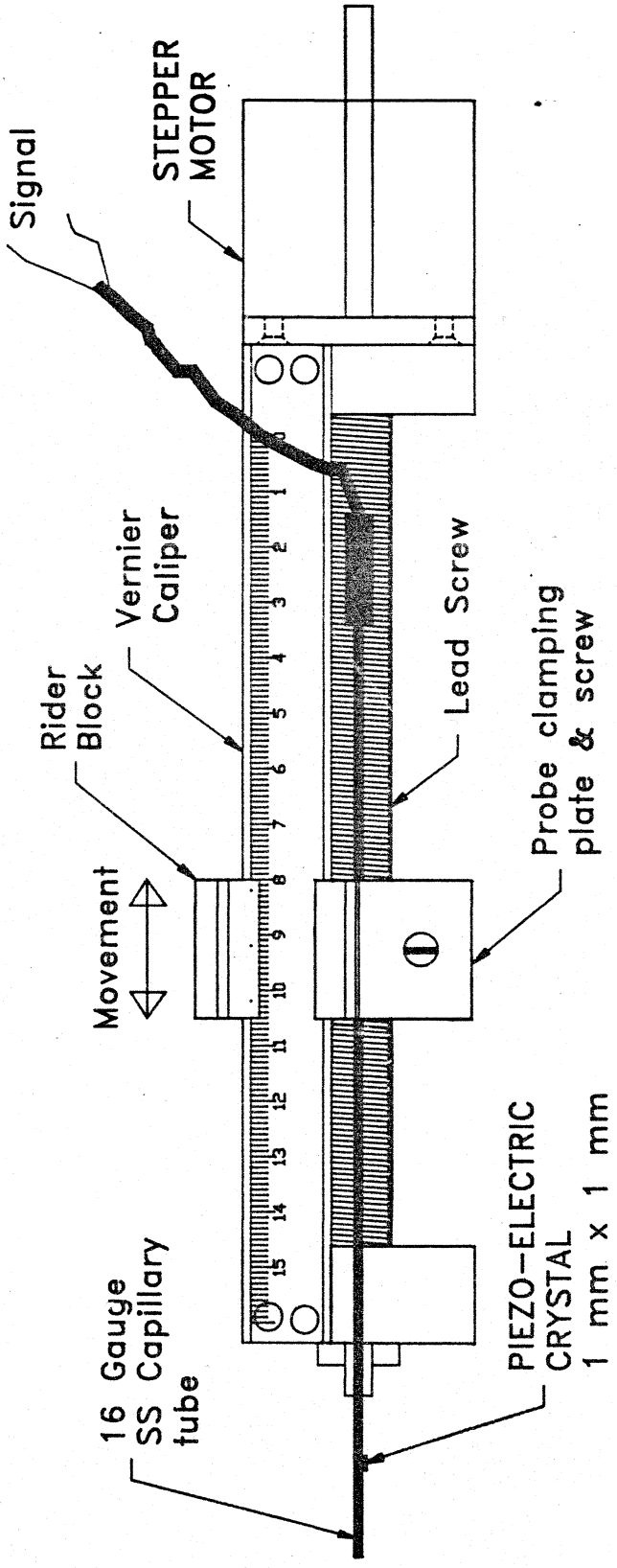

To obtain a continuous doppler signal of near uniform amplitude, the blood analogue was seeded with 0.15% (w/v) of polystyrene microspheres (Polysep 12% DVB, Polysciences Ltd., UK). The microspheres were dispersed using a surfactant (0.01% sodium lauryl sulphate) and the suspension was stabilised with 0.01% tetrasodium pyrophosphate (Black & How, 1989).

The probe was first carefully aligned so that the beam was parallel to the axis of the flow. This was carried out by using the valve mounting plate without a valve. Under steady flow, the probe was visually positioned at the centre of the flow channel. Then the probe was rotated on its axis to obtain a maximum doppler shift frequency. The probe was securely clamped in position and was not disturbed throughout the tests.

The velocity profiles were measured in the mitral flow channel using the steady flow set up (Fig.5.1) at a steady flow rate of 15 lpm[2]. This approximately corresponds to the peak flow rate at a mean output of 5 lpm under pulsatile conditions. The probe was moved in 0.5 mm steps using the computer control. At each step, 2000 samples were taken at a sampling rate of 400 Hz. The mean and standard deviation were calculated and stored in the memory. The mean velocity profile so obtained was then smoothed using a 5 point orthogonal function :

$$\bar{x}_o = \frac{(x_{-2}+3x_{-1}+5x_0+3x_1+x_2)}{13}$$

The width of the sample volume of the PUDVEL across the face of the crystal was 0.43 mm (Appendix F), which was less than

[2]At 15 lpm, Reynold's No.= 5000 at the valve i.d. of 2.2 cm

the 0.5 mm measurement step of the probe. Hence, spatial smoothening was used to eliminate any discontinuities in the measured profiles.

The smoothed velocity profiles were plotted along with ± one standard deviation in dotted lines. The standard deviation is equivalent to the root mean square (RMS) value of the fluctuating component of the velocity at a point and was taken as a measure of the intensity of flow disturbance at that point (Black & How, 1989). Hence a large deviation indicated increasingly higher levels of disturbed flow. This helped identify regions of disturbed flow downstream of the valve. Repeated measurements were carried out and it was seen that this disturbance was consistently produced showing that it was a flow property of the valve and not an artefact of the measurement system.

To start with, the probe was inserted 25 mm upstream of the valve in the inlet chamber and a velocity profile in the inlet section obtained. Velocity profiles were measured across the two principal diameters of the tilting disc valves as shown in Fig.7.3.

7.6 VELOCITY PROFILES & THEIR COMPARISON

Figure 7.5 was the velocity profile in the inlet section 30 mm ahead of the valve. At 15 lpm, the Reynolds number for the 38 mm diameter inlet side is 2900, which is in the region of turbulent flow resulting in a more flatter profile. The dotted line indicates the calculated mean velocity across the section assuming a totally flat profile. The cross-section of the 1.5 m

long entrance section made of commercial quality 38 mm (1.5") internal diameter PVC pipe was not exactly circular leading to a small discontinuity at the junction between it and the test section. This was reflected in the small step seen in the velocity profile near the walls. The small standard deviation (SD) of this profile was a clear indication of the stable velocity profile on the inlet side of the valve.

The measured velocity profile was integrated over the cross-section to yield a flow rate of 208.5 ml/s. This results in a 20% underestimate over the set flowrate of 250 ml/s (15 lpm). This large error could be due to one or more of the following causes :

a. Misalignment of the probe resulting in the ultrasound beam not being parallel to the axis of flow and the traverse not being across the diameter of the channel.

b. Underestimation of the doppler shift by the frequency tracking demodulator system, especially under the turbulent flow conditions.

This needs to be investigated in more detail, especially by measuring the velocity profiles under laminar and steady flow conditions in a cylindrical test section to establish the accuracy and provide a calibration for of the system. The second point needs more elaborate investigation, as it also involves the nature and concentration of the seeded particles used for reflecting the ultrasound and the stability of the suspension, which has been a problem in this study.

Figure 7.6 was the velocity profile downstream of the valve holder plate without any valve mounted. The dashed line

Figure 7.5
Inlet Section Velocity Profile

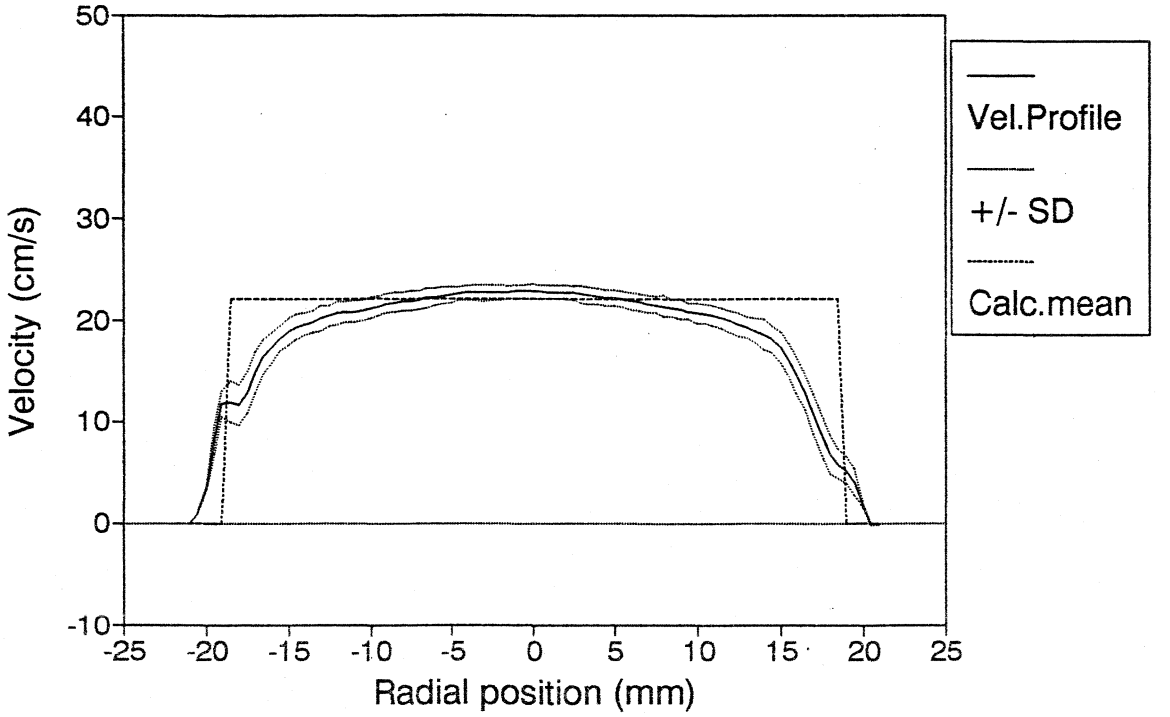

Figure 7.6
Holder Plate without Valve

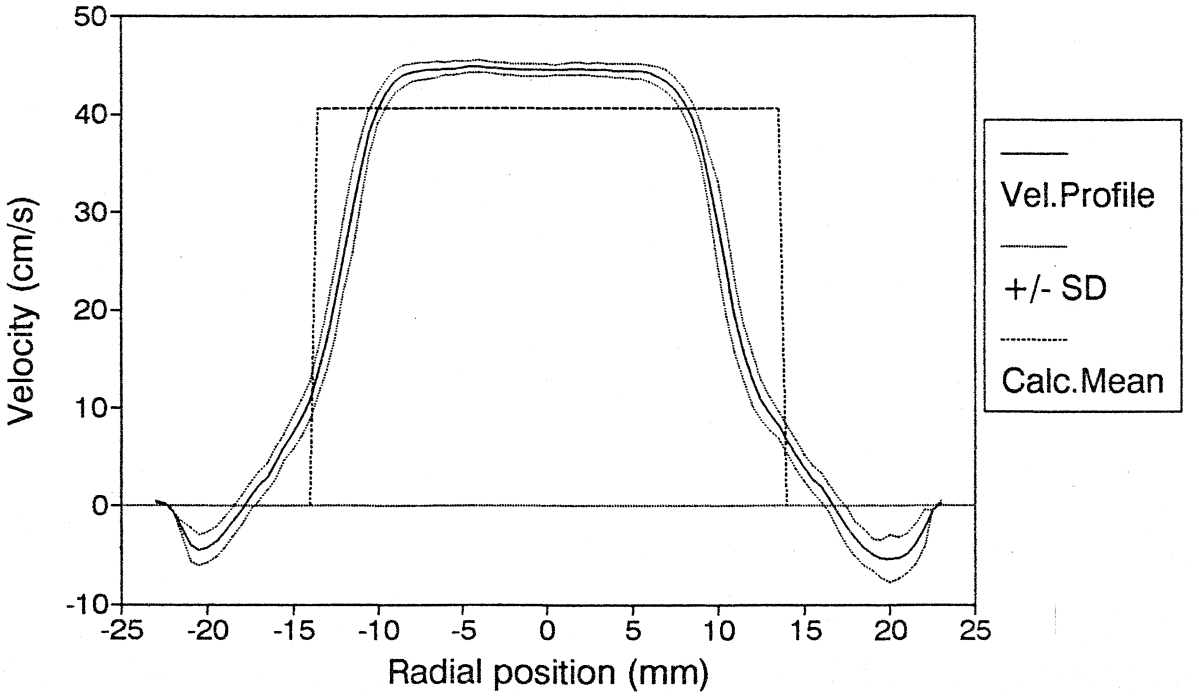

indicates the calculated mean velocity across this 28 mm diameter orifice[3]. Again the small SD indicates a stable flow.

Figures 7.7 (a) to (f) show the velocity profiles obtained perpendicular to the tilt axis of the 5 standard valves and the test valve TV42. For the tilting disc valves, the major orifice was on the left side. The flow through the major orifice of all the tilting disc valves was streamlined with minimal disturbance while that through the minor orifice was more disturbed. The improvement in the velocity of flow through the minor orifice of the TV42 valve over that of the present model of the Chitra valve is clearly seen. Further, the profile for this new model closely resembles that of the Medtronic-Hall valve as can be seen in **Figure 7.7(g).**

Though the volume flowrate through the minor-orifice of the BSM valve is large and comparable to the MHV (Fig.7.1), in this traverse, the velocities were considerably lower and more disturbed than the Chitra or MHV valves (fig.7.7(h)). This was due to the rather thick minor strut of the BSM, which gave rise to a large wake downstream of the strut. This resulted in a larger region of disturbed low velocity flow behind the disc. Further, the curved disc of the BSM resulted in a narrower outflow jet from the major orifice and which was directed more towards the wall on the left. This could cause high wall shear stresses and could lead to damage of the endothelial lining of the wall. Similar results have been reported by Chandran *et al.*, (1983d) for the Bjork-Shiley monostrut valve. Hence, from the velocity profile point of view, the use of curved C-C discs and thick

[3]Reynold's no.= 3960 at 15 lpm

Figure 7.7

VELOCITY PROFILES
Traverse Perpendicular to Tilt Axis

(a) Test Valve 42

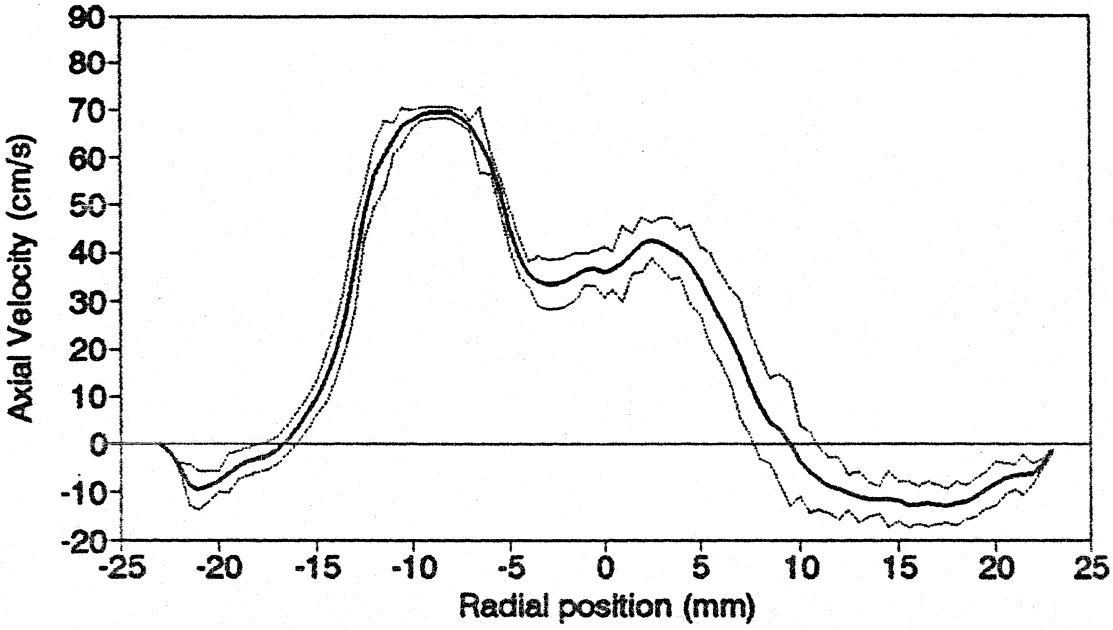

(b) Chitra Valve

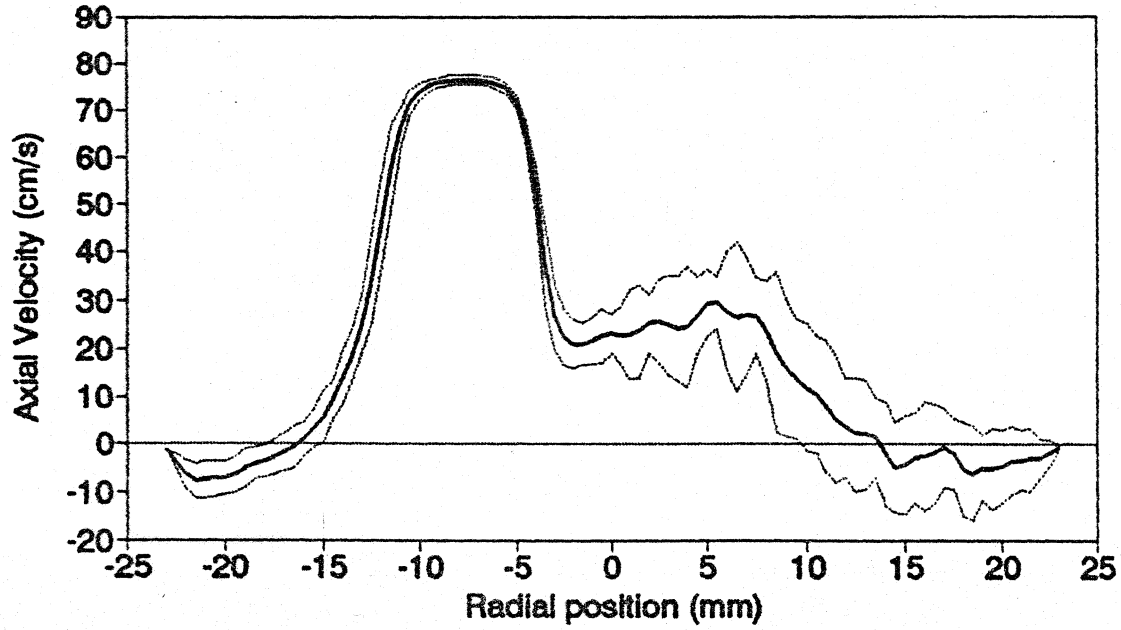

Figure 7.7

VELOCITY PROFILES
Traverse Perpendicular to Tilt Axis

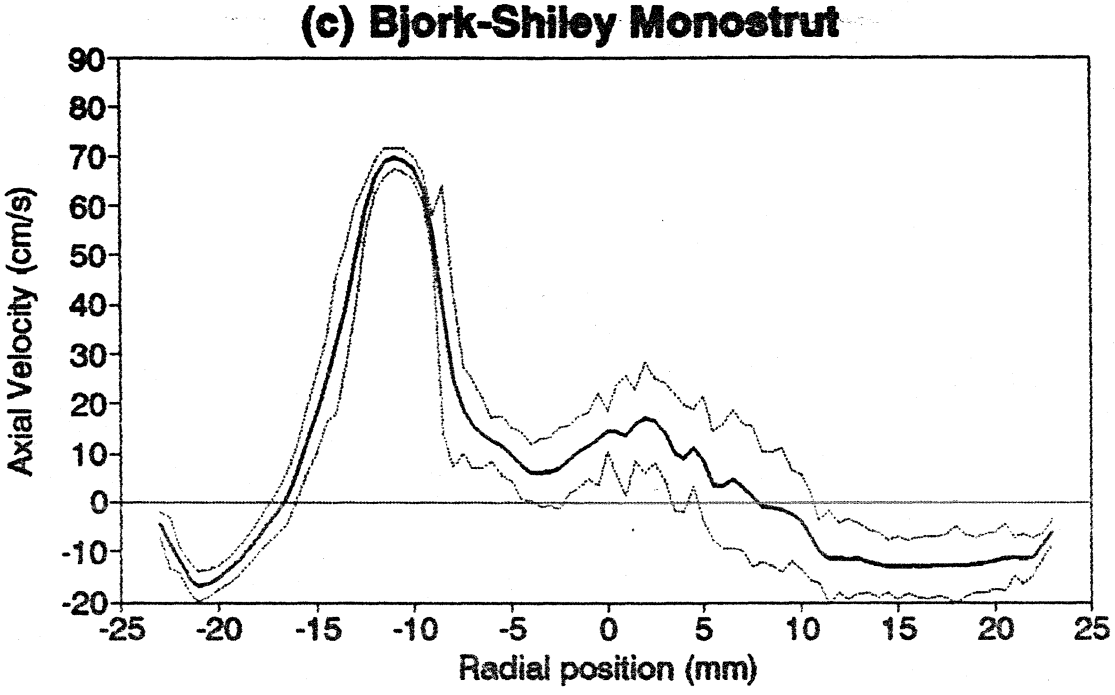

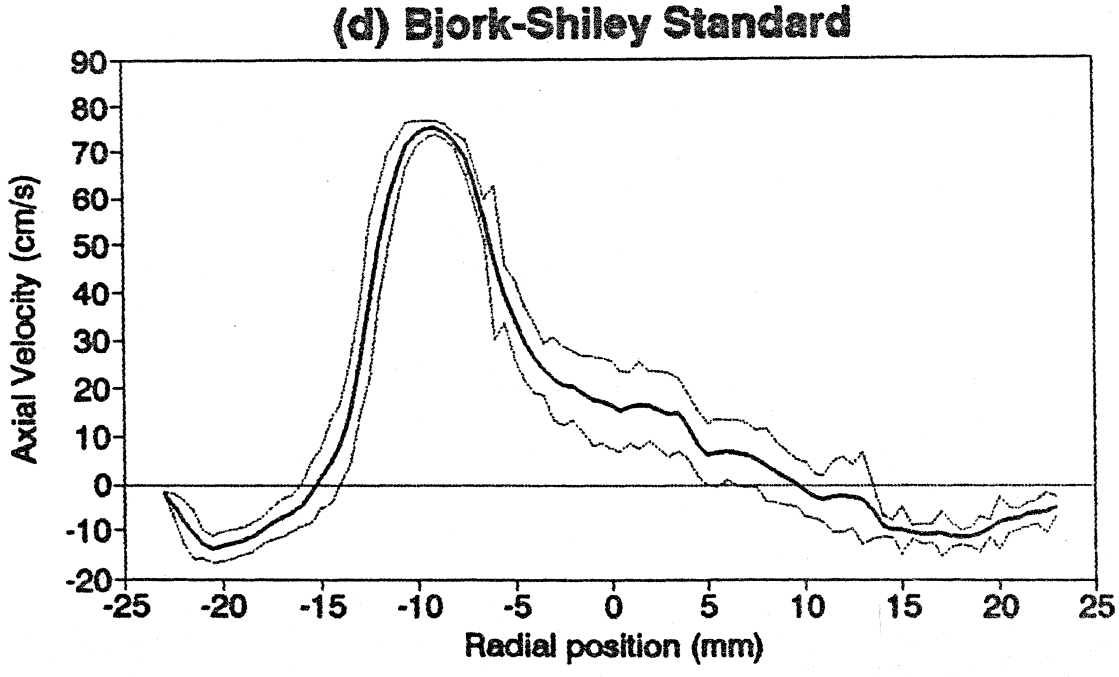

Figure 7.7

VELOCITY PROFILES
Traverse Perpendicular to Tilt Axis

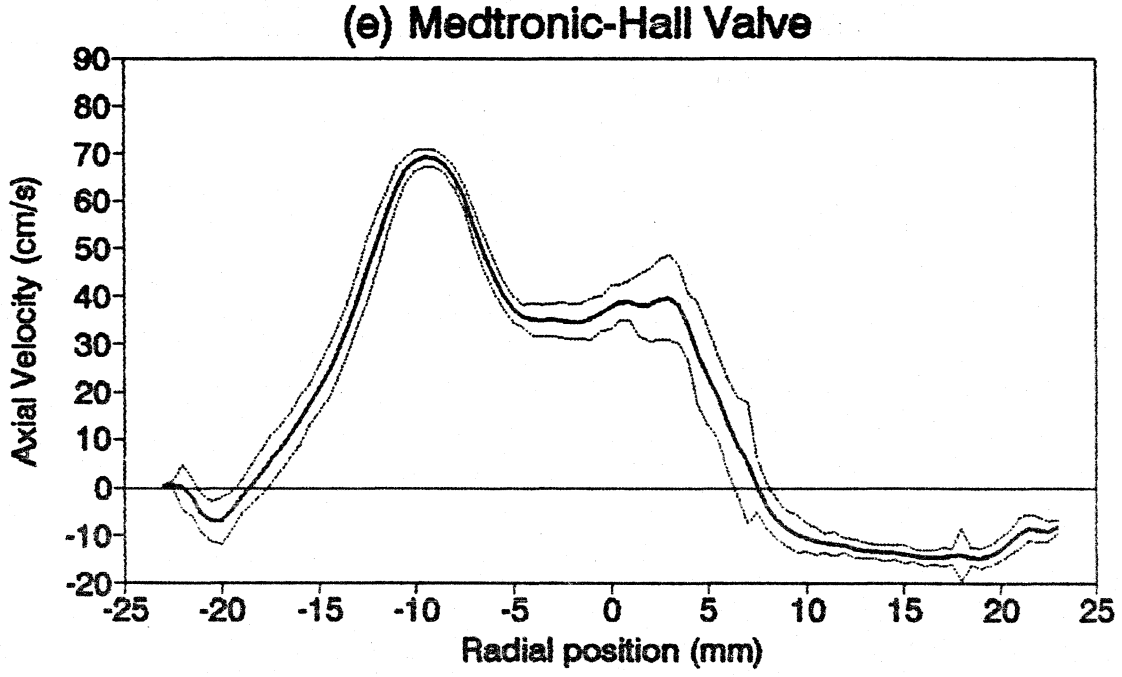

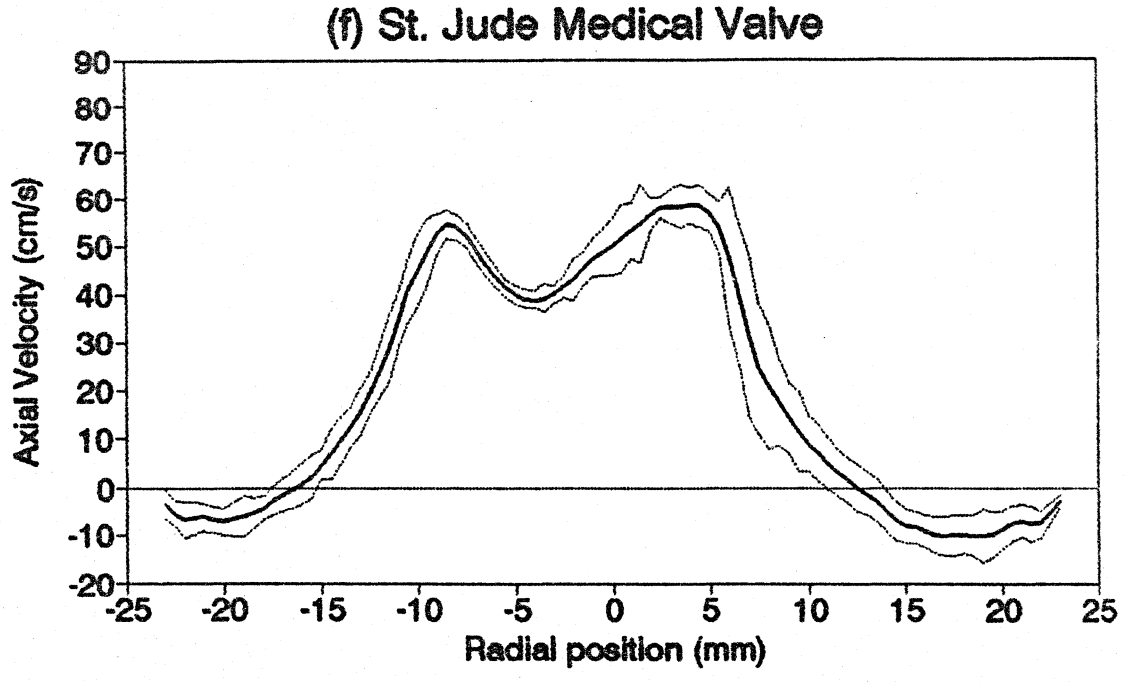

Figure 7.7

COMPARATIVE VELOCITY PROFILES
Traverse Perpendicular to the Valve Tilt Axis

(g) TV 42, Chitra & MHV Valves

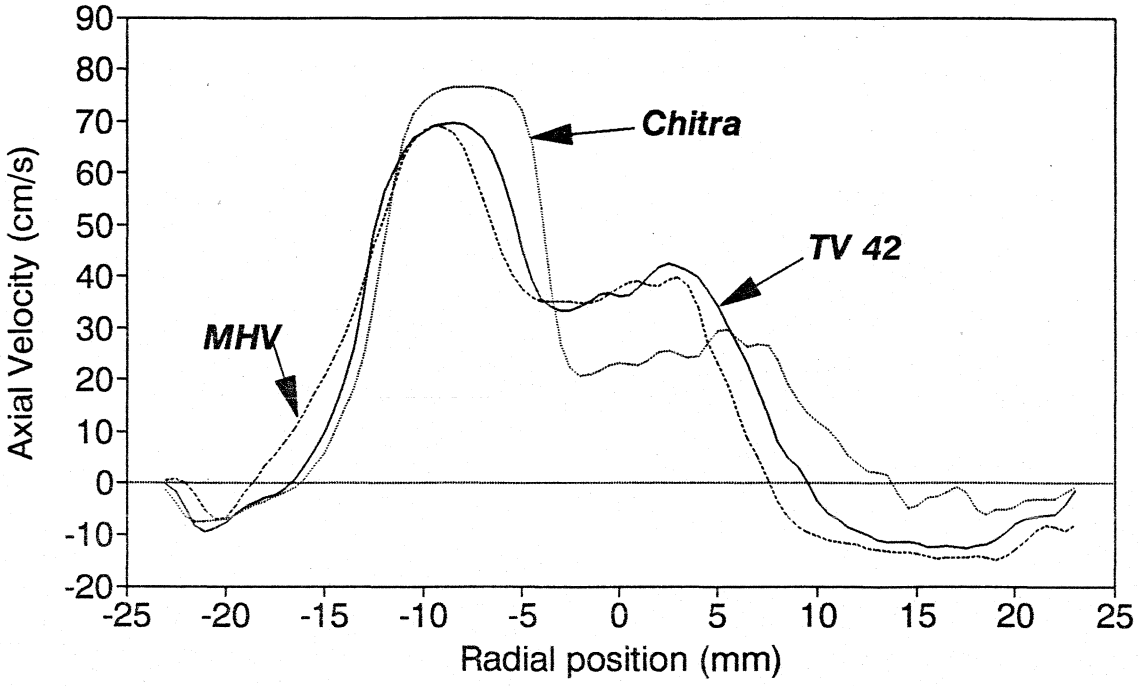

(h) TV 42, BSM, BSS & SJM Valves

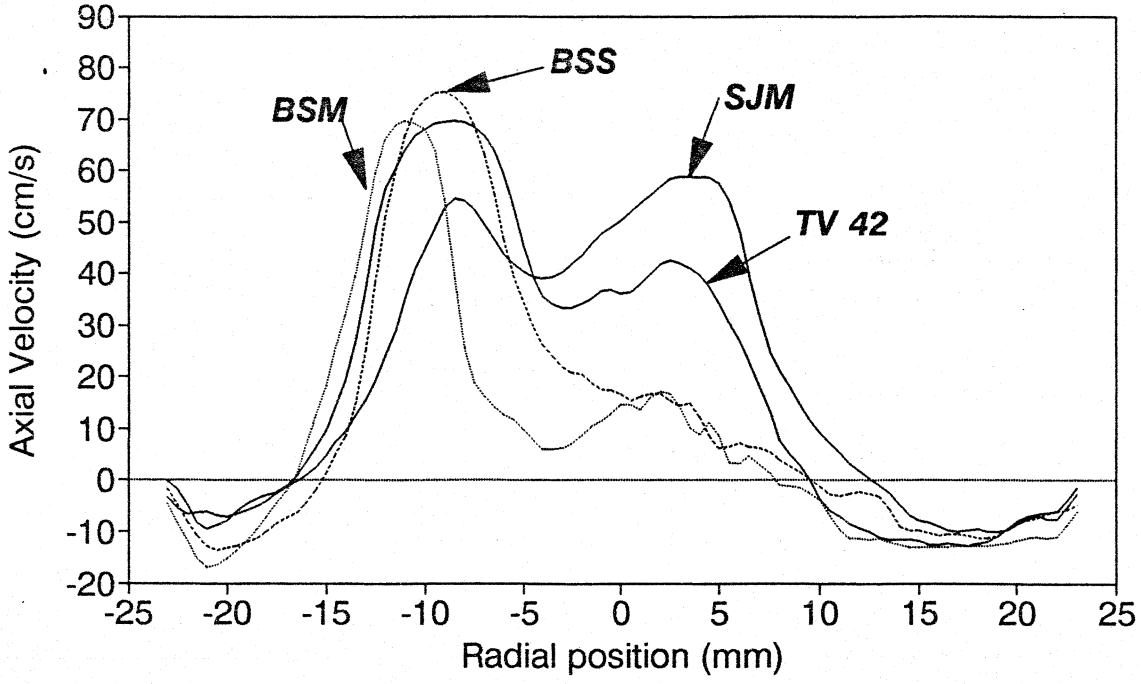

struts seem to be undesirable. Both the B-S valves exhibit a higher negative velocity region adjacent to the major orifice jet (left edge on the graphs) compared to the other tilting disc valves, indicating the presence of a stronger vortex there.

The MHV valve with its thinner minor strut gives rise to reduced flow disturbance in the minor orifice than the Chitra or TV42 valve. This clearly indicates the need to streamline the cross-section of the Chitra valve struts better than at present. The 75° opening angle of the TV42 results in a wider major orifice jet than the MHV.

The bileaflet St. Jude valve has a more central profile than the tilting disc valves as expected. An interesting feature was the unsymmetrical velocity profile obtained. This was probably due to the uneven opening of the leaflets resulting in the central jet getting deflected towards one of the leaflets. This pattern was confirmed by repeated measurements.

Figures 7.8 (a) to (f) show the velocity profiles with the measurement traverse parallel to the tilt axis. In this orientation, the traverse resulted in a measurement just downstream of the disc edge, on the minor orifice side as shown in fig.7.3. Again the improvement in the TV42 velocities over that of the present model is clear. The profile is similar to that of the MHV (fig.7.8(g)). The profile of the BSM was very disturbed and the velocities were significantly lower in magnitude indicating the presence of a large stagnation zone downstream of the disc. The BSS showed lower velocities consistent with the lower volumetric flowrate through it (Fig.7.8(h)).

Figure 7.8

VELOCITY PROFILES
Traverse Parallel to Tilt Axis

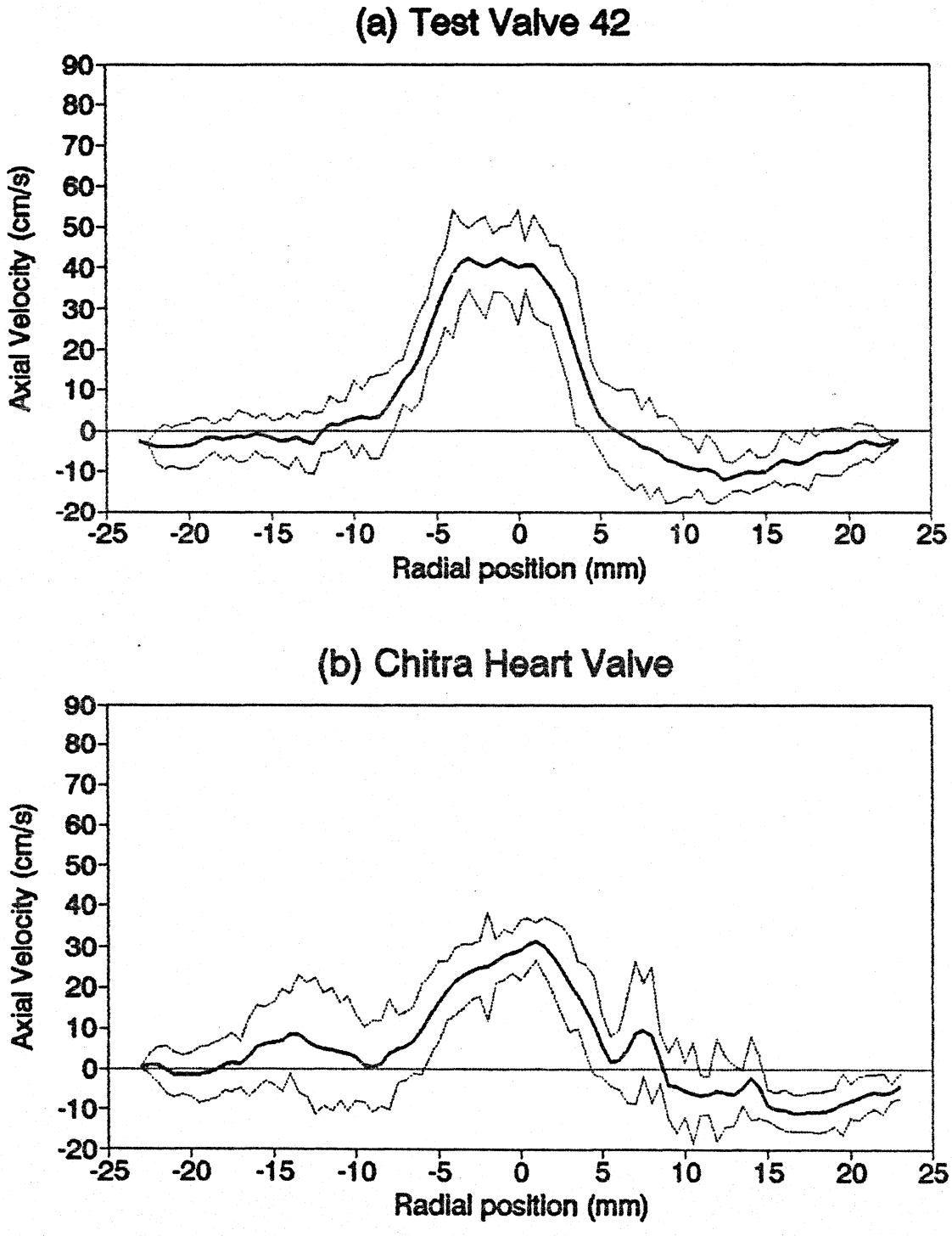

Figure 7.8

VELOCITY PROFILES
Traverse Parallel to Tilt Axis

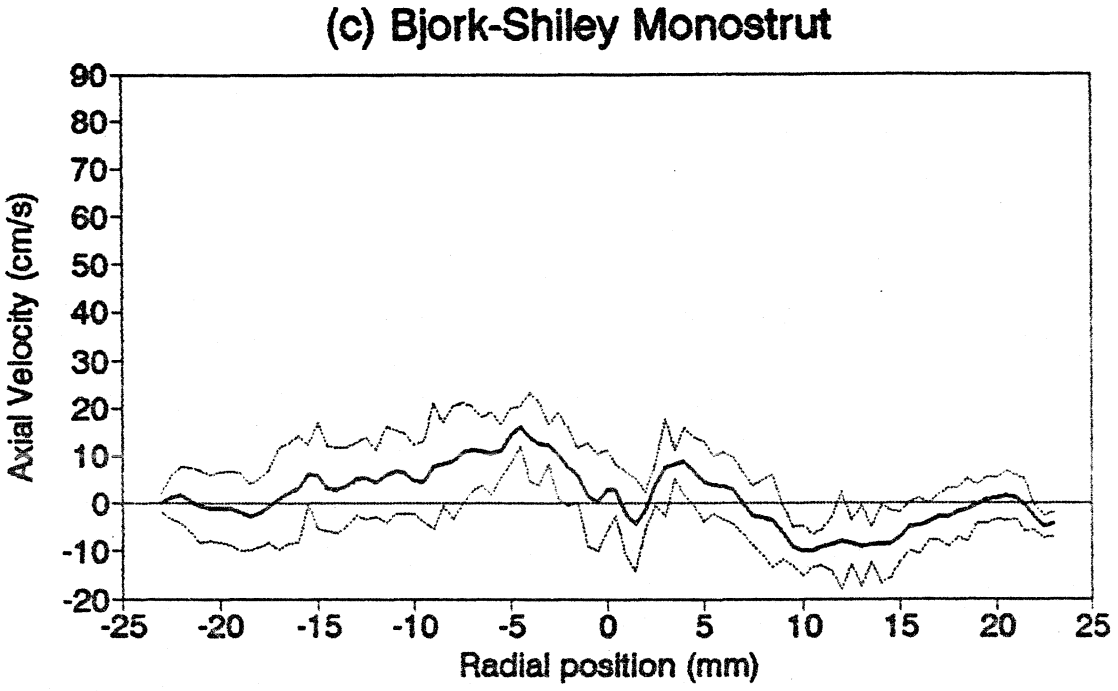

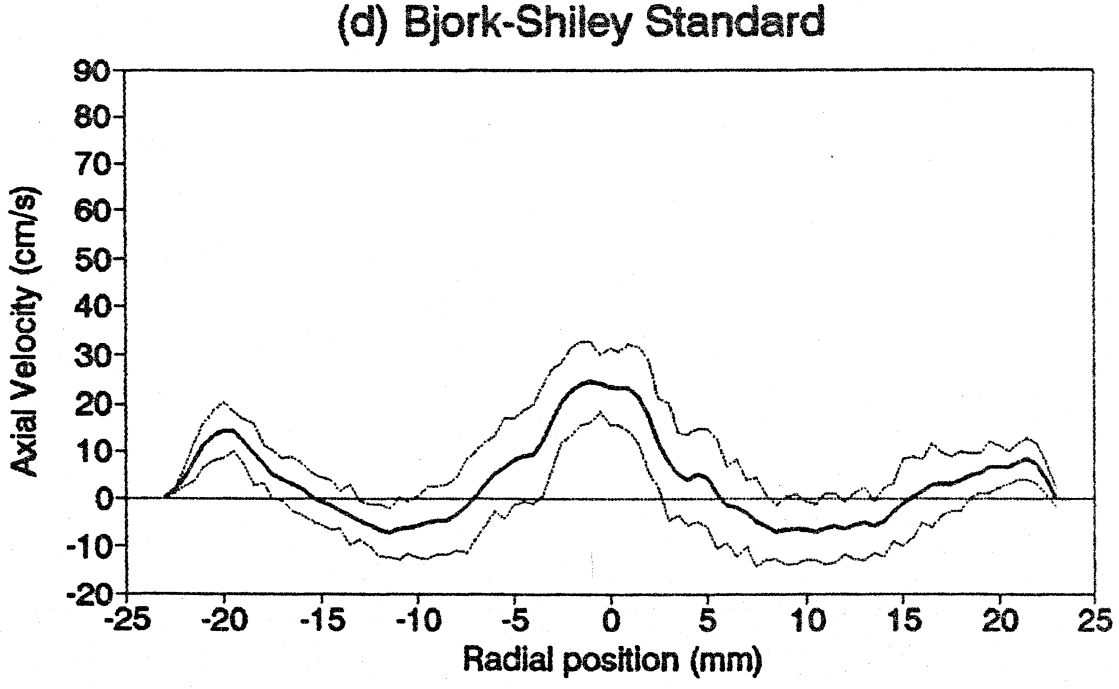

Figure 7.8

VELOCITY PROFILES
Traverse Parallel to Tilt Axis

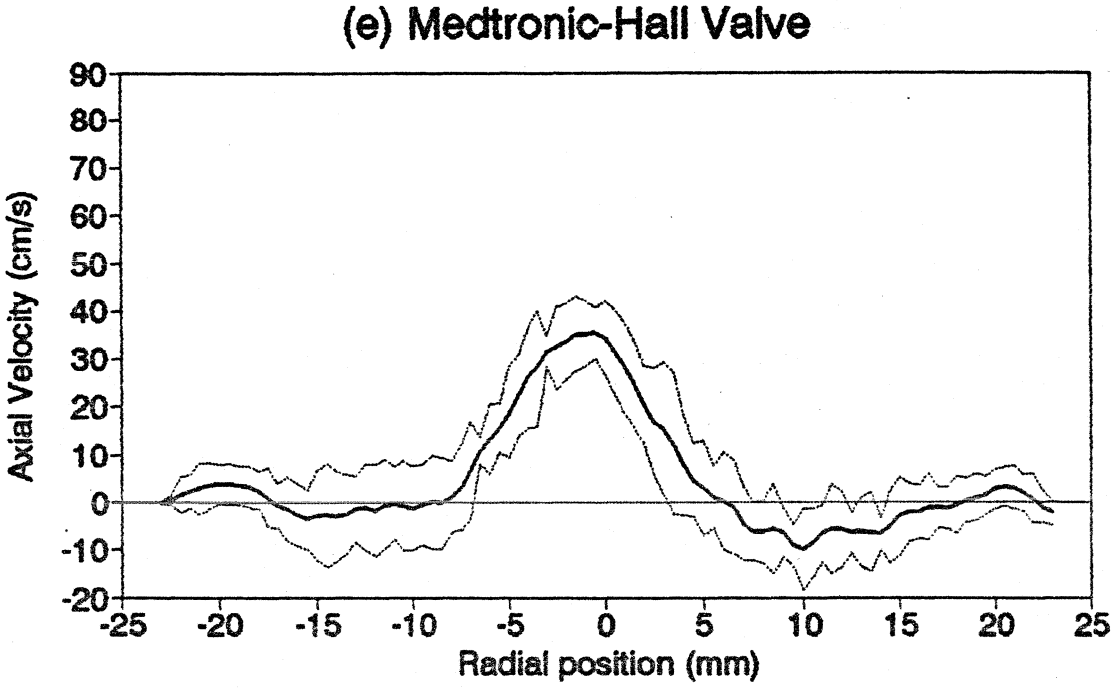

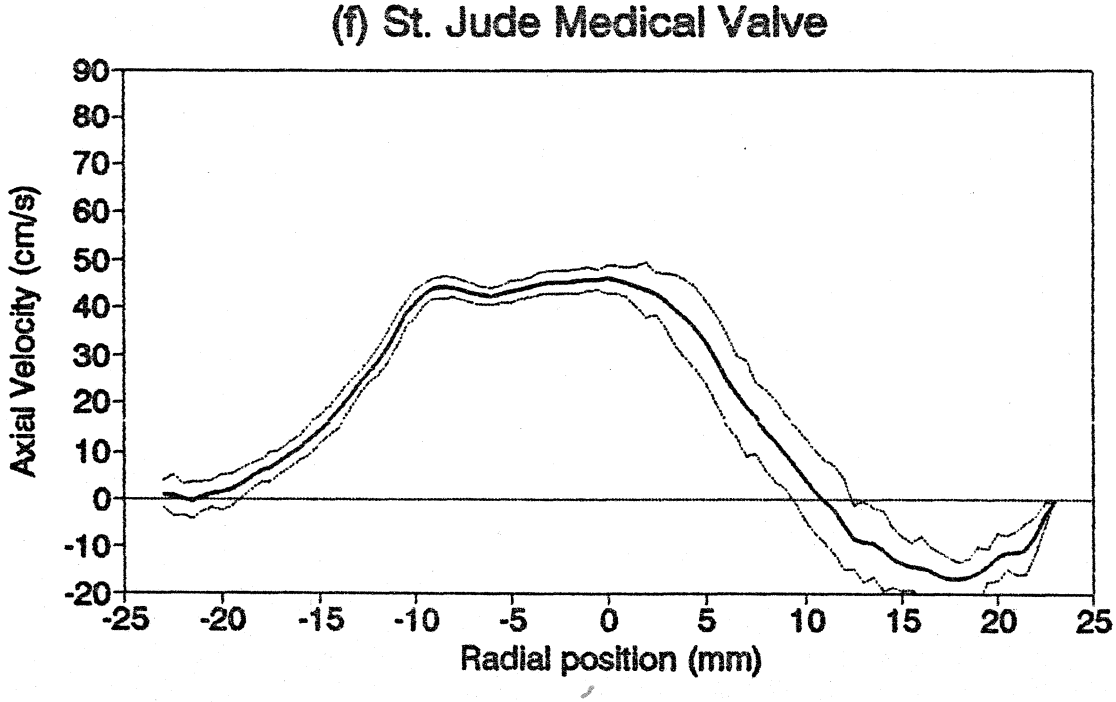

Figure 7.8

COMPARATIVE VELOCITY PROFILES
Traverse Parallel to the Valve Tilt Axis

(g) TV 42, Chitra & MHV Valves

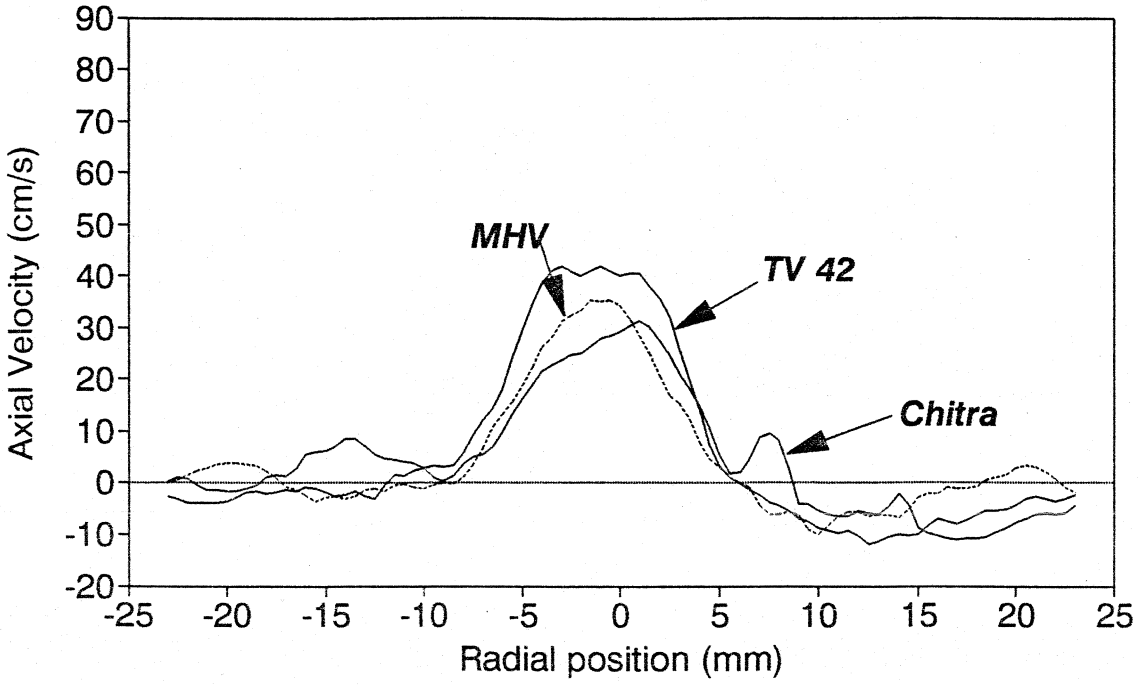

(h) TV 42, BSM, BSS & SJM Valves

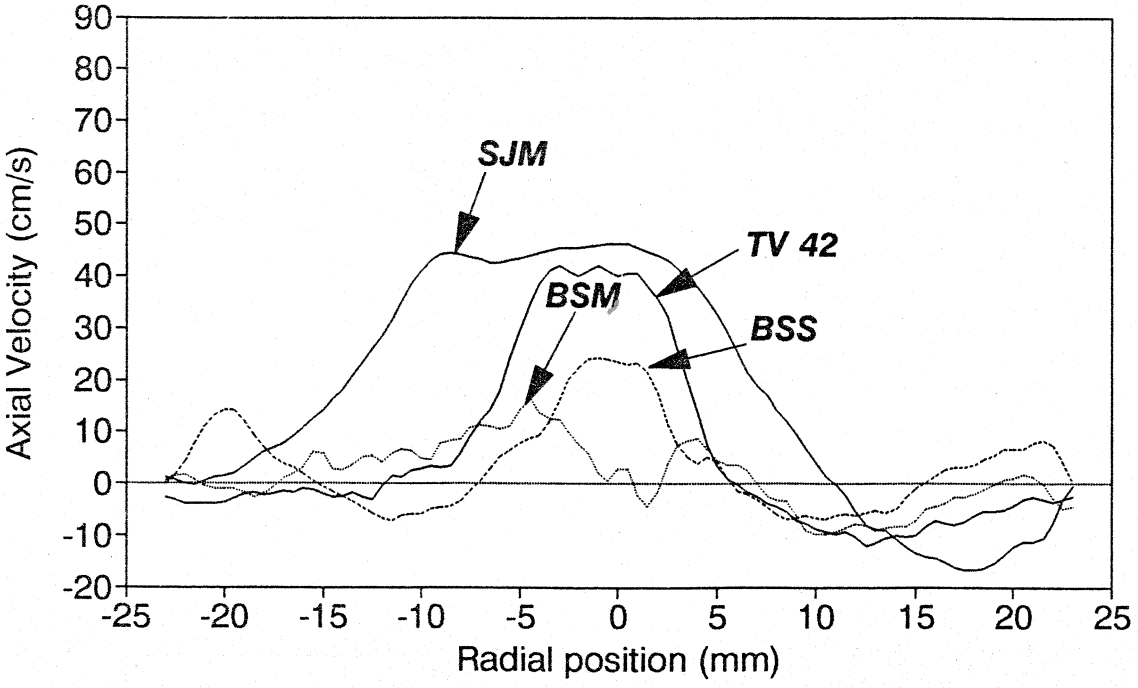

These velocity profiles are generally similar to those obtained using LDA by other workers for the same valve models (Chandran *et al.*, 1983d; Bruss *et al.*, 1983; Reul *et al.*, 1986; Yoganathan *et al.*, 1982b & 1988). But these studies have been performed in aortic positions and under pulsatile conditions. Chandran *et al.*, (1983d) have indicated that under pulsatile conditions, the velocity magnitudes in the minor orifice area are much higher than under steady flow conditions; while in the major orifice, the differences are small. This difference needs to be noted during interpretation of these results. The only report of LDA velocity profile measurements in mitral position is by Woo & Yoganathan (1986). They have reported (under pulsatile conditions) a peak velocity of 100-110 cm/s in the major orifice of Bjork-shiley C-C and MHV valves at a peak diastolic flowrate of 16 lpm, 14 mm downstream of the valve.

LDA suffers from one main disadvantage. It is difficult to apply where the flow chamber is not axisymmetric due to refraction problems. This is probably one of the main reasons, why LDA has not been widely used to study the velocity profiles downstream of mitral valves. As Woo & Yoganathan (1986) point out, although the general shapes of the velocity profiles produced by the mitral prostheses are expected to be qualitatively similar to those obtained with the aortic prostheses of the same type, the magnitude of the velocities and shear stresses as well as the flow field changes as it progresses downstream can be quite different. This will not be a limitation with the PUDVEL system, as the probe can be

generally inserted into the flow stream of any chamber with suitable design of the probe.

7.7 SUMMARY

The major aim of this study was to improve the flowrate through the minor orifice of the valve, which has been achieved. The choice of a plano-convex shape for the Chitra valve and a 70° opening angle has resulted in a 4% increase over the standard BS valve. The design changes in TV-42 model adds another 8% to the flowrate through the minor orifice.

The velocity profiles clearly indicate improved flow through the minor orifice of the TV-42 model in comparison to the present Chitra valve.

The velocity profiles show a large stagnation zone behind the BSM valve, inspite of the large volumetric flowrate through the minor orifice. This is due to the thick minor strut and is probably aided by the shape of the disc. The C-C disc also causes the jet like flow through the major orifice to be directed towards its nearside wall, which seems undesirable, as it can cause damage to the endothelial lining there. The thin minor strut of the MHV produces minimal disturbance to the flow field.

The PUDVEL system has proved to be satisfactory for the determination of velocity profiles under steady flow conditions. However, a detailed study needs to be carried out to establish its accuracy, especially under turbulent flow conditions. Improvements to the system are necessary to make it a more reliable instrument.

CHAPTER 8

CONCLUSIONS

The one and half decades of effort in the search for an indigenous valve ended with the third model of the Chitra valve entering clinical trial in December 1990. The evolution from the first to the third model occurred because of problems with the properties of materials or with techniques of fabricating valve components. In the history of valve development, the choice of appropriate materials, techniques of fabrication and the demonstration of satisfactory device function are more time consuming than the choice of a good design. Therefore, it was imperative to freeze the valve design early on, so that the developmental efforts could be concentrated on these more difficult problems. Hence considerations of any design improvement had to be postponed to this study.

During the late 80's, while the Chitra valve was becoming a reality, extensive data on fluid dynamics of the newer designs like the Medtronic-Hall, the Bjork-shiley Monostrut and the St. Jude valves were being published. Their improved clinical performance in comparison to the older models like the Bjork-shiley standard valves were also being reported. Hence, the time was ripe, when considerations for a major effort to improve the function of the Chitra valve could seriously be taken up.

The considerable experience gained during the development phase of the Chitra valve contributed greatly to a better understanding of the factors in play in the performance of prosthetic valves and the design of this present study. The fracture of the sapphire disc in 1986 and the reports on the fracture of the minor struts in the Bjork-Shiley convexo-concave valve during that time were the motivators for the development of the force transducer and measurement technique.

The following sections summarise the major contributions of this study, its limitations and further work that could be taken up.

8.1 NEW TECHNIQUES USED IN THIS STUDY

i. Force measurements :

The forces acting on valves have been measured with a force transducer designed and developed for this study. For the first time, magnitudes of the closing impact forces have been measured and the major factors affecting them have been identified. This probably gives some insight into the failure of the Bjork-Shiley C-C valves in clinical use and also the problems associated with valves in artificial hearts. The measurement of drag forces on the valve has also been demonstrated using this transducer.

ii. Pulsed Ultrasound Doppler Velocimeter (PUDVEL) :

Laser doppler anemometer has been the method of choice for in-vitro measurement of velocity profiles. Though highly

accurate, LDA is an expensive tool and difficult to set up for more routine use in the valve development laboratory.

A PUDVEL system has been set up and applied for the measurement of velocity profiles downstream of prosthetic heart valves. These data compare favourably with those obtained by LDA. The system at present gives an underestimate of the velocity and hence needs to be improved. Even then, it may not be as accurate as the LDA due to the larger sample volume and the need to introduce the probe into the flow field. However, it could be a low cost viable alternative to LDA for routine evaluation in a cardiac valve development laboratory.

iii. Semiconductor Differential Pressure Transducer for pressure drop measurement :

Pressure drop measurements across prosthetic valves have generally been measured by two techniques :

a. using two matched wire strain gauge transducers and electronically subtracting their outputs to obtain the differential signal.

b. using a wire strain-gauge differential pressure transducer.

The first method suffers from lower accuracy as it involves the use of two transducers matched under static conditions. Hence, their dynamic performance under pulsatile conditions have limited accuracy. The second method using a differential transducer directly eliminates this problem of matching. However, their sensitivity and dynamic frequency response have been limited.

Semiconductor differential pressure transducers have extremely high frequency response and a large signal sensitivity. They are however, not suitable for direct contact with water due to corrosion problems. This was overcome here by mounting the transducer in an acrylic holder and back-filling it with a silicone oil. This protects the sensor elements from the effects of water and at the same time enables direct fluid coupling for obtaining good frequency response and high signal output.

8.2 STEADY FLOW TEST DATA

i. Entrance & exit curvatures of the cage ring :

For the first time, the need for entrance and exit curvatures for the cage ring of tilting disc valves was addressed. This study clearly showed that the present practice of providing a radius at both the inlet and outlet edges of the valve cage ring was not optimum. The traditional flow-nozzle profile with an entrance curvature and a straight outlet showed the least pressure drop and as the best to employ.

ii. Effect of Pivot axis location & Disc shape on the Opening angle & Pressure drop :

The study brings out the dependence of disc opening angle on the disc shape and pivot axis location and shows that :-

a. The most central pivot axis location with full disc opening is obtained by using concavo-convex discs at pivot axis positions No.5 & No.6. However these models are not practically realisable designs with the present strut profiles, as the disc can escape through the inlet side of

the cage ring. A considerable change in the design of the cage is required to retain the disc in place.

b. For the plano-convex disc shape, the most central pivot axis location is No.3; the other more centrally pivoted valves being unacceptable due to reduced opening angle and higher pressure drops.

c. A concavo-convex disc with cage No.4 could be used to obtain full opening without sliding. This would however increase the complexity of fabrication. Also, as seen in pulsatile tests, the closing volumes and closing impact forces are increased. Hence, this design was also considered unacceptable.

d. Plano-convex disc No.2 with cage No.5 resulting in a higher sliding distance of 1.5 mm could also be used. However, there seemed a possibility of the disc getting stuck and hence was not studied. A more detailed study to optimise the sliding distance is also warranted.

iii. Optimum Opening-angle :

The family of curves on opening-angle vs. flowrate clearly indicates that the range of 70-75° as being an optimal opening angle. The reduction in pressure drops obtained at higher opening angles is not large enough to compensate for the increased closing volumes.

8.3 PULSATILE TEST DATA

i. Sewing Ring as a shock absorber :

The closing impact force tests have brought out the additional role of the sewing ring as a 'Shock absorber'. So far,

the sewing ring has been considered only as an interface for attachment and for sealing the periphery by tissue ingrowth.

By better absorbing the impact force, the stress on the sutures and the surrounding muscle are considerably reduced. This could have a major role in clinically reducing :

a. suture dehiscence and development of paravalvular leaks.

b. relative motion between the prosthesis and tissue interface leading to reduced inflammatory host response.

c. fatigue fracture and wear of the valve components.

Further, it also implies that there is considerable room for improving the performance of the sewing ring as a shock absorber by suitable design and choice of materials.

ii. Disc shape -- Concavo-convex vs Plano-convex :

The C-C disc valves TV-2C and BSM consistently show higher closing impact forces than their counterparts, TV-22 and BSS. The advantages of the C-C disc fade, when its disadvantages of more complex fabrication and increased closing volume & impact forces are taken into account.

Thus, the plano-convex shape of the disc as used presently seems to be the optimum choice at present.

iii. Effect of disc material specific gravity :

The static pulsatile tests bring out the effect of orientation on closing volume, when the disc material specific gravity differs from that of blood. The larger the difference, the larger the orientation effects. A material with the same density of blood seems ideal to minimise such orientation effects on valve performance. This could be achieved in the UHMW-PE discs by incorporating a metallic ring to act as a radio-opaque marker and at the same time helping to raise its density. It is also possible to consider the use of a filler like carbon fibres to raise the density of UHMW-PE to nearer that of blood.

8.4 COMPARATIVE PERFORMANCE

i. Pressure drops & Effective Orifice Area :

Among the standard valves, the St.Jude valve exhibits the lowest pressure drops under steady flow. The Chitra valve and TV-42 are next with almost comparable performance. Under pulsatile tests, the performance of all the tilting valves are generally comparable by present day standards.

ii. Closing volumes and closing impact forces :

The BSM clearly exhibits the maximum closing volumes and closing impact forces. The Chitra & TV-42 show less than the present day clinical standard Medtronic-Hall valve. The softer sewing ring and the plastic UHMW-PE disc definitely results in reduced impact forces of the indigenous valves.

iii. Relative flow through major & minor orifice areas :

TV-42 clearly shows the highest minor orifice flowrate in comparison, followed by the more recent improved models MHV & BSM. The present Chitra model shows better flow than the traditional BSS due to the use of the plano-convex disc shape. This might prove to be a major improvement in the performance of the TV-42 model

iv. Velocity Profiles :

The improved velocity in the minor orifice of the TV-42 over the present Chitra is clearly seen. The difference with MHV is small. Though the BSM exhibits a larger volumetric flow comparable to MHV through the minor orifice, the velocities are considerably lower and more disturbed behind the disc. This is probably due to the thicker minor-strut and disc shape. A thinner minor-strut and more stream-lined cross-sections as in the MHV is therefore a decided advantage.

The reduced impact forces of the Chitra valve can be used to further improve the profile of the minor strut.

8.5 A NEW DESIGN FOR THE CHITRA VALVE

Based on the steady flow and pulsatile tests, the valve model TV-42 emerges as the optimum choice, when constraints like cage design and ease of fabrication are imposed. This design has a pivot axis located at 0.34 diameters from the leading edge or equivalently 0.37 mitral ring diameters from the sewing ring and is close to the optimum value of 0.39 mitral ring diameters from

the anterior border of the mitral annulus as predicted by Peskin et al (1983) for a curved disc. **Figure 8.1** shows the TV-42 test valve alongside the current model TV-11.

The model uses a plano-convex disc with a well diameter such that the disc is permitted to slide down 1 mm during opening. This permits full opening of the valve upto 75° and also provides a clearance between the cage and the disc edge in the open position. The closing volumes and closing impact forces are marginally less than the current model of the Chitra valve while the effective orifice areas are equal. This proves that there is no degradation in performance due to the design changes.

The outlet curvature should be eliminated and struts should be well streamlined and have either an elliptical or a tear-drop cross-section with the minimum of thickness. Based on these data a new design for the Chitra Valve is proposed and is shown in **Figure 8.2.**

To minimise orientation effects, the disc of this new model could have a radio-opaque marker embedded or use a carbon fibre reinforced UHMWPE disc, making it of the same specific gravity as that of blood.

Further, with the cage design being kept similar to the existing model, no change in the fabrication technique is needed. In fact, the elimination of the radius at the outflow edge will simplify the cage machining to a some extent. This will ensure that there are no increased costs to the patient. With these improvements, it is hoped that this new model of the Chitra valve will result in reduced incidence of tissue overgrowth and thrombo-embolism in clinical use.

Figure 8.1

TEST VALVES TV-11 & TV-42

View from Inlet side

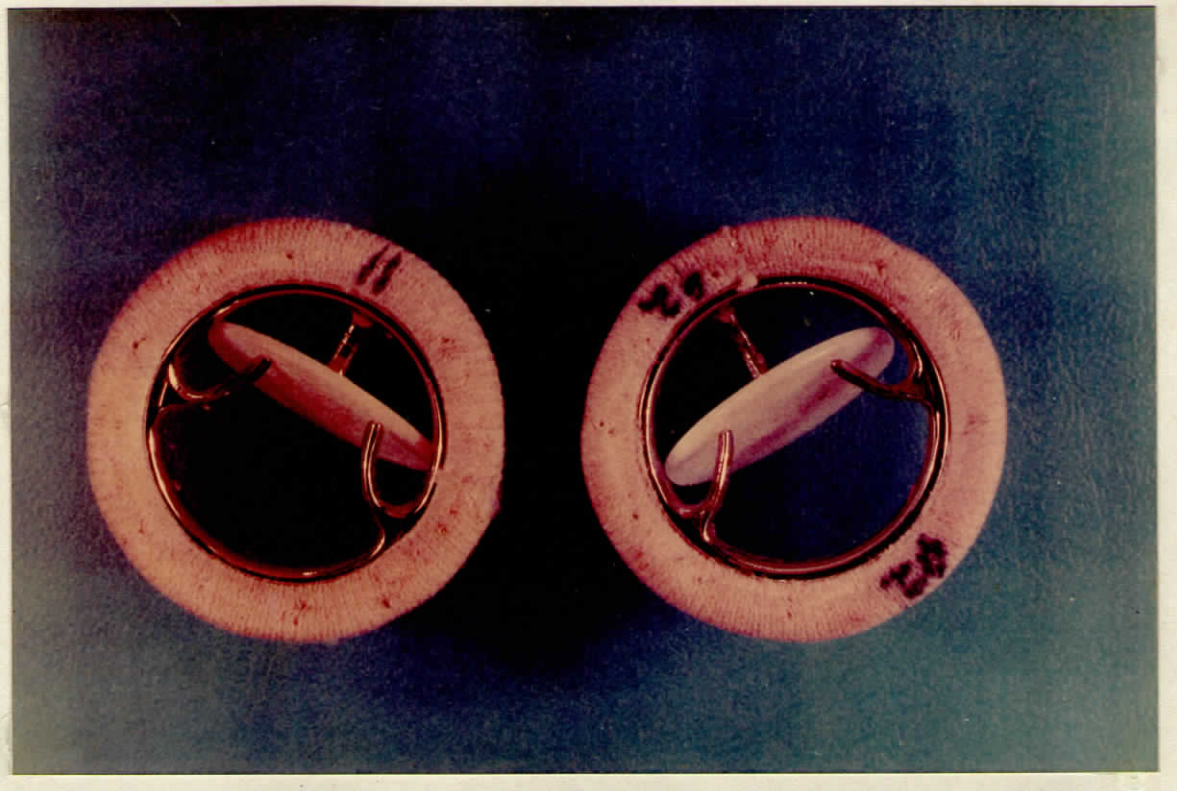

Figure 8.2

NEW DESIGN OF THE CHITRA VALVE

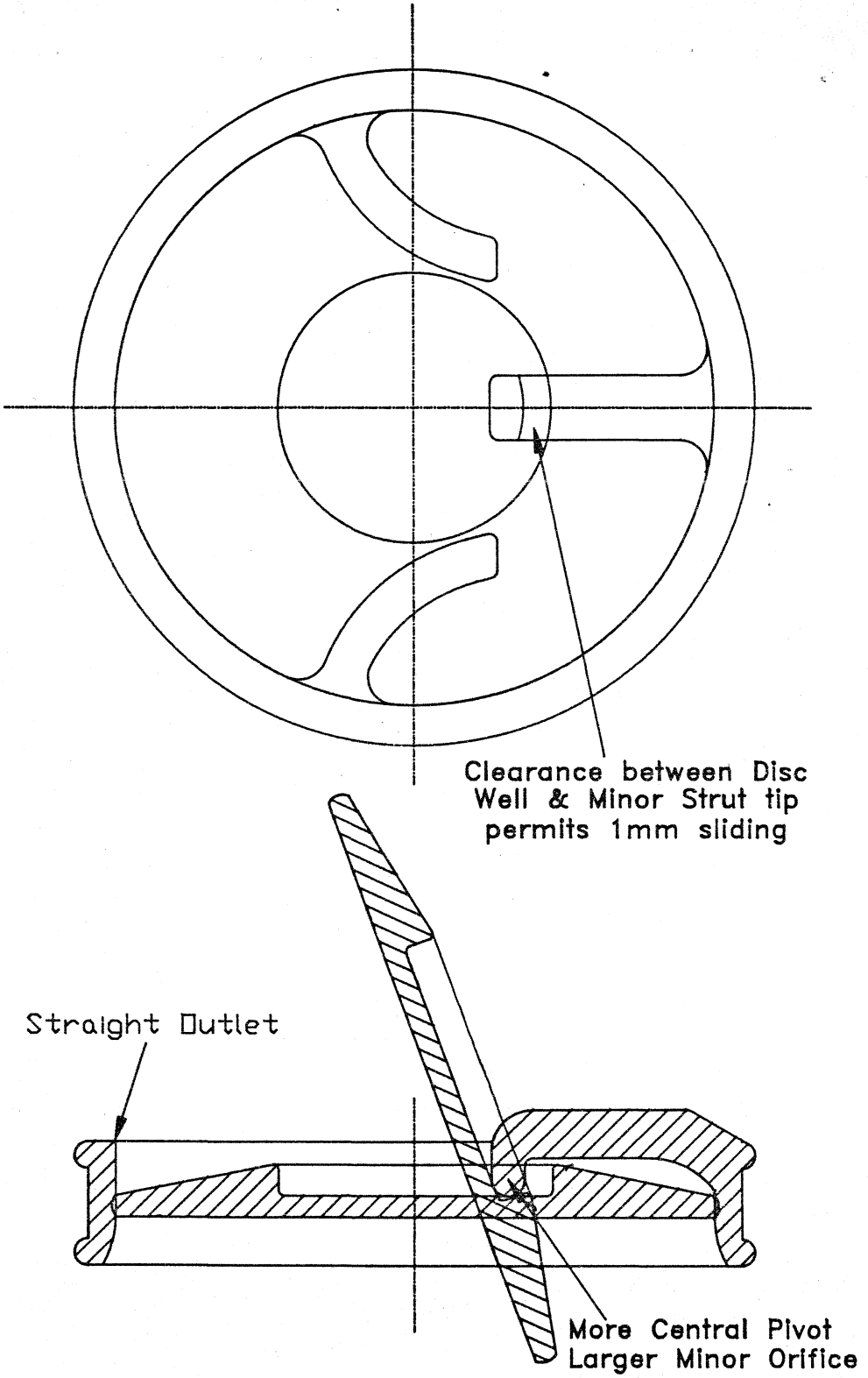

However, it is necessary to establish the durability of the valve in terms of its wear resistance and fatigue properties. It needs to be shown that the disc sliding introduced in this design does not result in increased wear of the disc, especially of its edge. Hence, the next stage in the development of the new model is to fabricate clinical quality prototypes for both accelerated durability testing and animal trials.

8.6 FURTHER INVESTIGATIONS

i. Drag force measurement :

The present technique of drag force measurement unfortunately was not sensitive enough to discriminate the effect of disc shape. This is one area where more detailed work is needed on improving the sensitivity of the transducer so that the effect of disc shape could be better understood. One could consider using an enlarged model with a larger transducer to achieve higher sensitivity. The effect of the struts, its cross-sectional profiles, etc., could probably be also studied.

ii. Sliding distance :

Initial assemblies of various combinations of cages and discs indicated that a sliding distance upto 1 mm seemed reasonable and acceptable. Higher sliding distance resulted in the disc edge hitting the ring too far out when closing and there seemed a possibility that it could get stuck. Under in-vivo conditions, the chances of the disc rubbing against the ventricular wall in mitral replacements are also increased.

Further, higher sliding distances could also result in higher edge wear of the disc. Hence, 1 mm was chosen as a reasonable comprise. However, with a detailed study, this distance could possibly be increased, in which case a more central pivot axis location may be possible.

iii. Closing impact forces and Sewing ring :

A comparative study of the closing impact forces of tissue valves and mechanical valves needs to be undertaken. This may help understand some of the differences in the clinical performance of these two types.

A detailed study is necessary to improve the design of the sewing ring to help absorb the closing impact force to the maximum. The use of foamed silicone rubber or other materials needs to be investigated. It may also be interesting to study the effect of reduced impact forces on tissue healing and blood damage in animal models.

iv. The PUDVEL system :

The accuracy of the system needs to be improved as indicated in earlier sections. Some of the parameters that need to be studied are crystal mounting, accuracy of tracking, accuracy of the doppler unit under turbulent flow conditions, probe movement, etc. Also a 20 MHz doppler unit may yield better results due to the stronger reflections at the smaller wavelengths. However, the range will be restricted to 10 mm.

In the present study, velocity profiles have been measured across two principal diameters only. However, it would be ideal

if the velocity profile across the whole cross-section of the flow channel could be mapped. This is possible with the present system by rotating the valve in small increments (say 5°) and obtaining the velocity profiles. But each such mapped profile for a single valve would require considerable amount of effort, time and computer storage space and hence was not attempted as a part of this study. But such velocity maps could lead to a better understanding of the differences in performance amongst tilting disc valves like the BSM and the MHV. It could also probably help correlate in-vitro data with clinical results. So far, there is only one report of a detailed mapping of downstream velocities. Hanle (1984) measured velocities at over 300 points, 31.8 mm downstream of Ionescu-Shiley, Bjork-shiley, St.Jude & Smellof **AORTIC VALVES** under both steady and pulsatile flow. However no detailed velocity maps from LDA studies are available in the open literature for mitral valves.

In the present study the velocity profile measurement using PUDVEL has been limited to steady flow measurements. However, the technique could be extended to pulsatile flow velocity profile measurements like in LDA. This would require the development of a more complex data acquisition and control software.

REFERENCES

Affeld K, Zartnack F, Mohnhaupt R & Bucherl ES (1976) "New methods for the in-vitro investigations of the flow patterns in artificial heart valves", ***Trans Am Soc Artif Int Organs*** 22:460-467.

Affeld K, Psolla J, Lehmann B & Mohnhaput R (1979) "Measurements of the unstationary flow field behind an artificial heart valve with the Laser Doppler anemometer", *Proc 2nd meeting ISAO* 439-441.

ASME Research committee report (1971) "***Fluid Meters***". Sixth Edition 1971, Editor Bean HS, The American Society of Mechanical Engineers, New York.

ASTM (1986) "Standard practice for reciprocating pin-on-flat evaluation of friction and wear properties of polymeric materials for use in total joint prostheses", ***ASTM report*** F732-82.

Baker DW & Yates WG (1973) "Technique for studying the sample volume of ultrasonic doppler devices", ***Med Biol Engng*** 11:766-770

Bhuvaneshwar GS, Ramani AV & Valiathan MS (1983) "A tilting disc valve - component materials and hydraulic function", ***Bull Mater Sc*** 3(2):111

Bhuvaneshwar GS, Muraleedharan CV, Ramani AV & Valiathan MS (1991a) "Evaluation of materials for artificial heart valves", ***Bull Mater Sci*** 14(6):1363-1374.

Bhuvaneshwar GS, Muraleedharan CV, Lal GAV, Ramani AV & Valiathan MS (1991b) "Synthetic Sapphire as an artificial heart valve occluder - Promise & Problems", ***Trans Indian Ceramic Soc*** 50:87-92

Biomedical Safety & Standards (1986) "Shiley Class I Recall of 60 degree convexo-concave heart valve complete", **16**:34, March 1, 1986.

Bjork VO & Olin C (1970) "A hydrodynamic comparison between the new tilting disc aortic valve prosthesis (Bjork-Shiley) & the corresponding prostheses of Starr-Edwards, Kay-Shiley, Smeloff-Cutter & Wada-Cutter in the pulse duplicator", *Scand J Thorac Cardiovasc Surg* 4:31

Bjork VO (1969) "A new tilting disc valve prosthesis", *Scand J Thorac Cardiovasc Surg* 3:1

Bjork VO (1970) "Experience with the Wada-Cutter valve prosthesis in the aortic area: one year follow-up", *J Thorac Cardiovasc surg* 60:26.

Bjork VO (1972a) "Delrin as implant material for valve occluders", *Scand J Thorac Cardiovasc Surg* 6:103.

Bjork VO (1972b) "The pyrolytic carbon occluder for the Bjork-Shiley tilting disc valve prosthesis", *Scand J Thorac Cardiovasc Surg* 6:109-113.

Bjork VO (1978) "The Improved Bjork-Shiley tilting disc valve prosthesis", *Scand J Thorac Cardiovasc Surg* 12(2):81-84.

Bjork VO, Olin C, Anstrom H (1969) "Results of aortic valve replacement with the Kay-Shiley disc valve", *Scand J Thorac Cardiovasc Surg* 3:93

Black RA & How TV (1989) "Pulsed Doppler ultrasound system for the measurement of velocity distribution and flow disturbances in arterial prosthesis", ***J Biomed Eng*** **11**:35-42

Bruss K-H, Reul H, Gilse JV & Knott E (1983) "Pressure drop and velocity fields at four mechanical heart valve prosthesis: Bjork-Shiley standard, Bjork-Shiley concave-convex, Hall-Kaster and St.Jude Medical", ***Life Support Systems*** **1**:3-22

Campbell JM (1950) "An artificial aortic valve", ***J Thorac Cardiovasc Surg*** **19**:312

Chandran KB, Ferguson TV Chen C-J & Khalighi B (1983a) "Experimental study of flow dynamics behind valve prosthesis", ***Am Soc Artif Int Organs J*** **6**:146-152.

Chandran KB, Yearwood TL Chen C-J & Falsetti HL (1983b) "Pulsatile flow experiments on heart valve prosthesis", ***Med & Biol Eng & Comput*** **21**:529-537.

Chandran KB, Khalighi B, Chen C-J, Falsetti HL, Yearwood TL & Hiratzka LF (1983c) "Effect of valve orientation on flow development past aortic valve prostheses in a model human aorta", ***J Thorac Cardiovasc Surg*** **85**:893-901.

Chandran KB, Cabell GN, Khalighi B & Chen C-J (1983d) "Laser anemometry measurements of pulsatile flow past aortic valve prostheses", ***J Biomechanics*** **16**(10):865-873.

Chang T-H, Guo GX, Hwag NHC, Kafesjian R & Quigano RC (1992) "The effect of suture ring compliance of a mechanical heart valve on the kinematics & acoustic characteristics observed during valve closure", presented XIX ESAO Congress, Rodos; ***J Artif Organs*** **15**:545 (abstract)

Davey TB, *et al.*, (1966) "Pulsatile flow studies of prosthetic heart valves", ***J Thorac Cardiovasc Surg*** 52:841

Davis KP, Myers JL, Pennock JL & Thiele BL (1985) "Strut fracture and disc embolization in Bjork-Shiley mitral valve prostheses: Diagnosis and Management", ***Ann Thorac Surg*** 40:65-68.

Dellsperger KC, Wieting DW, Baehr DA, Bard RJ, Brugger J-P & Harrison EC (1983) "Regurgitation of prosthetic heart valves: Dependence on heart rate and cardiac output", Am J Cardiol 51:321-328.

Dew PA, Olsen DB, Kessler TR, Coleman DL & Kolff WJ (1984) "Mechanical failures in in-vivo and in-vitro studies of pneumatic total artificial hearts", ***Trans Am Soc Artif Intern Organs*** 30:112-116.

Emery RW & Nicoloff DM (1979) "St.Jude Medical Cardiac valve prosthesis", ***J Thorac Cardiovasc Surg*** 78(2):269-276.

Emery RW, Palmquist WE, Mettler E & Nicoloff DM (1978a) "A new cardiac valve prosthesis: in-vitro results", ***Trans Am Soc Artif Internal Organs*** XXIV:550-556.

Emery RW, Palmquist WE *et al.*, (1978b) "A new cardiac prosthesis: all pyrolytic carbon bi-leaflet central flow valve", ***Circulation*** 58(Suppl II) pp83.

FDA (1985) "***Test protocol : interlaboratory comparison of prosthetic heart valve performance testing***", Food and Drug Administration, Rockville, Maryland, USA.

Fettel BE, Johnston DR & Morris PE (1980) "Accelerated life testing of prosthetic heart valves", ***Medical Instrumentation*** 14(3):161-164.

Fielder JH (1991) "Ethical issues in Biomedical engineering: the Bjork-Shiley heart valve", ***IEEE Eng in Med Biol*** March 1991, pp76-78

Figliola RS & Meuller TJ (1977) "Fluid stresses in the vicinity of disk, ball and tilting disk prosthetic heart valves from in-vitro measurements", ***J Biomech Engng*** 103:83-90.

Food & Drug Administration (1990) "***Replacement Heart Valves - Guidance for data to be submitted to the Food & Drug Administration in support of applications for premarket approval***", Draft version May 1990, FDA Rockville, Maryland, USA.

Frater RWM & Ellis FH Jr (1961) "Problems in the Development of a Mitral Valve Prosthesis", In ***Prosthetic Valves for Cardiac Surgery*** (Edited by Merendino KA), Springfield, Thomas, pp244-265

Gentle CR (1977) "A limit to hydraulic design of heart valve prostheses", ***Eng. in Medicine,*** 6-1,17-21

Gibbon JH Jr (1954) "Application of a mechanical heart and lung apparatus to cardiac surgery", ***Minn Med*** 37:171

Graf T, Fischer H, Reul H & Rau G (1991) "Cavitation potential of mechanical heart valve prostheses", ***Int J Artif Organs*** 14(3):169-174.

Hanle DD (1984) "***Fluid dynamics of prosthetic aortic heart valves in steady and pulsatile flow***" Ph.D Thesis, California Institute of Technology, CA, USA.

Harken DE, Soroff HS, Taylor WJ, Lefemine AA, Gupta SK & Lunzer S (1960) "Partial & complete prostheses in aortic insufficiency", ***J Thorac Cardiovasc Surg*** 40:744

Harken DE, Soroff HS, Taylor WJ, *et al.*, (1961) "Aortic valve replacement", In ***Prosthetic Valves for Cardiac Surgery,*** (Edited by Merendino KA), Springfield, Thomas, pp508-526

Hehrlein FW, Gottwik M, Graedrich G & Mulch J (1980) "First clinical experience with a new all-pyrolytic carbon bileaflet heart valve prosthesis", ***J Thorac Cardiovasc Surg*** 79:632-636.

Himount (1986) "***For the tough jobs 1900 UHMW polymer***", Himount USA Inc., Technical literature 500-675D rev 4-87.

Hufnagel CA & Harvey (1953) "The Surgical correction of aortic regurgitation", ***Bull Georgetown Univ Med Centre;*** 6:60

Hufnagel CA (1951) "Aortic plastic valvular prosthesis", ***Bull Georgetown U Med Cent*** 4:128

Hwang NHC, Lu PC, Sallam A & Reul H (1979) "Turbulent characteristics of prosthetic heart valves", ***Proc 14th AAMI Annual Meeting,*** Las Vegas p127.

Joyce C (1990) "Heart patients should be warned of faulty valve implant", ***New Scientist*** 125:1709 22

Kaster RL (1969) Discussion: In ***Prosthetic Heart Valves*** (Edited by Brewer LA III), Springfield, Thomas, p325

Kaster RL *et al.*, (1970) "The Lillehei-Kaster pivoting disc aortic prosthesis & a comparative study of its pulsatile flow characteristics with four other prosthesis", ***Trans Am Soc Artif Organs*** 16:233.

Klain M, Letiz KH, Kolff WJ (1969) "Comparative testing of artificial heart valves in a mock circulation", In ***Prosthetic Heart Valves, Springfield*** (Edited by Brewer LA III), Thomas, pp114-136.

Knight CJ (1973) "***The development of an artificial heart valve***", Ph.D. thesis, Univ. Edingburg

Knight Cj, Macleod N & Taylor DEM (1977) "Physical principles of the Edinburgh prosthetic heart valve", ***Med & Biol Eng & Computing*** 15:264-272.

Knott E, Reul H, Knoch M, Steinsiefer U & Rau G (1988) "In-vitro comparison of aortic heart valve prostheses - Part 1: Mechanical Valves", ***J Thorac Cardiovasc Surg*** 96:952-961.

Lefrak EA & Starr A (1979) "***Cardiac Valve Prostheses***", Appleton-Century-Crofts, New York,

Leyse RM, Quinton WE, Blumberg JB, Jarrison HG, May KJ Jr. & Merendino KA (1961) "A system for the study of cardiovascular flow patterns", In ***Prosthetic Valves for Cardiac Surgery,*** (Edited by Merendino KA), Thomas, Springfield, pp56-70.

Lindblom D, Bjork VO & Semb BKH (1986) "Mechanical failure of the Bjork-Shiley valve - incidence, clinical presentation and management", ***J Thorac Cardiovasc Surg*** 92:894-907.

Macleod N, Turina M, Wade JD, Wright JTM & Riemersmaa R (1976) "Further development of the Edinburgh prosthetic heart valve", ***Proc European Soc Artif Organs*** III pp146:151.

Macleod N, Turina M, Wade JD & Wheatley DJ (1977) "The principles and in vivo performance of the Edinburgh pivoted aerofoil disc prosthetic heart valve", ***Trans Am Soc Artif Intern Organs*** **XXIII**:80-87

Martin TRP & Black MM (1976) "Problems of In-vitro Testing of Heart Valve Replacements", ***Proc European Soc Artif Organs*** **III**, 131

McQueen DM & Peskin CS (1983) "Computer-assisted design of pivoting disc prosthetic mitral valves", ***J Thorac Cardiovasc Surg*** 86:126-135

McQueen DM & Peskin CS (1985) "Computer-assisted design of butterfly bileaflet valves for the mitral position", *Scand J Thorac Cardiovasc Surg* 19:139-148.

Medtronic Blood Systems (1980) "***Three year clinical evaluation of the Hall-Kaster Prosthetic Heart Valve***", Medtronic Inc., Plymouth, USA.

Olsen DB (1988) "Current & future valves for blood pumps", ***Artif Organs*** 12(3):239-241.

Olsen DB, Kolff J, Lawson J, Stellwag F, Ceccarelli V, Fukumasu H & Kolff WJ (1976) "Saving the aortic and pulmonary artery valves with total heart replacement", ***Trans Am Soc Artif Intern Organs*** **22**: (discussion) pp477-479.

Peskin CS (1977) "Numerical analysis of blood flow in the heart", ***J Comput Phys*** 25:220-252

Peskin CS & McQueen DM (1980) "Modelling prosthetic heart valves for numerical analysis of blood flow in the heart", ***J Comput Phys*** 37:113-132

Philips WM, Snyder A, Alchas P, Rosenberg G & Pierce WS (1980) "Pulsatile prosthetic valve flows", ***Trans Am Soc Artif Intern Organs*** 26:43-49

Pierce WS, Behrendt DM & Morrow AG (1968) "A hinged prosthetic cardiac valve fabricated of rigid components", ***J Thorac Cardiovasc Surg*** 56:pp229-235

Rabinowicz E (1965) "***Friction and wear of materials***", John Wiley Sons, New York pp113-118.

Ramani AV (1991) "India makes her own heart valve prosthesis", ***Current Science*** 61:74

Reif TH, Silver MD, Koppenhoefer H & Huffstutler Jr. MC (1986) "Estimation of the Abrasive wear coefficient in Lillehei-Kaster Cardiac Valve Prostheses", ***J Biomechanics*** 19:93-101

Reul H, (1983) "In-vitro evaluation of artificial heart valves", ***Adv cardiovasc Phys*** 5(Part IV):16-30.

Reul H, Minammitani H & Runge J (1975) "A hydraulic analog of the systemic and pulmonary circulation for testing artificial hearts", ***Proc European Soc Artif Organs*** II, 120-127.

Reul H, Giersiepen M & Knott E (1986) "Laboratory testing of prosthetic heart valves", in ***Proceedings - Heart Valve Engineering***, Institution of Mechanical Engineers, London, pp3-13.

Rodriguez L (1970) "Haemodynamic & angiographic findings in patients with isolated aortic valvular disease before and after insertion of a Starr-Edwards aortic ball valve prosthesis", ***Scand J Thorac Cardiovasc Surg*** [Suppl 5]:1

Scotten LN, Walker DK & Brownlee RT (1983) "The Bjork-Shiley and Ionescu-Shiley heart valve prostheses : In vitro comparison of their hydrodynamic performance in the mitral position", ***Scand J Thor Cardiovasc Surg*** **17**:201-209.

Stevenson DM, Yoganathan AP & Franch RH (1982) "The Bjork-Shiley Heart Valve Prosthesis : Flow characteristics of the New 70° Model", ***Scand J Thorac Cardiovasc Surg*** **16**:1-7

Swanson WM & Clark RE (1976a) "Cardiovascular system simulation requirements", ***J of Bioengng*** **1**:121-133.

Swanson WM & Clark RE (1976b) "A simple cardiovascular system simulator: design & performance", ***J of Bioengng*** **1**:135-145.

Swanson WM (1984) "Comparison of in-vitro valve pressure drop results from different investigators", ***Med Instrum*** **18**:115-117.

Swope RD & Falsetti HL (1976) "Velocity profiles in prosthetic heart valves under steady flow condition", ***Proc 29th ACEMB*** **18**:339 (abstract).

Teuvo KIL & Karkola P (1974) "Shrinkage & degradation of the Delrin occluder in the tilting disc valve prosthesis", ***J Thorac Cardiovasc Surg*** **68**:66-69.

Tindale WB, Black MM & Martin TRP (1982) "In-vitro evaluation of prothetic heart valves: anomalies and limitations", ***Clin Phys Physiol Meas*** **3**:115-130.

Turina M & Macleod N (1975) "Experimental evaluation of a new pivoting disc heart valve", ***Proc European Soc Artif Organs*** **II** pp30-32.

Valiathan MS, Bhuvaneshwar GS & Venkatesan VS (1978) "Comparative study of prosthetic and tissue valves in a pulse duplicator", ***Indian J Surg*** **40**(6):283-290.

Viggers RF, Robel SB, Wood SJ, Sawyer PN, Wesolowski SA & Sauvage LR (1968) "Improvement of aortic ball valve function by flow guidance", ***Surgery*** **63**:52-58.

Wada J (1967) "Knotless suture method and Wada hingeless valve", ***Jap J Thorac Surg*** **15**:88

Wada J (1969) Discussion in "***Prosthetic Heart Valves***", (Edited by Brewer LA III), Charles C Thomas, Springfield, p49.

Wada J, Komatsu S, Ikeda K, Kitaya T, Tanaka N & Yamada H (1969) "A new hingeless valve", In ***Prosthetic Heart Valves,*** (Edited by Brewer LA III), Charles C Thomas, Springfield, pp304-314.

Way S (1962) "Plates", in ***Handbook of Engineering Mechanics,*** (Edited by Flugge W) McGraw Hill, New York, Chapter 39.

Weiting DW (1969) "***Dynamic flow characteristics of heart valves***", Ph.D. thesis, Univ of Texas, Austin.

Weiting DW, Hall WC, Liotta D & DeBakey ME (1969) "Dynamic flow behaviour of artificial heart valves", In ***Prosthetic Heart Valves,*** (Edited by Brewer LA III) Charles C Thomas, Springfield pp34-49.

Whalen RL (1983) "Connective tissue response to movement at the Prosthesis/Tissue interface", in ***Biocompatible polymers, metals & composites,*** (Edited by Szycher M), sponsored by Soc of Plastics Eng Inc, Technomic Publishing Co Inc, Lancaster, USA; Chap 42:pp953-974.

White PD (1948) "*Heart Disease*", Ed.3 New York, Macmillan

Williams JB (1858) US Patent No.19323

Willshaw P, Biagetti M & Pichel RH (1986) "A comparative in-vitro study of the closing characteristics of Bjork-Shiley and Bicer-Val tilting disc mitral valve prostheses", *J Biomed Eng* 8:43-48.

Woo Y-R & Yoganathan AP (1986) "In-vitro pulsatile flow velocity and shear stress measurements in the vicinity of mechanical mitral heart valve prostheses", *J Biomechanics* 19(1):39-51

Woo Y-R & Yoganathan AP (1986a) "An instrument for the measurement of in-vitro velocity and turbulent shear stress in the immediate vicinity of prosthetic heart valves", *Life Support Syst* 4:47-62.

Wright JTM & Brown MC (1976) "A method for measuring the mean pressure gradient across heart valve prostheses under in-vitro pulsatile flow conditions", *Med Instrum* 11:110-113

Wright JTM & Temple LJ (1971) "An improved method for determining the flow characteristics of prosthetic mitral heart valves", *Thorax* 26:81-88.

Wright JTM & Temple LJ (1977) "A flow visualisation study of prosthetic and mitral heart valves in a model of the aorta and left heart", *Engineering in Medicine* 6(2):31-45.

Yoganathan AP & Corcoran WH (1979) "In-vitro velocity measurements in the vicinity of aortic prostheses", *J Biomechanics* 12:135-152.

Yoganathan AP & Letzing W (1983) ***"Prosthetic Heart Valves: A study of in-vitro performance Phase II"***, Final report, NTIS, USA.

Yoganathan AP, Corcoran WH, Harison EC & Carl JR(1978a) "The Bjork-Shiley aortic prosthesis: flow characteristics, thrombus formation and tissue overgrowth", ***Circulation*** 58:70-76

Yoganathan AP, Corcoran WH & Harrison EC (1978b) "Wall shear stress measurements in the near vicinity of prosthetic aortic heart valves", ***J Bioengineering*** 2:369-379.

Yoganathan AP, Reamer HH, Corcoran WH & Harrison EC (1979) "Laser-Doppler anemometer to study velocity fields in the vicinity of prosthetic heart valves", ***Med & Biol Eng & Comput*** 17:38-44

Yoganathan AP, Corcoran WH & Harrison EC (1979a) "Pressure drops across prosthetic aortic heart valves under steady and pulsatile flow - in-vitro measurements", ***J Biomechanics*** 12:153-164.

Yoganathan AP, Corcoran WH, Harrison EC & Carl J (1979b) "In-vitro measurements in the near vicinity of the Bjork-Shiley aortic prosthesis using a Laser-Doppler anemometer", ***Med & Biol Eng & Comput*** 17:453-459.

Yoganathan AP, Reamer HH, Corcoran WH & Harrison EC (1980) "The Bjork-Shiley aortic prosthesis: flow characteristics of the present model vs. the convexo-concave model", ***Scand J Thorac Cardiovasc Surg*** 14:1-5

Yoganathan AP, Chaux A, Gray RJ, Robertis MD & Matloff JM (1982a) "Flow characteristics of the St.Jude prosthetic valve : an in-vitro & in-vivo study", ***Artificial Organs*** 6:288=-294.

Yoganathan AP, Stevenson DM, Williams FP, Woo Y-R, Franch RH & Harrison EC (1982b) "In-vitro fluid dynamic characteristics of the Medtronic-Hall pivoting disc heart valve prosthesis", ***Scand J Thorac Cardiovasc Surg*** **16**:235-243

Yoganathan AP, Strand DM, Woo Y-R & Stevenson DM (1984) "An on-line method for evaluation of the in vitro pulsatile pressure drop and regurgitative characteristics of prosthetic heart valves", ***Medical Instrumentation*** 18:109-113

Yoganathan AP, Sung H-W, Woo Y-R & Jones M (1988) "In-vitro velocity and turbulence measurements in the vicinity of three new mechanical aortic heart valve prostheses: Bjork-shiley Monostrut, Omni-Carbon and Duromedics", ***J Thorac Cardiovasc Surg*** 95:929-39.

APPENDIX A

THEORY OF BENDING OF THIN ANNULAR PLATES

Figure A.1 shows the force transducer modelled as an annular plate with its central valve mounting orifice blocked by a rigid member and loaded by a hydraulic pressure P_0 on one side.

Way (1962) has given an analysis of the basic equations governing laterally loaded plates. From these, he has derived the equations governing the axially symmetric bending of annular plates. **Figure A.2** shows this situation of the force transducer as an annular plate loaded by the pressure P_0 on its annular surface and a shear force Q_1 along its inner edge. Q1 is the shear force per unit length of circumference.

From **Figure A.3** we have

$$Q_1 = P_0 b/2 \qquad (1)$$

This case of annular plate in axially symmetric bending can be analyzed by the superposition of three simpler cases as shown in **Figure A.4.** S.Way gives the deflection 'w' and the radial bending moment M_r at a point 'r' from the centre.

Figure A.1

Annular Plate with its central hole blocked and loaded by pressure P_o on one surface

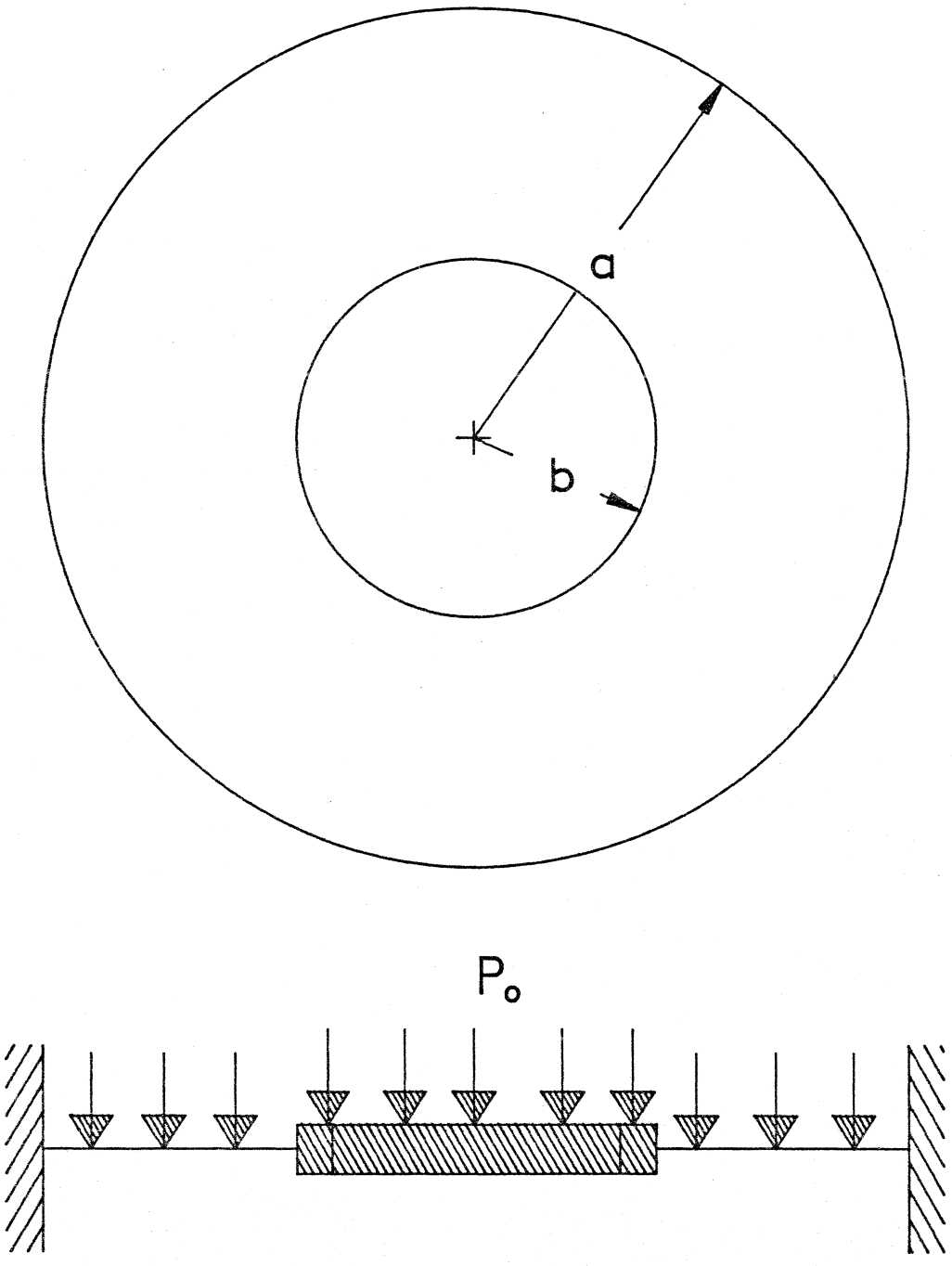

Figure A.2

Annular Plate loaded by Pressure P_o on its annular surface and Shear Force Q_1 on its inner edge

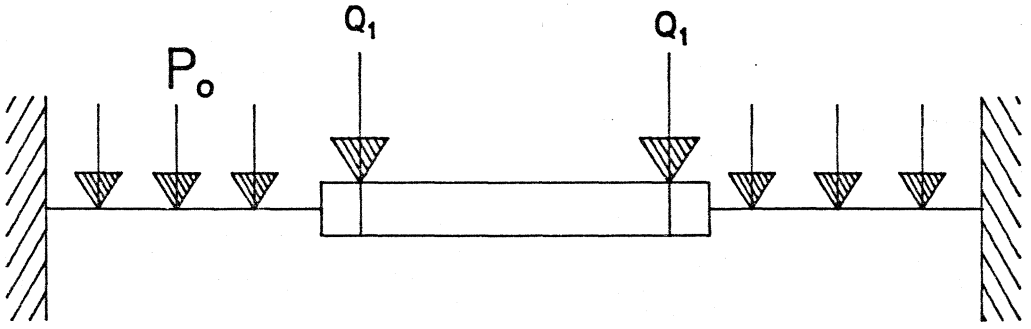

Figure A.3

Circular rigid plate with uniform pressure P_o and its equivalent shear force Q_1 along its circumference

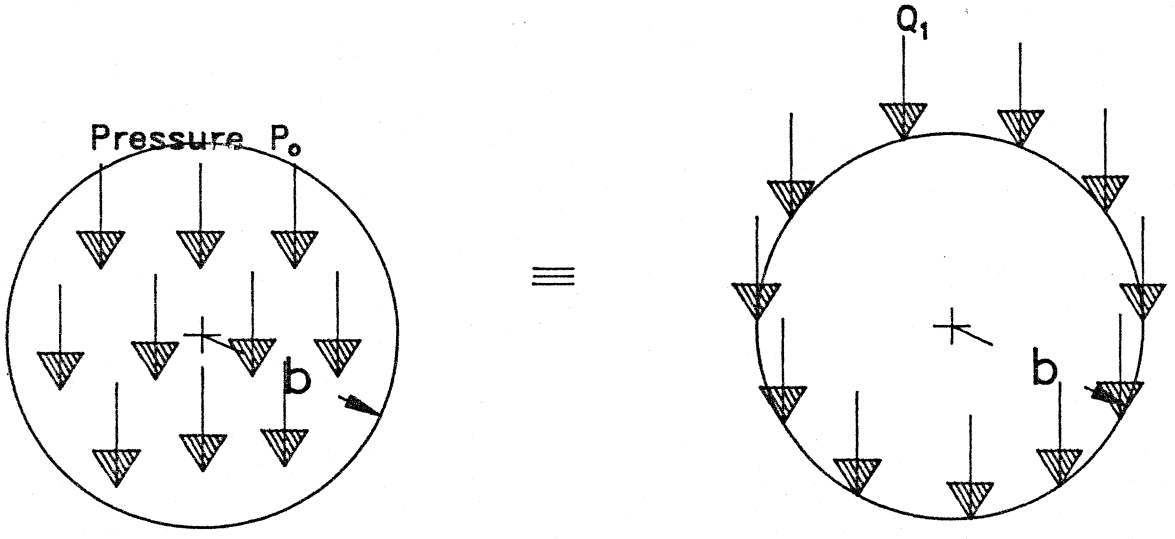

$$\Pi b^2 P_o = 2\Pi b Q_1$$

Figure A.4

Annular Plate in axially symmetric bending

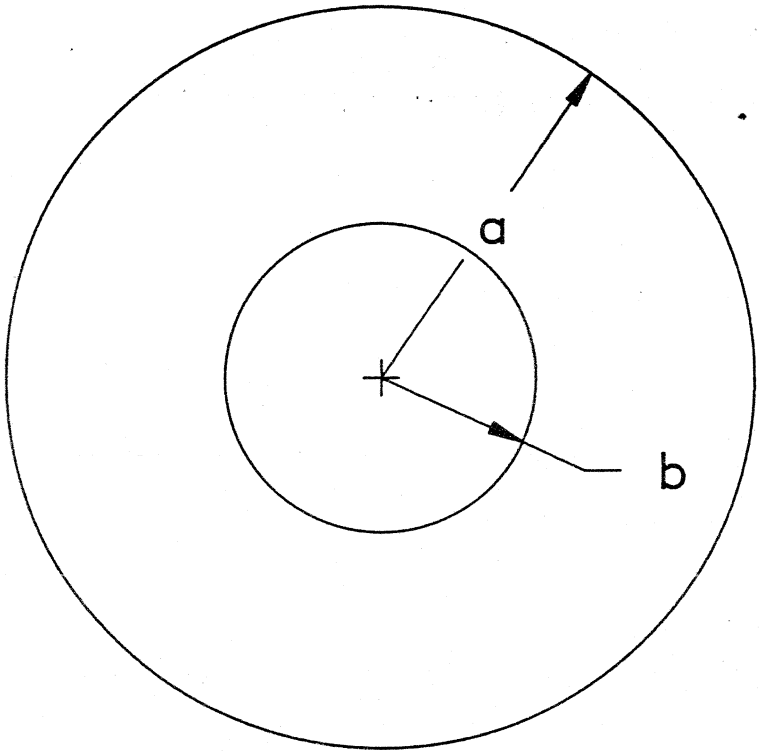

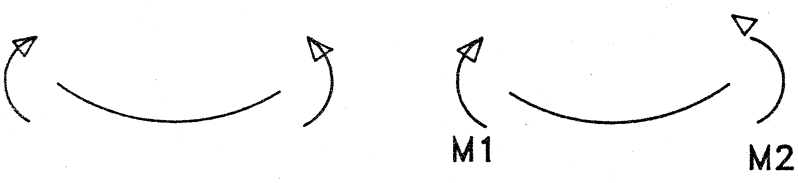

(a) Annular plate loaded by Edge moments

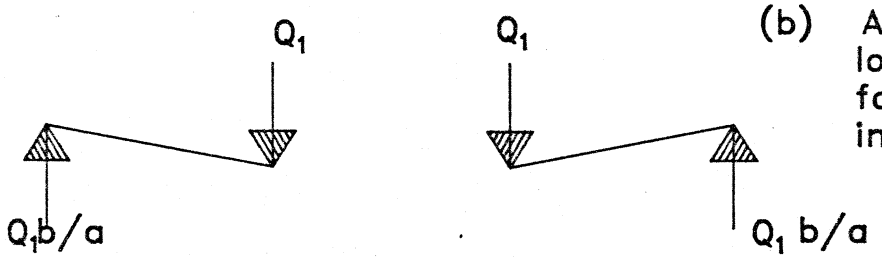

(b) Annular Plate loaded by shear force Q1 at the inner edge

(c) Annular Plate loaded by uniform pressure simply supported at the outer edge

In this analysis, the notations are :

Inner edge is at r = b
Outer edge is at r = a
Young's Modulus = E
Poissons Ratio = ν
Thickness of the plate = t

Then the flexural rigidity of the plate is given by :

$$K = \frac{Et^3}{12(1-\nu^2)} \qquad (2)$$

Case A : Annular Plate loaded by Edge Moments - Fig. A.4a

The deflection w_a and the radial bending moment M_r at a point 'r' from the centre of the plate is given by :

$$w_a = \frac{1}{2}\frac{r^2-a^2}{a^2-b^2}\frac{M_1b^2-M_0a^2}{(1+\nu)K} + \frac{a^2b^2}{a^2-b^2}\frac{M_1-M_0}{(1-\nu)K}\ln\frac{a}{b} \qquad (3)$$

$$M_r = -\frac{M_1b^2-M_0a^2}{a^2-b^2} + \frac{a^2b^2(M_1-M_0)}{r^2(a^2-b^2)} \qquad (4)$$

Case B : Annular Plate loaded by Shear Force Q1 at the Inner Edge - Fig. A.4b

The deflection w_b at a point 'r' from the centre of the plate for this shear load is given by :

$$w_b = B_0\left[\left(1-\frac{r^2}{a^2}\right)B_1 + \frac{r^2}{a^2}\ln\frac{r}{a} + B_2\ln\frac{r}{a}\right] \qquad (5)$$

where

$$B_0 = \frac{Q_1a^2b}{4K} \qquad (6)$$

$$B_1 = \frac{(3+\nu)}{2(1+\nu)} - \frac{b^2}{a^2-b^2}\ln\frac{b}{a} \qquad (7)$$

$$B_2 = \frac{2b^2}{a^2-b^2}\frac{1+\nu}{1-\nu}\ln\frac{b}{a} \qquad (8)$$

Case C : Annular Plate loaded by Uniform load, Simply supported at the outer edge and free inner edge - Fig. A.4c

The deflection w_c at a point 'r' from the centre of the plate due to this uniform load of P_0 is given by :

$$w_c = C_0\left[C_1 - \frac{r^2}{a^2}C_2 - \ln\frac{r}{a}C_3 + \frac{1}{8}\left(\frac{r}{a}\right)^4 - \frac{r^2b^2}{a^4}\ln\frac{b}{a}\right] \qquad (9)$$

where

$$C_0 = \frac{P_0a^4}{8K} \qquad (10)$$

$$C_1 = \frac{5+\nu}{8(1+\nu)} - \frac{b^2(3+\nu)}{4a^2(1+\nu)} + \frac{\left(\frac{b}{a}\right)^4}{1-\left(\frac{b}{a}\right)^2}\ln\frac{b}{a} \qquad (11)$$

$$C_2 = \frac{3+\nu}{4(1+\nu)}\left(1-\frac{b^2}{a^2}\right) + \frac{\left(\frac{b}{a}\right)^4}{1-\left(\frac{b}{a}\right)^2}\ln\frac{b}{a} \qquad (12)$$

$$C_3 = \frac{3+\nu}{2(1-\nu)}\left(\frac{b}{a}\right)^2 + \frac{2(1+\nu)}{1-\nu}\frac{\left(\frac{b}{a}\right)^4}{1-\left(\frac{b}{a}\right)^2}\ln\frac{b}{a} \qquad (13)$$

In the force transducer, the inner and outer edges of the diaphragm are rigidly fixed to stiff members (Fig. A.2). Hence, under loading, the slope of deflection at these two points must be zero.

By superposition, the total deflection 'w' is given as :

$$w = w_a + w_b + w_c \tag{14}$$

Hence, the slope of the deflection is :

$$\frac{dw}{dr} = \frac{dw_a}{dr} + \frac{dw_b}{dr} + \frac{dw_c}{dr} \tag{15}$$

Differentiating equations (3), (5) & (9) with respect to 'r',

$$\frac{dw_a}{dr} = \frac{M_1 b^2 - M_0 a^2}{(1+\nu)K} r + \frac{a^2 b^2}{a^2 - b^2} \frac{M_1 - M_0}{(1-\nu)K} \frac{1}{r} \tag{16}$$

$$\frac{dw_b}{dr} = B_0 \left[-\frac{2r}{a^2} B_1 + \frac{2r}{a} \ln\frac{r}{a} + \frac{r}{a^2} + \frac{B_2}{r} \right] \tag{17}$$

$$\frac{dw_c}{dr} = C_0 \left[-\frac{2r}{a^2} C_2 - \frac{C_3}{r} + \frac{r^3}{2a^4} - \frac{2rb^2}{a^4} \ln\frac{r}{a} - \frac{rb^2}{a^4} \right] \tag{18}$$

Applying the condition dw/dr=0 at the outer edge, where r = a and at the inner edge, where r = b gives :

$$\frac{M_1 b^2 - M_0 a^2}{(1+\nu)K} \frac{a}{a^2 - b^2} + \frac{M_1 - M_0}{(1-\nu)K} \frac{ab^2}{a^2 - b^2} = X_1 \tag{19}$$

where,

$$X_1 = B_0 [2B_1 - B_2 - 1] + C_0 \left[\frac{1}{a} \left(2C_2 + C_3 - \frac{1}{2} \right] + \frac{b^2}{a^3} \right] \tag{20}$$

and

$$\frac{M_1 b^2 - M_0 a^2}{(1+\nu)K} \frac{b}{a^2 - b^2} + \frac{M_1 - M_0}{(1-\nu)K} \frac{a^2 b}{a^2 - b^2} = X_2 \tag{21}$$

where,

$$X_2 = B_0\left[\frac{2b}{a}\left(\frac{B_1}{a}-\ln\frac{b}{a}\right)-\frac{b}{a^2}-\frac{B_2}{b}\right]+C_0\left[\frac{2b}{a^2}\left(C_2+\frac{b^2}{4a^2}+\frac{b}{a^2}\ln\frac{b}{a}\right)+\frac{C_3}{b}\right] \quad (22)$$

Multiplying equation (19) by 'a' and equation (21) by 'b' and then subtracting, we get :

$$\frac{M_1b^2-M_0b^2}{(1+\nu)K} = aX_1-bX_2 \quad (23)$$

Multiplying equation (21) by 'a' and equation (19) by 'b' and then subtracting, we get :

$$\frac{M_1-M_0}{(1-\nu)K}ab = ax_2-bX_1 \quad (24)$$

Solving equations (23) and (24) for M_1 and M_0, gives,

$$M_0 = \frac{Y_2-Y_1b^2}{b^2-a^2} \quad (25)$$

$$M_1 = \frac{Y_2-Y_1a^2}{b^2-a^2} \quad (26)$$

where,

$$Y_1 = \frac{aX_2-bX_1}{ab}(1-\nu)K \quad (27)$$

and

$$Y_2 = (aX_1-bX_2)(1+\nu)K \quad (28)$$

Substituting the values of M_1 and M_0 in equation (4), the radial bending moment M_r at any radial point 'r' from the centre of the diaphragm can be calculated.

The radial bending stresses in the outer diaphragm surface (i.e., t/2 from the neutral axis), is given by :

$$\sigma_r = \frac{6M_r}{t^2} \qquad (29)$$

Then for bending within the elastic region of the material, the surface strain in the radial direction can be calculated as :

$$\epsilon_r = \frac{\sigma_r}{E} \qquad (30)$$

APPENDIX B

FORCE TRANSDUCER STATIC CALIBRATION & PRESSURE DROP CORRECTION

Static calibration of the force transducer was carried out by suspending an aluminium pan using polyester threads and loading brass weights. The weights in the range of 1 to 200 gms from a weight box were accurate to ± 1 mg, when checked with an analytical electronic balance (0.1mg resolution). The transducer was calibrated in the range 0 to 400 gms in 50gm steps. The force transducer bridges were interfaced to the A/D board of the computer using 1000 gain single chip instrumentation amplifiers (INA101 Burr-Brown).

B.1 CENTRAL LOADING

A polyester thread was passed diametrically across the three pairs of mounting holes as shown in **Figure B.1.** The aluminium pan was suspended from the central intersection of the threads. Under these conditions, it was assumed that the two bridges would be loaded equally. However, repeated calibration by retying the threads showed variations, probably due to unequal tension in the threads. The data of the first order

Figure B.1

Force Transducer Calibration
Central Loading

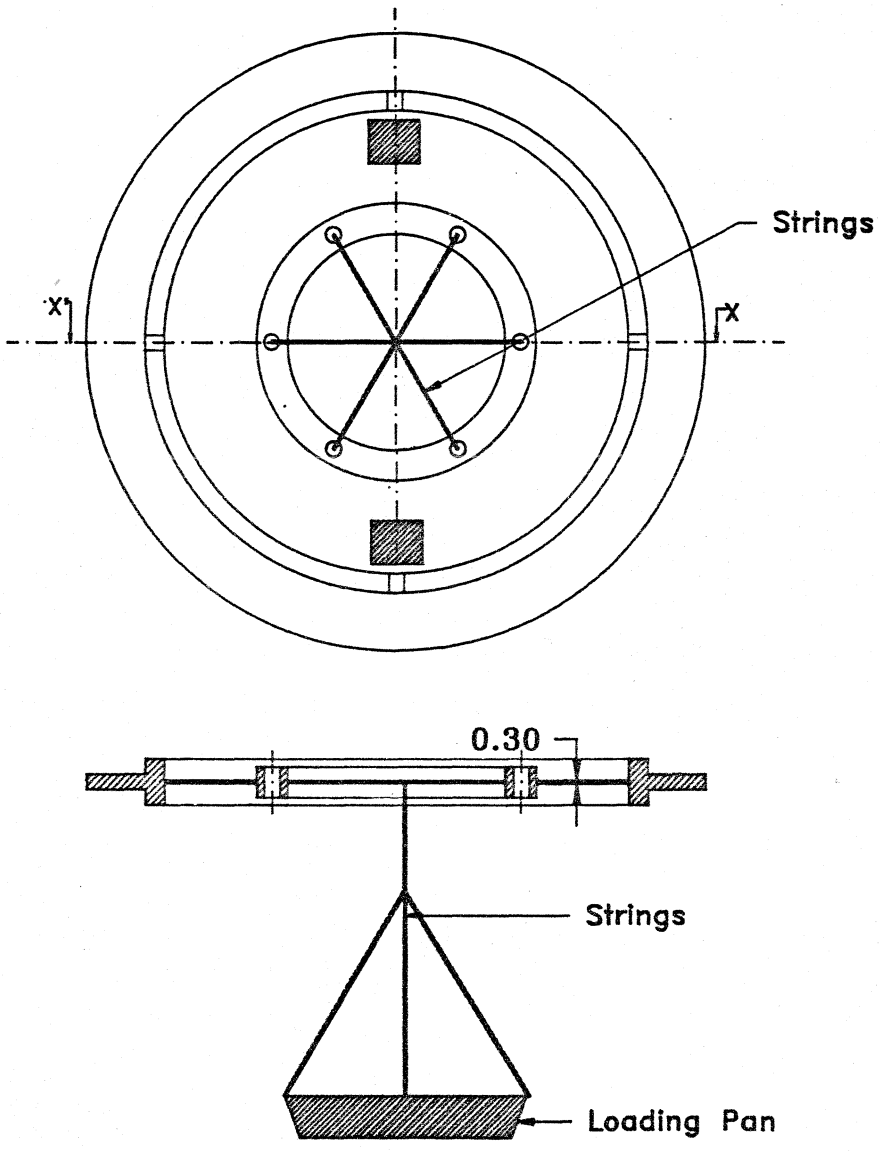

linear regression fit for one of the calibration tests is given in Table B.1.

Table B.1
Central Loading of force transducer

REGRESSION OUTPUT : CHANNEL A	
X coefficient	0.000632
Standard error of y estimate	0.001194
Coefficient of Determination - R^2	0.999061
No. of observations	19
REGRESSION OUTPUT : CHANNEL B	
X coefficient	0.000671
Standard error of y estimate	0.002072
Coefficient of Determination - R^2	0.997492
No. of observations	19

B.2 OFFSET LOADING

To obtain more consistent calibration, the thread was passed through adjacent two holes towards a bridge and the pan hung from it as shown in **Figure B.2.** The calibration was repeated on the opposite side also. The data for the two offset loading calibrations are given in Tables B.2 and B.3. The coefficient of 'x' of the nearside bridge is almost double of that obtained in the central loading and that of the farside bridge was very small - actually less than 4% of the nearside one. Hence, for a fair approximation, this offset loading could be assumed to produce strain on the nearside bridge only. These

Figure B.2

Force Transducer Calibration
Offset Loading

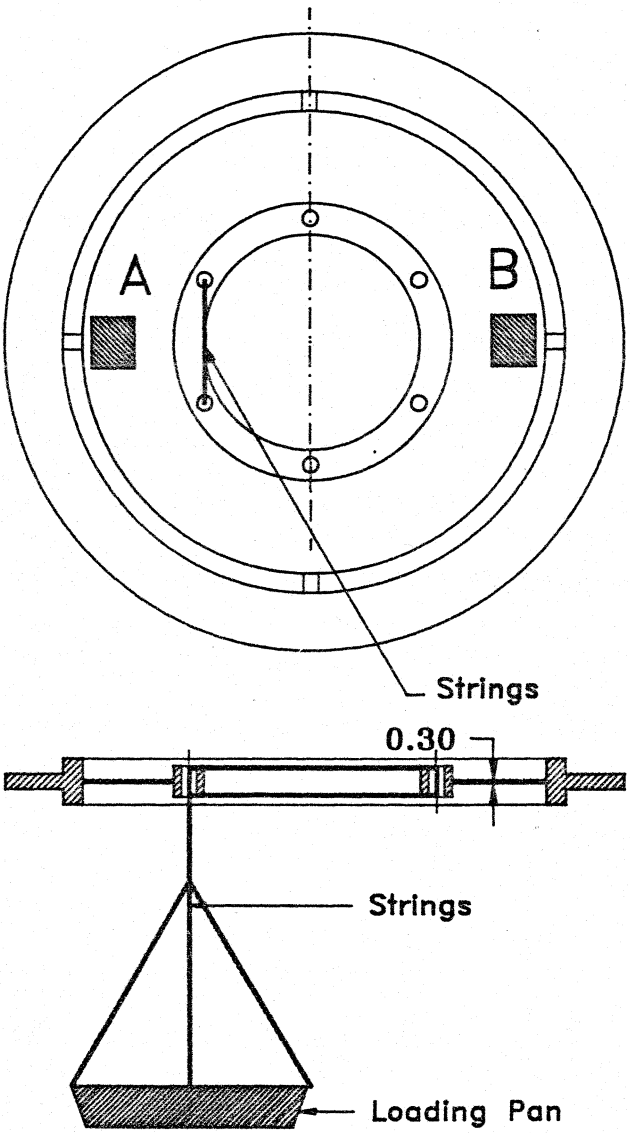

results were more reproducible and hence this calibration data was used in all calculations.

Table B.2
Offset Loading of force transducer towards Channel A

REGRESSION OUTPUT : CHANNEL A	
X coefficient	0.001226
Standard error of y estimate	0.000793
Coefficient of Determination - R^2	0.999980
No. of observations	9
REGRESSION OUTPUT : CHANNEL B	
X coefficient	0.000053
Standard error of y estimate	0.000985
Coefficient of Determination - R^2	0.984084
No. of observations	9

Table B.3
Offset Loading of force transducer towards Channel B

REGRESSION OUTPUT : CHANNEL A	
X coefficient	0.000043
Standard error of y estimate	0.000793
Coefficient of Determination - R^2	0.984463
No. of observations	9
REGRESSION OUTPUT : CHANNEL B	
X coefficient	0.001424
Standard error of y estimate	0.001020
Coefficient of Determination - R^2	0.999976
No. of observations	9

B.3 DIFFERENTIAL PRESSURE CALIBRATION

The transducer was mounted in the mitral chamber with its central mounting orifice blocked with silicone rubber as shown in Fig.5.3(b). The differential pressure transducer (LX06005D) was connected to the pressure taps P_3 & P_4. The transducer was interfaced to the A/D board using the 500 gain amplifier. The water level inside the top chamber was measured using a water manometer connected to the tap P_3 using a 3-way stopcock. After filling the top chamber with water, the level could be reduced gradually by draining water through the pressure tap P_1 and a 3-way stopcock.

The pressure drop and force signals were acquired into the computer. At each measurement point, 2000 samples were acquired at 100 samples/s and averaged.

First the pressure transducer was calibrated in-situ by setting the water levels carefully at 5 cm intervals. The linear regression coefficients of the data obtained are given in Table B.4. The coefficient of 0.356 volts/cm.H_2O was used in all further calculations. In the second set, the water level was reduced at approximately 2 cm intervals to obtain more data points. The data and linear regression fits are given in Table B.5.

Table B.4
Calibration of Pressure Transducer

REGRESSION OUTPUT	
X coefficient - volts/cm.H_2O	0.03559
Standard error of y estimate	0.0040
Coefficient of Determination - R^2	0.9999
No. of observations	7

Table B.5
Differential Pressure Calibration of Force Transducer

REGRESSION OUTPUT : CHANNEL A	
X coefficient - volts/ cm.H_2O	0.00952
Standard error of y estimate	0.00235
Coefficient of Determination - R^2	0.99930
No. of observations	21
REGRESSION OUTPUT : CHANNEL B	
X coefficient - volts/ cm.H_2O	0.01114
Standard error of y estimate	0.00314
Coefficient of Determination - R^2	0.99908
No. of observations	21

B.4 CALCULATION OF PRESSURE DROP CORRECTION FACTORS

The pressure drop correction factor for each of the force transducer channels was calculated from the calibration data. The coefficients used in the calculations are given below :

i. Force Bridges (static offset calibration) :

Channel A : 0.001226 volts/gmf.

Channel B : 0.001424 volts/gmf.

ii. Pressure drop transducer : 0.03559 volts/cm.H_2O

iii. Force Bridges (pressure difference calibration) :

Channel A : 0.00952 volts/cm.H_2O

Channel B : 0.01114 volts/cm.H_2O

The central hole for valve mounting has a diameter of 2.8 cm and the corresponding area is 6.158 cm^2. Therefore, the offset force on each bridge due to 1 cm of water was equal to 3.079 gmf/cm.H_2O.

iv. Voltage output due to 1 cm water on central area :

V_{CA} = 3.079 x 0.001226 = 0.003775 volts/cm.H_2O

V_{CB} = 3.079 x 0.001424 = 0.004384 volts/cm.H_2O

Therefore, the voltage output of the bridges due to the pressure drop across the diaphragm alone is equal to (iii) - (iv)

v. (iii) - (iv) gives :

V_{PA} = 0.00952 - 0.003775 = 0.005745 volts/cm.H_2O

V_{PB} = 0.01114 - 0.004384 = 0.006756 volts/cm.H_2O

Finally, the correction coefficients directly in pressure drop output are :

V_{PAC} = 0.005745/0.03559 = <u>0.16142 volts(force)/volts(pr.drop)</u>

V_{PBC} = 0.006756/0.03559 = <u>0.18983 volts(force)/volts(pr.drop)</u>

During steady flow measurements, the voltage output due to the pressure drop across the force transducer was multiplied by these coefficients to obtain the force corrections directly in volts.

APPENDIX C

VENTURI TUBE - DESIGN & CALIBRATION

The venturi tube belongs to the category of differential pressure flow meters, where the stream of fluid creates a pressure difference as it flows through the tube. The magnitude of this pressure difference depends upon the velocity and density of the fluid and the dimensional features of the tube.

C.1 THEORY

The equations of flow of fluids through a venturi tube are derived from the equations of continuity and energy and are available in any standard book on fluid dynamics and given succinctly by ASME (1971). Briefly, for incompressible liquids, at constant temperature, the continuity equation gives :

$$A_1 V_1 = A_2 V_2 \qquad (1)$$

where:

A_1 = Area of first or upstream section
A_2 = Area of second or downstream section
V_1 = Velocity at first section
V_2 = Velocity at second section

Ignoring the frictional losses, the general energy equation may be written as:

$$\frac{p_1}{\rho} + \frac{V_1^2}{2g_c} = \frac{p_2}{\rho} + \frac{V_2^2}{2g_c} \qquad (2)$$

where additionally :

ρ = Density of fluid
g = acceleration due to gravity
p_1 = pressure at first section
p_2 = pressure at second section

From equations (1) and (2), we get :

$$V_2^2 = 2g.\Delta p.\left[\frac{1}{1-(A_2/A_1)^2}\right] \qquad (3)$$

where :

Δp = $(p_1-p_2)/\rho$ is the pressure drop.

From (3), the theoretical volume flowrate $Q_T = A_2V_2$ can be obtained as :

$$Q_T = \sqrt{\left(\frac{2gA_2^2}{1-(A_2/A_1)^2}\right)\Delta p} \qquad (4)$$

In practical use, there is a 5 to 10% energy loss across the venturi probe and the actual flowrate 'Q' can be obtained as :

$$Q = C_d.Q_T$$

where :

C_d = is the discharge coefficient.

C.2 FABRICATION

The dimensions of the venturi tube as shown in **Figure C.1** were arrived at based on the dimensional proportions for a classical (Herschel) type as given by ASME (1971, p231). It basically consists of a short cylindrical inlet section of 19 mm diameter. This diameter was chosen so that the external diameter was identical to the EM flow probe and could be used interchangeably, if necessary. The inlet section was joined to the throat by a truncated conical section; the sections being joined by a smooth curve. The exit from the throat was lead off by another easy curve into a diffuser cone with an included angle of nearly 10°. The throat diameter was fixed at 12 mm by calculation so that, a pressure drop of 10 mmHg at 4 lpm and a pressure drop of 100 mmHg at 40 lpm could be obtained. With the semiconductor pressure transducer LX06005D (sensitivity 5 mV/psi at 5 volts excitation) and a 500 gain instrumentation amplifier, this resulted in an output voltage of approximately 50 mV at 4 lpm and 5 V at 40 lpm; thus enabling measurement over the range of 0 to 35 lpm.

The venturi tube was machined from a rod of Perspex (polymethyl methacrylate) with a smooth clear bore. The pressure taps were drilled as shown in the figure and connected to the transducer using luer fittings and rigid plastic tubes.

Figure C.1

Venturi Tube

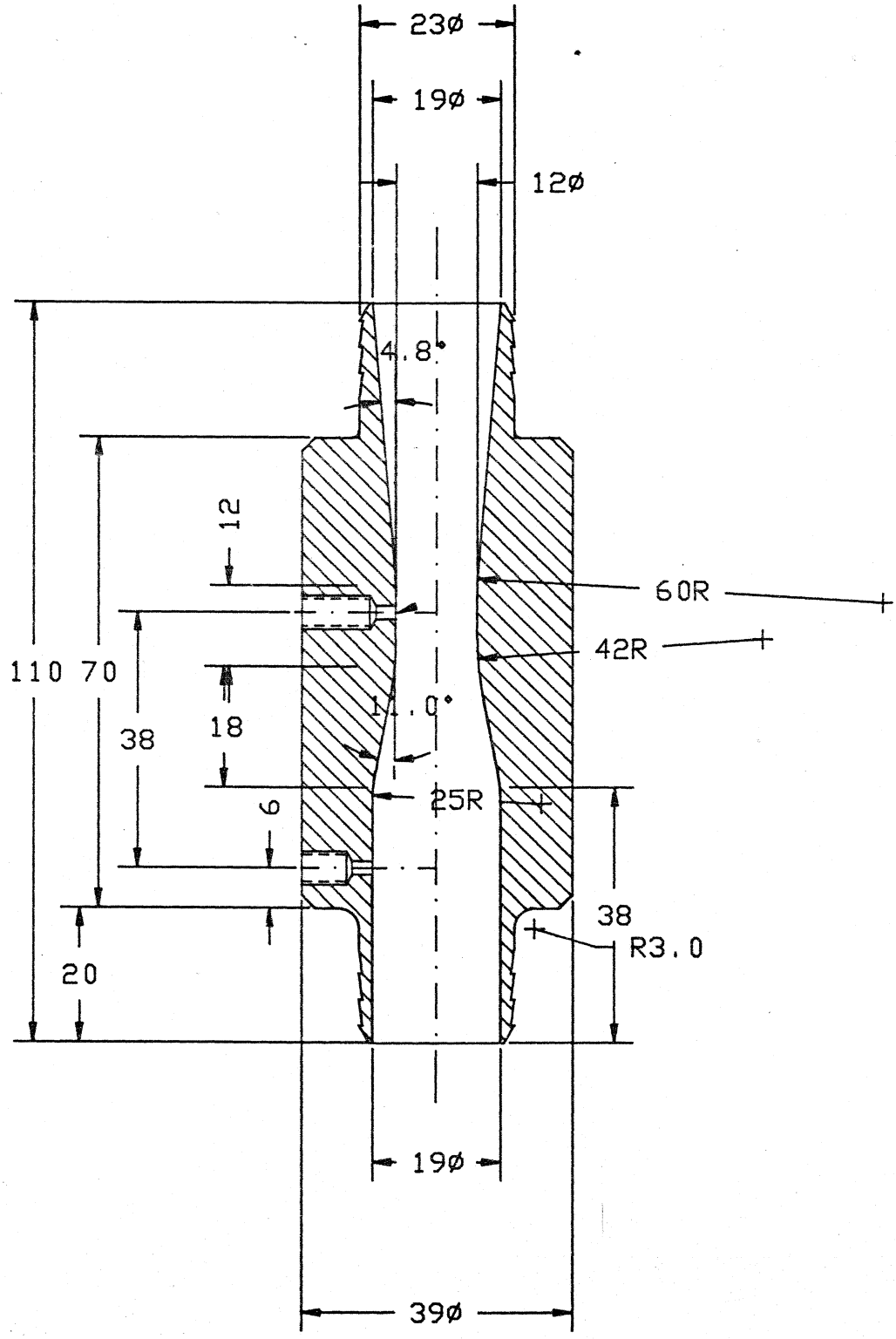

C.3 CALIBRATION

The calibration of the probe was basically carried out by timed collection. The pressure drop across the venturi probe was measured using a Sensym LX06005D semiconductor differential pressure transducer. The transducer was mounted in a perspex holder and backfilled with a silicone fluid under vacuum as described in §5.2.

The venturi measurement system under these conditions was directly calibrated in terms of the output voltage of the A/D board. The fluid used was the 1.08 specific gravity glycerine/water mixture at room temperature. The flowrate was determined by timing using a digital stopwatch, the time taken for a bucket of known volume (11.5 litres) to fill.

A linear least squares fit using a curve fitting software (Tablecurve, Jandel Scientific, USA) was carried out on the calibration data. Of the 3304 linear equations fitted by the software, the parabolic fit was the best with the highest F-value. This fitted equation related the measured output voltage to the fluid flowrate. The measured points and the fitted curve are shown in **Figure C.2.** The details of the fitted equation are :

$$y=a+bx^2$$

where,

a = 0.00286 volts
b = 0.002779 volts/(lpm)^2
Coefficient of determination = 0.99892
Standard error of y estimate = 0.02732 volts
F-value = 36064.8
No. of active points = 41

Figure C-2

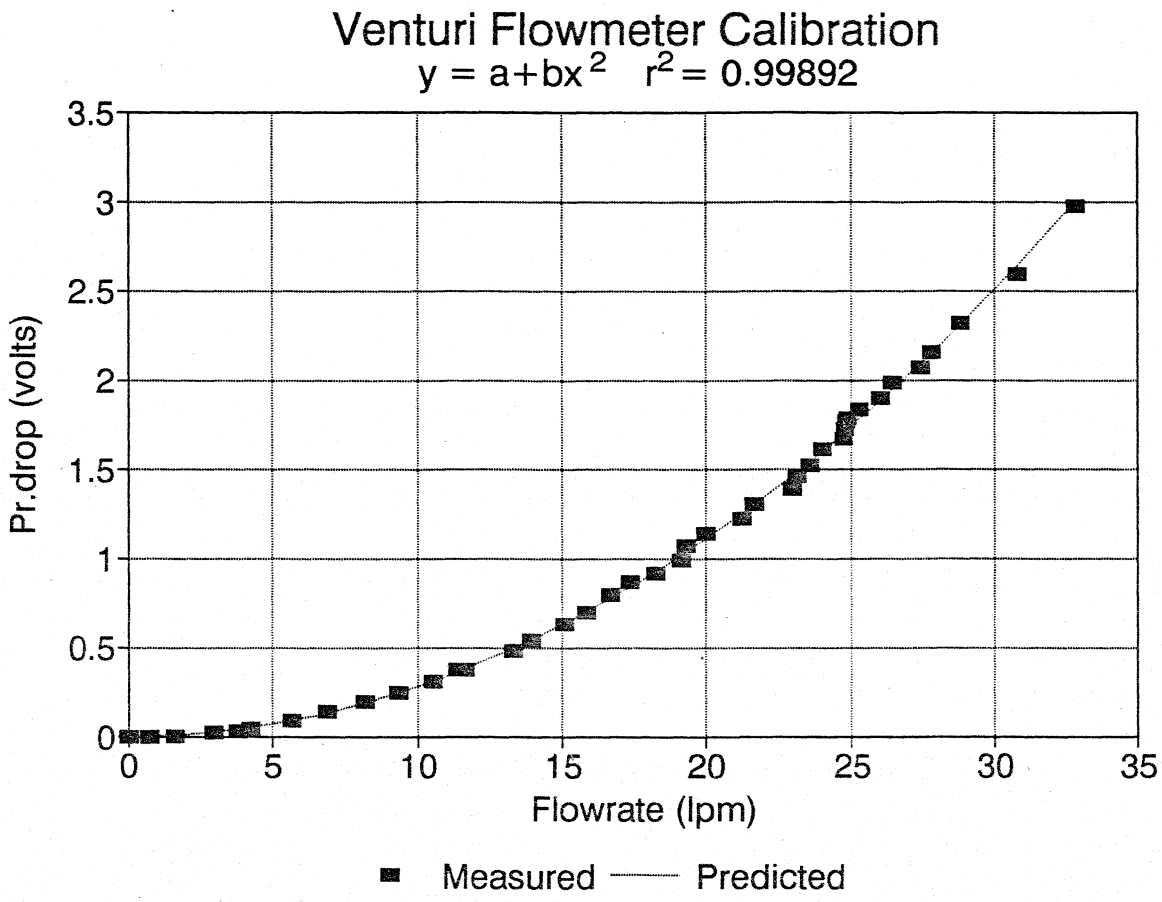
Venturi Flowmeter Calibration
y = a+bx 2 r2 = 0.99892
Pr.drop (volts)
3.5
3
2.5
2
1.5
1
0.5
0
0
5
10
15
20
25
30
35
Flowrate (lpm)
Measured
Predicted

It should be noted that the 12 bit A/D board in the range of ± 5 volts has a One bit error equivalent to ± 0.00244 volts and hence the constant 'a' in the fitted curve was ignored. The above data indicates an excellent fit to the measured data points and confirms the fact that venturi tubes can be used as primary flow measuring devices.

Using this fitted equation, a calibration table for setting the flowrates during the steady flow tests was determined as given in Table C.1.

Table C.1
Venturi Calibration Chart

Flow rate lpm	Pressure Drop volts
0	0.000
5	0.070
10	0.278
15	0.625
20	1.112
25	1.737
30	2.501
35	3.404

APPENDIX D

DESIGN OF SYSTEMIC IMPEDANCE FOR PULSE DUPLICATOR

A correct artificial load to model the left ventricle must mimic the input impedance of the systemic arterial tree. This fact was first appreciated by Westerhof *et al.*,(1971) in his studies of the isolated beating heart. Reul *et al.*,(1975) applied concept for the development of an artificial circulation to test total heart replacements. Martin & Black (1976) used these methods to design the systemic impedance for their pulse duplicator. The values of the components of the systemic impedance have been taken from this study for designing here. The component values are given in Table 6.1 and the electrical analogue used in Fig.6.2.

The physical realisation of the systemic impedance was achieved by using air reservoirs for compliance and an assembly of small bore stainless steel tubes (16G) for resistance.

D.1 DESIGN OF RESISTANCES

A quality factor Q can be defined for a resistance, which predicts the ratio between the resistive part (R) and the inertial part (wL). For $Q = R/wL \gg 1$, the resistance may be

considered as purely resistive with flow and pressure in phase. The ideal situation would be to keep Q >> 1 for the entire range of interest, which is given by the highest harmonic of interest in pressure or flow (generally assumed to be the 10th) (Reul *et al.*,1975).

Tubes of small bore are very suitable for the realisation of resistors of this type, because they have a favourable ratio of resistive to inertial properties. The resistance of a tube can be described by Poisseuille's law as :

$$R = \frac{8\mu l}{\pi r^4} \qquad (1)$$

and its inertia as :

$$L = \frac{\rho l}{A}$$

where :

μ = dynamic viscosity of the fluid
l = length of the tube
r = radius of the tube
ρ = density of the fluid
A = cross sectional area of the tube.

Hence it follows that

$$Q = \frac{R}{L} = \frac{8\nu}{r^2}$$

where $\nu = \mu/\rho$, is the kinematic viscosity.

This equation shows that Q increases with decreasing tube radius. A further prerequisite is a linear behaviour of the resistance over the entire flow range. This means that the flow must be laminar and the inlet length necessary for a development of a parabolic flow profile must be taken into account. If a non-linearity (due to the non-parabolic entrance

profile) of 10% is accepted, two governing equations for the tube length can be formulated (Westerhof *et al.*,1971).

$$l \geq 1.14x10^{-4} [\Delta P\, r^3\, \rho/\mu^2]$$

$$l^2 \geq \frac{11}{64} r\, [\Delta P\, r^3\, \rho/\mu^2]$$

where, ΔP describes the range of linearity for the resistance.

The tube length should be taken equal or greater than the greater of the two resulting values. For pressures in the physiological range and for tubes bores in the range of 0.2mm to 1mm diameter, the second equation determines the minimum necessary length.

Based on these equations, the resistances were designed using 16G SS capillary tubes with the following data :

viscosity of test fluid = 0.035 poise

radius of the tube = 0.06 cm

The resistances R_1 & R_2 were fabricated using a 1" PVC tube for the former and a 1/2" diameter for the latter for convenience of fabrication. This fixed the number of tubes that could be inserted in each to about 210 and 46 respectively. Using a spreadsheet software, for the values of the resistances required, the lengths of the tubes required could be determined and as also their quality factor. The data are given in Table C.1. It can be seen that the quality factors are reasonably good, though the linear pressure range of the first resistance is rather limited. It would have been ideal to use 18G SS tubing for R_1 to obtain better response range; but the number of tubes required increased substantially, making

fabrication more difficult. Also the chances of the tubes getting blocked are increased with reduced bore sizes.

Table D.1
Resistance Values & Quality Factor

PARAMETER	Sy	Units	R_1	R_2
Resistance	R	dyne.sec/cm^{-5}	108	1912
Length	l	cm	3.3	13
Radius	r	cm	0.06	0.06
Number of tubes	n	nos.	210	46
Pressure range	ΔP	mmHg	5	80
Quality factor for heart frequency of 1.16 Hz	Q		12.25	12.25

D.2 DESIGN OF COMPLIANCES

The compliances were fabricated from air chambers. For air, which can be assumed to be an ideal gas, it is well known that :

$$PV = RT$$

When, the temperature is constant, on differentiating we get :

$$PdV + Vdp = 0$$

or the compliance C as :

$$\frac{dV}{dp} = -\frac{V}{P} = C$$

The minimum values of V_1 & V_2 required for compliances C_1 & C_2 can be calculated, assuming a mean pressure (gauge) of 100mmHg or 860 mmHg (absolute) :

$$V_1 = 5.6x10^{-4} \times 860 \times 1333.2 = 642 \ cm^3$$

$$V_2 = 3.0x10^{-4} \times 860 \times 1333.2 = 344 \ cm^3$$

The required volumes were obtained by using 1 litre plastic containers fitted to a machined plastic base with suitable interconnections.

APPENDIX E

PNEUMOTACHOGRAPH – DESIGN & CALIBRATION

E.1 DESIGN

The resistance of the probe was designed using 18 G stainless steel capillary tubes with an internal radius of 0.4 mm. The maximum flowrates that would be encountered during test was taken as 600 ml/s (Willshaw *et al.,1986*). Since the driving pressure for valve at closure was 125 mmHg, a 10 mmHg pressure drop across the probe at this peak flowrate was considered reasonable. At this pressure drop, the output voltage of the A/D board was approximately 1.5 volts yielding a resolution of 1.0 ml/s.

The resistance was fabricated using 18 gauge thin walled stainless steel capillary tubing. The resistance value was calculated using Poisseuille's law as :

$$R = \frac{8\mu l}{\pi r^4 n} \qquad (1)$$

where :

R = resistance

μ = fluid viscosity = 0.000182 for air

l = length of the capillary = 5 cm

r = radius of the capillary = 0.04 cm

n = number of capillaries used.

For a pressure drop of 10 mmHg at 600 ml/s flowrate, the total resistance required is 22.6 dynes.sec/cm^5. Using 5cm length capillaries, it was determined that 40 tubes would be required. These 40 tubes could be conveniently fitted snugly into a bore of 9.5mm.

With this data, the pneumotachograph probe was designed as shown in **Figure E.1.** The inlet and outlet connectors were designed to fit the already existing mitral and aortic couplers.

E.2 CALIBRATION

The pressure drop across the probe was measured using the sensitive Sensym LX06001D semiconductor differential pressure transducer with a 5 volts excitation. At this excitation, the transducer had a sensitivity of 267.8 μV/mmHg (13.85 mV/psi). The transducer was interfaced to the A/D board of the computer using an instrumentation amplifier having a gain of 500. The probe was directly calibrated in terms of the A/D board output voltage using oxygen gas and an electronic mass flowmeter for oxygen (TopTrak, Sierra Instruments, USA). The mass flowmeter has an accuracy of ± 2% over the flowrate range of 0 to 10 lpm; the accuracy and calibration of this mass flowmeter being the same for air, oxygen and nitrogen. It was assumed that the error due to the calibration of the fabricated probe with oxygen and its actual use in air would be negligible as the difference in viscosity between oxygen and air is small.

Figure E.1

Pnuemotacho Probe

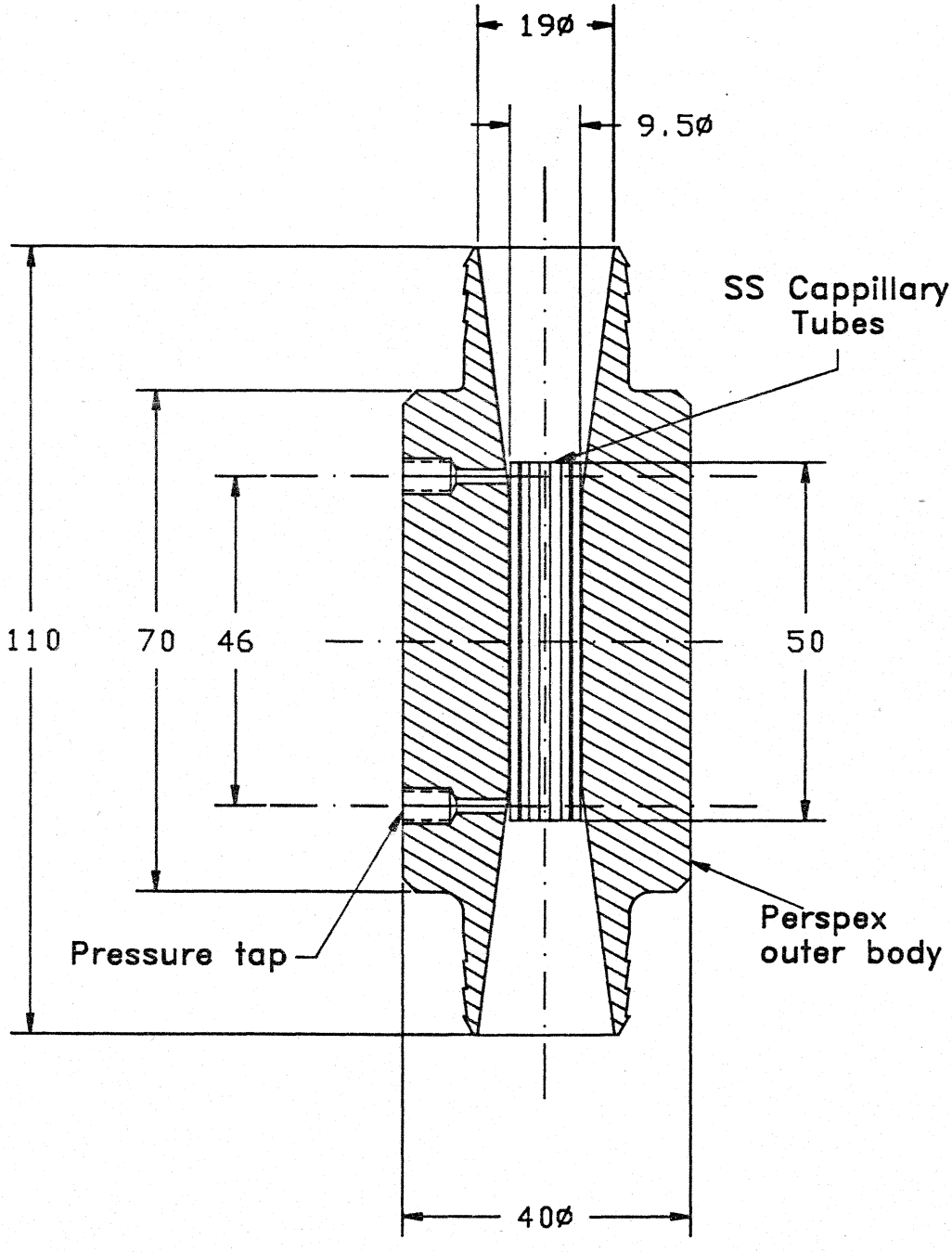

Linear least squares fits were made relating the output voltage to the gas flowrate over the ranges of 0-50 ml/s (0-3 lpm) and 50-166.7 ml/s (3-10 lpm). The data for the linear fits were :

1. Range : 0 to 50 ml/s (0 to 3 lpm).

   True flow = 511.2 x indicated voltage (ml/s)

   Coefficient of determination = 0.99901

   Standard error of flowrate = 0.5 ml/s

   No. of points = 16

2. Range : 50 to 166.7 ml/s (3 to 10 lpm)

   True flow = 427.2 x indicated voltage + 8.5 (ml/s)

   Coefficient of determination = 0.9995

   Standard error of flowrate = 0.8 ml/s

   No. of points = 15

APPENDIX F

PUDVEL - SAMPLE VOLUME DETERMINATION

The accuracy of any velocity profile measurement technique depends on the sample volume of the beam used - laser or ultrasound. The PUDVEL beam was characterised by using a fine jet of fluid produced by a 0.1 mm glass nozzle. The apparatus was based on that of Baker & Yates (1973). The nozzle, placed in a water bath, was connected to a plastic bag containing the test fluid with scattering polystyrene particles (§7.5). The bag was hung from a tall stand and under this pressure head, a fine well defined jet was produced by the nozzle. An exhaust tube placed several centimetres downstream of the nozzle, removed the spent particles of the jet to prevent contamination of the surrounding water in the bath. The ultrasound probe was moved in the axial and transverse planes. The sample volume was moved through the jet by incrementing the range gate of the velocimeter in steps of 0.1 mm and recording the output from the frequency tracker at each position. This procedure was repeated by moving the probe transversely in steps of 0.1 mm. The variation in the tracker output signal as a function of the range and transverse position was used to produce an

axonometric plot (**Figure F.1**) representing the spatial sensitivity of the transducer. Estimates of the sample volume dimensions was then obtained from it.

The dimensions of the sample volume depend on the dimensions of the crystal, the frequency of the ultrasound, the receiver pulse width and the sensitivity of the signal processing system. **Figure F.2** shows the variation in sensitivity along the beam of the ultrasound, averaged across the face of the transducer. The dimension along the beam was 0.4 mm (-3dB points) at a range of 8mm from the face of the crystal.

Figure F.3 shows the variation in beam intensity across the face of the crystal at distance of 8 mm from it. The -3dB width of the beam at this distance was 0.43 mm.

Assuming rotational symmetry about the axis of the beam, the sample volume can be taken to be less than 0.5 mm in all three directions.

Figure F.1

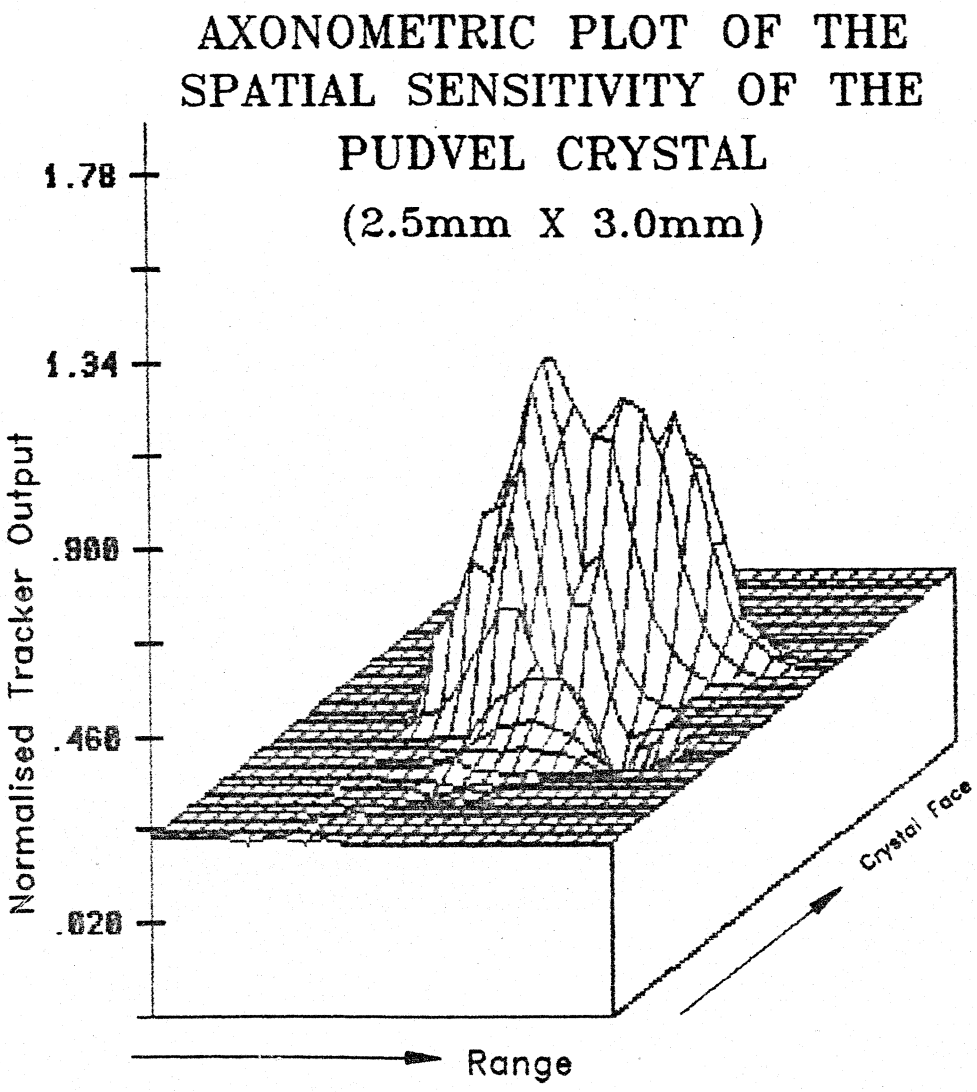
AXONOMETRIC PLOT OF THE
SPATIAL SENSITIVITY OF THE
PUDVEL CRYSTAL
(2.5mm X 3.0mm)
1.78
1.34
.900
.460
.020
Normalised Tracker Output
Range
Crystal Face

Figure F.2

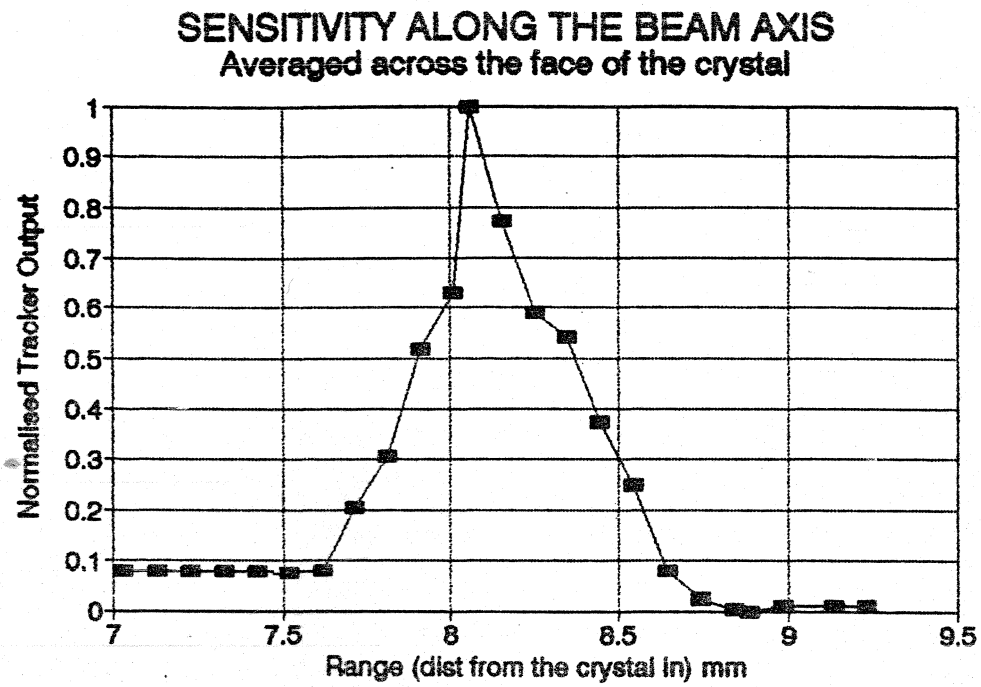

Figure F.3